



University
of Glasgow

Broad, John (2009) *A neurophysiological and proteomic study of cognitive enhancing strategies*. PhD thesis.

<http://theses.gla.ac.uk/1361/>

Copyright and moral rights for this thesis are retained by the author

A copy can be downloaded for personal non-commercial research or study, without prior permission or charge

This thesis cannot be reproduced or quoted extensively from without first obtaining permission in writing from the Author

The content must not be changed in any way or sold commercially in any format or medium without the formal permission of the Author

When referring to this work, full bibliographic details including the author, title, awarding institution and date of the thesis must be given

A Neurophysiological and Proteomic Study of Cognitive Enhancing Strategies

John Broad

A thesis presented for the degree of PhD
Division of Neuroscience and Biomedical Systems
Faculty of Biomedical and Life Sciences
University of Glasgow
G12 8QQ

November 2009

© Copies of this thesis may be obtained by photocopying

Abstract

Improving cognitive function is a growing area of interest for pharmaceutical companies. With an ageing population, cognitive decline is becoming a greater problem. Understanding the physiological effects of nootropic drugs and the changes that occur during cognitive enhancement will enable the design of safer treatments to enhance cognition. In this thesis cognitive enhancing strategies are investigated using neurophysiological and proteomic approaches. The effects of two classes of putatively cognitive enhancing drugs on emergent network oscillatory activities in hippocampal slices are investigated. The effect of an enriched environment, which causes an improvement in cognitive function, on the expression level of proteins in the hippocampus is also investigated.

The development of a new muscarinic acetylcholine receptor (mAChR) agonist that is selective for the M₁ mAChR subtype, called 77-LH-281, has recently been achieved. 77-LH-281 binds to an allosteric site of the M₁ mAChR which accounts for its increased selectivity over other mAChR agonists. This agonist causes gamma frequency oscillatory activity in hippocampal slices, a pattern of network activity that the *in vivo* equivalent of which is associated with cognitive processes. This gamma activity is dependent upon both excitatory and inhibitory networks. 77-LH-281 does not promote epileptiform-like activity in naïve slices as well as a range of models of epileptiform activity, unlike non-subtype selective mAChR agonists like oxotremorine-M. Oxotremorine-M changes the slow interictal-like events following application of 4-AP and NBQX into continuous beta frequency oscillations. This action is not mediated by the M₁ mAChR. Thus selective M₁ mAChR display a preferable range of oscillatory activities compared to non-subtype selective mAChR agonists.

Ampakines are a further class of nootropic drugs. Ampakines are positive modulators of AMPA-type glutamate receptors and they cause improvements in cognitive function of laboratory animals and humans. The ampakines investigated in this thesis are CX691, which increases the amplitude of currents through the AMPA receptor, and CX546, which increases the length of time the AMPA receptor is open. These ampakines do not induce oscillatory activity in naïve hippocampal slices, but they increase the frequency of interictal-like epileptiform activity. CX546 also induces ictal-like activity in the 4-AP induced epileptiform event model. Ampakines may therefore promote epileptiform activity in individuals that are susceptible to epilepsy.

Exposure to an enriched environment leads to improvements in cognitive performance. This behavioural change is mediated by changes at the level of the proteome. Exposure to an enriched environment changes the expression of many classes of proteins including signalling proteins and proteins that are involved in the structural changes that occur during cognitive enhancement. One of the proteins that significantly changes in expression is a protein that is associated with cognitive deficits, known as MeCP2. MeCP2 is a transcriptional repressor and increases in expression in the enriched environment.

This thesis demonstrates the diversity of molecular, cellular and network level approaches that can be used to induce and investigate cognitive enhancement. A combination of these approaches enables the *in vitro* evaluation of current cognitive enhancing strategies and may lead to the the development of novel approaches to enhance cognitive function.

Table of Contents

1	Introduction	13
1.1	General introduction	14
1.2	The hippocampus.....	14
1.3	Epilepsy	24
1.4	Cognitive Enhancement	29
1.4.1	Putative cognitive enhancers	31
1.4.2	Environmental Enrichment.....	33
1.5	Aims	34
2	Materials and Methods	36
2.1	In vitro Hippocampal Slice Experiments	37
2.1.1	Hippocampal Slice preparation	37
2.1.2	Electrophysiology.....	37
2.2	Environmental Enrichment experiments	41
2.2.1	Tissue Preparation	41
2.2.2	DiGE experiment.....	41
2.2.3	Western Blotting	44
2.3	Compounds	48
3	The effect of slice orientation on emergent oscillations	49
3.1	Introduction	50
3.2	Results.....	51
3.2.1	Kainate-induced oscillations	53
3.2.2	Oxotremorine-M induced oscillatory activity	53
3.2.3	The effect of 77-LH-281 on naïve hippocampal slices.....	56
3.3	Discussion	56
3.4	Conclusion.....	62
4	The effect of mAChR agonists on hippocampal neurophysiology.....	63
4.1	Introduction	64
4.2	Emergent network activity in the hippocampus and its modulation by mAChR agonists	66
4.2.1	The 4-AP-induced network activity model	66
4.2.2	Oxotremorine-M is pro-epileptogenic in the 4-AP epileptiform model	66
4.2.3	77-LH-281 has no effect on 4-AP-induced network activity	69
4.2.4	Bicuculline-induced network activity.....	69
4.2.5	Oxotremorine-M is pro-epileptogenic in the bicuculline epileptiform model.....	72
4.2.6	77-LH-281 increases bicuculline-induced inter-ictal-like event frequency.....	72
4.2.7	Low extracellular magnesium-induced network activity.....	75
4.2.8	Oxotremorine-M is pro-epileptogenic in the low extracellular magnesium epileptiform model 75	
4.2.9	77-LH-281 does not effect low extracellular magnesium-induced network activity.....	78
4.2.10	The 4-AP/NBQX- induced slow inter-ictal-like activity model	78
4.2.11	Oxotremorine-M induces beta frequency oscillations in the 4-AP/NBQX epileptiform model	81
4.2.12	The M ₁ mAChR does not mediate the oxotremorine-M -induced oscillations in the 4- AP/NBQX epileptiform model	83
4.3	The modulation of cellular properties of hippocampal pyramidal cells by mAChR agonists	86
4.4	The modulation of synaptic properties of the hippocampus by mAChR agonists	88

4.5	Discussion	90
4.6	Conclusion	101
5	The effect of ampakines on hippocampal neurophysiology	103
5.1	Introduction	104
5.2	The effects of ampakines on field excitatory post-synaptic potentials.....	105
5.2.1	The effect of CX546 on fEPSP	105
5.2.2	The effect of CX691 on fEPSP	107
5.3	Ampakines and emergent network activities	107
5.3.1	The effect of application of CX546 on 4-AP-induced inter-ictal-like activity	110
5.3.2	The effect of application of CX691 on 4-AP-induced inter-ictal-like activity	112
5.3.3	The effect of application of CX546 on bicuculline-induced inter-ictal-like activity.....	112
5.3.4	The effect of application of CX691 on bicuculline-induced inter-ictal-like activity	115
5.3.5	The effect of the application of CX546 on low extracellular magnesium-induced inter-ictal-like activity	115
5.3.6	The effect of the application of CX691 on low extracellular magnesium-induced inter-ictal-like activity	118
5.3.7	The effect of CX546 on 4-AP/NBQX-induced slow inter-ictal-like events	120
5.3.8	The effect of application of CX691 on 4-AP/NBQX-induced slow inter-ictal like events	120
5.4	Discussion	124
5.5	Conclusion	130
6	Changes in protein expression following environmental enrichment.....	132
6.1	Introduction	133
6.2	Effect of a model of environmental enrichment on global hippocampal protein expression	134
6.3	The change in expression of the proteins β-Actin, Rho A, and hnRNP K following exposure to a model of environmental enrichment	136
6.4	The change in expression of MeCP2 in response to a model of environmental enrichment.....	136
6.5	Discussion	139
6.6	Conclusion.....	143
7	Summary and conclusions	145
7.1	Introduction	146
7.2	The effect of mAChRs on hippocampal neurophysiology.....	146
7.3	The effect of ampakines in hippocampal slices	149
7.4	The environmental enrichment protocol.....	150
7.5	Combination of approaches investigating cognitive enhancement	151
7.6	Conclusions	151

List of Figures

Chapter 3

Figure 3.1 Trace examples of oscillations in the hippocampus.....	52
Figure 3.2.1 Characterisation of the effect of application of 400 nM kainate to hippocampal slices	54
Figure 3.2.2 Characterisation of the activity induced by the application of 10 μ M oxotremorine-M to naïve hippocampal slices prepared in the parasagittal and coronal orientations	55
Figure 3.2.3 Investigation into the extracellular oscillatory activity induced by 77-LH-281 in naïve hippocampal slices	57

Chapter 4

Figure 4.2.1 The response of naïve coronal hippocampal slices to 4-AP.....	67
Figure 4.2.2 Investigation into the effect of the application of 10 μ M oxotremorine-M on 4-AP-induced inter-ictal-like activity.....	68
Figure 4.2.3 Investigation into the effect of application of 10 μ M 77-LH-281 on inter-ictal-like activity induced by 20 μ M 4-AP.....	70
Figure 4.2.4 The effect of application of 20 μ M bicuculline (+ 5 mM K^+) to naïve hippocampal slices.....	71
Figure 4.2.5 Investigation into the effect of application of 10 μ M oxotremorine-M on inter-ictal-like activity induced by 20 μ M bicuculline (+ 5 mM K^+).....	73
Figure 4.2.6 Investigation into the effect of application of 10 μ M 77-LH-281 on 20 μ M bicuculline (+5 mM K^+)-induced inter-ictal-like activity	74
Figure 4.2.7 Investigation into the effect of low Mg^{2+} ACSF on naïve hippocampal slices	76
Figure 4.2.8 Investigation into the effect of the application of 10 μ M oxotremorine-M on inter-ictal-like activity induced by the removal of Mg^{2+} from the extracellular bathing medium.	77
Figure 4.2.9 Investigation into the effect of the application of 10 μ M 77-LH-281 on low extracellular Mg^{2+} -induced inter-ictal-like activity	79
Figure 4.2.10 Characterisation of 4AP/NBQX induced slow inter-ictal-like events.....	80
Figure 4.2.11 The effect of oxotremorine-M on 4-AP/NBQX-induced slow inter-ictal-like events	82
Figure 4.2.12.1 Investigation into the effect of application of 77-LH-281, a M_1 mAChR selective agonist to 4-AP/NBQX slow inter-ictal like events	84
Figure 4.2.12.2 Investigation into role of the M_1 mAChR in the oxotremorine-M induced suppression of 4-AP/NBQX slow inter-ictal like events and the induction of network activity.....	85
Figure 4.3 Characterisation of the CA1 pyramidal cell response to mAChR agonists.....	87
Figure 4.4 Characterisation of the effect of mAChR agonist application on the field excitatory post-synaptic potential.....	89

Chapter 5

Figure 5.2.1 Investigation into the effect of the ampakine CX546 on field excitatory post-synaptic potentials.....	106
Figure 5.2.2 Investigation into the effect of application of the ampakine CX691 on the amplitude of field excitatory post-synaptic potentials.....	108

Figure 5.3 Investigation into the effect of the application of ampakines on naïve hippocampal slices.....	109
Figure 5.3.1 Investigation into the effect of CX546 on hippocampal slices displaying inter-ictal-like activity induced by application of 4-AP	111
Figure 5.3.2 Investigation into the effect of CX691 on the frequency of inter-ictal-like events induced by 4-AP.....	113
Figure 5.3.3 Investigation into the effect of CX546 on the frequency of inter-ictal-like events induced by bicuculline (+5 mM K ⁺)	114
Figure 5.3.4 Investigation into the effect of CX691 on the frequency of bicuculline-induced inter-ictal-like events.....	116
Figure 5.3.5 Investigation into the effect of CX546 on low Mg ²⁺ induced inter-ictal-like activity.....	117
Figure 5.3.6 Investigation into the effect of CX691 on low Mg ²⁺ -induced inter-ictal-like events..	128
Figure 5.4.1 CX546 does not alter the frequency of 4-AP/NBQX induced slow inter-ictal-like events	121
Figure 5.4.2 CX691 does not alter the frequency of 4-AP/NBQX induced slow inter-ictal-like events	122

Chapter 6

Figure 6.2 The effect of an environmental enrichment protocol on the global protein expression of the hippocampus	135
Figure 6.3 The effect of an enriched environment upon the expression of β -Actin, Rho-A, and hnRNP K	137
Figure 6.4 Quantification of expression change of MeCP2 in response to enriched environment	138

List of Tables

Table 1- Preparation of Diluted Albumen (BSA) standards.....42

Table 2- Summary of effects of application of mAChR agonists on naïve coronal hippocampal slices and hippocampal slices displaying oscillatory activities.....90

Accompanying Material

Accompanying this thesis is the journal article McNair, K., J. Broad, et al. (2007). "Global changes in the hippocampal proteome following exposure to an enriched environment." published in the journal *Neuroscience*. This is included on page 170.

Acknowledgements

Initially I would like to take this opportunity to thank my supervisor Dr Stuart Cobb for giving me the chance to undertake such a fascinating and challenging thesis, and for his guidance and assistance throughout the course of my PhD studies. I would also like to thank my industrial supervisor, Dr Ceri Davies, for his invaluable help and guidance.

I would also like to thank all of the staff and students I have worked with over the last 3 years, especially Dr Imre Vida, Dr Kara McNair and Dr Helene Widmer, for their assistance in my practical work.

Finally I would like to thank all of my friends and family for their continued support and patience over the course of my degree, without whom I would certainly not have been able to get anywhere close to completing my thesis. A special thanks goes to my parents, siblings, Heather, Kirstie, Tony and Ruth, and the Farm.

Declaration

I declare that the work presented in this thesis is entirely my own, with the exception of fig 6.2, which is taken in part from McNair, K., J. Broad, et al. (2007). "Global changes in the hippocampal proteome following exposure to an enriched environment." from the journal *Neuroscience*.

Signature.....

John Broad

This work has not been presented in part or alone for any other degree course. Some of the work herein has been published in part. A list follows:

McNair, K., J. Broad, et al. (2007). "Global changes in the hippocampal proteome following exposure to an enriched environment." *Neuroscience* **145**, (P413-422), 2007

Broad, J. R., Davies, C. H., Cobb, S. R., Studies to investigate the pro-epileptogenic actions of ampakines in vitro. *British Neurosci. Assoc. Abstr.*, Vol **19**, (P87), 2007

Broad, J. R. , Davies, C. H., Cobb, S. R., A study comparing the pro-epileptogenic actions of a non-selective muscarinic acetylcholine receptor agonist and a specific M₁ receptor agonist in vitro. *Life Sciences 2007 Abstr.*, 2007

Definitions

Abbreviations

4-AP	4 amino pyridine
4-DAMP	1,1-Dimethyl-4-diphenylacetoxypiperidinium iodide
AC42	4-n-Butyl-1-[4-(2-methylphenyl)-4-oxo-1-butyl]-piperidine hydrogen chloride
ACh	Acetylcholine
AHP	After hyperpolarisation
AMPA	Alpha-amino-3-hydroxy-5-methyl-4-isoxazole propionic acid
AP5	D(-)-2-Amino-5-phosphonopentanoic acid
AQ RA-741	11-[[4-[4-(Diethylamino)butyl]-1-piperidinyl]acetyl]-5, 11-dihydro-6H-pyrido[2,3-b][1,4]benzodiazepin-6-one
BDNF	Brain derived neurotropic factor
CA	Cornu ammonis
CNS	Central nervous system
CRMP2	Collapsin response mediated protein 2
CX516	1-(quinoxalin-6-ylcarbonyl)piperidine
CX546	1-(1,4-Benzodioxan-6-ylcarbonyl)piperidine
DiGE	Differential in gel electrophoresis
EE	Environmental enrichment
EEG	Electroencephalogram
EPSC	Excitatory postsynaptic current
EPSP	Excitatory postsynaptic potential
GABA	γ -amino butyric acid
hnRNP.K	Heterogeneous nuclear ribonucleoprotein K
HRP	Horseradish peroxidase
IPG	Immobilised pH gradient
LTP	Long term potentiation
mAChR	Muscarinic acetylcholine receptor
MALDI-ToF	Matrix assisted laser desorption ionisation-time of flight
MeCP2	methyl CpG binding protein 2
mGluR	Metabotropic glutamate receptor
MK801	(+)-5-methyl-10,11-dihydro-5H-dibenzo[a,d]cyclohepten-5,10-imine maleate
MS/DBB	Medial septum/diagonal band of Broca
MT-7	Muscarinic toxin 7
nAChR	Nicotinic acetylcholine receptor
NMDA	N-methyl D-aspartate
PAGE	Polyacrylamide gel electrophoresis
PVDF	Polyvinylidene Fluoride,
RT-PCR	Reverse transcriptase polymerase chain reaction
SDS	Sodium dodecyl sulphate
SLM	Stratum lacunosum moleculare
SO	Stratum oriens
TBST	Tris buffered saline solution (+ Tween)
TM	Trans-membrane

1 Introduction

1.1 General introduction

This thesis investigates different cognitive enhancement strategies in the hippocampus, a structure in the brain responsible for many cognitive processes including learning and memory formation. Cognitive enhancement, as defined by this thesis, is a measurable improvement in brain function. Strategies to improve cognition are important in ameliorating the symptoms of cognitive decline that occur in many neurological disorders including Alzheimer's Disease and schizophrenia.

The major focus of this thesis is the investigation of the effect that putative cognitive enhancing drugs have on the communication between cells and networks within the hippocampus. These compounds are tested in both physiological models of brain activity and in several models of epileptiform activity. The compounds investigated are muscarinic acetylcholine receptor agonists and positive allosteric modulators of AMPA type glutamate receptors, called ampakines. These compounds were chosen for their propensity to affect synaptic transmission between neurones and emergent network activities in the hippocampus.

A secondary focus of this thesis is the investigation of the effects of a model of cognitive enhancement on the global protein expression of the hippocampus. The expression of a range of selected proteins is investigated following exposure to an enriched environment, which is known to lead to improvements in cognitive function.

These strategies will allow the evaluation of current opinions in the field of cognitive enhancement, as well as providing further insight into the mechanisms of action of a range of nootropic drugs.

1.2 The hippocampus

The hippocampus is the most well characterised cortical brain region and is ideally suited for studying network activity due to its highly laminar structure. In humans the hippocampus is located in the temporal lobe below the neocortex and is involved in mnemonic processing and the representation of place in the environment (O'Keefe and Dostrovsky, 1971; Scoville and Milner, 1957). The hippocampus is so named due to its resemblance to a seahorse (*hippos* = horse, *kampos* = monster, sea monster; Greek).

The hippocampal formation is divided into four sub-fields- the *cornu ammonis* (CA) 1-4 (Lorento de No, 1934), and the dentate gyrus. The CA3 and CA1 regions occupy most of

the hippocampus. The dentate gyrus projects to the cells of the CA3 region along the mossy fibre pathway, and the CA3 region projects to the CA1 and dentate gyrus regions along the Schaffer collaterals. Cells from the CA1 region project through the subiculum and project out to the entorhinal cortex layer V neurones.

Both the hippocampus and the dentate gyrus are three-layered cortices. The dentate gyrus contains the polymorphic layer (the *hilus*) containing the granule cell axons, the granule layer (the *stratum granulosum*) containing the granule cell bodies, and the molecular layer (*stratum moleculare*) containing the granule cell dendrites. The hippocampus contains a polymorphic layer (the *stratum oriens*) containing the basal dendrites of the pyramidal cells, a pyramidal cell layer (the *stratum pyramidale*) containing the pyramidal cell bodies, and a molecular layer (the *stratum radiatum* and the *stratum lacunosum-moleculare*) containing the distal apical dendrites of the pyramidal cells. The principal cells make up about 90% of the neurones within the hippocampus, and these cells form projections to the adjacent area.

The dentate gyrus acts as a gate for sensory inputs from the entorhinal cortex entering the hippocampus (Finnerty and Jefferys, 1993). Inputs into the dentate gyrus come from the perforant pathway and axons from the dentate gyrus project to both the CA3 and the CA1 regions of the hippocampus. The CA3 region contains recurrent axonal arborizations that innervate local pyramidal cells within the CA3 region. The Schaffer collaterals then project to the CA1 region.

The CA1 region receives inputs from the Schaffer collaterals from the CA3 region. The CA1 region also receives inputs from the entorhinal cortex and projects through the subiculum into the entorhinal cortex. The unidirectional perforant path-dentate gyrus-CA3-CA1 series of connections is known as the trisynaptic loop of the hippocampus, and is made by excitatory connections between the principal cells of each area.

The hippocampus is made up of two major classes of neurones- pyramidal cells and interneurones. Pyramidal cells are the principal cells of the hippocampus. These bipolar neurones have their cell bodies in the *stratum pyramidale* and have spiny dendritic trees that project basally to apically. These cells are glutamatergic and excitatory.

Interneurones account for only 8-10% of neurones in the hippocampus but display a much greater diversity than the relatively homogenous population of pyramidal cells (Freund and Buzsaki, 1996). There are at least 21 different classes of interneuron identified in the CA1

region of the hippocampus. The interneurons have many different neurochemical, pharmacological, anatomical and electrophysiological properties, although many do have restricted target regions, lack spines, and are GABAergic.

The interneurons are categorised by these different parameters. The interneurons innervate either pyramidal cells, excitatory inputs into the hippocampus, or other interneurons. The major classes of interneurons that innervate pyramidal cells are the basket cells, axo-axonic cells, bistratified and oriens-lacunosum moleculare interneurons. These synapse onto the soma, axon initial segment, and stratum oriens and stratum radiatum/lacunosum moleculare respectively (Klausberger and Somogyi, 2008). These interneurons express parvalbumin or cholecystekinin, as well as a variety of other biochemical markers (Klausberger et al., 2005). This diversity allows highly variable functionality and resonances to exist within the interneuronal population, important in the generation and pacing of oscillatory activities.

Neurotransmitters within the hippocampus

The cells within the hippocampus release neurotransmitters that act mainly upon two different classes of receptors at the synapses between cells. The first class is ligand gated ion channels, or ionotropic receptors, which act within 1-100 ms. When activated, these receptors open a pore in the cell membrane that allows current to flow through the pore. The second major type of receptor is the metabotropic receptors, or G-protein coupled receptors. G-protein coupled receptors act over 100-2000 ms and activate intracellular second messenger systems in order to change the cellular excitability or gene expression within the target cell (Marinissen and Gutkind, 2001).

Glutamate receptors

It was only in the 1960s that amino acids were first identified as being able to mediate synaptic transmission. We now know that glutamate is the major excitatory neurotransmitter within the central nervous system (Fonnum, 1984). Glutamate activates both ionotropic receptors- known as AMPA, kainate, and NMDA receptors (Dingledine et al., 1999) and metabotropic receptors, known as metabotropic glutamate receptors (mGluRs) (Pin and Duvoisin, 1995).

AMPA receptors are the most highly expressed neurotransmitter receptor within the central nervous system. They are ionotropic glutamate receptors and are expressed at the majority

of the excitatory synapses within the brain. They are made up of 4 subunits (Matsuda et al., 2005), and these individual subunits are called GluR1-4. Each subunit has 3 transmembrane (TM) domains and an M2 re-entrant loop that forms the functional inner pore of the receptor. The channel properties depend on the expression of the individual subunit composition. AMPA receptor subunits contain a Q/R editing site and a flip/flop domain (Dingledine et al., 1999), allowing for a large range of channel conductances, open times and desensitisation kinetics. AMPA receptors are mainly monovalent cation channels and allow Na^+ and K^+ to pass through the ion pore. However, AMPA receptors that do not contain the GluR2 subunit are permeable to Ca^{2+} (Hollmann et al., 1991).

Kainate receptors are a subset of ionotropic glutamate receptors that also conduct fast excitatory synaptic transmission. These receptors contain the GluR 5-7, KA1 or KA2 subunits (Dingledine et al., 1999), and they are named as they have a higher affinity for kainate than AMPA. They are highly expressed upon interneurons and application of nanomolar concentrations of kainate has been shown to produce oscillatory rhythms within the hippocampus (Fisahn, 2005; Fisahn et al., 2004).

NMDA receptors are a further class of ionotropic glutamate receptor. NMDA receptors are again made up of 4 subunits. The receptor must contain 2 NR1 subunits, as well as 2 NR2A-D subunits to be functional (Laube et al., 1998). Heterodimeric subunits are common, although heterotrimeric subunits exist (Brothwell et al., 2008). The NMDA receptor is often blocked at polarised potentials by the presence of a Mg^{2+} ion (Nowak et al., 1984). Strong depolarisation leads to the removal of the Mg^{2+} block of the NMDA receptor and allows current to flow through the receptor (Jahr and Stevens, 1990). The NMDA receptor is a non-selective cation channel, and as such allows Ca^{2+} entry into the cell (MacDermott et al., 1986). This process mediates one form of long-term potentiation (LTP), a long lasting change in synaptic strength that is thought to underlie memory formation (Kandel, 1997).

The final class of glutamate receptors is the metabotropic glutamate receptors (mGluRs). There are 8 mGluRs and they modulate excitatory and inhibitory transmission. They are large 7 transmembrane domain proteins that activate diverse G-proteins, which in turn can activate phospholipase C and activate or inhibit adenylate cyclase (Nakanishi, 1992). Agonists of mGluRs can cause oscillatory activity within the hippocampus (Cobb et al., 2000).

GABA receptors

GABA is the major inhibitory neurotransmitter within the central nervous system, aside from the spinal cord. Like glutamate receptors, GABA activates ionotropic receptors, the GABA_A receptors, and metabotropic receptors, the GABA_B receptors. GABA provides the major inhibitory drive to the hippocampus in adults. However, GABA can be excitatory during early development (Ben Ari et al., 1989) and seizures (Ben Ari, 2006), due to a disruption of the chloride gradient.

The GABA_A receptor is a ligand gated ion channel that is made up of 5 subunits (Nayeem et al., 1994). For a functional ion channel at least one α and β subunit must be present, with the other subunits made up of α , β , γ , δ , ϵ , π , θ or ρ subunits (Sieghart et al., 1999). Again, the different expression of the channels leads to different channel properties. Each subunit is made up of 4 transmembrane domains and the M2 transmembrane domain lines the pore and forms the selectivity filter for the ion channel. When two molecules of GABA bind to the receptor, the ion channel opens and allows the movement of anions, primarily Cl⁻ ions and to a lesser degree bicarbonate (HCO₃⁻) ions (Bormann et al., 1987).

The GABA_B receptor is the corresponding metabotropic receptor that mediates inhibitory synaptic transmission on a slower time course. The GABA_B receptor is a 7 transmembrane domain receptor and has a requirement to form heterodimers of GABA_BR1 and GABA_BR2 to allow functional expression of GABA_B (Marshall et al., 1999). The GABA_B receptor is linked through the G_{oi} G-protein and activation of the GABA_B receptor causes an inhibition of presynaptic Ca²⁺ channels (Wu and Saggau, 1995) and opens postsynaptic K⁺ channels (Dutar and Nicoll, 1988). At postsynaptic loci GABA_B receptor activation leads to hyperpolarisation of the cell through the activation of inwardly rectifying K⁺ channels, acting to decrease excitability of the network. At presynaptic loci GABA_B activation inhibits the release of neurotransmitters including GABA (Misgeld et al., 1995), leading to an increase in local excitability (Leung et al., 2005). High doses of GABA_B antagonists and the genetic depletion of GABA_B R1 (Brown et al., 2003; Schuler et al., 2001) are pro-convulsive, indicating the network effect of GABA_B activation is to decrease excitability predominately through postsynaptic mechanisms.

Acetylcholine receptors

Acetylcholine receptors are highly expressed in the hippocampus. They consist of both nicotinic ionotropic and muscarinic metabotropic receptors. The nicotinic acetylcholine

receptors (nAChRs) are made up of 5 subunits, much like the GABA_A receptors described above (Changeux and Edelstein, 1998). They contain 4 transmembrane spanning domains, with the TM2 region as the selectivity filter. They are permeable to monovalent cations. Only the nAChR made up entirely of $\alpha 7$ subunits is permeable to Ca²⁺ (Seguela et al., 1993).

Muscarinic acetylcholine receptors have been shown to be present in the many different areas of the central nervous system, initially by radioligand binding studies, then by the use of oligonucleotide probes (Buckley et al., 1988), and finally by the use of immunocytochemistry (Levey et al., 1995). In the hippocampus, the different receptor subtypes are found differentially expressed in different areas. The M₁ receptor subtype is strongly expressed in the pyramidal cell layer of the hippocampus and the granule cell layer of the dentate gyrus. The M₂ receptor is found mainly in non-pyramidal neurones and in discrete bands of fibres surrounding the pyramidal cells; out with the hippocampus it is found in the medial septum and the diagonal band of Broca, important cholinergic inputs to the hippocampus (Hajos et al., 1998). The M₃ receptor is enriched in pyramidal neurones, the stratum lacunosum-moleculare and in the outer third of the molecular layer of the dentate gyrus. The M₄ receptor is expressed in non-pyramidal neurones, fibre pathways and in the inner third of the molecular layer. The M₁ and M₃ receptors are largely found postsynaptically, whereas the M₂ and M₄ receptors are localised pre-synaptically, and the distribution of the receptors is highly complementary. M₁ receptors display 3-fold higher expression level than M₃ receptors in the hippocampus, and the receptor reserve of the M₁ receptor is estimated to be above 75% (Porter et al., 2002). The M₁ receptor is therefore the predominant excitatory muscarinic acetylcholine receptor subtype found in the hippocampus.

The receptors also have a complementary expression in the perforant pathways (the main excitatory input into the hippocampus) and associational/commissural projections (the major pathways for integration of information along the septotemporal axis) (Rouse et al., 1999). In the perforant pathway, the M₂, M₃ and M₄ receptors are found presynaptically, with the M₃ receptor dominant in the lateral perforant pathway. The M₂ and M₄ receptors are found presynaptically on the associational pathway, and the M₄ receptor is also found on the commissural pathway. This differential expression all over the hippocampus allows complex regulation of the differing physiological responses mediated by cholinergic pathways.

The mAChRs act through a number of different second messenger cascade systems in the central nervous system. M_1 , M_3 and M_5 predominantly act through $G\alpha_q$ as postsynaptic receptors, and the M_2 and M_4 receptors act mainly through $G\alpha_{i/o}$ as presynaptic receptors. Cholinergic excitation is known to cause depolarisation of pyramidal cells, with an associated increase in input resistance. Cholinergic receptor activation leads to the blockade of a calcium activated potassium conductance, depression of the after hyperpolarisation (AHP) and increases in cell firing, (Cole and Nicoll, 1984b). The M-current is also blocked (Cole and Nicoll, 1983). The M_1 receptor is known to depolarise the pyramidal cells via increases in I_H (a hyperpolarisation activated current) and I_{cat} (a calcium activated non-specific cation current) (Mann and Paulsen, 2005). The M_3 receptor is thought to block the leak potassium conductance (Pitler and Alger, 1990; Porter et al., 2002). Cholinergic excitation is known to release calcium from intracellular stores in CA1 pyramidal neurones, mediated by inositol 1,4,5 triphosphate (Power and Sah, 2002). This leads to a rise in free intracellular calcium in the soma and nuclear regions.

Muscarinic receptors are known to regulate the release of several neurotransmitters in the hippocampus. Although mAChR activation excites GABAergic interneurons, GABA release is reduced (Behrends and ten Bruggencate, 1993) via the M_2 and M_4 mAChR induced suppression of the pre-synaptic release machinery of the GABAergic interneurons (Zhang et al., 2002). In turn, muscarinic receptor mediated transmission is regulated by several receptors. $GABA_B$ receptors, via pre- and post-synaptic mechanisms, prevent muscarinic mediated excitation of CA1 pyramidal cells (Morton et al., 2001). There is therefore a reciprocal inhibition between acetylcholine and GABA transmission. The tonic activation of pre-synaptic adenosine A1 receptors inhibits muscarinic mediated depolarisation of CA1 pyramidal cells.

Oscillations in the hippocampus

One of the most noticeable features of the brain, when recording electro-encephalograms (EEGs) using scalp electrodes from mammals, is the presence of regular patterned oscillatory activity. This activity is a function of neuronal assemblies and can be grouped into distinct frequency bands, and recorded from the rodent hippocampus during different activities. Low frequency oscillations (0.5-2 Hz) can be observed during slow wave sleep, whereas rhythmic components with medium frequencies (5-10 Hz) and fast frequencies (40-100 Hz) are found during REM sleep and exploratory activities. Similar rhythms can be observed in hippocampal slice preparations, in which application of various agonists to the slice leads to several different types of emergent network activity. The oscillations that

occur *in vitro* in hippocampal slices are also grouped in discrete frequency bands. These include delta frequency oscillations, with oscillation frequencies that lie between 0.5 and 4 Hz, theta frequency oscillations, with oscillation frequencies that lie between 4 and 12 Hz, beta frequency oscillations, with oscillation frequencies that lie in the range of 13 to 30 Hz, gamma frequency oscillations, with oscillation frequencies that lie in the range of 30 to 100 Hz, and fast ripples, with oscillation frequencies that lie in the range of 100 to 400 Hz (these are sometimes known as high frequency oscillations). Some of the physiological oscillations that occur in the hippocampal slices investigated in this thesis are detailed in figure 3.1.A.

Pathophysiological oscillations are also found *in vivo* and *in vitro* in the hippocampus and in other cortical structures. These are often associated with CNS disorders such as epilepsy, schizophrenia and Parkinson's disease. Rectifying these aberrant oscillations has been suggested as an approach to evaluate the therapeutic benefit of treatments of these diseases (Cobb and Davies, 2005).

Theta frequency oscillations

The theta frequency oscillation is thought to be critical for temporal coding and the modification of synaptic strengths, with LTP enhanced during theta frequency oscillations (Huerta and Lisman, 1993). The major currents that underlie theta frequency oscillations are generated by the entorhinal input, the CA3 Schaffer collaterals, and voltage dependent Ca^{2+} currents in pyramidal cell dendrites.

An intact septal input from the medial septal-diagonal band of Broca (MS-DBB) is necessary for *in vivo* theta oscillations (Fischer et al., 1999) leading to the hypothesis that a rhythmic input from the septal projections was required to impose the rhythmic activity. The MS-DBB contains both cholinergic and GABAergic projections to the hippocampus. The MS-DBB is able to generate and maintain its own theta rhythm *in vitro* (Garner et al., 2005).

The extracellular field is composed of the summed IPSPs on the soma and EPSPs on the dendrites of pyramidal cells. It has been proposed that the interplay between the inhibitory feed-forward input from the septum and the excitatory input from the perforant pathway generates the theta frequency oscillation. EPSPs from the perforant path act to provide rhythmic excitation to the pyramidal cells, and cholinergic projections from the MS-DBB slowly depolarise pyramidal cell dendrites. The activity of cholinergic neurones also leads

to a slow depolarisation of basket cell interneurons, whilst the activity of the GABAergic neurons projecting from the MS-DBB rhythmically hyperpolarises basket cell interneurons. Basket cell interneurons in turn provide phasic inhibition of the soma of pyramidal cells. The tonic cholinergic excitation of interneurons, coupled with the theta frequency phasic inhibition of interneurons by GABAergic projections from the MS-DBB, may be responsible for the phasic output of interneurons (Buzsaki, 2002).

These oscillations can, however, also be observed in cultured hippocampal cells and septally de-afferated hippocampi, with *in vivo* micro-infusion of carbachol and bicuculline (Colom et al., 1991). This suggests the hippocampus must have an intrinsic network oscillator, in order to synchronise emergent activity.

The primary intrinsic hippocampal network oscillator is thought to be found in the CA3 region of the hippocampus, although it has also been suggested that the intrinsic oscillator is the CA2 region (Fischer, 2004). Carbachol cannot stimulate theta frequency oscillations in the CA1 region in the absence of the CA3 region (Williams and Kauer, 1997). The propagation of the oscillatory activity is dependent on synaptic transmission via AMPA receptors and also dependent on NMDA receptors. The oscillation is initiated by the depolarisation of the CA2/CA3 pyramidal cells by activation of muscarinic acetylcholine receptors, causing pyramidal cells to discharge (Fischer, 2004). However, activation of the M₁ mAChR on pyramidal cells alone is too slow to account for the generation of theta frequency membrane potential oscillations. mAChR activation depolarises pyramidal cells which leads to the modulation of intrinsic membrane currents like I_M, I_h and I_A, and the pyramidal cells show resonant frequency preferences within the theta frequency range (Pike et al., 2000). Stratum oriens/lacunosum moleculare (O-LM) interneurons also display a resonant frequency within the theta frequency range. Theta frequency subthreshold membrane oscillations can be induced in O-LM interneurons by the activation by mAChRs located on the interneurone (Chapman and Lacaille, 1999). These interneurons also can provide phasic inhibition to pyramidal cell dendrites, pacing the oscillation.

Gamma frequency oscillations

As mentioned above, another major relevant oscillatory rhythm recorded both *in vivo* and *in vitro* is the gamma frequency oscillation, which is thought to allow some forms of cognitive processing and perceptual binding to occur (Gray and Singer, 1989; Mann and Paulsen, 2005), including storage of memories and consciousness. It provides a temporal

structure to co-ordinate the activity of individual neurones. Gamma frequency oscillations are often found superimposed upon the theta oscillations *in vivo* in the hippocampus, an interaction which can be disrupted by the blockade of mAChRs (Hentschke et al., 2007).

Gamma oscillations can be induced in the hippocampus *in vitro* by the application of kainate, the application of mGluR agonists, and the application of cholinergic agonists such as carbachol (Buhl et al., 1998; Fisahn et al., 1998). Although these oscillations are within the same frequency band they display a differential pharmacology. Kainate and mGluR agonist-induced oscillations are maintained in the presence of AMPA receptor antagonists (Fisahn et al., 2004), whereas cholinergic induced oscillations are blocked by AMPA receptor antagonists (Fisahn et al., 1998). All gamma oscillations are dependent on fast inhibition mediated by GABA_A receptors.

The predominant class of interneurone that is assumed to underpin gamma frequency oscillatory activity within the hippocampus is the parvalbumin expressing perisomatic fast spiking basket cell. These interneurons make up ~20% of the interneurons in the hippocampus (Freund and Buzsaki, 1996), display an intrinsic resonance of about 40 Hz (Pike et al. 2000), fire an action potential at 1 per gamma cycle, display mutual inhibitory connections between basket cells, and the current sinks and sources of the gamma frequency oscillation is located in the perisomatic region (Mann et al., 2005). As basket cells can innervate ~1000 pyramidal cells they are ideally placed to synchronise pyramidal cell activities (Cobb et al., 1995).

Gamma frequency oscillations have been modelled extensively *in silico*, in order to gain further mechanistic understanding of the oscillation. Initially, in a model by Traub et al (Traub et al., 1996), the frequency of oscillations was dependent on GABA_A conductance, time delay and the driving current to interneurons. A synchronised inhibitory synaptic conductance occurs if a sufficiently large population of neurones fire within a short space of time. In this model the tonic excitatory driving current needs to be homogenous to allow synchronisation to occur and strong inhibitory synapses are required to maintain global synchronicity. The introduction of shunting inhibition between basket cells in a model of gamma frequency oscillations allows greater coherence to emerge with an increased heterogeneity in tonic excitatory drive and firing frequency (Vida et al., 2006).

Beta frequency oscillations

Beta frequency oscillations (Boddeke et al., 1997) are possibly the least well characterised of all the cholinergic induced hippocampal oscillatory activities. They are often grouped together with gamma frequency oscillations, as they are rarely observed in absence of gamma oscillations, and seem to have a similar physiology and pharmacology (Shimono et al., 2000). The functional significance of beta oscillations within the hippocampus is currently unknown. A twice gamma oscillation threshold tetanic stimulus to the CA1 region causes a shift from gamma oscillations to beta oscillations (Traub et al., 1999). This stimulation is associated with a loss of synchrony in the network, and is thought to be due to an increase in the Ca^{2+} -dependant AHP current. Subthalamic network oscillations within the beta frequency range arise during dopamine deficiency in Parkinson's disease, and these oscillations are associated with reduced movement (Levy et al., 2002).

1.3 Epilepsy

The hippocampus is able to generate oscillatory activity due the high levels of recurrent interconnectivity that is present in this area. Most of this oscillatory activity is of a physiological nature, as mentioned previously, and is associated with different states of alertness and cognitive tasks (Gray and Singer, 1989). However, pathological oscillations, such as those associated with epilepsy, can also arise from the hippocampus. The hippocampus and the entorhinal cortex play a predominant role in the causation of seizures in temporal lobe epilepsy (Goddard et al., 1969).

Epilepsy is a common major neurological disorder, affecting over 0.5 % of the world population (Kaneko et al., 2002). Epilepsy is manifest in a range of ways, stretching from absence seizures, in which patients stare vacantly, right up to tonic-clonic seizures in which patients lose consciousness and jerk violently. It was defined by Jackson (1890; see Swash 2005) as an

“episodic disorder of the nervous system arising from the excessively synchronous and sustained discharge of a group of neurones”.

Seizure activity is characterised by excessive activity of neurones in the central nervous system. The term epilepsy refers to repetitive and numerous seizures, which occur at unpredictable occasions. Seizures are characterised by excessive bursting of CNS neurones. At the cellular level, epilepsy events can be observed as paroxysmal depolarisation shifts and action potential firing in principal cells (Matsumoto and Marsan,

1964). Epilepsy can be caused by many factors, including cerebral trauma, injury, toxins, tumours, and genetic causes, whilst the cause of some idiopathic epilepsies are poorly understood.

Seizures are manifest at the EEG level as periodic large amplitude oscillatory activity known as ictal events. Ictal events are associated with repetitive firing of pyramidal cells, and the depolarisation block of interneurons (Ziburkus et al., 2006). They are manifest at the extracellular level as hypersynchronous bursting discharges as observed in figure 3.1 B. Inter-ictal events, which are characterised as single population events, are often present between these ictal events. The presence of inter-ictal events is used as a biomarker to diagnose epilepsy (Jefferys, 1993).

Particular types of epilepsy are initially characterised by the location at which the seizures are generated, and whether the seizures are localised or generalised. A degree of hyperexcitability and hypersynchrony of neurones leads to seizure generation. Hyperexcitability can occur following excessive depolarisation of neurones. Hypersynchrony can occur when too many neurones are depolarised at the same time (Najm et al., 2001). Throughout the central nervous system neurones are activated by depolarisation, and in turn innervate and depolarise other neurones. Neurones require some degree of excitability and synchronicity, as in the generation of oscillatory activity. It is the unregulated depolarisations of many neurones within a narrow time frame that leads to the generation and propagation of seizures.

The hippocampus is particularly susceptible to the generation of seizures due to the high levels of interconnectivity and excitatory synaptic transmission that occurs in this brain region (Schwartzkroin, 1993). Over half of partial epilepsies originate in temporal lobe structures (Luciano, 1993). The seizure susceptibility of the hippocampus arises due to the strong and recurrent excitatory connections between the CA3 pyramidal cells (MacVicar et al., 1982). The elements that allow physiological oscillations within the hippocampus also underlie the susceptibility of the hippocampus to pathological oscillatory activity.

The approach to treating epilepsy is to decrease the excitability and synchronicity of neurones. This is achieved mainly through two ways- a suppression of function of sodium or calcium ion channels that mediate cellular depolarisation (such as phenytoin or ethosuximide), or the enhancement of GABA receptor mediated synaptic inhibition (the use of benzodiazepines or barbituates). Other drugs such as phencyclidine, ketamine or MK-801 have anticonvulsant effects through their action as NMDA glutamate receptor

antagonists, but are not used clinically as they have psychological side effects (Krystal et al., 1994). The majority of patients with epilepsy respond well to therapy but approximately 20% of patients with primary generalised epilepsy and 35% of patients with focal epilepsy display seizures that cannot be retracted (Reutens and Berkovic, 1995; Spencer et al., 1981).

Many compounds have the potential to cause or exacerbate epilepsy, acting through the modulation of ion channels or receptors. For a drug to be pro-epileptogenic the drug must promote hyperexcitability and hypersynchrony of neurones. Both the modulation of glutamatergic and cholinergic synaptic transmission have been implicated previously in epileptogenesis (Sakai et al., 2001; Turski et al., 1989; Wong et al., 2002). The pro-epileptogenic nature of putatively cognitive enhancing drugs must be extensively investigated, as any effective cognitive enhancing strategy must not also lead to the generation of seizures.

Experimental models of epilepsy

In order to evaluate the potential of compounds to be pro- or anti-epileptogenic, several animal models are used. The *in vitro* hippocampal slice model allows the easy application of drugs at a known concentration and the manipulation of environmental factors. Several drugs and conditions are used to model the epileptic hippocampus. The models all increase the excitability of neurones and cause a synchronisation of the output of these neurones (Gulyas-Kovacs et al., 2002) and they induce ictal like and inter-ictal like activity.

The *in vitro* models used to investigate the mechanisms of epileptiform activity in this thesis include:

1. The application of the K^+ channel blocker 4-AP.
2. The application of bicuculline, a $GABA_A$ receptor antagonist.
3. The removal of Mg^{2+} from the extracellular medium to allow NMDA mediated transmission
4. The use of a combination of 4-AP and the AMPA/kainate glutamate receptor antagonist NBQX

These mechanistically distinct models of epileptiform activity were chosen as they modulate different and complementary parts of the hippocampal network. 4-AP changes the intrinsic excitability of hippocampal neurones, bicuculline removes fast GABAergic inhibitory transmission, and the zero Mg^{2+} model enhances NMDA transmission. In the combined 4-AP/NBQX model an attempt was made to isolate the interneurone network to allow the further investigations into hippocampal networks.

The 4-AP model

Inter-ictal-like activity is induced in hippocampal slices following the application of the K^+ channel blocker 4-AP. 4-AP can induce epileptiform activity *in vivo* (Szente and Baranyi, 1987) and *in vitro* (Perreault and Avoli, 1992). Application of 4-AP leads to three main actions: (1) the blockade of the fast K^+ A current (I_A) and the slower delay (D) current (I_D), increasing axonic and presynaptic excitability, and (2) direct actions on voltage dependent calcium channels (Lundh and Thesleff, 1977).

I_A is the current responsible for the fast repolarisation of the action potential after firing. At the concentrations used in this and other studies ($<75 \mu M$) 4-AP does not significantly block the I_A current (Storm, 1988). The I_D current, which is a slowly inactivating K^+ current, allows the cell to integrate synaptic inputs over tens of seconds. Without this current, inputs into the pyramidal cells quickly summate and action potentials occur (Storm, 1988). The I_{ADP} , which is the current that regulates burst firing in neurones (Brown and Randall, 2009), is increased by a reduction of I_A and I_D and the increase of the magnitude of this current leads to paroxysmal depolarising shifts at the intracellular level (Perreault and Avoli, 1991). The inter-ictal activity that is induced by application of 4-AP originates in the CA3 region and propagates to the CA1 region (Perreault and Avoli, 1992).

The bicuculline model

Bicuculline is a competitive GABA_A receptor antagonist acting at the orthosteric GABA binding site. Blockade of fast inhibition prevents feed-forward and feedback inhibition in the network and decreases the inhibitory drive to the network (Miles and Wong, 1987). Application of bicuculline leads to seizure activity *in vivo* (Ben-Ari et al., 1981). The activity induced within the hippocampal slice model is reminiscent of the inter-ictal spike activity that occurs in the epileptic EEG.

GABAergic feedback inhibition normally exerts tight control over the pyramidal cells within the CA3 region. When fast inhibition is removed by the block of GABA_A receptors recurrent synaptic connections between pyramidal cells facilitates the propagation of depolarising action potentials through the network. Following the application of bicuculline subthreshold excitatory postsynaptic potentials can trigger paroxysmal depolarisation shifts in the membrane potential (Psarropoulou and Descombes, 1999). CA3 pyramidal cells respond to mossy fibre stimulation as if the fibres were stimulated several times as opposed to the single occasion, again due to the removal of feedback and feed-forward inhibition within the network.

Methyl derivatives of bicuculline have been reported to block SK channels, which mediate the afterhyperpolarisation potential (AHP) (Khawaled et al., 1999). The AHP is responsible for spike frequency adaptation in pyramidal cells, an important regulator of excitability. The block of the AHP by bicuculline methyl derivatives would lead to an increased excitability of the network, presumably contributing to the emergence of inter-ictal-like events in hippocampus.

The low magnesium model

The removal of Mg²⁺ ions from the extracellular bathing medium of the hippocampal slice leads to the eventual emergence of inter-ictal-like events. Although low Mg²⁺ solutions would be expected to lower the firing threshold for action potentials (Hille et al., 1975), the removal of the Mg²⁺ block of the NMDA receptor is enough for the generation of synchronous activity (Traub et al., 1994). This is reinforced by the sensitivity of these events to NMDA receptor antagonists. Paroxysmal depolarising shifts, the intracellular correlate of the inter-ictal-like activity observed at the extracellular level, are observed in the CA3 pyramidal cells following the removal of Mg²⁺ ions from the bathing medium. As the low Mg²⁺ model does not directly interfere with the interneurone network, the model is useful for the study of the role of the GABA_A receptor in the generation and spread of oscillatory activity (Tancredi et al., 1990), although the effects of this receptor that are mediated through the NMDA receptor are greatly reduced following the removal of the Mg²⁺ block.

The combined 4-AP and NBQX model

The 4-AP/NBQX is a model of epileptiform activity in the hippocampus first identified by Perrault and Avoli in 1992. In this model the inter-ictal-like events induced by the

application of 4-AP described above are modulated by the application of the AMPA/kainate glutamate receptor antagonist NBQX. This model putatively isolates the interneurone network, and as such is used in this thesis to determine the effect potentially epileptogenic compounds on the interneuronal network. However, several caveats to the interpretation of the activities observed in this model need to be observed.

Initially, the concentration of 2 μ M NBQX used in this thesis may not completely block AMPA/kainate receptors. NBQX is a competitive antagonist at these receptors (Honore et al., 1988; Sheardown et al., 1990), and as 4-AP strongly increases glutamate release (Pena and Tapia, 2000; Tapia, 1996), NBQX antagonism may be overcome. Secondly, although Perrault and Avoli confirmed the necessity for GABA_A mediated synaptic transmission in their events, this does not mean the events are solely carried by the interneurone network. GABA may rather have a role in the initiation or pacing of these events as for the oscillatory activity described above. Thirdly, the important role of NMDA receptors in oscillatory activity is not considered in this model. In the interpretation of the data from the 4-AP/NBQX model these caveats will be observed and discussed.

1.4 Cognitive Enhancement

Many strategies, including the use of drugs, exercise and environmental conditions have produced measurable changes in the ability of rodents, primates and humans to complete cognitive tasks (Carey et al., 2001; Ingvar et al., 1997; Varty et al., 2000).

Cognitive deficits occur in many disorders of the central nervous system, including Alzheimer's disease, schizophrenia and in some forms of epilepsy. An attempt to delay and even reverse the cognitive decline that occurs following these disorders is an important therapeutic area for pharmaceutical companies. Drugs that increase nicotinic acetylcholine receptor function are currently used to ameliorate the cognitive and mnemonic decline in Alzheimer's disease sufferers (Newhouse et al., 1997). Memory loss in Alzheimer's disease is thought to be associated with a loss of cholinergic projections, and boosting cholinergic activity with anticholinesterase inhibitors or nAChR agonists prevents the progression of cognitive decline observed in Alzheimer's disease sufferers (Friedman, 2004). Nicotinic receptor drugs may also be useful in controlling the positive symptoms of schizophrenia (Martin et al., 2004). Unfortunately, nAChR agonists can promote epileptiform activity (Roshan-Milani et al., 2003), and so other strategies to promote cognitive function are currently under investigation.

The enhancement of glutamatergic function has also long been associated with enhancing cognition. The enhancement of both NMDA and non-NMDA mediated excitatory transmission causes cognitive enhancement in animal models (Kandel, 1997; Lynch, 2002). As mentioned above, the NMDA receptor mediates one form of LTP. LTP is understood to be the cellular basis of memory formation (Kandel, 1997). The blockade of NMDA receptors by MK-801 or ketamine leads to impairment of memory formation (Sharma and Kulkarni, 1991). The use of positive modulators of AMPA receptors, known as ampakines, leads to cognitive enhancement in rodents and humans (Hampson et al., 1998; Ingvar et al., 1997; Ito et al., 1990).

The activation of mAChRs has been reported to be pro-cognitive. Activation of mAChRs can facilitate memory formation (Markram and Segal, 1990). Conversely the mAChR antagonists atropine and scopolamine are known to prevent memory storage in rodents (Blozovski et al., 1977; Grauer and Kapon, 1996) and humans. A partial agonist of the M₁ receptor, sabcomeline, improves the reversal learning of primates (Harries et al., 1998). Also, application of a M₂ mAChR antagonist, which causes dose-dependent increases in acetylcholine release, leads to improvements in passive avoidance tasks and working memory in primates.

The enhancement of oscillatory activity has been implicated in cognitive enhancement. Carbachol can enhance LTP through cholinergically induced oscillations (Huerta and Lisman, 1993), but this effect is abolished following the knock-out of the M₁ mAChR (Shinoe et al., 2005). As noted above, agonists of mAChRs induce gamma frequency oscillatory activity (Fisahn et al., 1998). Following the genetic depletion of the M₁ subtype of mAChR gamma frequency oscillations are not induced by mAChR agonists (Fisahn et al., 2002). Gamma frequency oscillations are associated with cognitive function and aberrant gamma frequency oscillations are associated with schizophrenia (Tallon-Baudry and Bertrand, 1999). Consequently the M₁ subtype mAChR is a potential target for cognitive enhancing strategies.

Aside from the use of nootropic drugs, some environmental conditions can lead to the enhancement of cognition in rodents. The environmental enrichment protocol causes spatial re-mapping in the hippocampus, and leads to behavioural changes and improvements in cognitive function.

1.4.1 Putative cognitive enhancers

The M₁ mAChR agonist 77-LH-281

The compound used in this thesis to investigate the role of M₁ receptor in physiological oscillatory activity, epileptogenesis and the possible enhancement of cognition is 77-LH-281. This is an allosteric full agonist of M₁ receptors (Langmead et al. 2008). 77-LH-281 is a chemical analogue of AC-42, which binds to an ectopic site on the M₁ muscarinic acetylcholine receptor (Langmead et al., 2006). This site is thought to be located in the N-terminus/TM1 and the third outer loop/TM7 domains of the M₁ receptor (Spalding et al., 2002), away from the orthosteric acetylcholine binding site located in TM3. In contrast, N-desmethylclozapine, a clozapine metabolite with affinity for the M₁ receptor, occupies a binding site that overlaps the orthosteric binding site of the M₁ mAChR (Spalding et al., 2006).

Activation of the M₁ receptor by carbachol (Marino et al., 1998) and N-desmethylclozapine (Sur et al., 2003) potentiates NMDA receptor currents in CA1 pyramidal cells. As NMDA receptor mediated currents are responsible for one form of LTP enhancement this potentiation may increase mnemonic function and enhance cognition. M₁ mAChR agonists have also been implicated in the treatment of Alzheimer's Disease (Fisher et al., 1996). It is interesting therefore to investigate the potential of 77-LH-281 to enhance cognitive function, and attempt to assess the potential unwanted effects of this agonist in epileptiform models.

Ampakines

Aside from muscarinic acetylcholine receptor agonists, another class of nootropic drug are ampakines. Ampakines are positive allosteric modulators of AMPA type glutamate receptors (Arai and Kessler, 2007). Different ampakines exert their effect through decreasing desensitisation of AMPA receptors, lengthening open times in response to agonist application, improving the binding of glutamate to AMPA receptors and increasing the conductance of the AMPAR channel. Therefore in the presence of ampakines fast glutamatergic transmission is more efficient and a similar release of glutamate will cause a greater depolarisation of the postsynaptic membrane potential than in the absence of ampakines. As ampakines enhance excitatory glutamatergic transmission, they can facilitate synaptic plasticity and enhance learning (Lynch, 2004).

There are two major structural classes of ampakines, both of which positively modulate AMPAR transmission but have different effects on the AMPA mediated current.

Benzothiazides, which include the drugs cyclothiazide and IDRA-21, one of the earliest ampakines identified, block the desensitisation of AMPA receptors (Xia and Arai, 2005) but they have little effect on the deactivation of AMPA receptors. Deactivation and desensitisation of AMPA receptors occurs on a time scale fast enough to affect the excitatory postsynaptic current (Lynch, 2004).

Benzamide drugs have effects on the open times and conductance of AMPA receptors. They all reduce the deactivation kinetics of AMPA receptors and they slow the rate at which the synaptic responses decay (Arai et al., 2004; Nagarajan et al., 2001). However, different compounds have different actions depending on the chemical structure of the ampakine. For example CX546 has been shown to greatly prolong the decay of AMPA receptor mediated excitatory postsynaptic currents (EPSCs) but has little effect on the amplitude of the EPSC (Nagarajan et al., 2001). In contrast, CX516 increases the amplitude of the excitatory post-synaptic current but has a much smaller effect on the rate of decay of synaptic responses (Arai et al., 2004). The concentration of CX516 needs to be much higher (within the millimolar range) to observe this effect on EPSC decay time than the effect on response amplitude. CX691 also increases the amplitude of the EPSC, and is 20-50 times more potent than CX516 (Johnson et al. 1999).

As well as effects at the cellular level, ampakines have effects at the synaptic level. At the Schaffer collateral-CA1 pyramidal neurone synapse, application of some ampakines increases the amplitude of fEPSPs. Under an LTP paradigm, application of ampakines facilitates the induction of LTP *in vivo* (Staubli et al., 1994) in response to theta burst stimulation. Depending on the specific ampakine, the effect on LTP can vary *in vitro*. Application of CX546 increases the amplitude of LTP whereas cyclothiazide does not. Both CX546 and cyclothiazide lower the threshold for LTP induction.

In a model of epileptiform activity in which inter-ictal-like events are induced by the removal of Mg^{2+} ions from the extracellular bathing medium, subsequent application of the ampakine cyclothiazide causes a significant increase in the length of defined seizure-like events in hippocampal slices (Lasztocki and Kardos, 2006). Cyclothiazide also produces epileptiform activity in hippocampal cultures and *in vivo* (Qi et al., 2006). This effect is partially due to the effect of cyclothiazide blocking GABA_A receptors (Deng and Chen, 2003), much like the bicuculline model of epileptiform activity described above. The other classes of ampakines, which do not delay receptor desensitisation but do increase the

AMPA receptor open time or EPSP amplitude, may be less prone to the generation of epileptiform activity in the hippocampus as the receptor can still desensitise under high levels of stimulation. They are more specific for the AMPA receptor than cyclothiazide as they have little affinity for the GABA_A receptor.

1.4.2 Environmental Enrichment

Environmental enrichment and cognitive enhancement

An enriched environment is an environment that exposes animals to a spatially complex inanimate stimulation and increased social contact. Hebb (1949) noticed rats raised in his home performed better in cognitive tasks than rats raised in the lab, indicating that increased stimuli at home could be responsible for this effect (Toscano et al., 2006). As such environmental enrichment is a model of cognitive enhancement as animals perform better than control rats in a number of measurements of cognitive ability. This is mediated through the modulation of the structure and growth of neuronal cells (Nilsson et al., 1999). Such changes may be responsible for the increase in the synaptic strength of the perforant path in the hippocampi of animals exposed to an enriched environment. Environmental enrichment can also induce the production of new neurones, which occurs, amongst other areas, within the subgranular layer of the dentate gyrus in the hippocampus. Neurogenesis and gliogenesis (the production of new neuronal and glial cells respectively) is known to occur at levels five times greater in animals in the enriched environment than in control animals. However, neurogenesis is not required for the behavioural effects observed in animals exposed to the enriched environment (Meshi et al., 2006).

Environmental enrichment can also ameliorate cognitive deficits induced by a number of conditions (Guilarte et al., 2003; Toscano et al., 2003) including developmental lead exposure and exposure to prenatal ethanol.

It is known that changes in the expression of genes occur following exposure to an enriched environment (Rampon et al., 2000). It was therefore decided to investigate the changes that occur at the global proteomic method using a gel electrophoresis approach combined with mass spectrometry to identify the specific protein changes that occur following environmental enrichment. This approach allows measurement of changes at the proteome level that underlie the improvement in cognitive function. Possible future therapeutic targets for nootropic drugs and biomarkers for the protein changes that occur following cognitive enhancement may be elucidated using this approach.

Expression of MeCP2 and environmental enrichment

Rett syndrome is a postnatal developmental disorder within the autism spectrum affecting the development of 1 in 10000 girls aged 6-12 months. The disorder is due to mutations in a gene called *MECP2* that encodes for a Methyl-CpG binding protein that regulates gene expression. It consists of a methylated CpG binding domain, a transcriptional repression domain and a C-terminal domain, as well as a pair of nuclear localisation signals (Chahrour and Zoghbi, 2007). MeCP2 is postulated to be a transcriptional repressor, because when it binds to CpG dinucleotides it recruits the co-repressor Sin3a and histone deacetylases 1 and 2. Environmental enrichment induces histone modification and inhibitors of histone deacetylases have been shown to restore learning and memory (Fischer et al., 2007). This leads to the compacting of chromatin, which prevents promoter regions binding and gene expression to occur. Aberrant, mosaic expression of MeCP2 leads to mental and physical abnormalities with neurones encoding the mutant protein displaying the mutant phenotype. This is not a neurodegenerative disorder as the neurones do not die, but it is rather a neurodevelopmental disorder. Recently it was shown (Guy et al., 2007) that this phenotype can be reversed in a mouse model of Rett syndrome following the conditional re-expression of wild-type MeCP2. One of the target genes for MeCP2 is the gene encoding brain-derived neurotrophic factor (BDNF), a protein critical for the formation and maintenance of long term potentiation (Kang et al., 1997), a cellular mechanism implicated in the genesis of memory. A lack of activity dependent transcription of BDNF has been postulated to be one of the underlying causes of the Rett syndrome phenotype. As a decreased level of MeCP2 in the brain leads to cognitive impairment, likewise it is possible that an increased level of MeCP2 may occur in the environmental enrichment model of cognitive enhancement. Several previous studies have investigated the effect of environmental enrichment alleviating the symptoms of Rett syndrome (Kondo et al., 2008; Nag et al., 2009). Therefore it is worthwhile investigating the expression of MeCP2 following exposure to an enriched environment.

1.5 Aims

In this project there are three main aims:

1. To investigate the effect of putative nootropic compounds, mAChR agonists and ampakines, on physiological and pathophysiological network properties of the hippocampus.

2. To gain mechanistic insight into the networks that underlie the oscillatory activity induced by the application of these nootropic compounds.
3. To investigate the change in expression of putative cognition related proteins following exposure to an enriched environment

A range of pharmacological, physiological and proteomic approaches are used to investigate these cognitive enhancing strategies. Insight into the effect of these strategies on hippocampal networks and protein expression will enable the evaluation of each strategy and allow further development of the field of cognitive enhancement.

2 Materials and Methods

2.1 In vitro Hippocampal Slice Experiments

2.1.1 Hippocampal Slice preparation

Animals were supplied by Harlan UK Ltd. and housed in group cages under controlled environmental conditions (temperature 19-23°C, 12hr light/dark cycles). Animals had *ad libitum* access to food and water.

Male Wistar rat (3 weeks) were cervically dislocated and decapitated in accordance with UK home office guidelines under the authority of the UK Animals (Scientific Procedures) Act, 1986. A scalpel was used to make an incision along the middle of the skin on the top of the head, revealing the skull. Ice-cold (0-4°C) ACSF (composition (mM) NaCl 124, KCl 3, NaHCO₃ 26, NaH₂PO₄ 1.25, MgSO₄ 1, D-glucose 10 and CaCl₂ 2) was then poured over the skull to wash away excess blood and to cool the brain. Incisions were then made at either side of the neck bones using sharp dissecting scissors and the skull was cut from back to front along the midline to reveal the brain. The sides of the skull were pulled back and the brain placed into ~70 ml of ice cold ACSF using a small spatula. The cerebellum and pre-frontal cortex was then removed and the brain was hemisected in the sagittal plane down the midline. Depending on the orientation of slice required, the brain was glued onto a wax block using cryoacrylate adhesive at the back of the brain on the cut that the cerebellum had been removed with for coronal sections, or on the sagittal plane of the midline for horizontal sections. Slices were cut to a thickness of 450 µm using a vibrating microtome (Campden Instruments, UK) in ice cold ACSF, the hippocampus removed and the hippocampal slices transferred to an interface holding chamber containing room temperature oxygenated (95% O₂/ 5% CO₂) ACSF (23°C) using a large bore pipette. The slices were maintained at room temperature and allowed to recover for 1 hour before use.

2.1.2 Electrophysiology

2.1.2.1 Recording set-up

The recording chamber (Digitimer Research Instruments, UK), microscope (Koyawa, Japan) and manipulators holding recording and stimulating electrodes were all mounted on a pressure sensitive anti-vibration table (Intracel, U.K) surrounded by a Faraday cage. All of the remaining electrical recording equipment, including an Axoclamp 2B current and voltage clamp analyser (Molecular Devices, USA), a signal processor (Brownlee precision 440, Brownlee, USA), Humbug noise subtraction device (Quest Scientific), analogue-to-

digital converter (Digidata 1320 series, Molecular Devices, CA) and PC, were mounted on racks out side of the Faraday cage.

An interface type chamber (Digitimer Research Instruments, UK) was chosen for extracellular and intracellular recordings. This consisted of 2 separate 15 mm diameter chambers in which the slices were placed on nylon netting and a 1 cm² piece of lens tissue (Whatman, UK). The slices were kept in a warm, humidified oxygen enriched atmosphere at the interface of warmed ACSF. The ACSF was perfused at a rate of ~2 ml/min using a peristaltic pump (Gilson, France).

Recording electrodes for extracellular and intracellular recordings were pulled from standard-wall (1.2 mm external diameter/0.69 mm internal diameter) borosilicate glass capillaries on a Brown and Flaming-type horizontal electrode puller model P-87 (Sutter Instruments, USA). Extracellular recording electrodes were pulled to a standard D.C. resistance of <1 M Ω and filled with ACSF. Intracellular recording electrodes were pulled to a resistance of between 80-120 M Ω and filled with 3M potassium methyl sulphate and 2% Neurobiotin (Vectastain, US if the cells were later to be processed for morphology).

Filled electrodes were then mounted into electrode holders, where the filling solution came into contact with silver chloride-coated silver wire. The electrode was then inserted into a unity-gage head stage (current gain 0.1: Axon Instruments) and connected to the Axoclamp 2B amplifier. A silver chloride-coated silver reference electrode connected to the head stage was placed into the bath.

Nickel/chromium bipolar stimulation electrodes were constructed from 2 lengths of 0.05 mm diameter nickel/chromium (80%/20%) wire, twisted together and cut at the tip to allow focal stimulation. An isolated stimulator box (Digitimer Ltd., England) provided electrical stimulation, triggered by the output of the Digidata from the P.C. All stimulating and recording electrodes were mounted on micromanipulators (Narishinge MC35, Japan). This allowed for precise electrode placement as the electrodes could be moved in a coarse or fine manner in all axes.

2.1.2.2 Extracellular Field Recordings

These experiments were performed in an interface recording chamber, using ACSF-filled microelectrodes with a resistance of <1 M Ω .

Spontaneous emergent network activity

In order to assess the effect of compounds on the emergent activity of neuronal networks, extracellular recordings were made, in the majority of slices, from the CA3 region of the hippocampus. This configuration allows the effect of compounds on populations of cells to be examined. 1 hour after hippocampal slices were made, slices were then transferred to the recording chamber and allowed to equilibrate from room temperature to the recording chamber temperature (34 ± 1 °C).

The recording electrodes were then gently placed in contact with the surface of the hippocampal slice, close to the *stratum pyramidale* towards the *stratum radiatum* within the CA3 area. The slices were then covered to retain the humidity of the chamber using a glass slide, preventing the slice from drying. Positive and negative trace deflections as measured by the extracellular field electrodes in the external space were the indication of synchronous population activity. These trace deflections were then amplified 2000 times by a Brownlee 440 signal processor, either in one operation or in 2 stages of 10 and then 200 times amplification. The recordings were band pass filtered at 1 to 1 kHz to remove extraneous noise and 50 Hz line frequency noise was subtracted using a humbug device (Quest Scientific, Canada). This processed analogue signal was then digitised using a Digidata 1320A converter at 10 kHz, and then fed to a P.C. to be captured on hard disk using pClamp 8.0 software (Axon Instruments, Union City, CA, USA).

Evoked field excitatory post-synaptic potential (fEPSP) recordings

Extracellular recordings were made in the CA1 region of the hippocampus. Recording electrodes were placed onto the stratum radiatum of the hippocampus. Stimulating electrodes were placed on the Schaffer collaterals and a stimulus was given at 20 s intervals. The fEPSPs were recorded at a rate of 20 kHz and the data were captured using WinLTP software. The stimulus consisted of a square wave pulse of 100 μ s duration and 0-30 mA constant current amplitude, to generate a half-maximal response for each experiment.

2.1.2.3 Intracellular current clamp recordings

For intracellular recordings, electrodes (80-120 M Ω) were filled with 3 M potassium methyl sulphate using a 0.2 μ m syringe filter. The electrodes were pulled to a fine point to

allow minimal damage to the pyramidal cells upon entry. Intracellular recordings were made from the *stratum pyramidale* of the CA1 region of the hippocampus.

The pyramidal cells were impaled by advancing the recording electrode through the CA1 stratum pyramidale using a Narishige (MC35, Japan) water hydrolic drive. Square negative current pulses (0.1 nA) were applied through the recording electrode to provide an indication of when the tip was approaching a cell membrane, signified by an increase in resistance and a consequent increase in the voltage response to the current pulse. When the tip of the electrode was touching the cell membrane, an oscillatory 'buzz' was applied to break into the cell. The cellular response to 500 ms 0.1 nA positive and negative current steps was assessed, before the application of a 60 s bolus of the compound of interest was added. The membrane potential was continuously recorded for 30 s before and 4-6 mins after the application of the 60 s bolus in current clamp bridge mode. The cellular response to 500 ms 0.1 nA positive and negative current steps was assessed again.

2.1.2.4 Data analysis

For the extracellular recordings of drug-induced emergent network activity frequency analysis was performed after 30 mins drug application. For network oscillations of the delta, theta, beta, gamma types and ictal-like events, 5 s epochs of trace were randomly selected within the 30th minute and power spectral analysis was performed on the trace. For inter-ictal-like events, the frequency of events over 1 minute of recording was determined. For the 4-AP/NBQX induced slow inter-ictal-like events, the frequency of events over 5 minutes of recording was determined due to the inherent infrequent nature of these events.

For the EPSP recordings, the mean amplitude of 15 events (over 5 minutes) 30 minutes after drug application was used to determine drug effects.

For the intracellular current clamp recordings, the input resistance was measured using hyperpolarising 0.1 nA current injections and measuring the change in the membrane potential just prior to, and 5 minutes after drug application. Membrane potential was also determined just prior to and 5 minutes after drug application.

Comparisons between the effect of drugs on membrane potential and input resistance were made using paired Student's T test. Comparisons between the effect of drugs on fEPSP amplitude and inter-ictal-like event frequency were performed using Wilcoxon signed rank paired non-parametric tests. Tests were performed using GraphPad Prism software, and

significance was assumed at $P < 0.05$, denoted by * in the figures. $P < 0.01$ is denoted by **, and $P < 0.001$ by ***.

2.2 Environmental Enrichment experiments

The following methods are reproduced in the methods section of the paper referred to in the appendix (McNair et al. 2007).

2.2.1 Tissue Preparation

2.2.1.1 Animals

Animals were supplied by Harlan UK Ltd. and housed in group cages under controlled environmental conditions (temperature 19-23°C, 12 hr light/dark cycles). Animals had *ad libitum* access to food and water. At three weeks of age the environmental enrichment protocol was initiated. Animals were transferred to black Perspex cages (100 x 50 x 60 cm) containing several novel objects including tubes, a running wheel, ladders, platforms and beams, as well as food corner, a suspended water bottle, and sawdust base. The enrichment objects were rearranged every 3 days to ensure a degree of spatial novelty. The animals in the poor environment had none of the novel enrichment objects. The enrichment protocol lasted for 6 weeks, and each of the cages contained 6 animals.

2.2.1.2 Tissue extraction

After 6 weeks of the environmental enrichment protocol, the animals were killed by cervical dislocation followed by decapitation in accordance with local ethical guidelines and U.K. legislation. Brains were rapidly transferred to ice cold (0-3°C) oxygenated ACSF. Hippocampi were dissected free, snap frozen in liquid nitrogen and stored at -80°C until required.

2.2.2 DiGE experiment

For each individual protein sample the CA1 region from three to four hippocampal slices were pooled and lysed in 150 µl of buffer containing 10 mM tris pH 8, 5 mM magnesium acetate, 8 M urea and 2 % ASB14. Lysed tissue was then subjected to five freeze thaw cycles and left at room temperature for 1 hour to aid solubilization of proteins. Samples were subsequently sonicated (4 x 4 minute cycles, with 2 minutes between each cycle to prevent overheating) and centrifuged at 13,000 r.p.m. for 15 minutes. Following sample

clean up using an ammonium precipitation, protein pellets were re-suspended in approximately 70 μl of lysis buffer and protein concentration determined using Pierce's BCA Protein assay kit.

2.2.2.1 Protein concentration determination

Sample protein concentration was determined using a Pierce BCA (bicinchoninic acid) protein assay reagent kit (Pierce, U.S.A.) using the microplate protocol. A BSA standard curve was produced using the protocol with a working range of 20-20000 $\mu\text{g/ml}$, diluted using the lysis buffer. The following dilutions were used:

Volume of Diluent	Volume and Source of BSA	Final BSA Concentration
0	300 μl of Stock	2000 $\mu\text{g/ml}$
125 μl	375 μl of Stock	1500 $\mu\text{g/ml}$
325 μl	325 μl of Stock	1000 $\mu\text{g/ml}$
175 μl	175 μl of vial B dilution	750 $\mu\text{g/ml}$
325 μl	325 μl of vial C dilution	500 $\mu\text{g/ml}$
325 μl	325 μl of vial E dilution	250 $\mu\text{g/ml}$
325 μl	325 μl of vial F dilution	125 $\mu\text{g/ml}$
400 μl	100 μl of vial G dilution	25 $\mu\text{g/ml}$
400 μl	0	0 $\mu\text{g/ml}$ = Blank

Table 1. Preparation of Diluted Albumen (BSA) standards

The working reagent was then prepared in excess according to the protocol. 3 samples per replicate were used, with a 1 in 10 dilution (10 μl in 100 μl lysis buffer) to preserve the protein extract. 25 μl of each BSA dilution or sample and 200 μl working reagent was added to each well, mixed on a plate shaker for 1 minute, and incubated at 37 $^{\circ}\text{C}$ for 30 minutes in a water bath. The plate was allowed to cool to room temperature and the absorbance was measured using an Opsys MR plate reader (Dynex Technologies, U.K.) and Revelation Quickline software (version 4.03, Dynex Technologies, U.K.) at a wavelength of 562 nm. The standard curve was plotted automatically using a quadratic curve fit and the concentration of each unknown standard was obtained from this curve.

2.2.2.2 Sample CyDye labeling

The experiments detailed below (until section 2.2.3) were performed by K.M McNair. Fifty micrograms of each protein sample was labeled with 400 pmol of either Cy2, 3 or 5 according to the manufacturer's instructions (GE Healthcare, Amersham, Little Chalfont, UK). Treatment samples were assigned randomly across six to eight gels. Prior to the 1st

dimension Cy2, 3 and 5 samples were pooled and added to the same volume of 2× sample buffer containing 8 M urea, 2 % ASB14, 20 mg/ml DTT and 2 % IPG buffer and then corrected to a final volume of 450 µl using rehydration buffer (8 M urea, 2% ASB14, 2 mg/ml DTT and 1% IPG buffer).

2.2.2.3 2D gel electrophoresis

The 1st dimension of the 2D gel electrophoresis process was performed using the rehydration method (Rabilloud et al., 1994). Isoelectric focusing was carried out on pH 3–10 non-linear (NL) 24 cm IPG strips. The second dimension was run on 12.5%, homogenous polyacrylamide gels poured between low fluorescence glass plates (GE Health Care). Gels were scanned immediately after the running of the second dimension on a Typhoon™ 9400 variable mode imager.

2.2.2.4 DiGE gel analysis

Gel images were analyzed in differential in-gel analysis (DIA) mode in DeCyder software with spots displaying greater than 1.5-fold change in spot density being tentatively defined as being differentially expressed. All experiments incorporated a Cy2 internal standard. Following gel-to-gel matching of spots, statistical analysis (Student's t-test) of normalized protein abundance changes between samples was performed using a BVA software module as described (Alban et al., 2003).

2.2.2.5 Spot picking and mass spectrometry analysis

Protein spots shown to be significantly different ($P < 0.05$) from control following treatment were picked, digested (Porcine trypsin 0.2 µg, Promega, UK) and spotted onto a Voyager DE-Pro Maldi-Tof target plate for subsequent mass spectrometry analysis (Perceptive Biosystems, CA, USA) using the Ettan Spot Handling Workstation (GE Health Care). Maldi-Tof mass spectrometry was performed in positive reflector mode using a laser setting around 2350. The low mass gate setting was set at 750 Da, and the spectra were acquired over a range of 750–3500 Da. The accelerating voltage was 20 kV, the grid voltage set to 76 % and the guide wire voltage set to 0.006 %, with an extraction delay time of 160 ns. One hundred shots per spectrum were collected, with a combination of three spectra per spot.

Spectra were then exported to Data Explorer™ (version 4, Applied Biosystems, Cheshire, UK) where they were internally calibrated using the 842.5099 and 2211.1046 trypsin peaks, processed to reduce background noise, and a monoisotopic peak list was generated and entered into the Mascot peptide mass fingerprint (PMF) database. Data were searched using the NCBI Inr database.

Those peptide mixtures that were unidentified by Maldi-Tof analysis were sent for tandem MS analysis. Tryptic peptides were solubilized in 0.5 % formic acid and fractionated by nanoflow HPLC on a C18 reverse phase column, eluting with a continuous linear gradient to 40 % acetonitrile over 20 min. The eluate was analyzed by online electrospray tandem mass spectrometry using a Qstar Pulsar (Applied Biosystems). Mass spectrometric analysis was performed in IDA mode (AnalystQS software, Applied Biosystems), selecting the four most intense ions for MSMS analysis. A survey scan of 400–1500 Da was collected for 3 s followed by 5 s MSMS scans of 50–2000 Da using the standard rolling collision energy settings. Masses were then added to the exclusion list for 3 min. Peaks were extracted using the Mascot script (BioAnalyst, Applied Biosystems) and automatically exported to the Mascot (Matrix Science, London, UK) search engine.

For both the PMF and MS/MS searches, proteins were matched with the identified peptides and each protein was assigned a Mascot score, which was a probability-based Mowse score (Perkins et al., 1999). In the case of PMF the significance threshold was 62, and in the case of MS/MS this threshold was 36.

2.2.3 Western Blotting

Both 1D and 2D western blotting techniques were used to analyse the expression of proteins identified. For each hippocampus 600 µl of ASB14 lysis buffer was added and the tissue was ground in a 1.5 ml centrifuge tube using a plastic pestle. Samples were then freeze-thawed five times in liquid nitrogen and a water bath heated to 30°C. The samples were then left at room temperature for 1 hour to aid solubilisation before 4 cycles of 4 minutes sonication, with one minute between cycles. The samples were then centrifuged at 13000 rpm for 15 minutes on a lab bench centrifuge (MSE microcentaur, Scotlab, UK) and the supernatant collected, before 10 µl was removed to determine the protein concentration (see above).

2.2.3.1 1D Western Blotting techniques

Samples of 25 µl containing 30 µg protein, 10 % sample reducing agent and 25 % loading buffer (Invitrogen, U.K.) were loaded into each well of a pre-cast 4-10 % 12-well sodium dodecyl sulphate polyacrylamide gel electrophoresis (SDS-PAGE) gel (Invitrogen, U.K.) to separate the proteins by charge. One lane contained rainbow markers (Amersham, U.K.). Five replicates for each sample were loaded onto the gel. The gels were placed in gel tanks and covered in NuPAGE MOPS 1x running buffer (Invitrogen, U.K.) containing 0.25 % NuPAGE antioxidant (Invitrogen, U.K.). The remainder of the gel tank was filled with 1x MOPS running buffer containing antioxidant. The gels were run at 200 V for 60 minutes or until the gel front was close to the base of the gel.

2.2.3.2 2D Western Blotting techniques

Gel loading

The protein mixtures were initially separated for their charge using isoelectric focusing on Amersham's Ettan™ IPGphor™ system. Samples were run on 7 cm non linear 3-10 immobilised pH gradient (IPG) Dry Strip gels, using the rehydration method (Rabilloud et al, 1994). For rehydration loading, 75 µg protein was added to a total volume of rehydration buffer (8 M urea, 2% ASB14, 5 mg/ml DTT, 0.5% IPG buffer) to a total volume of 125 µl. Dithiothreitol (DTT) and non-linear pH 3-10 IPG buffer were added fresh to the rehydration buffer prior to the 1st dimension run.

1st Dimension run

This mixture was spread evenly along the base of a 7 cm ceramic IPG strip holder and the strip was placed gel side down onto the sample mixture. The strip was placed ensuring that no bubbles were present between the strip and the coffin, with the anodic end of the strip placed towards the pointed end. 300 µl of silicone oil (Dry strip cover fluid, Amersham Biosciences, U.K.) was pipetted over the top of the IPG strip and the coffin lid replaced, to prevent the strip from drying out. The IPG strip was positioned to ensure that both the electrodes in the holder were touching the strip, and the holder itself made contact with the anode and cathode of the IPG-phor. Samples were run using a pre-set 7 cm program:

Step 1	Step and hold	30 V	14 h or 420 VHrs
Step 2	Step and hold	500 V	1 h or 500 VHrs
Step 3	Step and hold	1000 V	1 h or 1000 VHrs
Step 5	Step and hold	5000 V	4 h or 20000 VHrs

at 20°C and 50 mA per gel.

Successful 1st dimension runs were considered to be runs in which the total volt hours exceeded 20000 Vh on the IPG-phor reader. The strips could then be used immediately or stored at -80°C for up to 3 months.

2nd Dimension- Equilibration and run

The strips were used immediately after the 1st dimension run or used straight from -80°C freezer, to prevent migration of the proteins. Strips were placed in plastic falcon tube containing 4 ml of equilibration buffer 1 (containing DTT) for 13 minutes and shook gently at room temperature. The buffer was removed and immediately replaced with 4 ml of equilibration buffer 2 (containing iodoacetamide), and the strips were again gently shook for 13 minutes at room temperature. Buffer 1 preserved the fully reduced state of the proteins, whereas buffer 2 prevented reoxidation of the thiol groups by alkylation, and thus preventing gel distortion. Equilibrated IPG strips were then run on pre-cast 12 % single well sodium dodecyl sulphate polyacrylamide gel electrophoresis (SDS-PAGE) gels (Invitrogen, U.K.) to separate the proteins by charge. The gels were placed in gel tanks and the covered in NuPAGE MOPS 1x running buffer (Invitrogen, U.K.) containing 0.25 % NuPAGE antioxidant (Invitrogen, U.K.). The remainder of the gel tank was filled with 1x MOPS running buffer containing no antioxidant. The strips were placed with the (anode/cathode) to the left-hand side of the gel, ensuring there were no air gaps between the strip and the gels. 0.5 ml of agarose sealant solution was then pipetted over the length of the strip to ensure contact was maintained with the SDS-PAGE gel. The gels were run at 200 V for 60 minutes.

2.2.3.3 Gel Transfer

The proteins from the gels were immediately transferred onto a 0.45 µm pore size PVDF membrane. The components for the membrane transfer were all soaked in NuPAGE

transfer buffer containing 10 % Methanol, for 10 minutes prior to use. The PVDF membrane was initially soaked in pure methanol to enhance hydrophobic protein transfer. The NuPAGE transfer cassette (Invitrogen, U.K.) was assembled as the manufacturer's instructions. The gel was removed from its casing and placed onto a piece of buffer-soaked filter paper, on top of several blotting sponges inside the cassette. The PVDF membrane was then placed on top of the gel followed by another piece of filter paper and several blotting sponges. The blot cassette was filled with clean transfer buffer containing 0.1 % antioxidant and the rest of the module was filled with water. The transfer was run at 30 V for 1 h and at room temperature.

2.2.3.4 Blocking

The PVDF membrane was removed from the blot cassette and washed briefly in distilled water. The membrane was then placed in ~10 ml 3% milk TBST solution for 2-3 h at room temperature. The membrane was placed on a plate shaker to gently wash the membrane. Blocking times were increased for antibodies that gave high background staining (indicated in figures).

2.2.3.5 Primary antibody incubation

Following blocking, the membranes were transferred to a plastic wallet containing 2 ml of the primary antibody at the correct dilution, diluted in 1 % milk TBST solution. The wallet was sealed, ensuring there were no air bubbles, and the wallet was placed onto a vibrating shaker overnight (~14 h) at 4°C. The following morning the membrane was removed from the wallet and washed 4x for 10 minutes in TBST.

2.2.3.6 Secondary antibody incubation

The membrane was then transferred to a second plastic wallet, containing 2 ml of the relevant secondary antibody conjugated to horseradish peroxidase enzyme (HRP) at a concentration of 1:1000. The antibody was diluted in 1% milk TBST solution. The wallet was again sealed and placed on a vibrating shaker at room temperature for 1 h. After this the membrane was removed from the wallet and washed 4x in TBST for 10 minutes before being revealed.

2.2.3.7 Protein detection using enzyme chemi-luminescence (ECL)

Following the final TBST wash, the membrane was blotted to remove excess moisture. 5 ml of a 40:1 mix of Amersham ECL Western Blotting Detection System (Amersham, U.K.) buffers A and B was then placed over the membrane, and the membrane was shook gently for 5 minutes. Excess buffer was blotted off the end of the membrane, and the membrane was then placed into a clear plastic envelope and inside a dark box (Amersham, U.K.).

2.2.3.8 X-ray film development

The membrane inside the development box was then taken to a dark room to reveal the location and intensity of the protein of interest. Amersham Hyperfilm (Amersham, U.K.) was placed over the membrane and the box closed. The film was left in the box for between 10 s and 5 minutes depending on the strength of the signal, and the film was then developed using a Kodak X-OMAT 1000 machine (Kodak, U.K.).

2.2.3.9 Analysis

As several protein spots were revealed on each membrane, some due to non-specific antibody staining, there was a need to ensure the protein spot identified was the protein of interest. The protein spots were initially compared to known protein band sizes to observe the size migration of the protein. For the 2D western blots the proteins were then checked to establish whether the spots were at the correct pH position in the 1st dimension. The 1D western blots were scanned with a Canon LiDE scanner and band intensity quantified using a 1D gel analysis programme within the Totallab v2003 image analysis software package (Nonlinear Dynamics Ltd, Newcastle upon Tyne). Data were analysed using Student's T test and refutation of the null hypothesis taken as $p < 0.05$.

2.3 Compounds

All drugs were purchased from Sigma, (4-aminopyridine, oxotremorine-M, 2-AP5, CX546), Tocris Bioscience (bicuculline methochloride, kainate, NBQX, atropine) or were kind donations from GlaxoSmithKline (77-LH-281, CX691, MT-7). All drugs were stored as 10 mM stock solutions in H₂O or DMSO at -20 C and dissolved on day of use.

3 The effect of slice orientation on emergent oscillations

3.1 Introduction

The emergent network properties of neuronal networks will depend upon many factors but one of the principal factors amongst these is the underlying circuitry that is present in the network. Although hippocampal slices retain much of the network within the slice differences in the circuitry of a particular slice will be apparent depending on the orientation in which the slice is made. As such different slices may show different preferences for particular emergent activities.

In this chapter the effect of the orientation of the hippocampal slice on patterns of displayed oscillatory activity is investigated. Two orientations were investigated; the sagittal orientation, in which slices were made parallel to the midline of the brain; or the coronal orientation, in which slices were made along the long axis of the hippocampus.

There are several types of oscillation that were obtained during the data collection for this thesis, both physiological oscillations and pathophysiological oscillations (see fig 3.1.A). Gamma oscillations (Traub et al., 1998) are thought to occur during the processing of incoming sensory signals (Gray and Singer, 1989) and were manifest as continuous low amplitude oscillatory activity in hippocampal slices. Beta frequency oscillations (13-29 Hz) were also characterised by continuous oscillatory activity and also occur during mental activity. These fast oscillations are thought to be responsible for the binding of different sub-regions of the brain together (Engel et al., 1991). Theta frequency oscillations are involved in exploratory behaviour *in vivo* (Buzsaki, 2002; Vanderwolf, 1969), and these oscillations observed in the EEG are mimicked in hippocampal slices by the application of, amongst other things, carbachol (Williams and Kauer, 1997). Slower, continuous oscillations, of a frequency of <4 Hz were also observed on occasion. These oscillations were designated delta frequency oscillations and were identified as a sinusoidal waveform, as for the oscillatory activity detailed above.

The other oscillations observed throughout this thesis were likely to be indicative of pathophysiological states in slices. The ictal activity observed in slices (see fig 3.1 B) is characterised by several seconds of oscillatory activity followed by periods of quiescence and are reminiscent of EEG recordings and field recordings that are made *in vivo* during seizure activity. Inter-ictal events, characterised by large positive and negative field deflections *in vitro* (Rutecki et al., 1987), are reminiscent of the events observed between seizures in EEG recordings from epileptic patients. These events, with a frequency of

occurrence of <2 Hz, differed from the 'delta' oscillations as they were independent events as opposed to a sinusoidal oscillation.

As the hippocampus is arranged in an orthogonal fashion, the connectivity and the morphology of the slice differs depending on the orientation in which the slice is made. As oscillations depend upon the underlying synaptic connectivity and morphological processes of the cells that generate the oscillations, different slice orientations display differing oscillation frequency preferences (Gloveli et al., 2005). This chapter investigates some of the oscillations generated by the application of kainate and mAChR agonists in coronal and parasagittal hippocampal slices.

Aims

The aims of this chapter are:

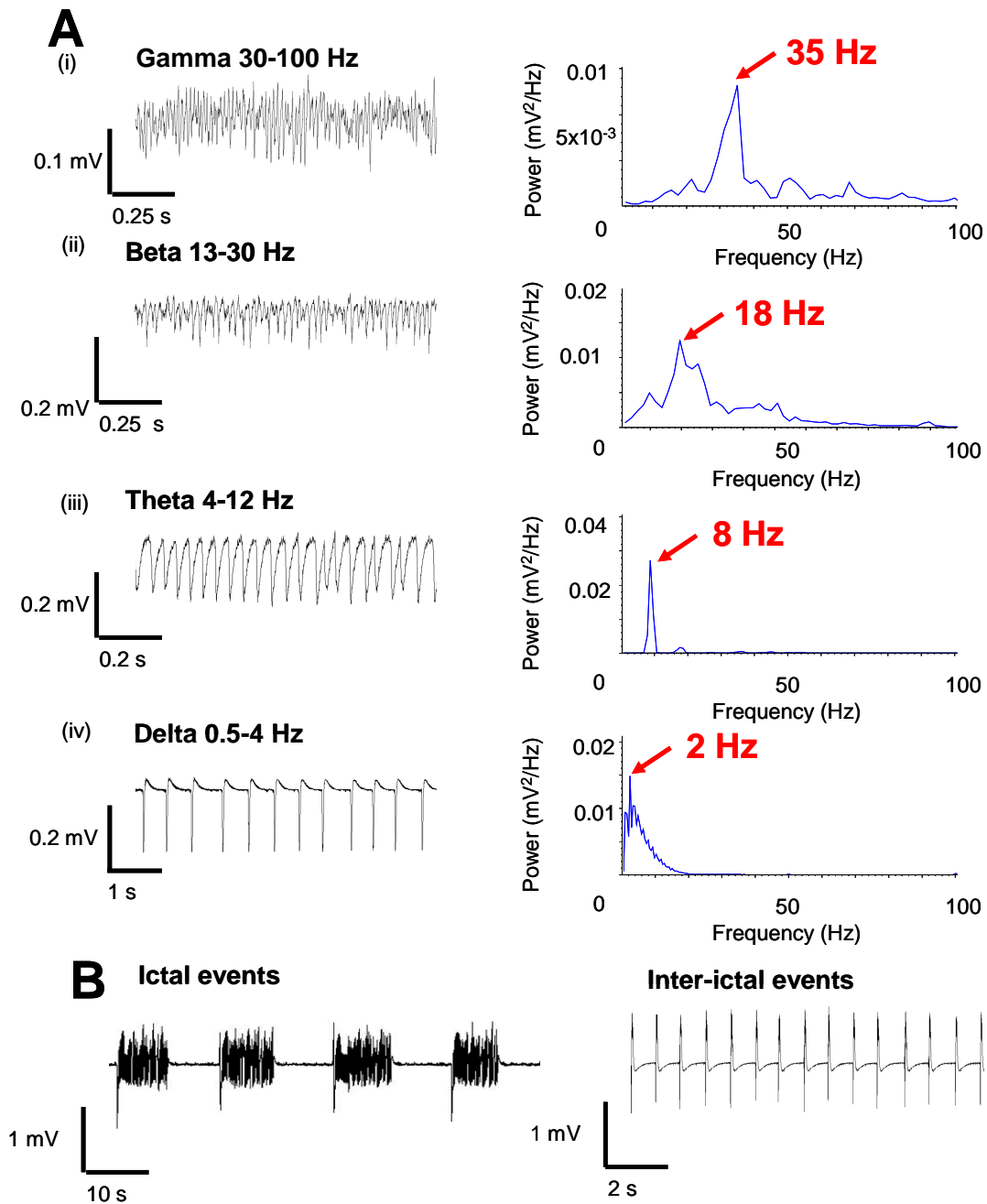
1. To investigate the emergent network activities in parasagittal and coronal slices induced by application of kainate.
2. To compare differences between slice orientations in oscillations induced by oxotremorine-M.
3. To investigate the effect of applying 77-LH-281, a novel M_1 subtype selective mAChR agonist, to parasagittal and coronal slices.

Extracellular field recordings were performed to observe the emergent network oscillatory activity induced by the application of the above drugs.

3.2 Results

A range of oscillatory activities (examples of which can be seen in figure 3.1) were observed in hippocampal slices of either the coronal or parasagittal slices response to the application of kainate and the mAChR agonists. The major results are summarised in the other three following figures.

Fig 3.1 Trace examples of oscillations in the hippocampus



A Representative examples from hippocampal slices displaying (i) gamma oscillations, (ii) beta oscillations, (iii) theta oscillations and (iv) slow wave oscillations. Power spectra are shown. **B**. Representative trace examples showing (i) ictal-like epileptiform activity and (ii) inter-ictal like events.

3.2.1 Kainate-induced oscillations

Application of the glutamate receptor agonist kainate to hippocampal slices led to different modes of oscillatory electrical activity depending on the orientation of the hippocampal slice. Application of 400 nM kainate to hippocampal slices prepared in the sagittal orientation led to the emergence of a regular inter-ictal-like bursting activity in the majority of slices tested (67%, $n = 29/43$ of slices, mean burst frequency = 1.91 ± 0.12 Hz [S.E.M.]).

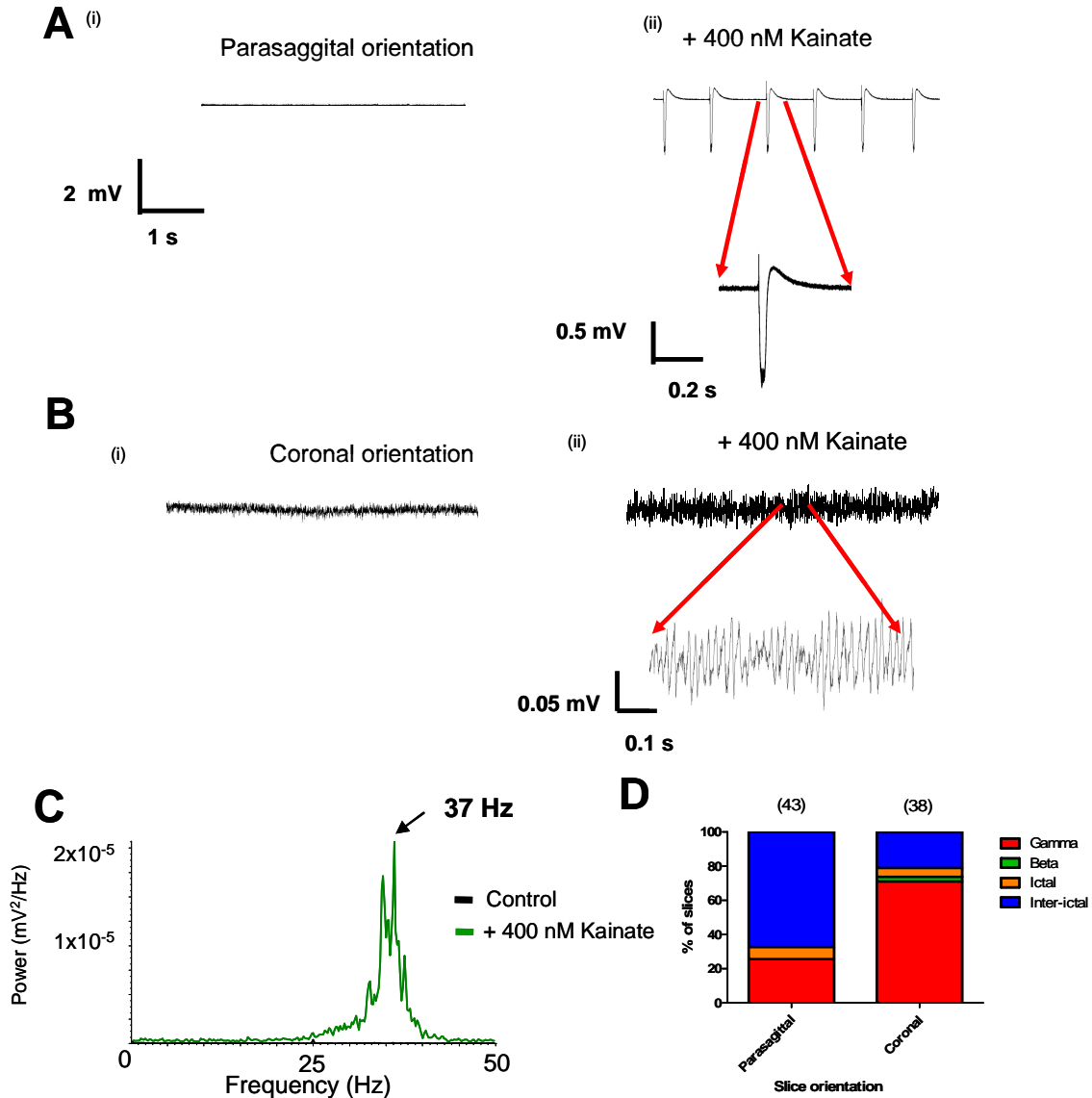
Whilst inter-ictal-like bursting represented the predominant form of activity, other less common modes of oscillatory activity were observed including rhythmical field potential oscillations in the gamma (mean frequency = 31.6 ± 1.3 Hz, 26 %, $n = 11$ of 43 slices) and theta (mean frequency = 7.4 ± 1.6 Hz, 7%, $n = 3$ of 43 slices) frequency ranges. This distribution of oscillatory responses is summarised in figure 3.2.1 D

In comparison to responses seen in parasagittal slices, application of 400 nM kainate to hippocampal slices prepared in the coronal orientation led to emergent network oscillatory activity mainly in the gamma frequency range (71%, $n = 27/38$ of slices; mean frequency = 31.46 ± 1.15 Hz). In addition to gamma frequency oscillations, 400 nM kainate was less commonly found to generate a range of other oscillatory activities including an inter-ictal-like response (21%, $8/38$ of slices; mean frequency = 2.0 ± 0.3 Hz), theta frequency network oscillatory activity (5%, $2/38$ of slices; mean frequency = 6.3 ± 2.4 Hz) and beta frequency activity (2.5%, $1/38$ of slices; frequency = 17.5 Hz) as indicated in figure 3.2.1.D.

3.2.2 Oxotremorine-M induced oscillatory activity

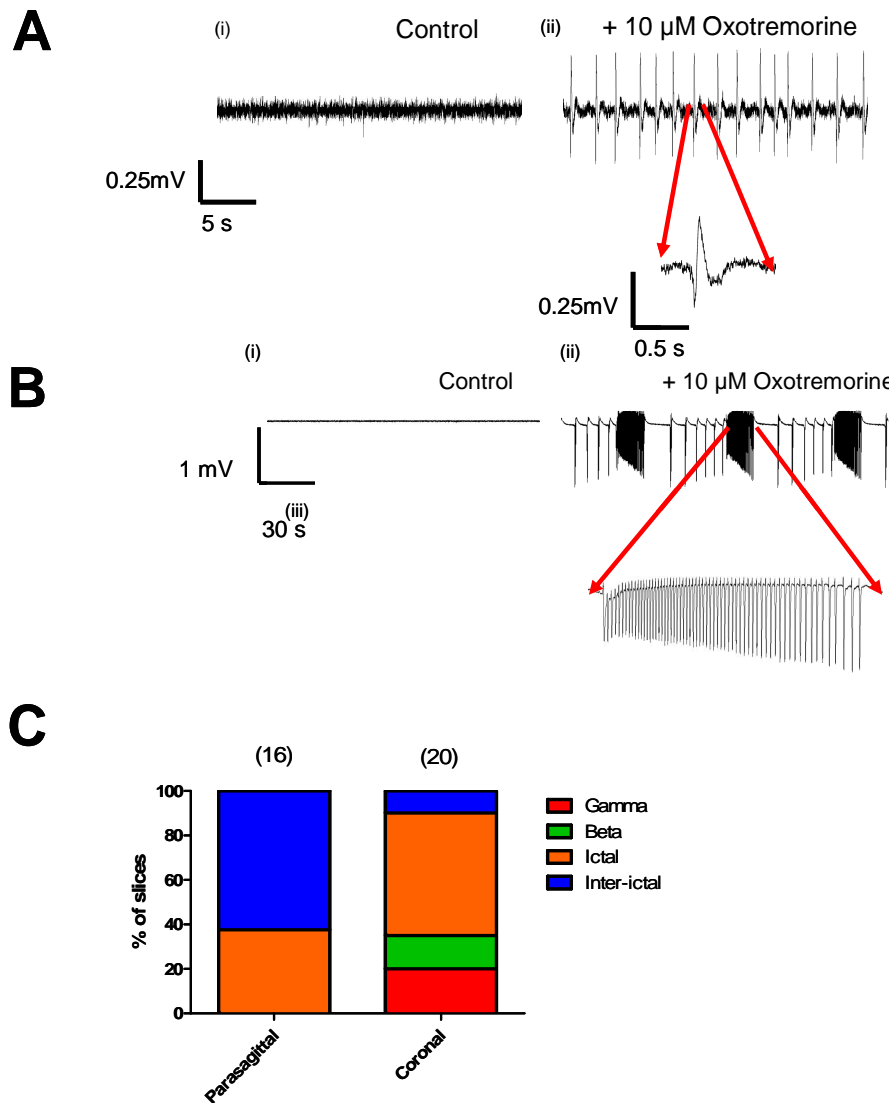
Application of the mAChR agonist oxotremorine-M (10 μ M) to slices prepared in the sagittal orientation led to the emergence of inter-ictal-like oscillatory events in the majority of slices tested (62.5%, $10/16$ of slices; mean frequency = 0.396 ± 0.086 Hz; figure 3.2.2 A). Ictal-like events were observed in a subset (37.5%, $6/16$) of slices. Both ictal-like and inter-ictal-like activities were sensitive to subsequent application of the specific mAChR antagonist atropine (10 μ M) confirming the role of mAChRs in this activity.

Fig 3.2.1 Characterisation of the effect of application of 400 nM kainate to hippocampal slices



A. Representative extracellular field recording trace showing (i) the naïve parasagittal hippocampal slice and (ii) inter-ictal-like events following the application of 400 nM kainate to the naïve hippocampal slice (*inset*- expanded interictal event). Note there is no emergence of network gamma oscillatory activity. **B.** Representative field recordings showing the (i) the naïve coronal hippocampal slice and (ii) subsequent application of 400 nM kainate. Note the induction of network oscillatory activity. **C.** Power spectrum analysis of the above network oscillation shows the frequency of the oscillation to be at 37 Hz, within the gamma range. **D.** Bar chart showing the relative prevalence of oscillations induced by application of agonists to each slice orientation. Inter-ictal-like events were more predominant than gamma frequency oscillations in parasagittal slices, whereas the reverse is true in slices prepared in the coronal orientation (n shown in brackets above).

Fig 3.2.2 Characterisation of the activity induced by the application of 10 μ M oxotremorine-M to naïve hippocampal slices prepared in the parasagittal and coronal orientations



A. Representative extracellular recording trace examples showing (i) the naïve hippocampal parasagittal slice, (ii) interictal-like network activity induced by the application of 10 μ M oxotremorine-M (*inset*- expanded interictal event)
B. Representative trace examples showing (i) naïve slices (ii) ictal-like activity following application of 10 μ M Oxotremorine-M (*inset*- expanded trace)
C. Bar chart showing the relative distribution of emergent network activity following application of 10 μ M oxotremorine to slices prepared in parasagittal and coronal orientations. Inter-ictal-like activity was the dominant emergent oscillatory activity in parasagittal slices, whereas a wide range of oscillations occurred following application of oxotremorine in coronal slices.

In contrast oxotremorine-M more regularly induced ictal-like activity in slices made in the coronal orientation than in the parasagittal orientation. The most common types of oscillatory activity observed in slices made in the coronal orientation following application of 10 μ M oxotremorine-M were ictal-like activity (55%, 11/20 of slices, 10.6 ± 1.0 Hz) and inter-ictal-like activity (30%, 6/20 of slices, 1.14 ± 0.43 Hz). Subsequent application of 10 μ M atropine or the AMPA/kainate receptor antagonist NBQX (2 μ M) or led to an attenuation of the ictal-like and inter-ictal-like activity induced by oxotremorine-M. Interestingly, in the presence of the M_1 mAChR irreversible antagonist MT-7, application of oxotremorine-M led to the emergence of ictal-like activity in the majority (66 %, 4/6) of slices tested. This indicates the M_1 mAChR is not necessary for the emergence of oxotremorine-induced oscillations.

3.2.3 The effect of 77-LH-281 on naïve hippocampal slices

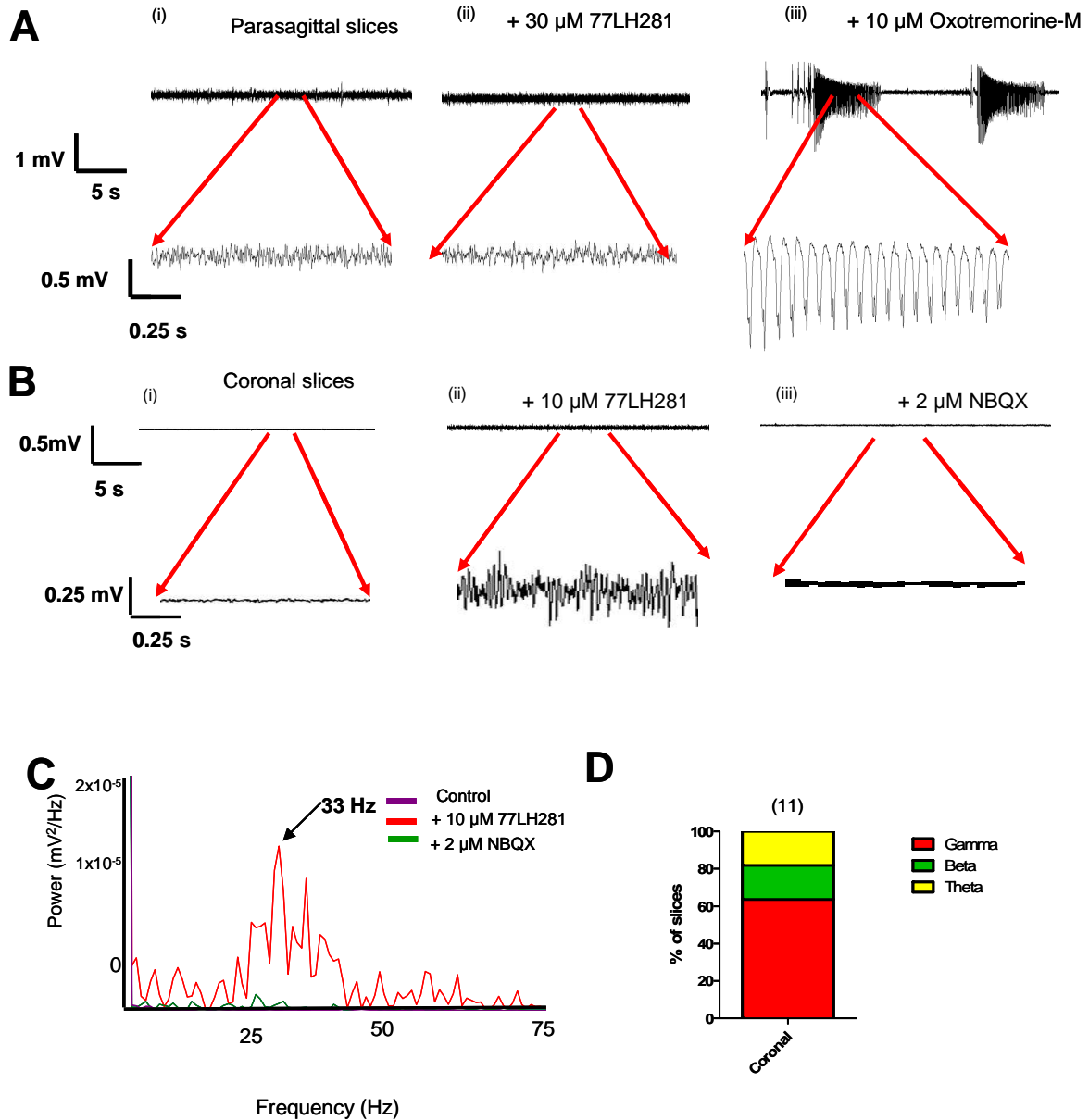
The specific M_1 mAChR agonist 77-LH-281 induced gamma frequency network activity in the majority (64%, 7/11) of coronal hippocampal slices but had no effect in parasagittal hippocampal slices (see fig 3.2.3). The mean frequency of the observed gamma oscillations was 36.6 ± 1.9 Hz following application of 77-LH-281. These oscillations were abolished in the majority (73%, 8/11) of slices by the subsequent application of 2 μ M NBQX. No gamma frequency activity was observed in all (12/12) slices made in the parasagittal orientation following application of 10-100 μ M 77-LH-281. Subsequent application of 10 μ M oxotremorine-M induced either inter-ictal or ictal-like activity in all 12 parasagittal slices tested.

3.3 Discussion

The main findings of this chapter are as follows:

1. Both kainate and mAChR agonists display differential oscillations depending on slice orientation.
2. Kainate and oxotremorine-M can induce pathophysiological epileptiform-like oscillatory activity, whereas the selective M_1 mAChR agonist only induces physiological activities.
3. Slices prepared in the coronal orientation are more prone to display activity within the theta, beta and gamma ranges than slices prepared in the parasagittal orientation.

Fig 3.2.3 Investigation into the extracellular oscillatory activity induced by 77-LH-281 in naïve hippocampal slices



A & B. Representative trace showing the emergent network activity following the application of 10 μM 77-LH-281 to naïve slices. **A** Trace examples showing application of 10 μM 77-LH-281 has no effect in parasagittal slices. Subsequent application of 10 μM oxotremorine-M leads to ictal-like activity (12/12 slices). **B.** Trace examples showing application of 10 μM 77-LH-281 to naïve coronal slices (i) leads to network oscillatory activity (ii) that is sensitive to subsequent application of the AMPA receptor antagonist NBQX (2 μM) (iii). **C.** Power spectrum of trace excerpt in **B** showing this oscillatory activity is within the gamma frequency range (33.1 Hz). **D.** Bar chart showing in the majority of slices activity within the gamma frequency range is induced by 77-LH-281. No oscillatory activity was induced by application of 77-LH-281 to coronal hippocampal slices.

It is likely that the difference in cellular and network connectivity between coronal and parasagittal slices underlies the difference in oscillatory activity initiated by drug application to these slices.

Kainate

Initially the differing effect of nanomolar concentrations of kainate upon hippocampal slices prepared in the coronal and parasagittal orientations was investigated. Kainic acid is a highly potent agonist at GluR 5-7 and KA1 and 2 receptors (Dingledine et al., 1999). Activation of kainate receptors leads to EPSCs in both pyramidal cells (Castillo et al., 1997) and interneurons (Frerking et al., 1998) and can pre-synaptically reduce the release of GABA from interneurons (Rodriguez-Moreno et al., 1997). In coronal slices application of kainate leads to gamma frequency oscillatory activity (Fisahn et al. 2004; Fisahn 2005) in both the entorhinal cortex (Cunningham et al., 2003) and the hippocampal formation (Mann and Paulsen, 2005). The oscillation is maintained in the presence of AMPA receptor antagonists but abolished following application of the GABA_A receptor antagonist bicuculline (Fisahn 2005).

Basket cell interneurons innervate the somatic regions of pyramidal cells and other basket cells (Cobb et al., 1997). These interneurons can pace gamma frequency oscillations due to the existence of mutual fast synaptic inhibition between basket cells (Bartos et al., 2002; Mann et al., 2005). The interneurone network is well placed to regulate oscillatory activity as the extensive axonal arborisation of basket cells can provide large numbers of principal cells with synchronous inhibition at the frequency within the gamma range (Penttonen et al., 1998). The gamma frequency oscillations that are observed in the coronal sections are likely to be controlled by the perisomatic targeting interneurons like the basket cells, as they have extensive arborisations within the transverse plane (Gloveli et al., 2005). The absence of an extensive O-LM interneurone axonal arborisation in the transverse plane allows the oscillation frequency to be controlled by the basket cells.

In a small proportion of coronal slices gamma frequency oscillatory activity could be observed on occasion in the absence of applied compounds. This occurred only 1-1½ hours following the preparation of slices. As such, it is likely that glutamate released during the slicing process is able to initiate these oscillations. This type of oscillation has been shown to be mediated by a mechanism that is distinct from the kainate-induced oscillation

(Pietersen et al, 2009), calling into question which oscillation best represents the *in vivo* situation.

In parasagittal slices, application of kainate does not induce gamma frequency network oscillations in the majority of slices. The principal emergent oscillatory activity is inter-ictal-like activity, with a mean frequency of ~2 Hz. This activity is clearly different from the gamma frequency oscillatory activity observed following application of kainate to coronal slices. An extensive OLM interneurone arborisation is present in slices prepared in the parasagittal direction (Gloveli et al., 2005). The OLM interneurons display a distinct frequency preference for rhythmic slow oscillations (Pike et al., 2000). Thus, the larger arborisations of OLM cells that are present in parasagittal slices as opposed to coronal slices means that the parasagittal slices display slow ictal-like activity preferentially to gamma frequency oscillatory activity. Comparison of intracellular recordings from basket cell and OLM interneurons in both orientations may provide a clearer indication of the role of these interneurons in the inter-ictal-like and gamma frequency oscillations that emerge following the application of kainate. Pairing these recordings with recordings from pyramidal cells would allow further insight into role interneurons play in pacing oscillation frequency.

Acetylcholine

Acetylcholine receptors, comprising nicotinic and muscarinic receptors, are widely expressed within the hippocampus (Fabian-Fine et al., 2001; Levey et al., 1995). The network activity that emerged from the slices following application of muscarinic agonists was dependent on both the mAChRs activated by the agonists and the orientation of the slice used.

Oxotremorine-M shows little functional selectivity between the 5 subtypes of muscarinic receptors (Birdsall et al., 1978; Kukkonen et al., 1996). In coronal slices application of oxotremorine-M mainly led to the emergence of ictal-like activity, whereas in parasagittal slices inter-ictal activity is the dominant oscillation. Ictal-like oscillatory activity is well described in the hippocampus both *in vivo* (Colom et al., 1991) and *in vitro* (Fellous and Sejnowski, 2000; Fischer et al., 1999; Traub et al., 1992).

Ictal activity is characterised by periods of oscillatory activity followed by quiescence. During ictal events, pyramidal cells discharge strongly and GABAergic inhibition from interneurons is reduced, either through the depolarisation block of the interneurons

(Ziburkus et al., 2006), or by depolarising GABAergic synaptic transmission following a reversal of the chloride gradient (Isomura et al., 2003). The afterdischarge potential which occurs following tetanic stimulation is used as one model of ictal events. In this model GABAergic synaptic transmission becomes excitatory, and the depolarising GABAergic EPSPs are synchronised with pyramidal cell discharge (Fujiwara-Tsukamoto et al., 2003). In contrast, in a model of drug induced ictal events, depolarisation block of interneurons occurs throughout the ictal-like episodes, with a return of interneurone activity implicated in the termination of the ictal-like event (Ziburkus et al., 2006).

mAChR agonists display a differential effect on the hippocampal pyramidal cells and interneuronal subtypes, which allows the emergence of ictal-like activity. Hippocampal pyramidal cells are depolarised to threshold by the application of mAChR agonists (Cole and Nicoll, 1984a), following which they undergo a cycle of depolarisation and hyperpolarisation (Williams and Kauer, 1997). Lacunosum moleculare interneurons are directly depolarised by mAChR activation, which also induces voltage dependent oscillations in these neurons (Chapman and Lacaille, 1999). Other interneurons, including basket cells, can be depolarised, hyperpolarised, or unresponsive following mAChR activation (Widmer et al., 2006)

For a difference in the propensity of different oscillations to emerge occur between slice orientations, there must be an underlying difference in the neurons that pace the oscillatory activity. As described previously, the OLM interneurons are the primary pacemaker neurone of the parasagittal slices, whereas the basket cell interneurons are the dominant pacemaker cell of the coronal slices (Gloveli et al., 2005). Following tetanic stimulation OLM interneurons hardly discharge during the afterdischarge potential, whereas fast spiking cells, including basket cells and chandelier cells, show spiking that is synchronous with pyramidal cell firing (Fujiwara-Tsukamoto et al., 2004). This mechanism could readily explain the different propensities of the emergence of ictal-like events for each slice orientation.

However, the ictal like activity that emerges following application of mAChR agonists is likely to differ from that which emerges following tetanic stimulation. In a contrasting model of ictal events, following application of 4-AP profound depolarisation block of interneurons is observed during ictal episodes (Ziburkus et al., 2006). As the majority of interneurons recorded in this study were OLM interneurons, this finding does not directly contradict the above hypothesis. It is possible that fast spiking interneurons do not undergo depolarisation block to the same extent as OLM interneurons, allowing the

basket cells to continue to set the dominant oscillatory frequency. It is also possible that basket cells (amongst other interneurons) are required only for the initiation of ictal events. Thus in coronal slices the extensive arborisations of basket cells can initiate ictal events prior to undergoing depolarisation block, whereas in the parasagittal slices the decreased abundance of basket cell arborisations decreases the likelihood of ictal episodes. Paired recordings of basket cells and pyramidal cells during ictal and inter-ictal events in each plane would provide further insight into the cellular mechanisms of this activity.

The ictal-like oscillation occurs predominantly within the theta frequency range, and this frequency is likely to be predominantly dependent on the intrinsic membrane properties of the pyramidal cells. This contrasts the classical theta model (Buzsaki 2002) in which phasic cholinergic excitatory and GABAergic inhibitory projections from the medial septum-diagonal band of Broca (MS/DBB) control the output of basket cell interneurons, leading to phasic inhibition of pyramidal cells. This combined with the depolarisation of pyramidal cell dendrites by mAChRs and excitatory drive from the perforant path leads to the emergence of theta frequency oscillations. Interneuronal inhibition is removed by either the depolarisation block of interneurons during ictal events, or the reversal of the chloride gradient. The emergence of theta frequency oscillatory activity must arise from the intrinsic pyramidal cell properties or possibly from depolarising GABAergic events. Indeed, pyramidal cells display a resonant frequency within the theta frequency range (Pike et al., 2000).

The M_1 mAChR induced gamma frequency rhythm is similar in frequency to the kainate-induced rhythm. However, in the majority of slices the cholinergic induced gamma frequency rhythm is dependent upon both fast phasic excitation and phasic inhibition, and can be stopped by the blockade AMPA/kainate receptors (Mann et al., 2005). Kainate induced oscillatory activity has previously been shown to be independent of fast glutamatergic transmission (Bartos et al., 2007; Fisahn et al., 2004). In the CA3 region, kainate receptors are expressed on interneurons (Fisahn 2005), and depolarisation of these interneurons following application of nanomolar concentrations of kainate leads to the emergence of the mutual basket cell-basket cell interactions that underlie gamma frequency oscillatory activity (Hajos et al., 2004). In contrast, the cholinergically initiated gamma frequency oscillation is dependent on phasic excitatory drive as the M_1 mAChRs are primarily located upon pyramidal cells (Rouse et al., 1999). Therefore fast excitatory transmission from the pyramidal cell network appears to be required to drive the oscillation. However, in a minority of slices, gamma frequency oscillatory activity occurred following application of AMPA/kainate receptor antagonists. It is possible that

once AMPA/kainate receptors have initiated the oscillation, recurrent inhibition is able to carry the oscillation. However, in a highly active network a large amount of glutamate release occurs (Szerb, 1984). In this case a competitive antagonist (like NBQX used in this study) may be overcome by increased amount of glutamate. In this case an increased concentration may have completely abolished gamma frequency oscillations.

Application of the M_1 mAChR specific agonist 77-LH-281 leads to gamma frequency oscillatory activity in coronal hippocampal slices but not in parasagittal slices. The slice orientation determines the predominant interneurone axonal arborisation. The arborisation of the basket cells in the coronal slices are ideally suited to pace gamma frequency oscillatory activity, whereas the predominant interneurons in the parasagittal slices are the OLM cells and these have a frequency preference of low theta frequency ranges (Pike et al., 2000). Thus selective M_1 agonists may not produce oscillatory activity in parasagittal slices due to the absence of enough basket cell-basket cell recurrent synaptic connections to allow the emergence of gamma frequency activity.

3.4 Conclusion

In this chapter an attempt was made to investigate the effect of application of a range of compounds in both parasagittal and coronal hippocampal slices. The orientation of the slice had profound effects on the emergent activity that arose from the networks within the slices. It is likely that the different arborisations within the interneurone networks in the different slices underpin this change in network activity. Coronal slices are more conducive in allowing the emergence of network oscillatory activity in the theta, beta and gamma frequency ranges, whereas parasagittal slices tend to display slower oscillations. As the coronal slices displayed a higher propensity to display oscillatory activities, this orientation was used for the remainder of this thesis.

Also, in comparison with oxotremorine-M, application of the M_1 mAChR agonist 77-LH-281 does not promote pathophysiological oscillatory activity in naïve hippocampal slices of either orientation, but rather promotes gamma frequency oscillations. Gamma frequency oscillations are thought to be important in cognitive function (Slobounov et al., 2000; Tallon-Baudry and Bertrand, 1999; Tallon et al., 1995), and therefore compounds like 77-LH-281 that promote gamma frequency oscillations have the potential to enhance cognition.

4 The effect of mAChR agonists on hippocampal neurophysiology

4.1 Introduction

In this chapter, two mAChR agonists are investigated in a range mechanistically distinct epileptiform models. These agonists are oxotremorine-M, a non-subtype selective mAChR agonist, and 77-LH-281, an M₁ mAChR selective agonist. The effect of these agonists on different models allows the evaluation and comparison of the pro-epileptiform potential of these agonists, as well as mechanistic insight into the mode of action of oscillations induced by mAChR agonists.

Compounds that promote cholinergic signalling are of interest in potential cognitive enhancement strategies for several reasons. The cholinergic system can enhance learning and memory within the hippocampus mostly through the activation of mAChRs (Bartus et al., 1982; Fibiger, 1991; Nilsson et al., 1992). Conversely, mAChR antagonists like scopolamine and atropine can disrupt hippocampal mnemonic processes (Grauer and Kapon, 1996; von Linstow Roloff et al., 2007). Enhancing cholinergic signalling is used clinically as prolonging ACh action at the synapse through the use of acetylcholinesterase inhibitors (such as rivastigmine or donepezil) improves cognitive performance in Alzheimer's disease (Perry et al., 1985). An approach to ameliorate the cognitive impairment associated with schizophrenia using mAChR agonists has also been proposed (Friedman, 2004).

It has been suggested that the M₁ mAChR is primarily involved in mediating alterations in learning and memory (Hunter and Roberts, 1988; Messer et al., 1990). Studies have also shown the application of a functionally selective M₁ mAChR receptor agonist, sabcomeline, significantly improved reversal learning in marmosets (Harries et al., 1998). As such, enhancement of mAChR activity through specific M₁ mAChR receptor agonism is a potential therapeutic strategy to develop novel nootropic drugs.

Activation of cholinergic projections from the medial septum/diagonal band of Broca initiates oscillatory activity in the hippocampus (Brazhnik and Fox, 1999) which can be mimicked by application of cholinergic agonists like carbachol directly to the hippocampal formation. Application of carbachol promotes theta frequency oscillatory activity *in vivo* (Bland et al., 1994) and *in vitro* (Chapman and Lacaille,

1999; Williams and Kauer, 1997), which enhances synaptic plasticity in CA1 pyramidal neurones (Huerta and Lisman, 1993). Theta frequency oscillatory activity occurs during exploratory states in rodents (Vanderwolf, 1969) and hippocampal place cells (which encode spatial memory) discharge in relation to an underlying theta frequency oscillation (O'Keefe and Recce, 1993).

Aside from the pro-cognitive potential of mAChR agonists, activation of mAChRs is pro-epileptogenic (Cobb et al., 1999; MacVicar and Tse, 1989; Williams and Kauer, 1997). Application of pilocarpine, a mAChR agonist, can cause seizure activity *in vivo* (Cavalheiro et al., 1991). Epileptiform activity can be induced in hippocampal slices following the application of mAChR agonists (Egorov et al., 2003; Nagao et al., 1996) and disinhibition-induced epileptiform activity is enhanced by the acetylcholinesterase inhibitor physostigmine (Gruslin et al., 1999). Epileptiform activity can be induced in hippocampal slices through the blockade of the mAChR sensitive K^+ current (I_M) in hippocampal slices (Pena and Alavez-Perez, 2006). It is therefore important to investigate the pro-epileptogenic potential of the novel specific M_1 mAChR subtype selective agonist 77-LH-281 (Langmead et al., 2008).

The major aim of this chapter is to investigate the effect of application of oxotremorine-M and 77-LH-281 on four mechanistically distinct models of epileptiform activity. The effect of application of oxotremorine-M and 77-LH-281 on the intrinsic electrical properties of CA1 pyramidal cells and excitatory synaptic transmission will also be investigated. The effect of oxotremorine-M and 77-LH-281 on naïve slices is shown in the preceding chapter.

Extracellular and intracellular electrophysiological recordings from coronal hippocampal slices are performed to determine the pro-epileptiform potential of M_1 selective and non-subtype selective mAChR agonists, and allow insight into the oscillations induced by mAChR agonists.

4.2 Emergent network activity in the hippocampus and its modulation by mAChR agonists

The effects of the mAChR agonists oxotremorine-M and 77-LH-281 on experimental models of epileptiform activity were investigated. Four different epileptiform models were used: a 4-AP-induced block of K^+ currents; a bicuculline-induced block of the $GABA_A$ receptor, alongside a raised extracellular $[K^+]_o$ to 5 mM; the removal of Mg^{2+} ions from the extracellular medium, ACSF, to remove the voltage-dependent magnesium site block of the NMDA receptor channel; and the combined use of 4-AP to activate the network and NBQX to reduce AMPA/kainate mediated ionotropic glutamatergic synaptic transmission.

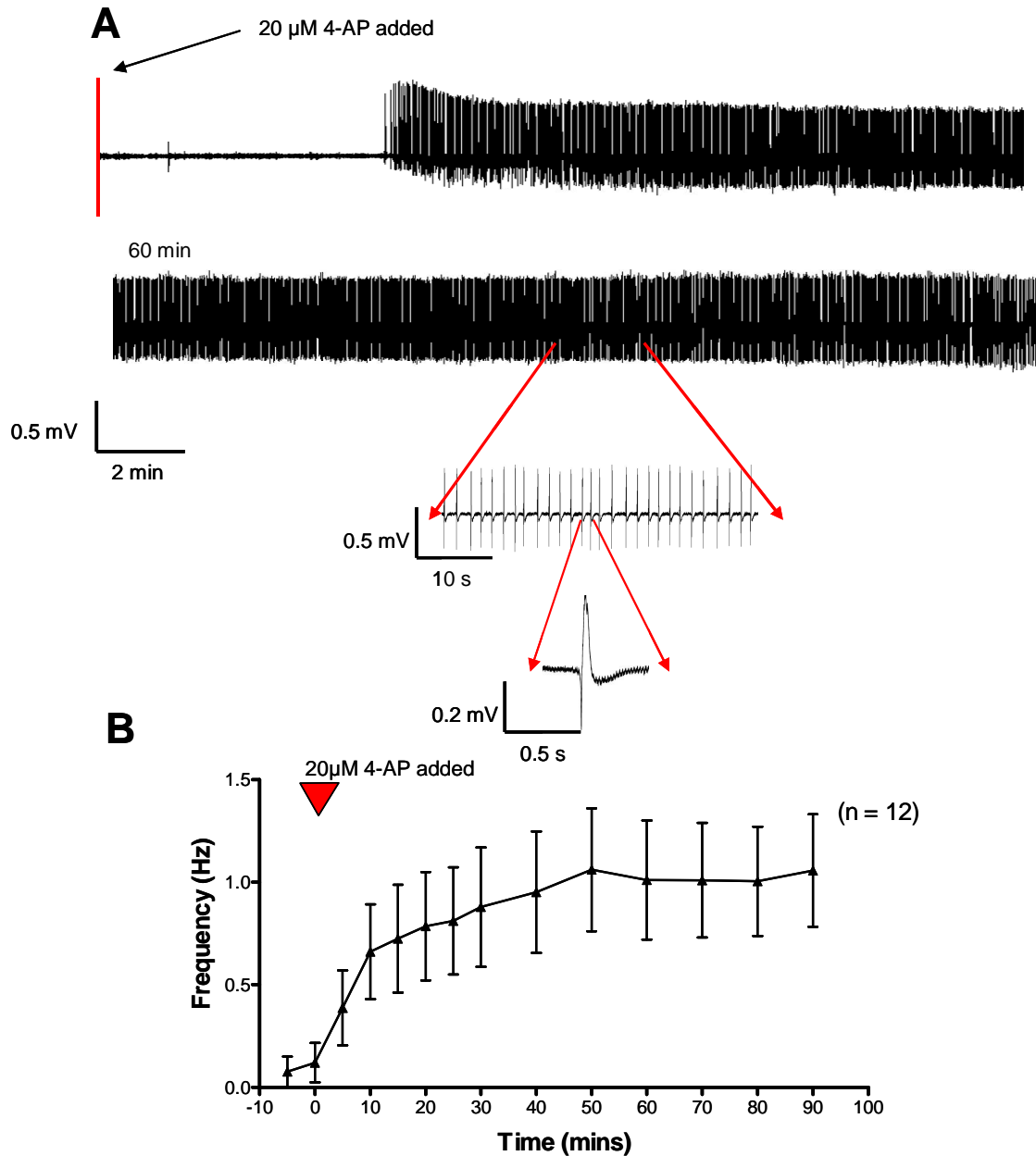
4.2.1 The 4-AP-induced network activity model

Application of 20 μ M 4-AP led to inter-ictal-like epileptiform activity in coronal hippocampal slices (Fig 4.2.1). Inter-ictal-like events started to appear with a latency of 8.0 ± 1.8 minutes (mean \pm S.E.M., $n = 11$) after the initial application of 4-AP. Following the initial inter-ictal-like event, there was a gradual increase in the inter-ictal-like event frequency, as shown by fig 4.2.1 B. The frequency of inter-ictal events stabilised approximately 30-40 minutes after application of 20 μ M 4-AP, with a mean event frequency of 1.02 ± 0.02 Hz ($n = 12$) 40 minutes after 4-AP application. The rate of change in frequency after 40 minutes does not differ significantly from zero ($P = 0.95$, $r^2 = 0.00007$).

4.2.2 Oxotremorine-M is pro-epileptogenic in the 4-AP epileptiform model

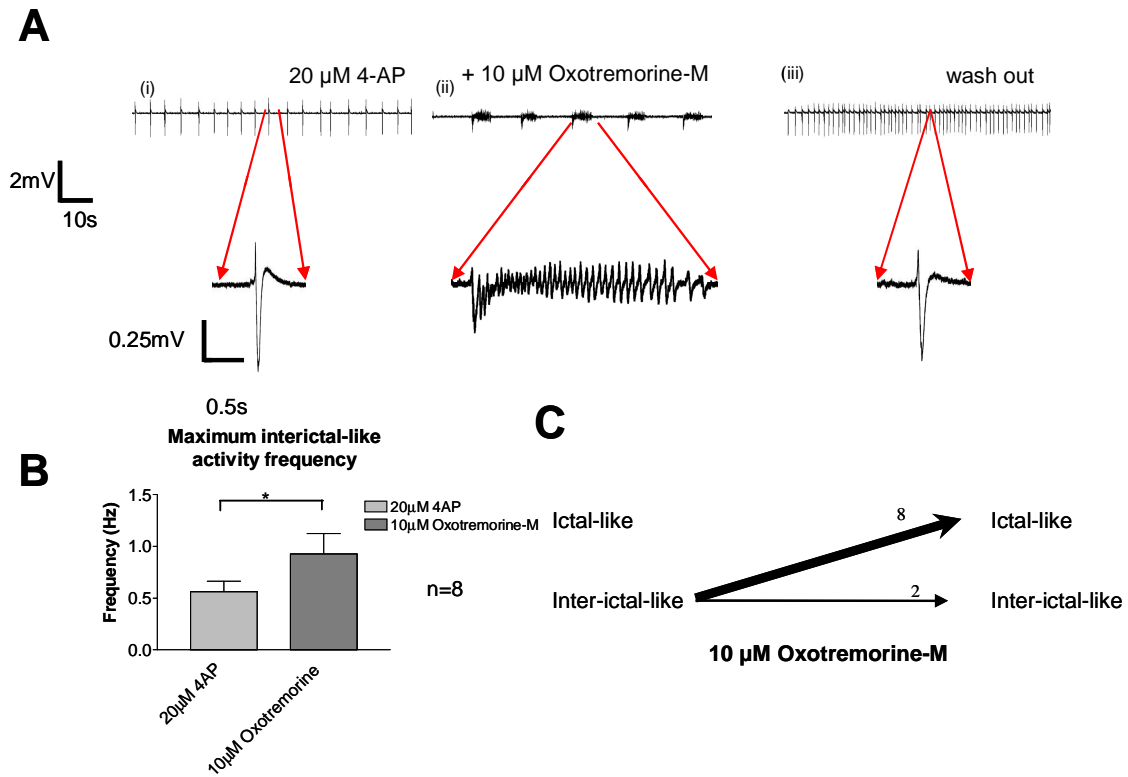
Application of 10 μ M oxotremorine-M to 20 μ M 4-AP-induced inter-ictal-like events led to the emergence of ictal-like bursting events in the majority (80%, 8/10) of slices with a mean occurrence frequency of 0.17 ± 0.06 Hz.

Fig 4.2.1 The response of naïve coronal hippocampal slices to the application of 4-amino pyridine (4-AP)



A. Representative trace example showing the emergence of regular inter-ictal-like activity 5-10 minutes after application of 20 μ M 4AP to coronal hippocampal slices. This oscillation persists regularly for over 90 minutes. *Expanded trace*- it can be seen that in this example the rate of inter-ictal-like activity is approximately 0.5 Hz. *Inset*- an example of a 4AP-induced inter-ictal-like event. **B.** Pooled frequency data from 12 hippocampal slices. It can be seen that the frequency of inter-ictal-like events stabilises 30-50 minutes after application of 20 μ M 4-AP.

Fig 4.2.2 Investigation into the effect of the application of 10 μM oxotremorine-M on 4-AP-induced inter-ictal-like activity



A. Representative trace example showing (i) inter-ictal-like activity induced by the application of 20 μM 4-AP, (ii) subsequent application of 10 μM oxotremorine-M and (iii) wash out of the 10 μM oxotremorine-M. Regular inter-ictal-like activity (~ 0.5 Hz (i)) is converted into ictal-like events, with an intra-burst oscillation frequency of 11 Hz, following the application of oxotremorine-M. **B.** Summary histogram showing oxotremorine-M induces a significant increase in inter-ictal-like frequency before the activity changes to ictal-like activity. **C.** Trend chart showing the effect of 10 μM oxotremorine-M application on 20 μM 4-AP-induced activity. As can be seen, of the 10 slices displaying inter-ictal-like activity, the majority (8) display ictal-like activity following oxotremorine-M application.

Prior to the change in mode of activity induced by oxotremorine-M application, the agonist initially caused a significant ($P = 0.039$) increase (0.56 ± 0.10 to 0.92 ± 0.20 Hz, $n = 8$) in the inter-ictal-like event frequency (fig 4.2.2 B) before the activity changed to ictal-like activity. The oscillatory frequency within the episodes lies within the theta frequency range (9.54 ± 0.70 Hz).

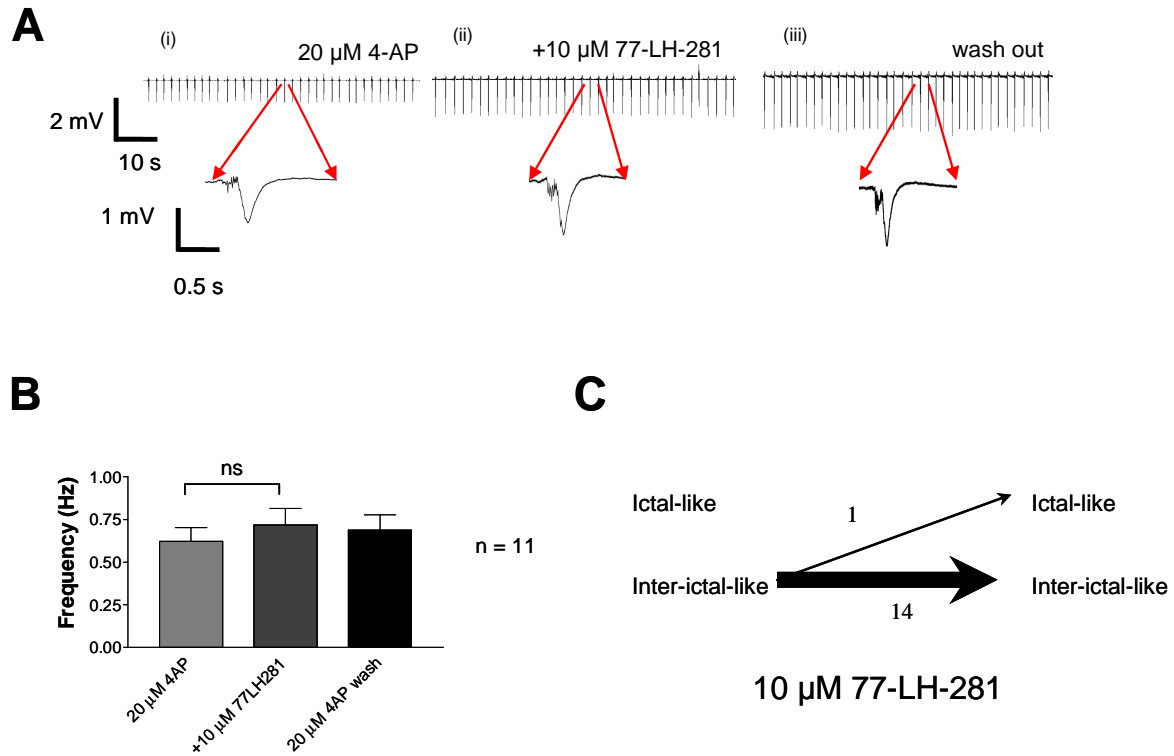
4.2.3 77-LH-281 has no effect on 4-AP-induced network activity

Next the effect of the M_1 mAChR selective agonist 77-LH-281 on 4-AP induced activity was investigated in order to elucidate the role of the M_1 receptor in the mAChR-induced ictal-like activity. In contrast to the effect of $10 \mu\text{M}$ oxotremorine-M, application of 77-LH-281 ($10 \mu\text{M}$) did not change the mode, or frequency, of 4-AP-induced epileptiform activity. The summary histogram in fig 4.2.3 B shows application of $10 \mu\text{M}$ 77-LH-281 did not cause a significant change ($P = 0.17$) in the frequency of inter-ictal-like events induced by the application of $20 \mu\text{M}$ 4-AP (0.62 ± 0.08 to 0.72 ± 0.10 Hz, $n = 11$). The trend chart (fig 4.2.3 C) shows the majority (93%, 14/15) of slices do not display a change in the mode of activity following application of $10 \mu\text{M}$ 77-LH-281. $100 \mu\text{M}$ 77-LH-281 also did not change the mode or frequency of the observed network activity. Mechanistically distinct models of epileptiform activity were used to investigate further the oscillations induced by mAChR agonists.

4.2.4 Bicuculline-induced network activity

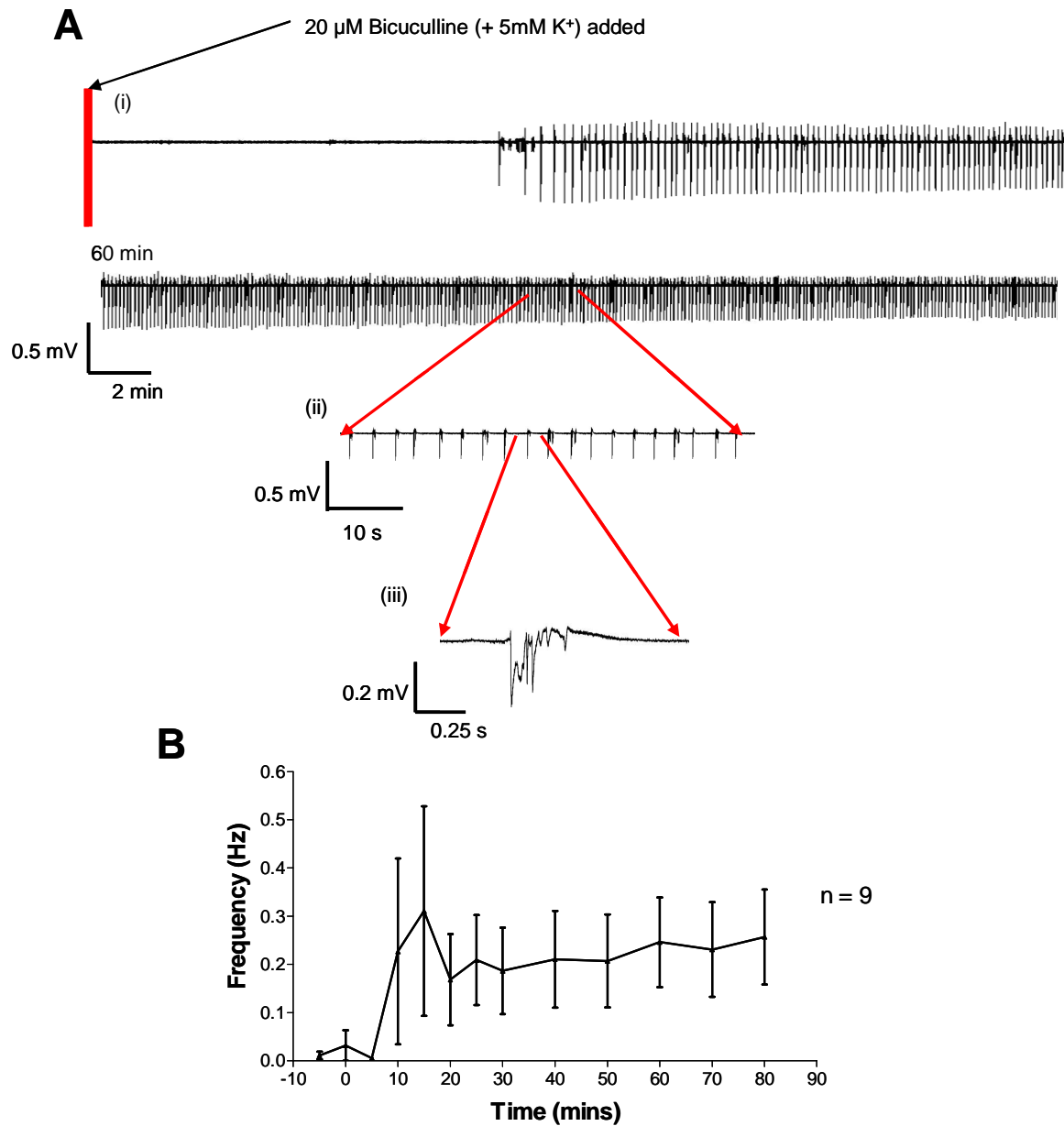
Figure 4.2.4 shows the effect of $20 \mu\text{M}$ bicuculline on coronal hippocampal slices. The inter-ictal-like activity induced by application of bicuculline, a GABA_A receptor antagonist, had a much lower frequency than the frequency of inter-ictal-like activity induced by the application of $20 \mu\text{M}$ 4-AP. A raised $[\text{K}^+]_o$ (5 mM) in the circulating ACSF was used to increase the frequency of inter-ictal-like events towards the frequency of inter-ictal-like events induced by application of $20 \mu\text{M}$ 4-AP.

Fig 4.2.3. Investigation into the effect of application of 10 μM 77-LH-281 on inter-ictal-like activity induced by 20 μM 4-AP



A. Representative trace showing (i) inter-ictal-like bursting induced by 20 μM 4-AP (*inset*- single inter-ictal-like burst) (ii) the effect of subsequent application of the M_1 mAChR agonist 77-LH-281 (10 μM) on this activity (*inset*- single inter-ictal-like burst) and (iii) wash out of 77-LH-281. **B.** Summary histogram showing there is no significant change in inter-ictal-like event frequency. No overt change in oscillatory activity from inter-ictal-like activity is observed, as shown in the trend chart (C) in which only 1 of the 15 slices displaying inter-ictal-like activity display ictal-like activity following application of 10 μM 77-LH-281.

Fig 4.2.4 The effect of application of 20 μM bicuculline (+ 5 mM K^+) to naïve hippocampal slices



A. Representative trace example showing the effect of 20 μM bicuculline (+5 mM K^+) on naïve hippocampal slices. 10-15 minutes after 20 μM bicuculline (+5 mM K^+) application inter-ictal-like activity appears. The frequency of inter-ictal-like events increases with time. Expanded trace (ii)- in this example it can be seen that the event frequency is approximately 0.3-0.4 Hz. *Inset* (iii)- note the change in the inter-ictal-like event from the 4-AP induced event (see fig 4.2.1). B. Time-frequency plot showing the mean (\pm S.E.M.) inter-ictal-like activity (n = 9) increases in frequency until it stabilises between 30-40 mins post bicuculline application.

Despite the increased $[K^+]_o$ the inter-ictal-like event frequency induced by 20 μM bicuculline is lower than the inter-ictal frequency induced by 20 μM 4-AP. Inter-ictal-like events started to appear with a mean latency of 8.4 ± 1.6 minutes ($n = 9$) following bicuculline application, with characteristic positive and negative voltage deflections (fig 4.2.4 A). The time frequency plot illustrated in fig 4.2.4 B shows the mean oscillatory frequency as bicuculline washed into the slice. There was a sharp increase in inter-ictal-like event frequency over the initial 10-20 minutes following bicuculline application, before the frequency of events stabilised after 40 minutes (0.23 ± 0.01 Hz, $n = 9$) with no significant change in the frequency of inter-ictal-like events after this time point ($P = 0.70$, $r^2 = 0.004$).

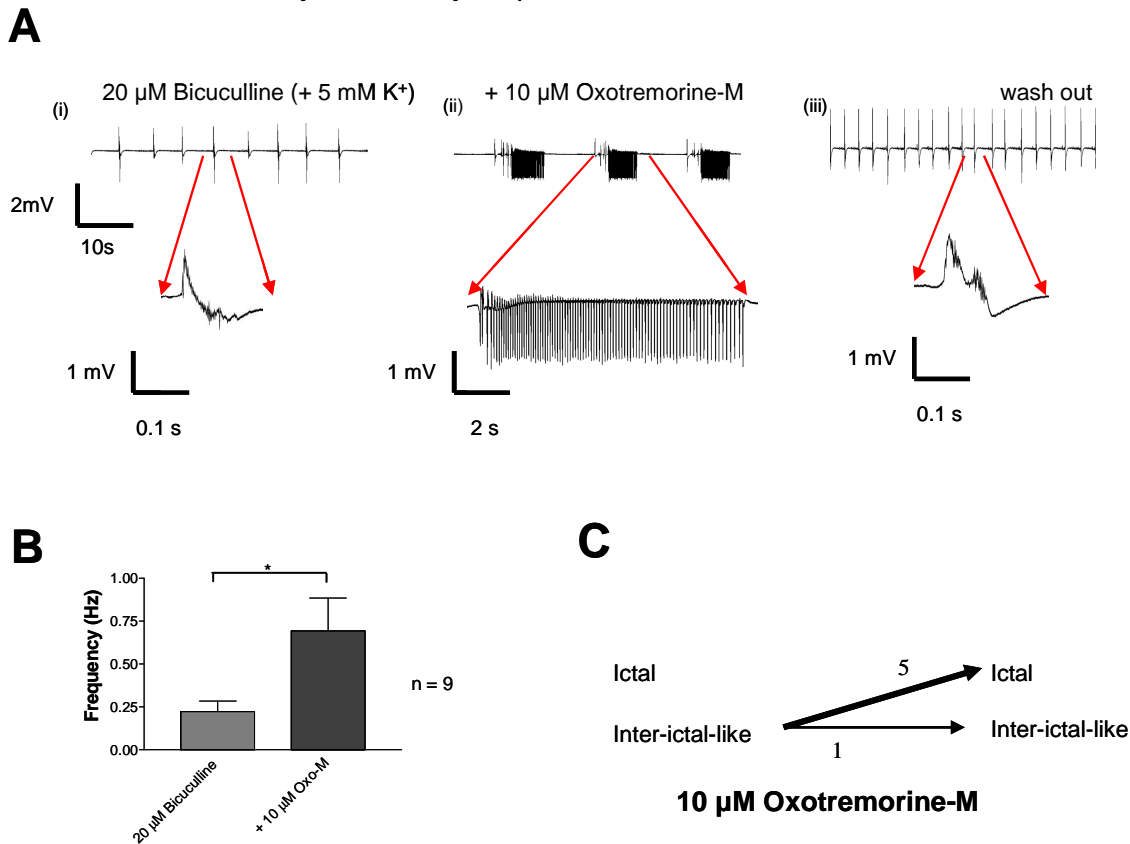
4.2.5 Oxotremorine-M is pro-epileptogenic in the bicuculline epileptiform model

Application of 10 μM oxotremorine-M to hippocampal slices displaying bicuculline-induced inter-ictal-like activity changed the mode of activity from inter-ictal-like activity to ictal-like activity in the majority of slices tested (83%, 5/6 slices) with a mean occurrence frequency of 0.12 ± 0.03 Hz. The frequency of the oscillation within the ictal-like event was predominantly within the theta frequency range (mean = 12.65 ± 0.44 Hz). There was a significant ($P = 0.0078$) increase in the inter-ictal-like event frequency following addition of 10 μM oxotremorine-M (0.22 ± 0.06 to 0.69 ± 0.19 Hz, $n = 9$) (see fig 4.2.5.B), prior to the emergence of ictal-like activity. Inter-ictal-like activity re-emerged upon wash out of oxotremorine-M.

4.2.6 77-LH-281 increases bicuculline-induced inter-ictal-like event frequency

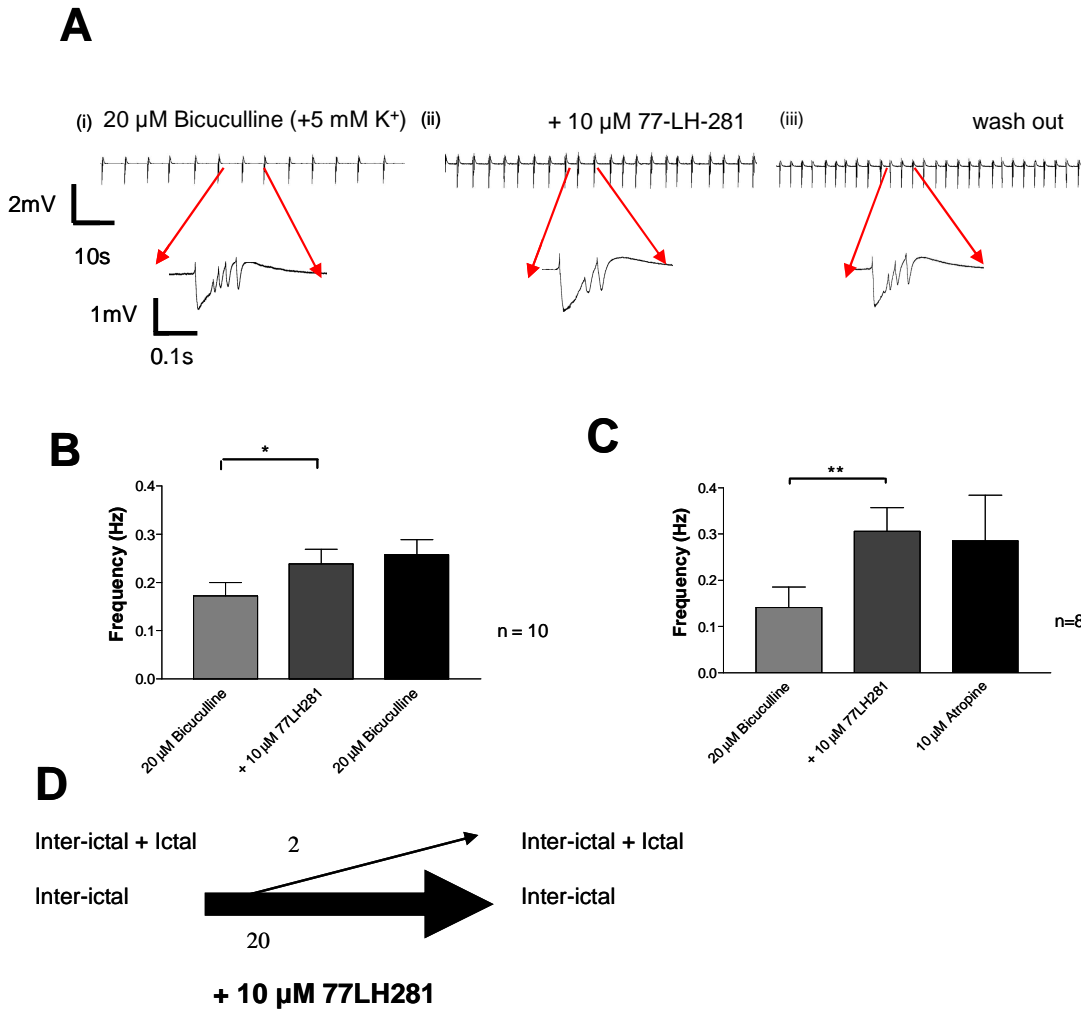
The effect of the application of the M_1 mAChR subtype selective agonist 77-LH-281 on bicuculline induced inter-ictal-like activity was then investigated to allow the elucidation of the role of the M_1 mAChR subtype in the mAChR induced ictal-like activity. Application of 10 μM 77-LH-281 to bicuculline induced inter-ictal-like events caused a significant ($P = 0.027$) increase in the frequency (0.16 ± 0.02 to 0.27 ± 0.03 Hz, $n = 18$) of inter-ictal-like events. This effect was not reversible upon wash out of 10 μM 77-LH-281 (0.24 ± 0.03 to 0.26 ± 0.03 Hz, $n = 10$, fig 4.2.6.B).

Fig 4.2.5 Investigation into the effect of application of 10 μM oxotremorine-M on inter-ictal-like activity induced by 20 μM bicuculline (+ 5 mM K^+)



A. Representative trace showing (i) inter-ictal-like activity induced by 20 μM bicuculline (+ 5 mM K^+) (*inset*-inter-ictal-like event), (ii) the effect of the application of 10 μM oxotremorine-M on bicuculline-induced inter-ictal-like activity (*inset*- ictal-like event) and (iii) wash out of oxotremorine-M (*inset*-inter-ictal-like event). **B.** Summary histogram showing a significant increase in the frequency of inter-ictal-like events in response to the application of 10 μM oxotremorine-M prior to changing the mode of activity to ictal-like activity. **C.** Trend chart showing the effect of 10 μM oxotremorine-M on inter-ictal-like activity induced by 20 μM bicuculline (+ 5 mM K^+). 5 of 6 slices displaying inter-ictal-like activity displayed ictal-like activity following application of 10 μM oxotremorine-M.

Fig 4.2.6. Investigation into the effect of application of 10 μM 77-LH-281 on 20 μM bicuculline (+5 mM K^+)-induced inter-ictal-like activity



A. Representative trace showing (i) 20 μM bicuculline (+5 mM K^+)-induced oscillatory activity (*inset*- single inter-ictal-like event), (ii) the effect of subsequent application of the M_1 specific agonist 77-LH-281 (10 μM) on 20 μM bicuculline (+5 mM K^+)-induced inter-ictal-like activity (*inset*- single inter-ictal-like event) and (iii) wash out of 77-LH-281 (*inset*- inter-ictal-like event). **B & C.** Summary histograms showing the effect the effect of the application of 10 μM 77LH281 on bicuculline (+5 mM K^+)-induced interictal-like activity. There is a significant increase in the frequency of interictal-like activity induced by the application of 10 μM 77-LH-281 Note this effect is not reversible upon wash out of 77-LH-281 (**B**), or when all mAChRs are blocked by the mAChR antagonist atropine (**C**). **D.** Trend chart showing application of 10 μM 77-LH-281 to 20 μM bicuculline (+5 mM K^+)- induced inter-ictal-like activity did not change the mode of activity into ictal-like activity in 20 of 22 slices.

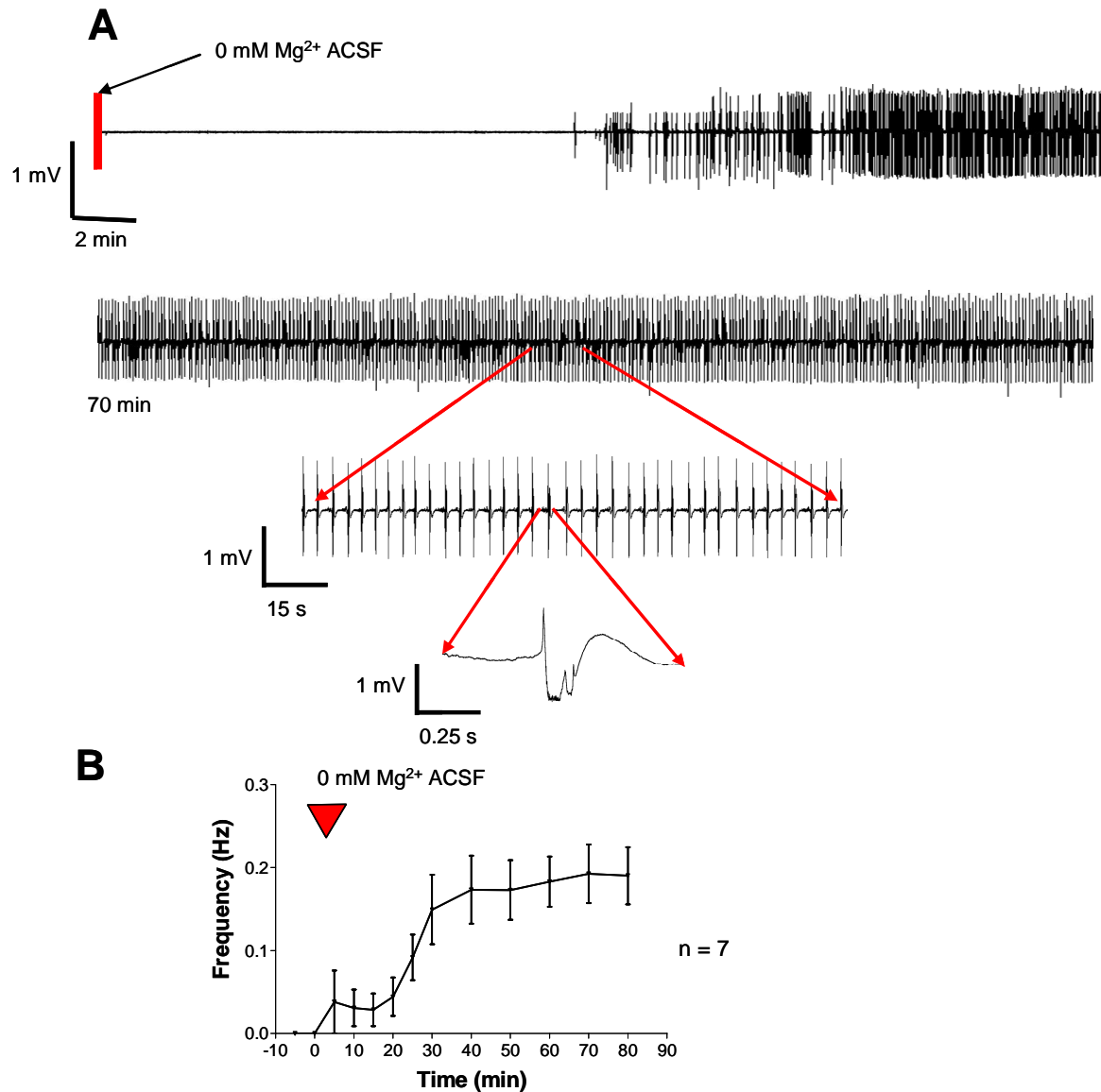
Only a small subset (8.3%, 2/24) of slices displayed ictal-like activity following addition of 10 μM 77-LH-281. In order to investigate further the irreversibility of 10 μM 77-LH-281 induced frequency potentiation upon wash out, 10 μM atropine (a non-selective mAChR antagonist) was subsequently applied to slices (fig 4.2.6.C). Atropine did not significantly reverse (0.31 ± 0.05 to 0.29 ± 0.10 Hz, $P = 0.46$, $n = 8$) the increase in inter-ictal-like event frequency induced by application of 10 μM 77-LH-281 suggesting M_1 mAChR activation leads to a potentiation of inter-ictal-like event frequency that is not dependent on continuous M_1 mAChR activation.

4.2.7 Low extracellular magnesium-induced network activity

The effect of removing Mg^{2+} ions from the extracellular bathing medium was to induce inter-ictal-like events (fig 4.2.7) as previously reported (Tancredi et al., 1990; Traub et al., 1994). Removal of Mg^{2+} ions relieves the voltage-dependent block of the NMDA receptor, which leads to an increase in excitability of the network. The inter-ictal-like events appeared after 13.0 ± 2.6 minutes ($n = 8$) and there was no statistically significant change the frequency of the events after 40 minutes (fig 4.2.7.B, $P = 0.62$, $r^2 = 0.007$). The mean frequency following this point was 0.18 ± 0.01 Hz, indicating the frequency of the events is slower than both the 4-AP and bicuculline induced events. As inter-ictal-like events in the low extracellular magnesium took on average longer to appear and stabilise than the 4-AP and bicuculline-induced events, at least 60 minutes following removal of Mg^{2+} from the ACSF were allowed to elapse before further pharmacological experimentation was carried out.

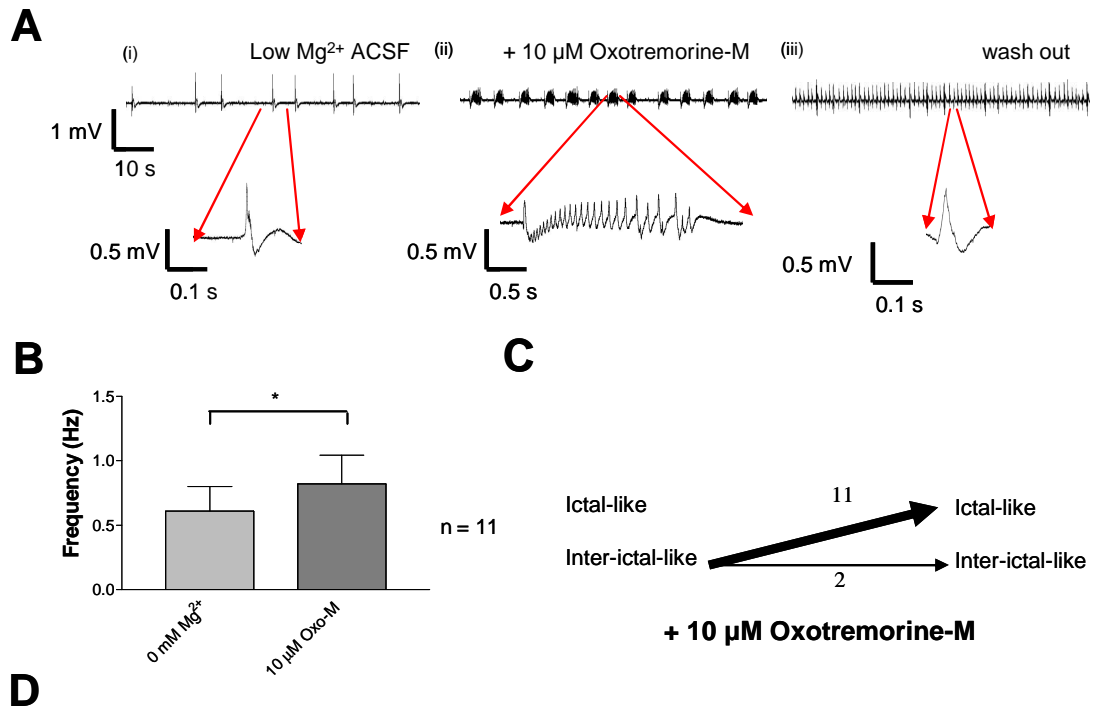
4.2.8 Oxotremorine-M is pro-epileptogenic in the low extracellular magnesium epileptiform model

Application of 10 μM oxotremorine-M to both of the previously studied epileptiform models and naïve hippocampal coronal sections predominantly led to ictal-like activity. Likewise, application of 10 μM oxotremorine-M to low extracellular magnesium-induced inter-ictal-like activity led to a change in the mode of oscillatory activity from inter-ictal-like to ictal-like events (11/13 slices tested, fig 4.2.8.C).

Fig 4.2.7 Investigation into the effect of low Mg^{2+} ACSF on naïve hippocampal slices.

A. Representative trace showing the gradual emergence of inter-ictal-like events 30-40 minutes following the removal of Mg^{2+} ions from the extracellular bathing medium to give a nominally zero extracellular $[Mg^{2+}]$. *Expanded trace*- the rate of inter-ictal-like activity is approximately 0.2 Hz in this example. *Inset*- the inter-ictal-like burst event. **B** Time-frequency plot of the mean (\pm S.E.M.) inter-ictal-like activity ($n = 7$) following the removal of Mg^{2+} ions from the extracellular bathing medium. Note the stability of the frequency of inter-ictal-like events after 40-50 minutes.

Fig 4.2.8 Investigation into the effect of the application of 10 μM oxotremorine-M on inter-ictal-like activity induced by the removal of Mg^{2+} from the extracellular bathing medium.



A. Representative trace showing (i) inter-ictal-like activity from hippocampal slices in which extracellular $[\text{Mg}^{2+}]$ is nominally zero (*inset*- inter-ictal-like event), (ii) the effect of 10 μM oxotremorine on this inter-ictal-like activity (*inset*- ictal-like event), and (iii) wash out of oxotremorine-M (*inset*- inter-ictal-like event). **B.** Summary histogram showing a significant increase in inter-ictal-like event frequency before the mode of activity changes from inter-ictal-like activity to ictal-like activity. **C.** Trend chart showing the effect of application of 10 μM oxotremorine on inter-ictal-like activity induced by low extracellular Mg^{2+} . The majority (11/13) of slices change from inter-ictal-like activity to ictal-like activity.

The ictal-like events occurred at a frequency of 0.30 ± 0.08 Hz, and the frequency of the oscillatory activity within the ictal-like discharges (mean = 9.44 ± 0.71 Hz) was within the theta frequency range. This change from inter-ictal-like to ictal-like events was reversed by subsequent wash out of oxotremorine-M or by subsequent application of atropine ($10 \mu\text{M}$). Prior to the occurrence of ictal-like events, the inter-ictal-like event frequency (fig 4.2.8.B) significantly ($P = 0.032$) increased (0.61 ± 0.19 to 0.82 ± 0.22 Hz, $n = 11$) as $10 \mu\text{M}$ oxotremorine-M washed into the slice.

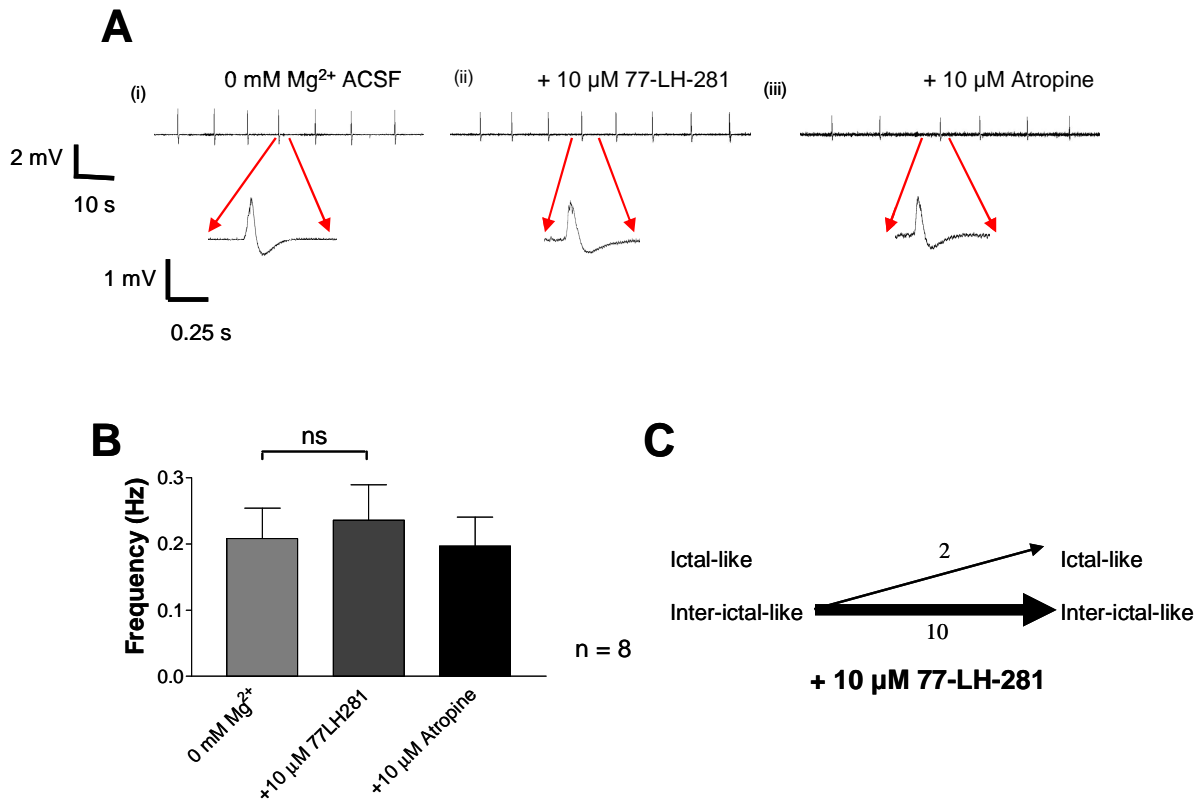
4.2.9 77-LH-281 does not effect low extracellular magnesium-induced network activity

The effect of the 77-LH-281 was then investigated in the low magnesium model. Unlike the effect of $10 \mu\text{M}$ oxotremorine-M on low magnesium-induced inter-ictal-like activity, application of $10 \mu\text{M}$ 77-LH-281 did not induce ictal-like activity in the majority (10/12, see fig 4.2.9 C) of slices tested. Furthermore, application of $10 \mu\text{M}$ 77-LH-281 to inter-ictal-like activity induced by low-magnesium conditions did not lead to a significant ($P = 0.22$) change (0.21 ± 0.05 to 0.24 ± 0.05 Hz, $n = 8$) in the frequency of inter-ictal-like activity. Subsequent application of atropine ($10 \mu\text{M}$) reversed the increase (0.24 ± 0.05 to 0.20 ± 0.04 , $n = 8$) in frequency of oscillatory activity.

4.2.10 The 4-AP/NBQX- induced slow inter-ictal-like activity model

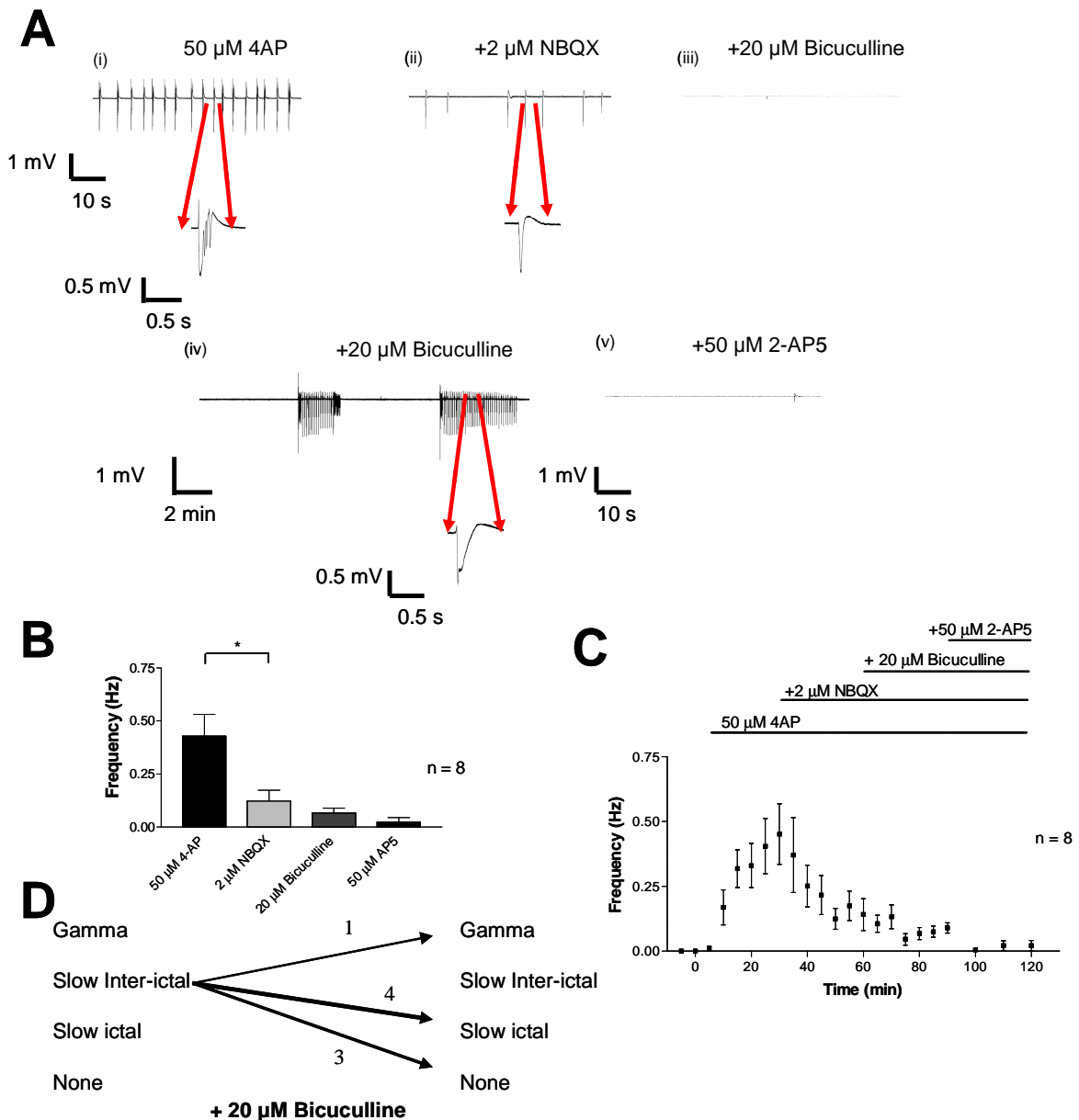
In order to investigate further the role of mAChR acetylcholine receptors in the physiology of oscillatory network activity, it was decided to investigate the role of mAChR activation in a model of reduced excitatory drive. This was achieved by the initial application of 4-AP, as for the epileptiform activity model described previously, and the subsequent application of the AMPA/kainate receptor antagonist NBQX to block AMPA/kainate receptor mediated synaptic transmission in the hippocampal slice. Application of $2 \mu\text{M}$ NBQX caused a significant ($P = 0.039$) decrease in the rate of $50 \mu\text{M}$ 4-AP-induced inter-ictal-like activity (from 0.43 ± 0.07 to 0.15 ± 0.04 Hz, $n = 8$, see fig 4.2.10.B). These events are similar in appearance to inter-ictal like events, but occur much less frequently, and are designated slow inter-ictal-like events henceforth.

Fig 4.2.9. Investigation into the effect of the application of 10 μM 77-LH-281 on low extracellular Mg^{2+} -induced inter-ictal-like activity



A. Representative trace examples showing (i) low-extracellular Mg^{2+} induced inter-ictal-like activity (*inset*- interictal-like event) (ii) the effect of the application of 10 μM 77-LH-281 on low-extracellular Mg^{2+} induced inter-ictal-like activity and (iii) the effect of the subsequent application of the mAChR antagonist atropine (10 μM) (*inset*- interictal-like event). **B.** Summary histogram showing there is no change in inter-ictal-like event frequency upon application of 10 μM 77-LH-281. **C.** Trend chart showing the effect of application of 10 μM 77-LH-281 on low- Mg^{2+} -induced oscillatory activity. Only 2/12 slices change the mode of activity following application of 10 μM 77-LH-281.

Fig. 4.2.10 Characterisation of the 4-aminopyridine/NBQX events.



A. Representative extracellular trace showing intermittent burst discharges in response to application of 50 μ M 4-AP (i). Subsequent co-application of the AMPA receptor antagonist NBQX (2 μ M) results in a slowing and smoothing of the field potential events (ii). Such events were subsequently abolished by application of the GABA_A receptor antagonist bicuculline in 4/8 slices (iii, 20 μ M) suggesting that GABA_A mediated synaptic transmission is implicated in the events. In a number of slices tested (4 of 8) infrequent episodes of field events were noticed (iv) but which occurred at very low frequency (every 243 to 746 s, mean 495 s) and were abolished by NMDA receptor antagonist 2-AP5 (v, 50 μ M). **B.** Summary histogram and **(C)**, time course scatter plot showing effect of cumulative AMPA, GABA_A and NMDA receptor blockade on the frequency of 4-AP-induced hippocampal field events. **D.** Trend chart showing switches in 4-AP/NBQX network activity upon application of bicuculline. Note that the predominant response is a suppression of the slow inter-ictal-like events and the emergence of ictal-like discharges.

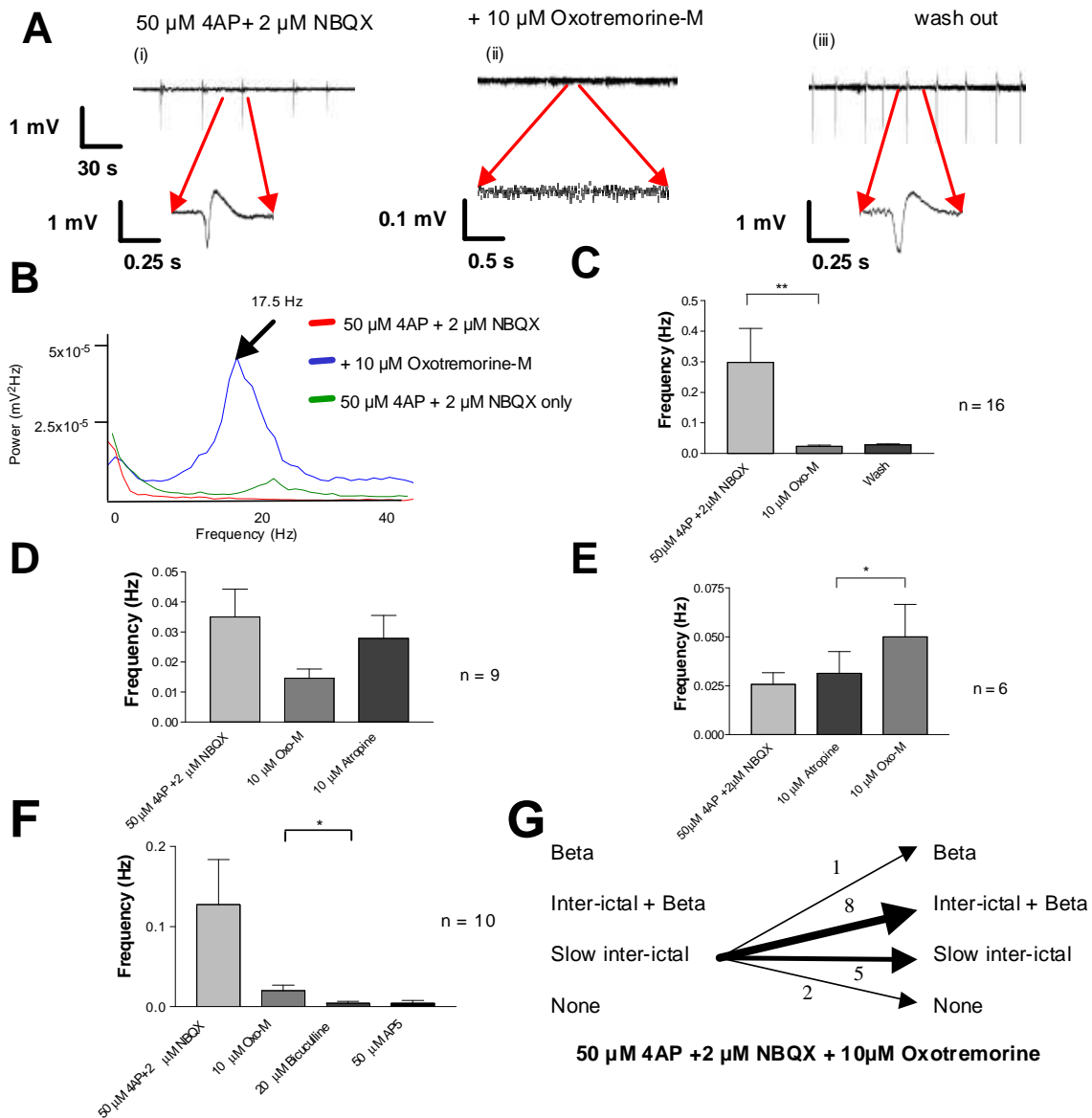
Application of 20 μM bicuculline abolished the slow inter-ictal-like events in 4 slices and led to the emergence of very slow and infrequent ictal-like events in the other 4 of the slices ($0.002 \text{ Hz} \pm 0.001 \text{ Hz}$, $n = 4$). Application of 50 μM 2-AP5 caused near abolition of all remaining activity, with very infrequent field events remaining in 2 slices ($0.02 \pm 0.01 \text{ Hz}$). This is also displayed in the time-frequency scatter plot (fig 4.2.10.C), in which the sequential addition of the above compounds leads to a decrease in field event frequency following each addition. The trend chart (fig 4.2.10.D) shows that application of 20 μM bicuculline abolished the slow inter-ictal-like events in all slices, with 4/8 slices displaying slow ictal-like activity (see fig 4.2.10.A (iv)), and one slice displayed gamma frequency oscillatory activity.

4.2.11 *Oxotremorine-M induces beta frequency oscillations in the 4-AP/NBQX epileptiform model*

The effect of mAChR agonists on a model of reduced excitatory drive was then investigated. As seen above it is possible to isolate slow inter-ictal like events by co-application of 4-AP and NBQX (see fig 4.2.10). Subsequent application of oxotremorine-M allowed insights into the effect of mAChR activation on the interneuronal network. Application of 10 μM oxotremorine-M to 50 μM 4-AP/2 μM NBQX-induced slow inter-ictal like events caused a significant ($P = 0.0012$) mean attenuation (from 0.30 ± 0.11 to $0.024 \pm 0.004 \text{ Hz}$, $n = 16$) in slow inter-ictal like event frequency and an initiation of a beta frequency oscillatory activity in the majority of (9/16) slices (figs 4.2.11.C and G). The decrease in the slow inter-ictal like event frequency was very partially reversible upon wash out of 10 μM oxotremorine-M (the mean event frequency increased from 0.024 ± 0.04 to $0.029 \pm 0.003 \text{ Hz}$).

The majority of the network oscillatory activity induced by the application of 10 μM oxotremorine-M (mean = $17.88 \pm 1.9 \text{ Hz}$, $n = 16$) occurred within the beta frequency range. Both the slow inter-ictal like events and the beta frequency oscillatory activity could be observed concurrently in 50% (13/26) of slices. Network oscillatory activity remained in a subset of (3/9, 33%) slices for at least 30 minutes after washout of oxotremorine-M.

Fig 4.2.11 The effect of oxotremorine-M on 4-AP/NBQX-induced slow inter-ictal-like events



A. Representative trace examples showing (i) regular slow inter-ictal like events observed in response to co-application of 50 μ M 4-AP and 2 μ M NBQX. A regular network oscillation is observed following subsequent application of 10 μ M oxotremorine-M (ii), which is reversible on wash out (iii). **B.** Power spectrum showing this network oscillatory activity to lie within the beta frequency range. **C-F.** Summary histograms showing the frequency of slow inter-ictal-like events. **C.** Application of 10 μ M oxotremorine-M causes a significant decrease in the frequency of the slow inter-ictal-like events. **D.** This effect is reversed by the application of 10 μ M atropine. Application of atropine also abolished the oxotremorine-induced beta frequency oscillation (6/6 slices, data not shown). **E.** Pre-incubation of atropine prevents oxotremorine-induced suppression of slow inter-ictal-like events. There is a significant increase in the frequency of slow inter-ictal-like events. Both the oscillatory activity induced by the application of 10 μ M oxotremorine-M and any residual inter-ictal-like events are abolished by the application of bicuculline (**F**, 20 μ M). **G.** Trend chart showing changes in activity mode following oxotremorine application. Note the induction of beta frequency activity in 9/16 slices investigated following application of 10 μ M oxotremorine-M.

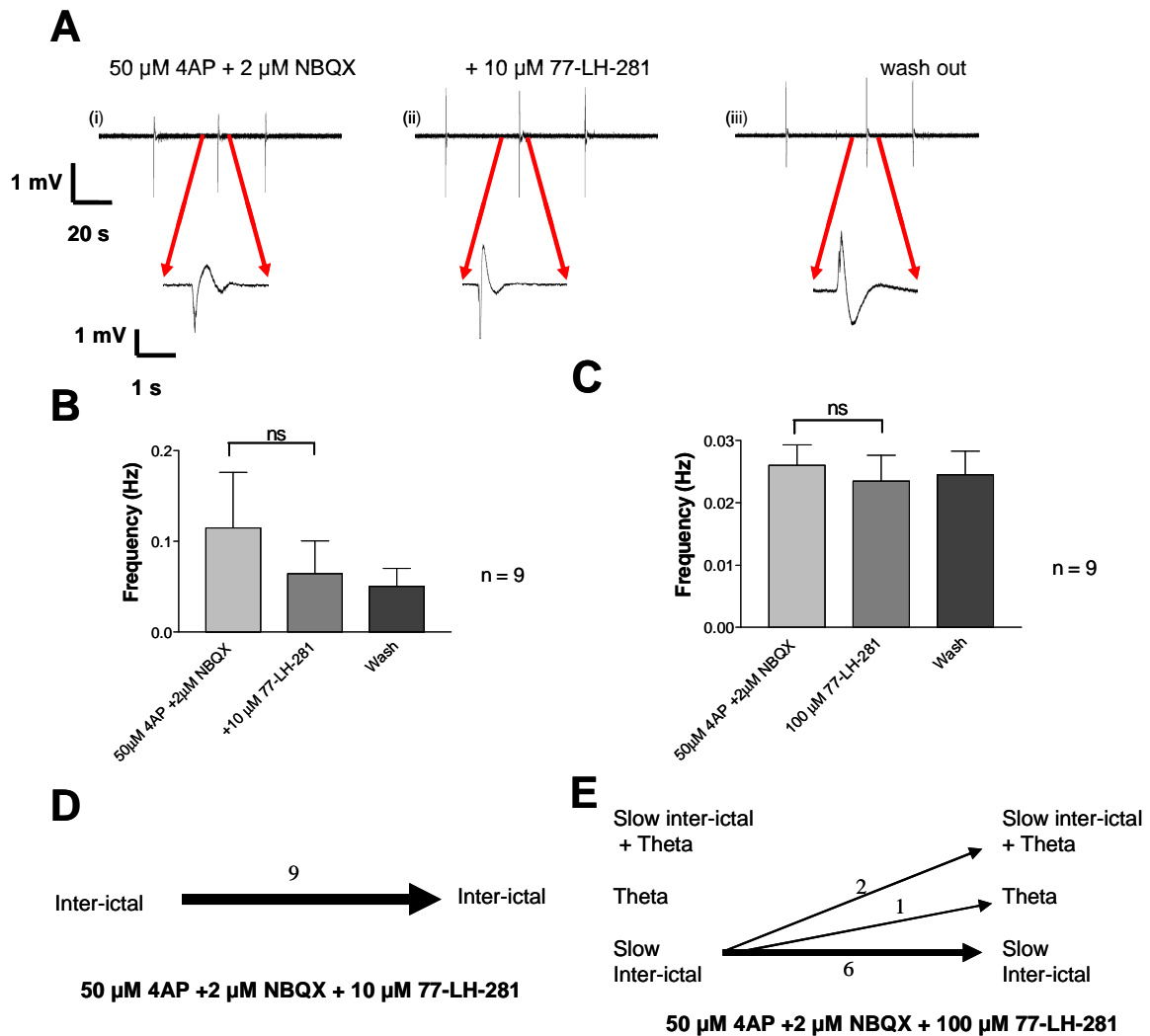
Application of the mAChR antagonist atropine (10 μ M) to the co-applied 50 μ M 4-AP/ 2 μ M NBQX and 10 μ M oxotremorine induced network activity (fig 4.2.11.D) caused an increase in slow inter-ictal like event frequency (0.015 ± 0.003 to 0.028 ± 0.008 Hz, $n = 9$). In other experiments, prior application of 10 μ M atropine prevented attenuation of the 4-AP/NBQX slow ictal-like event frequency by 10 μ M oxotremorine-M (fig 4.2.11.E) indicating that these effects were mediated by mAChRs. There was a significant ($P = 0.031$) increase in the mean slow inter-ictal like event frequency (from 0.031 ± 0.011 to 0.050 ± 0.016 Hz, $n = 6$) following application of 10 μ M oxotremorine-M (fig 4.2.11.E), possibly through nAChR activation. Network oscillatory activity was also prevented by the prior application of 10 μ M atropine ($n = 6$). Application of the GABA_A receptor antagonist bicuculline (20 μ M) abolished the predominant beta frequency network oscillatory activity induced by oxotremorine-M in all slices tested (8/8). The slow inter-ictal like events that were not attenuated by oxotremorine-M were almost abolished (from 0.02 ± 0.006 to 0.004 ± 0.002 Hz, $n = 10$) by subsequent application of 20 μ M bicuculline (fig 4.5.1.F), and the events that remained were small in amplitude and sporadic in occurrence.

4.2.12 *The M₁ mAChR does not mediate the oxotremorine-M-induced oscillations in the 4-AP/NBQX epileptiform model*

Activation of mAChRs changes the mode of activity from 4-AP/NBQX induced slow inter-ictal like events (fig 4.2.10) to beta frequency oscillatory network activity (fig 4.2.11). As selective tools were available to study the M₁ mAChR the role of this receptor in the suppression of 4-AP/NBQX events and induction of beta frequency oscillations was investigated.

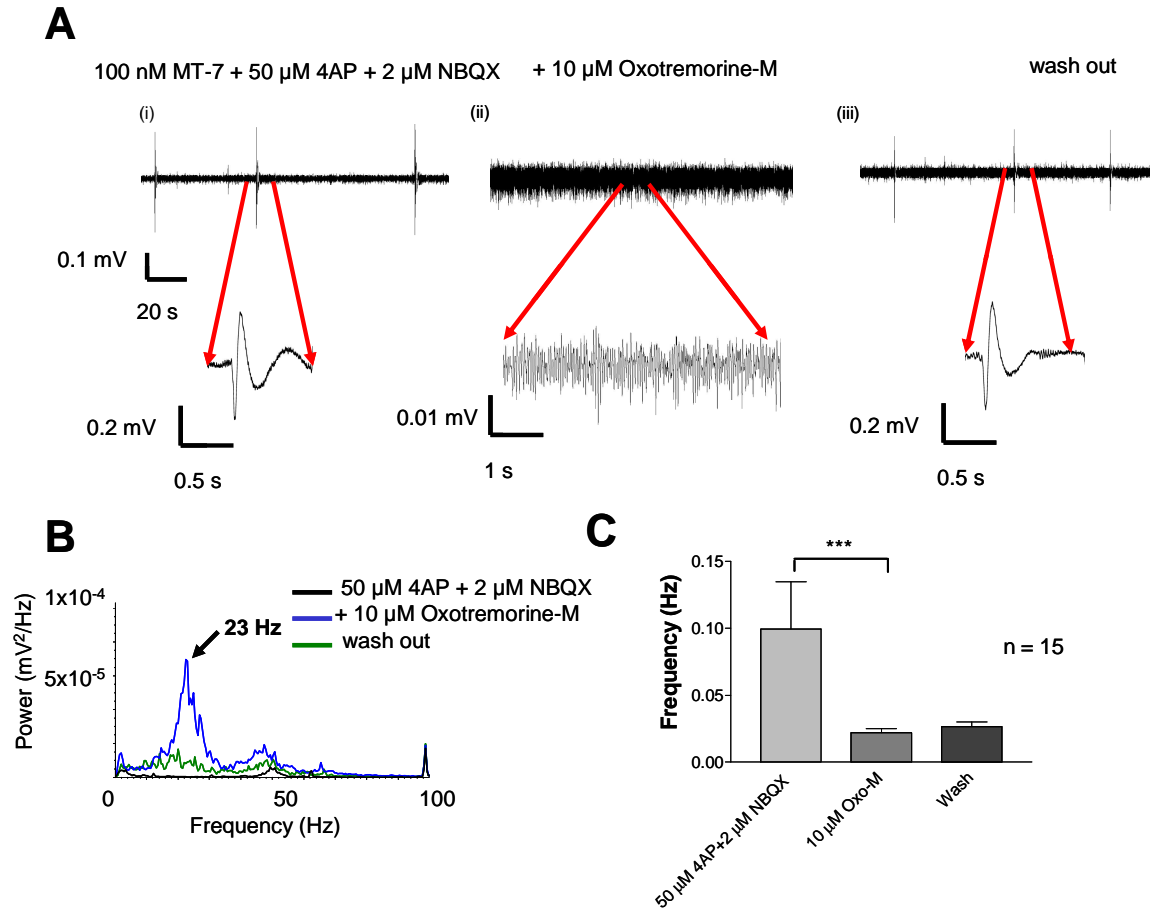
Application of 77-LH-281 (10 μ M) to 4-AP/NBQX induced slow inter-ictal-like events did not lead to significant ($P = 0.36$) attenuation (from 0.11 ± 0.06 to 0.06 ± 0.04 Hz, $n = 9$) of the frequency of the slow inter-ictal-like events (fig 4.2.12.1.B) and did not change the mode of events in any of the slices tested (10/10 slices, fig 4.2.12.1.D). Even at a concentration of 100 μ M (fig 4.2.12.1.C), 77-LH-281 did not significantly ($P = 0.73$) change the slow inter-ictal-like event frequency (from 0.026 ± 0.004 to 0.023 ± 0.003 Hz, $n = 9$).

Fig 4.2.12.1 Investigation into the effect of application of 77-LH-281, a M_1 mAChR selective agonist to 4-AP/NBQX slow inter-ictal like events



A. Representative trace examples showing (i) 4-AP/NBQX-induced slow inter-ictal-like events. The frequency of these events did not change following application of the selective M_1 mAChR agonist, 77-LH-281 (10 μ M) (ii), and did not change upon wash out of 77-LH-281 (iii). **B-C** Summary histograms showing no change in the frequency of slow inter-ictal-like events occurred following application of 10 μ M 77-LH-281 (**B**). **C.** No change in the frequency of slow inter-ictal like events was observed following application of 100 μ M 77-LH-281. **D-E.** Trend charts showing (**D**) no change in network activity following application of 10 μ M 77LH281 to slow inter-ictal like events. Oscillatory network activity is only occasionally observed in response to the application of 100 μ M 77-LH-281 (**E**).

Fig 4.2.12.2 Investigation into role of the M_1 mAChR in the oxotremorine-M induced suppression of 4-AP/NBQX slow inter-ictal like events and the induction of network activity



A. Representative trace examples showing (i) 4-AP/NBQX-induced slow inter-ictal-like events (ii) the effect of 10 μ M oxotremorine-M application and (iii) wash out. The M_1 mAChR was blocked prior to the experiments by application of the specific irreversible M_1 mAChR antagonist MT-7 (100 nM). Application of 10 μ M oxotremorine-M to the 100 nM MT-7, 50 μ M 4AP and 2 μ M NBQX model caused an induction of oscillatory activity within the beta frequency range, shown in the power spectral analysis (**B**). **C.** Summary histogram showing an associated significant decrease in 4-AP/NBQX-induced inter-ictal-like event frequency showing block of the M_1 mAChR has no effect on the suppression of inter-ictal-like event frequency by oxotremorine-M.

At this concentration some theta frequency network oscillatory activity (9.43 ± 1.93 Hz, $n = 3$) was observed in only a minority (33 %, 3/9) of slices.

The M_1 mAChR subtype specific irreversible antagonist MT-7 was used to block the M_1 mAChR receptor. Slices were pre-incubated for >2 hours with 100 nM MT-7 prior to the initiation of 4-AP/NBQX-induced slow inter-ictal like events. In naïve slices this was able to prevent initiation of gamma frequency oscillatory activity (see fig 3.2.3) by the subsequent application of 10 μ M 77-LH-281, but not the emergence of ictal like events following application of 10 μ M oxotremorine-M ($n = 6$, data not shown). Application of 10 μ M oxotremorine-M significantly ($P = 0.0005$) attenuated slow inter-ictal-like event frequency (from 0.10 ± 0.04 to 0.02 ± 0.003 Hz, $n = 15$) and induced oscillatory network activity (fig 4.2.12.2.A) in 55 % (10/18) slices (mean frequency = 14.29 ± 1.9 Hz, $n = 10$). The decrease in slow inter-ictal-like event frequency was partially, but not significantly ($P = 0.44$) reversed following wash out of oxotremorine-M (0.03 ± 0.004 Hz on washout).

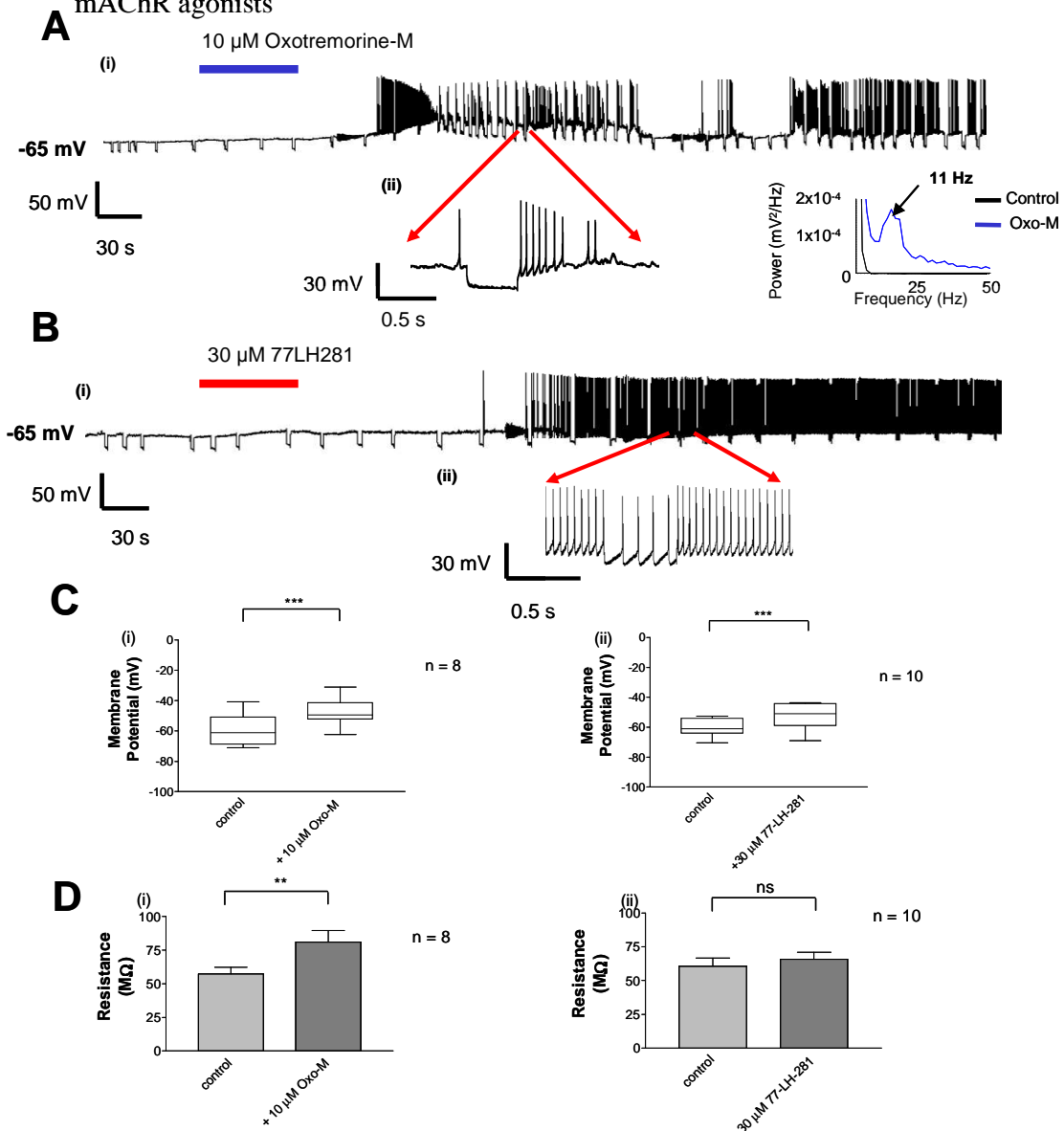
4.3 The modulation of cellular properties of hippocampal pyramidal cells by mAChR agonists

The activation of mAChRs alters the intracellular excitability of neurones (Cole and Nicoll, 1983; , 1984a). This section concerns the effect of the non-selective mAChR agonist oxotremorine-M and the M_1 mAChR subtype specific agonist 77-LH-281 on the intracellular properties of CA1 pyramidal cells.

Comparison of the effects of application of oxotremorine-M and 77-LH-281 on the intracellular properties of CA1 pyramidal cells

Transient application of a bolus of 10 μ M oxotremorine-M for 60 s caused a depolarisation of pyramidal cells and action potential firing (fig 4.3.A). Application of a 60 s bolus of the M_1 mAChR agonist 77-LH-281 (30 μ M) also led to action potential firing and membrane depolarisation (fig 4.3.B). The membrane potential depolarisations induced by both 10 μ M oxotremorine (from -59.1 ± 3.8 to -47.5 ± 3.3 mV, $n = 8$) and by 30 μ M 77-LH-281 (-60.0 ± 1.8 to 52.5 ± 2.6 mV, $n = 10$) (fig 4.3.C) were statistically significant ($P < 0.001$).

Fig 4.3 Characterisation of the CA1 pyramidal cell response to the application of mAChR agonists



A. Representative current clamp recording from a CA1 pyramidal neurone showing (i) the response of the cell to a 60 s application of 10 μ M Oxotremorine-M (ii) expanded trace showing action potential firing (*inset*- power spectrum showing theta frequency sub-threshold membrane potential oscillation). Note the strong suprathreshold depolarising response. **B.** Representative current clamp recording from a CA1 pyramidal cell showing (i) the response of the cell to a 60 s application of 30 μ M 77-LH-281 (ii) expanded trace showing action potential firing. Hyperpolarising membrane deflections in response to 0.1 nA current injections can be observed in both **A** and **B**. **C.** Box plots showing the significant depolarisation of the pyramidal cell induced by the application of (i) 10 μ M Oxotremorine-M and (ii) 30 μ M 77-LH-281. **D** Summary histograms showing (i) the significant increase in input resistance with application of 10 μ M Oxotremorine-M ($P < 0.01$) and (ii) no change in input resistance following the application of 30 μ M 77-LH-281.

The mean input resistance of the pyramidal cells significantly ($P = 0.0078$) increased from 57.3 ± 5.0 to 80.8 ± 8.7 M Ω in response to application of 10 μ M oxotremorine-M whereas there was no significant change in the input resistance (from 60.6 ± 6.0 to 65.7 ± 5.1 M Ω , $P = 0.28$, $n = 8$) following application of 30 μ M 77-LH-281 (fig 4.3.D).

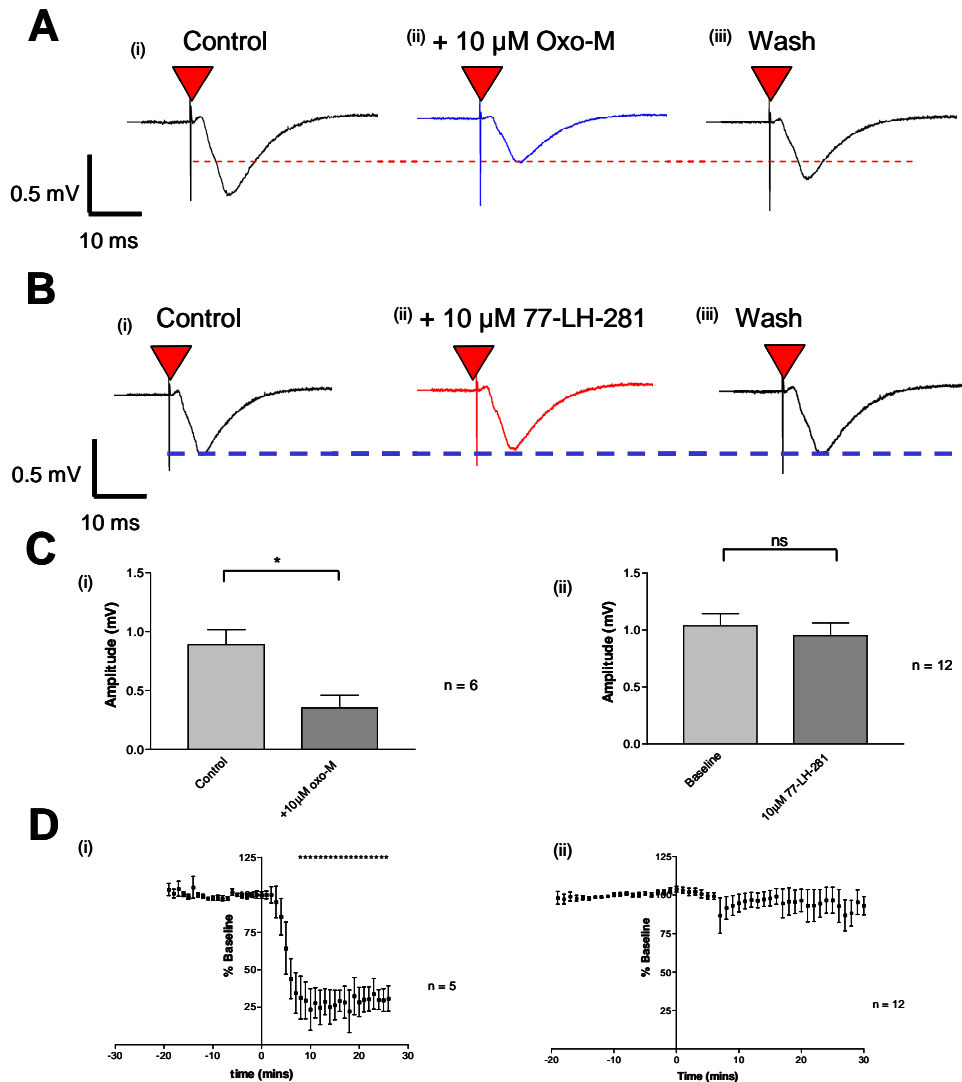
4.4 The modulation of synaptic properties of the hippocampus by mAChR agonists

The effect of the application of mAChR agonists on the synaptic properties of the hippocampus can be investigated by stimulating the Schaffer collaterals in the *stratum radiatum* and recording the field excitatory post-synaptic potential (fEPSP) in the same lamina of the CA1 region. Parameters of the fEPSP, including the amplitude, can be modulated by compounds that affect synaptic transmission at the Schaffer collateral to CA1 pyramidal cell synapse.

Comparison of the effects of oxotremorine-M and 77-LH-281 on the field excitatory post-synaptic potential

Application of 10 μ M oxotremorine-M significantly ($P = 0.031$) reduced the mean ($n = 6$) amplitude of the fEPSP (from 0.89 ± 0.13 mV to 0.35 ± 0.11 mV) (mean \pm S.E.M.). In contrast the mean ($n = 12$) amplitude of the fEPSP was not significantly altered (1.04 ± 0.11 mV to 0.95 ± 0.11 mV, $n = 12$, $P = 0.47$) by 10 μ M 77-LH-281 (fig 4.4.C). Application of 100 μ M 77-LH-281 also did not have a significant effect on the amplitude of the fEPSP. The mean ($n = 6$) amplitude of the fEPSP was significantly reduced 6 minutes after application of 10 μ M oxotremorine-M (all $P < 0.05$ following this time point) whereas application of 10 μ M 77-LH-281 produced no significant change in the mean ($n = 12$) amplitude of the fEPSP at any time point (fig 4.4.D).

Fig 4.4 Characterisation of the effect of mAChR agonist application on the field excitatory post-synaptic potential



A. Representative trace examples showing (i) the field excitatory post-synaptic potential (fEPSP), (ii) the effect of application of 10 μ M oxotremorine-M on the fEPSP and (iii) washout of oxotremorine-M. Triangle shows the point of stimulus. **B.** Representative trace examples showing (i) fEPSP, (ii) the effect of application of 10 μ M 77-LH-281 on the fEPSP and (iii) wash out of 77-LH-281. **C.** Summary histograms showing the amplitude of the fEPSP as measured 30 minutes after application of 10 μ M oxotremorine-M compared to 5 minutes before oxotremorine application. Application of 10 μ M oxotremorine-M leads to a significant decrease in the amplitude of the fEPSP whereas application of 10 μ M 77-LH-281 has no effect on the amplitude of the fEPSP. **D.** Time course showing the significant decrease of the amplitude of the fEPSP in response to application of 10 μ M oxotremorine-M (i) and no significant change in the amplitude of the fEPSP in response to application of 10 μ M 77-LH-281 (ii).

4.5 Discussion

This chapter investigates the effect of mAChR agonists upon network oscillatory activity within the hippocampus. In the previous chapter oxotremorine-M induced ictal-like events whilst the M₁ mAChR selective agonist 77-LH-281 led to persistent gamma frequency network oscillatory activity. In order to gain mechanistic insight into the different oscillations that were displayed, and to evaluate whether M₁ mAChR selective agonists display a similar pro-epileptogenic potential to non-subtype selective agonists, 77-LH-281 and oxotremorine-M were applied to four mechanistically distinct models of epileptiform activity. The cellular and synaptic effects of 77-LH-281 were also investigated and compared with oxotremorine-M. A summary of activities induced by mAChR agonists in hippocampal slices is displayed in table 2 below.

Table 2- Summary of effects of mAChR agonists in naïve coronal hippocampal slices and hippocampal slices displaying oscillatory activities

Drug	Naïve slices	4-AP-induced events	Bicuculline-induced events	Low Mg ²⁺ -induced events	4-AP/NBQX-induced events
Control conditions (vehicle)	No activity	Inter-ictal	Inter-ictal	Inter-ictal	Slow inter-ictal
Oxotremorine-M	Theta oscillations	Ictal Events	Ictal events	Ictal events	Beta oscillations
77-LH-281	Gamma oscillations	No effect	Increase in inter-ictal-like event frequency	No effect	No effect

4-AP-induced events

The mAChR agonists were initially applied to 4-AP-induced inter-ictal type network activity. 4-AP blocks K⁺ channels that mediate, including others, the I_D current, a slowly inactivating K⁺ current (Storm, 1988) and the I_A current, a transient outward K⁺ current (Huguenard et al. 1991). As 4-AP washes into the hippocampal slice, the

blockade of these K^+ currents leads to paroxysmal depolarising shifts within the pyramidal cells of the CA3 region (Perreault and Avoli, 1991). The synchronised activity of large numbers of pyramidal cells, specifically currents within the dendrites of pyramidal cells, produces the potential difference measured in hippocampal extracellular recordings. The depolarising shifts are likely to arise from the synaptic activation of a large number of cells (Gutnick et al., 1982). This is measured as the characteristic inter-ictal-like event as shown in figure 4.2.1., which can be abolished by bicuculline (Avoli et al., 1996), and reduced in frequency by NBQX (see fig 4.2.10; (Perreault and Avoli, 1992). Thus both glutamatergic and GABAergic networks are activated following application of 4-AP (Rutecki et al., 1987).

Application of oxotremorine-M produced an initial increase in inter-ictal event frequency, followed by the eventual emergence of ictal-like activity. As was mentioned in the previous chapter, application of oxotremorine can activate all subtypes of mAChRs (Birdsall et al., 1978; Kukkonen et al., 1996). The M_1 or M_3 mAChRs are located principally on pyramidal cells (Levey et al., 1995; Rouse et al., 1999) and they couple through $G\alpha_q$ G-proteins. Activation of these receptors depolarises pyramidal cells, as shown in figure 4.3. The paroxysmal depolarising shift frequency is independent of the membrane potential of individual pyramidal cells, but is dependent on $[K^+]_o$ (Rutecki et al., 1985). As depolarisation of pyramidal cells and consequent action potential firing of pyramidal cells can cause activity dependent increases in $[K^+]_o$ (Poolos et al., 1987), this is one possible mechanism for the increase in frequency of inter-ictal-like events. This is clearly related to the level of depolarisation in each pyramidal cell, but the effect is observed at the level of the network. It is likely that the number of action potentials within the network, which is proportional to the level of depolarisation of the pyramidal cells within the network, regulates the frequency of paroxysmal depolarisation shifts within pyramidal cells. In short, a depolarisation of pyramidal cells will act to increase the frequency of inter-ictal-like events.

Oxotremorine-M also activates the inhibitory M_2 and M_4 mAChRs. The majority of these receptors are located on pre-synaptic interneurons (Kitaichi et al., 1999; Rouse et al., 1999). They act to decrease $GABA_A$ mediated inhibition to pyramidal cells by

disrupting the release of GABA where $M_{2/4}$ mAChRs are expressed. As observed in the bicuculline model, reducing GABA_A mediated inhibition is pro-epileptogenic. They also act to decrease GABA_B activation through reduced GABA release. Both agonists of GABA_B, through the activation of pre-synaptic GABA_B receptors and inhibition of GABA release (Motalli et al., 1999), and antagonists, through the block of post-synaptic GABA_B mediated inhibition of pyramidal cells (Motalli et al., 2002), have been shown to be pro-convulsant in models of epileptiform activity. This indicates that the effects of presynaptic disruption of GABA release and consequent removal of GABA_B activation by $M_{2/4}$ mAChR activation are complex. Pre-synaptic GABA_B activation leads to inhibition of transmitter release by a reduction in Ca^{2+} entry (Huang et al., 2006), whereas post-synaptic GABA_B activation acts to hyperpolarise pyramidal cells through the action of inwardly rectifying potassium channels (Andrade et al., 1986; Pham and Lacaille, 1996).

In the main this increase in inter-ictal-like event frequency caused by oxotremorine-M is superseded by the emergence of ictal-like events. As mentioned in the previous chapter, ictal-like events emerge following a reduction of inhibition from interneurons either by depolarising block of the interneurons (Ziburkus et al., 2006), or by a reversal of the chloride gradient allowing GABA_A activation to become excitatory (Isomura et al., 2003). To induce ictal activity in the network oxotremorine-M must also remove inhibition from interneurons. This may be through a direct inhibition of GABA release through $M_{2/4}$ mAChRs as described above. It is also possible that an increased excitatory drive to the pyramidal cells leads to either a feed-forward depolarisation block of interneurons, or an activity dependent reversal of the chloride gradient (Fischer et al., 1999).

77-LH-281 did not have an effect on the network activity that emerged from hippocampal slices in which inter-ictal-like events were ongoing following the application of 4-AP. The M_1 mAChR induced depolarisation of pyramidal cells, which should increase the probability of, and therefore frequency of, paroxysmal depolarising shifts, did not lead to a subsequent significant increase in frequency of inter-ictal-like events. It is possible that increased pyramidal cell activity led to a consequent increase in inhibitory feedback from the interneurons in the network. Without the reduction in inhibition following $M_{2/4}$ mAChR activation, the inter-ictal-

like event frequency remained constant. It is also possible that M_3 mAChRs, located on the pyramidal cells, are required in combination with M_1 mAChRs to increase the frequency of inter-ictal-like events.

Following application of the M_1 specific mAChR agonist 77-LH-281 ictal events are not observed. This indicates that the removal of GABAergic inhibition that occurs during ictal-like events does not occur following activation of the M_1 mAChR alone. This could be due to the absence of $M_{2/4}$ mAChR mediated inhibition of interneurons. As M_1 mAChRs do not increase the rate of inter-ictal-like events it is also possible feed-forward depolarisation block of interneurons, or an activity dependent change in the equilibrium potential of GABA, does not occur. As there are a range of possible mechanisms for the absence of ictal-like events following application of 77-LH-281, mechanistically distinct epileptiform models were used to investigate the differences between M_1 -selective and non subtype selective mAChR agonists.

Bicuculline-induced events

Bicuculline is an antagonist of $GABA_A$ receptors, which are the most widely expressed ligand gated anion channels in the central nervous system. Blockade of these channels leads to a removal of fast $GABA_A$ mediated potentials in the hippocampus. The emergence of epileptiform phenomena is dependent upon the balance of excitation and inhibition (Bernard, 2005). Removal of $GABA_A$ mediated synaptic transmission leads to the gradual emergence of inter-ictal-like events through the removal of IPSPs, and consequent increased summation of EPSPs within each pyramidal cell (Pouille and Scanziani, 2001), leading to more supra-threshold action potential firing. This is manifest as paroxysmal depolarising shifts within pyramidal cells and inter-ictal-like events throughout the network.

Activation of M_{1-5} mAChRs by oxotremorine-M leads to an increase in inter-ictal-like event frequency and the emergence of ictal-like events. This indicates that a reduction in $GABA_A$ mediated synaptic transmission is not the sole driving force behind a mAChR-induced increase in inter-ictal-like event frequency or the emergence of ictal-like activity. As for the 4-AP model described above, a depolarisation of pyramidal

cells through M_1 and M_3 mAChR activation would lead to an activity dependent increase in the frequency of paroxysmal depolarisation shifts within pyramidal cells. Through the action of M_2 and M_4 mAChRs pre-synaptic disruption of GABA release occurs. However, as $GABA_A$ receptors are blocked in this model, any change in the level of inhibition will be mediated by the reduction in pre-synaptic and post-synaptic $GABA_B$ activation.

In the presence of bicuculline, activation of M_{1-5} mAChRs often leads to the emergence of ictal-like activity. As mentioned above, there are two hypotheses concerning the emergence of ictal-like activity in hippocampal slices. In the first, a depolarising block of interneurons contributes to the removal of inhibition from the network (Ziburkus et al., 2006); in the second a reversal of the chloride gradient allows $GABA_A$ -mediated synaptic transmission to become depolarising (Isomura et al., 2003). In the presence of bicuculline, a removal of inhibition, rather than depolarising GABA transmission, is likely to contribute to ictal-like activity. As ictal-like events are not induced by bicuculline, other reductions in inhibitory drive must occur, most likely through the modulation of $GABA_B$.

Pyramidal cells display a long sustained depolarisation during an ictal-like event (Ziburkus et al., 2006). These transient depolarisations are correlated with the depolarisation block of interneurons. It is possible that postsynaptic $GABA_B$ mediated potentials tonically prevent the emergence of ictal-like events within pyramidal cells, and the disruption of these by a reduction in GABA release by $M_{2/4}$ mAChRs may allow ictal-like events to occur (Kitaichi et al., 1999; Levey et al., 1995; Rouse et al., 1999).

The depolarisation block of interneurons is possible contributor to the removal of $GABA_B$ mediated inhibition. This could arise following direct activation of mAChRs on interneurons (Chapman and Lacaille, 1999), or increased feed-forward activation of interneurons following increased pyramidal cell activity due to actions of mAChR agonists.

Further evidence for the key role interneurons (and therefore $GABA_B$ receptors) play in mediating ictal-like events is the absence of ictal-like events in the bicuculline

model following selective M_1 mAChR activation by 77-LH-281. The predominant pyramidal cell expression of M_1 mAChRs means subtype-selective activation of the M_1 mAChR would not disrupt GABA release from interneurons.

In the presence of bicuculline application of the M_1 mAChR agonist 77-LH-281 causes a significant increase in the frequency of inter-ictal-like events. In the presence of GABA_A mediated synaptic inhibition, M_1 mAChR activation does not increase the frequency of inter-ictal-like events. The depolarisation of pyramidal cells caused by M_1 mAChR activation, in combination with the removal of feedforward inhibition allows an increase in the frequency of paroxysmal depolarising shifts.

Zero Mg^{2+} -induced events

The removal of Mg^{2+} ions from the extracellular bathing solution surrounding the hippocampal slice removes the Mg^{2+} block of NMDA receptors, which leads to inter-ictal-like network activity emerging from the CA3 region (Tancredi et al., 1988). The NMDA receptors are located on the dendrites of pyramidal cells and are normally quiescent at polarised potentials following glutamate release due to the Mg^{2+} block. However, strong activation of AMPA/kainate receptors leads to a removal of the Mg^{2+} block by depolarisation, which opens the NMDA receptor channel to allow Na^+ and Ca^{2+} entry and further depolarisation (Dingledine et al., 1999). In low- Mg^{2+} bathing solution, the level of basal NMDA receptor-mediated transmission is enough to induce synchronous activity in the hippocampus (Traub et al., 1994). This depolarisation of the pyramidal cell decreases the seizure threshold (Tancredi et al., 1990) and leads to the emergence of inter-ictal-like events.

As in the previous models, oxotremorine-M initially increases the frequency of inter-ictal-like events and eventually induces ictal-like activity in the low Mg^{2+} model. The increase in inter-ictal like event frequency is likely to be due to an increase in the probability of action potential firing following depolarisation of pyramidal cells, in combination with a reduction of GABAergic inhibition through the action of $M_{2/4}$ mAChRs. Similarly, ictal-like events emerge during a transient further reduction of (potentially GABA_B) mediated inhibition. The mAChRs associated with the increase in inter-ictal-like event frequency and induction of ictal events exerts their effects

through mechanisms distinct from the modulation of the voltage dependency of the NMDA receptor.

In contrast to the bicuculline-induced model of epileptiform activity, application of the M_1 mAChR agonist 77-LH-281 does not increase the frequency of inter-ictal-like events induced by the removal of extracellular Mg^{2+} ions. M_1 mAChR activation has been shown to regulate NMDA receptor function, including increasing NMDA receptor mediated LTP (Marino et al., 1998; Shinoe et al., 2005). As the M_1 mAChR agonist has no effect in this model, it is possible the effects of the M_1 mAChR activation are occluded by the removal of the Mg^{2+} block of the NMDA receptor. If this is the case then the M_1 mAChR may have little or no role in the induction of ictal-like events caused by oxotremorine-M, as robust ictal-like events are induced even whilst the M_1 mAChR is functionally occluded. Further evidence for this is the ability of oxotremorine-M to initiate ictal events in the presence of MT-7.

Application of nicotinic acetylcholine receptor (nAChR) agonists has previously been demonstrated to enhance the frequency of inter-ictal-like events in the three epileptiform models investigated above (Roshan-Milani et al., 2003). Oxotremorine-M enhances the 4-AP-induced events by $80 \pm 34\%$, the bicuculline induced events by $270 \pm 112\%$, and the low- Mg^{2+} induced events by $105 \pm 79\%$. This corresponds to the enhancement of 4-AP-induced events by approximately 50%, the bicuculline induced events by 220%, and the low- Mg^{2+} induced events by 100% by nAChR agonists. The similarity in the ratios of enhancement in the three models may be due to convergence of the mechanisms of frequency potentiation by the acetylcholine receptor agonists in the individual models. Also, the maximum possible degree of frequency potentiation, and the initial frequency of the oscillatory activity, is dependent on the paradigm used to induce the inter-ictal-like activity.

4-AP/NBQX induced events

Application of NBQX to 4-AP-induced events leads to the abolition of the majority of AMPA/kainate mediated synaptic transmission within the hippocampus. All inter-ictal-like activity, which is underpinned by paroxysmal depolarising shifts, is not abolished by glutamate receptor block. EPSPs received from other pyramidal cells

through AMPA/kainate receptors are significant contributors to paroxysmal depolarisation shifts within pyramidal cells (Chamberlin et al., 1990). The slow inter-ictal-like activity that occurs in the presence of NBQX indicates that other mechanisms must be able to initiate paroxysmal depolarisations. It is possible that the competitive block of AMPA/kainate receptors is overcome due to increased glutamate release in an active network (Hamberger et al., 1979), or another mechanism, such as depolarising GABAergic potentials from interneurons (Perreault and Avoli, 1992), synchronously activates the pyramidal cell network. The remaining slow inter-ictal-like events are abolished by bicuculline, indicating that the GABA_A receptor mediated signalling is critically important for the slow inter-ictal-like events. NMDA receptors are functional in this model as well, as the GABA_A antagonism reveals very infrequent 2-AP5 sensitive ictal-like-events in 50% of the slices. NMDA antagonists were not routinely used in as subsequent addition of NMDA antagonists does not affect inter-ictal-like event frequency in the presence of AMPA/kainate antagonists (Perreault and Avoli, 1992). It is possible therefore, that the effect of the NMDA receptor is only revealed following removal of the dominant GABA_A component of the oscillatory activity.

The strident differences between the effect of oxotremorine-M in this and the 4-AP model indicate NBQX is effective in reducing AMPA/kainate glutamatergic synaptic transmission. In hindsight, if a dose response relationship between inter-ictal-like event frequency and NBQX concentration was constructed, a concentration that had more evidence for the complete block of AMPA/kainate receptors could have been chosen.

Application of the mAChR agonist oxotremorine-M significantly decreases the frequency of slow inter-ictal-like events and predominantly induces beta frequency network oscillations. The oscillation and the slow inter-ictal-like events are not mutually exclusive, as in up to 50% of slices both occurred simultaneously. The suppression of the slow inter-ictal-like events and the beta frequency oscillation in the presence of NBQX are clearly dissimilar to the increase in inter-ictal-like event frequency and ictal-like events induced by oxotremorine-M and 4-AP alone. In the absence of AMPA/kainate receptor blockade mAChR agonists increase the frequency of inter-ictal-like events due to the depolarisation of pyramidal cells and a decrease of

GABAergic inhibition (see above). In the presence of AMPA/kainate receptor antagonists, mAChR agonists decrease the frequency of slow inter-ictal-like events.

The decrease in slow inter-ictal-like event frequency is possibly due to a change in the $[K^+]_o$, which could be investigated using ionic electrodes. It is more likely to be due to a change in the network connections involved in the initiation of the slow inter-ictal-like events. One way this decrease in frequency could occur would be to decrease GABA release from interneurons (Behrends and ten Bruggencate, 1993). Inter-ictal-like events are correlated with an increase in EPSPs within pyramidal cells. If these EPSPs are received through depolarising GABA_A potentials (as suggested by the Avoli group) a mAChR mediated decrease in GABA release would act to decrease the frequency of inter-ictal-like events. Another would be to activate different classes of interneurons directly, or through the modulation of NMDA receptor mediated transmission, to initiate other forms of synchronous activity within pyramidal cells. It is unlikely that these changes in oscillation mode and frequency are direct effects of mAChR activation on pyramidal cells, as M₁ mAChR activation does not replicate the decrease in slow inter-ictal-like event frequency.

Rather than the induction of ictal-like events, oxotremorine-M induced beta frequency oscillatory activity. This oscillation was sensitive to the subsequent application of bicuculline, indicating that the oscillation was dependent upon GABA_A receptors, and thus interneurons play a continuous role in the oscillation. A feature of ictal-like events is the depolarisation block of interneurons, or a shift in the chloride reversal potential so that GABA becomes excitatory. Stratum oriens-lacunosum moleculare interneurons undergo depolarisation block during ictal-like events (Ziburkus et al., 2006), whereas fast spiking and non-fast spiking perisomatic-targeting interneurons are able to continue to fire action potentials (Fujiwara-Tsukamoto et al., 2004). These are likely to be the dominant class of interneurone in the coronal slices, are depolarised by the action of mAChR s and therefore potentially able to pace beta frequency oscillatory activity (McMahon et al., 1998).

Given the requirement of GABA_A receptors signalling, and the absence of AMPA/kainate mediated EPSPs, an attractive mechanism for the generation of the beta frequency oscillation is a depolarising GABA_A signal, with GABAergic IPSPs at

beta frequencies acting as the pacemaker. Another possible component of the oscillation is the depolarising block of interneurons removing GABA_B mediated inhibition and allowing the emergence of the beta frequency oscillatory activity.

In order to confirm this, intracellular recordings from pyramidal cells and perisomatic targeting interneurons would need to be performed, alongside labelling the interneurons to assess their morphology. This experiment would give great insight into the mechanism of the network shift from slow inter-ictal-like events into beta frequency oscillatory activity. It would be interesting to investigate the role of NMDA receptors in the oscillation, as it is possible these receptors are revealed by a change in the GABA mediated synaptic transmission following activation of mAChRs.

Beta oscillations have previously been reported in the hippocampus following application of carbachol (Arai and Natsume, 2006; Shimono et al., 2000), metabotropic glutamate receptor agonists (Boddeke et al., 1997), and tetanic stimulation (Traub et al., 1999). In all of the models the oscillation is insensitive to block of fast glutamatergic synaptic transmission and sensitive to block of synaptic inhibition, indicating that the beta oscillation that occurs in the presence of 4-AP/NBQX/oxotremorine-M has a similar pharmacological profile as previously reported beta frequency oscillations.

Activation of the M₁ mAChR has no effect on the slow inter-ictal-like event frequency and does not induce beta frequency oscillatory activity. This suggests that the M₂₋₅ mAChRs mediate the induction of the beta frequency oscillation and the suppression of slow inter-ictal-like event frequency. This is expected with the majority of M₁ mAChRs being expressed on pyramidal cells (Rouse et al., 1999). The absence of effect of 77-LH-281 in this model is consistent with the reported absence of effect of NMDA antagonists, as M₁ mAChRs modulate NMDA receptors (Shinoe et al., 2005; Perreault and Avoli, 1992).

The effect of mAChR agonists on pyramidal cells

Application of mAChR agonists to CA1 hippocampal pyramidal cells leads to a depolarisation of pyramidal cells by approximately 8 mV and action potential firing,

which corresponds to previous studies (Cole and Nicoll, 1984a; Williams and Kauer, 1997). There is an increase in input resistance within pyramidal cells following application of oxotremorine-M, which is not apparent following application of 77-LH-281. Activating M_1 mAChR alone can depolarise pyramidal cells. The selective activation of the M_1 mAChR activates the hyperpolarisation activated current, I_h , and the non-specific cation conductance, I_{cat} (Fisahn et al., 2002). Opening these channels would, if anything, decrease input resistance. The depolarisation that occurs following M_1 mAChR activation is likely to be mediated by both of these mixed cation currents, as the reversal potential of I_h is around -17 mV and the reversal potential of I_{cat} is around -20 mV (Colino and Halliwell, 1993; Maccaferri et al., 1993).

The increase in input resistance that occurs following application of oxotremorine-M is due to the action of the M_{2-5} mAChRs on a range of conductances. Non subtype selective mAChR agonists modulate a range of conductances including the activation of the I_h and I_{cat} , as mentioned above, and the suppression of a slow Ca^{2+} -activated K^+ current I_{AHP} , the voltage and time dependent K^+ current I_M , and the voltage and time independent I_{leak} (Cole and Nicoll, 1984a; Colino and Halliwell, 1993; Halliwell and Adams, 1982). Previous reports suggest the increase in input resistance is mainly from the suppression of the I_{AHP} and the I_M and the closing of the channels associated with these conductances (Cole and Nicoll, 1984a). There is no significant change in input resistance following the selective activation of the M_1 mAChR by 77-LH-281, as selective activation of the M_1 mAChR does not affect these currents. The absence of activation of I_M by M_1 mAChR selective agonists is another possible contributing factor in the lack of epileptogenic effects of these agonists, as activation of I_M has been shown to be pro-epileptogenic (Pena and Alavez-Perez, 2006).

The effect of mAChR agonists on evoked potentials

The fEPSP experiments were conducted at the Schaffer collateral to CA1 pyramidal cell synapse. Application of oxotremorine-M leads to a significant decrease in the amplitude and the slope of the fEPSP, whereas application of 77-LH-281 has no significant effect on the fEPSP. This strongly supports the suggestion that the decrease of the amplitude and the slope of the fEPSP induced by mAChRs is not mediated by the M_1 mAChR subtype. Previous studies have shown that synaptic

transmission at the Schaffer collateral-CA1 pyramidal cell synapse is reduced in amplitude by mAChR activation by approximately 40% in the stratum radiatum (SR), whereas in the stratum lacunosum-moleculare (SLM) synaptic transmission is reduced by up to 90% (Hasselmo and Schnell, 1994). As wide low resistance electrodes were utilised in these experiments it is possible that both the SR and SLM were recorded from, as demonstrated by the approximately 60% reduction in fEPSP amplitude by oxotremorine-M.

It is likely that the fEPSP is decreased by the action of the M_2 and/or M_4 receptors, as they are located presynaptically (Levey et al., 1995) and are linked to a decrease in Ca^{2+} entry into the neurone through N-type Ca^{2+} channels, a process vital for synaptic vesicle release (Caulfield and Birdsall, 1998). Paired pulse experiments have shown that the mAChR effect on the Schaffer collateral-CA1 synapse is a presynaptic effect (de Sevilla et al., 2002; Kuhnt and Voronin, 1994).

4.6 Conclusion

In this chapter the networks that underlie cholinergic induction of oscillatory activity in the hippocampus was investigated. The M_1 subtype selective mAChR agonist 77-LH-281 does not induce ictal-like activity in a range of models of epileptiform activity in the hippocampus, whereas application of the mAChR agonist oxotremorine-M leads to ictal-like activity.

As well as this, insight into the mechanisms that underlie the ictal events observed in the hippocampus can be gained. Fast glutamatergic transmission is required for both the M_1 -induced gamma frequency oscillation and ictal-like activity (see chapter 3), but fast $GABA_A$ mediated transmission is not required for ictal-like events.

Only in the presence of bicuculline does selective activation of the M_1 mAChR lead to an increase in the frequency of inter-ictal-like events. M_1 mAChR agonists acting through the activation of I_{cat} depolarise pyramidal cells, leading to an increased probability of action potential firing. In the bicuculline model as there would be no increase in IPSPs on pyramidal cells as interneurons are activated, the frequency of paroxysmal depolarisations increases. In the absence of fast glutamatergic

transmission activation of the M_1 mAChR receptor has no effect on the network activity. Therefore the M_1 mAChR is almost certainly acting predominantly through pyramidal cells of the CA3 region.

The above chapter indicates that M_1 subtype selective mAChR agonists display many of the desirable characteristics required for a nootropic compound. These include the potential to initiate gamma frequency oscillations, and a lower potential than classical mAChR agonists to promote epileptiform activity. Although many further safety and efficacy studies would need to be performed to confirm both the safety profile and potential of this compound to be pro-cognitive, these studies indicate that M_1 subtype selective mAChR agonists are a safer class of compound to use than non-subtype selective mAChR agonists as cognitive enhancing drugs.

5 The effect of ampakines on hippocampal neurophysiology

5.1 Introduction

This chapter investigates the effect of ampakines on hippocampal slices. Ampakines are positive allosteric modulators of AMPA-type glutamate receptors, which are the most highly expressed receptor in the central nervous system (Dingledine et al., 1999). AMPA receptors are ionotropic glutamate receptors and mediate fast excitatory synaptic transmission. Ampakines positively modulate AMPA receptors by (i) increasing the conductance of the AMPA receptor, (ii) increasing the time to channel deactivation, or (iii) preventing desensitisation of the AMPA receptor (Lynch, 2004).

Ampakines are known to be pro-cognitive in rats (Lockhart et al., 2007), and humans (Ingvar et al., 1997). Ampakines enhance LTP *in vitro* (Arai et al., 2004) and *in vivo* (Staubli et al., 1994), a change in synaptic function thought to underpin learning and memory (Kandel, 1997), and cause the release of BDNF (Lockhart et al., 2007), a pro-cognitive gene regulator which enhances LTP (Kang et al., 1997). Ampakines increase synaptic transmission at the excitatory synapses in the hippocampus and increase depolarisation by increasing EPSCs (Lynch and Gall, 2006). This increase in the post-synaptic depolarisation and enhancement of synaptic transmission underlies the nootropic properties of ampakines (Lynch, 2004).

However, by increasing post-synaptic depolarisation it has been suggested that ampakines could be pro-epileptogenic as well as pro-cognitive. Cyclothiazide, an ampakine that prevents desensitisation of AMPA receptors, is pro-epileptogenic *in vivo* (Qi et al., 2006) and *in vitro* (Lasztocki and Kardos, 2006). In this chapter, the effect of two recently developed ampakines, CX546 and CX691, will be investigated in a series of models to evaluate their pro-epileptic potential. CX546 is a first generation type 1 ampakine that causes increases in the hippocampal EPSC duration (Xia and Arai, 2005). CX691 is a second-generation ampakine that increases the amplitude of the EPSC.

As such, the aims of this chapter are as follows;

1. To evaluate the effect of application of the ampakines CX546 and CX691 on evoked field excitatory post-synaptic potentials.
2. To investigate the potential of CX546 and CX691 to initiate emergent oscillatory activity in naïve hippocampal slices.

3. To investigate the effect of application of CX546 and CX691 on hippocampal slices in which epileptiform-like activity has been initiated.

This will allow an investigation into the effect of CX546 and CX691 on physiological synaptic and network activity, and the potential pro-epileptogenic nature of these ampakines.

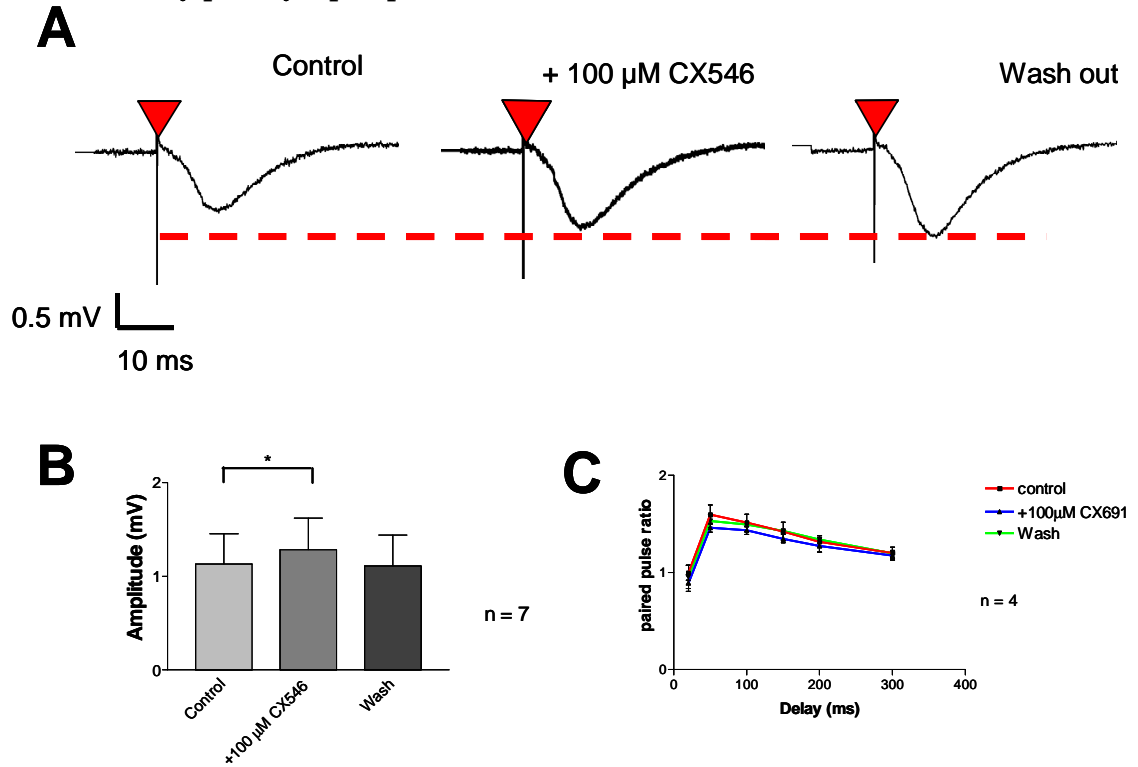
5.2 The effects of ampakines on field excitatory post-synaptic potentials

The modulation of the biophysical properties of AMPA receptors by ampakines is likely to affect Schaffer collateral-CA1 pyramidal cell synaptic transmission as the synapse is glutamatergic (Hollmann and Heinemann, 1994). A change in the properties of synaptic transmission by modulation of AMPA glutamate receptors will be manifest in a change in the magnitude of the field excitatory post-synaptic potential (fEPSP) measured from the CA1 region of the hippocampus.

5.2.1 The effect of CX546 on fEPSP

Application of 100 μ M CX546 to hippocampal slices caused an increase in the amplitude of the fEPSP (fig 5.2.1.A). The mean ($n = 7$) amplitude of the fEPSP was significantly ($P = 0.031$) increased (1.13 ± 0.32 to 1.28 ± 0.34 mV) by the application of 100 μ M CX546. This effect was reversible upon wash out (1.11 ± 0.33 mV, fig 5.2.1.B). There was no change in the paired pulse ratio of the amplitude at all time points tested following application of 100 μ M CX546 (fig 5.2.1.C). These data suggest that the facilitation of the fEPSP by CX546 occurred at a postsynaptic locus consistent with the proposed action of ampakines.

Fig 5.2.1 Investigation into the effect of the ampakine CX546 on field excitatory post-synaptic potentials



A. Representative trace examples showing (i) a field excitatory post-synaptic potential (ii) the increase in the amplitude of the field potential in response to the application of 100 μM CX546 and (iii) washout of the ampakine CX546. **B.** Summary histogram showing the significant increase in the amplitude of the field excitatory post-synaptic potentials in response to the application of the ampakine CX546. **C.** Paired-pulse protocols showing there is no difference in the facilitation of the amplitude of the fields between the presence and absence of CX546 (100 μM).

5.2.2 The effect of CX691 on fEPSP

The mean amplitude of the fEPSP was significantly ($P = 0.027$) increased (from 0.79 ± 0.19 to 0.81 ± 0.22 mV, $n = 12$) by $10 \mu\text{M}$ CX691; subsequent application of $100 \mu\text{M}$ CX691 further increased the amplitude (to 0.88 ± 0.23 mV) of the fEPSP (fig 5.2.2.B). Wash out of $100 \mu\text{M}$ CX691 decreased the amplitude of the fEPSP to 0.77 ± 0.22 mV. $100 \mu\text{M}$ CX691 induced no changes in the paired pulse ratio of the amplitude of fEPSP at all time points tested (fig 5.2.2.C). This indicates the increase in the magnitude of the fEPSP by CX691 occurred at a postsynaptic locus.

5.3 Ampakines and emergent network activities

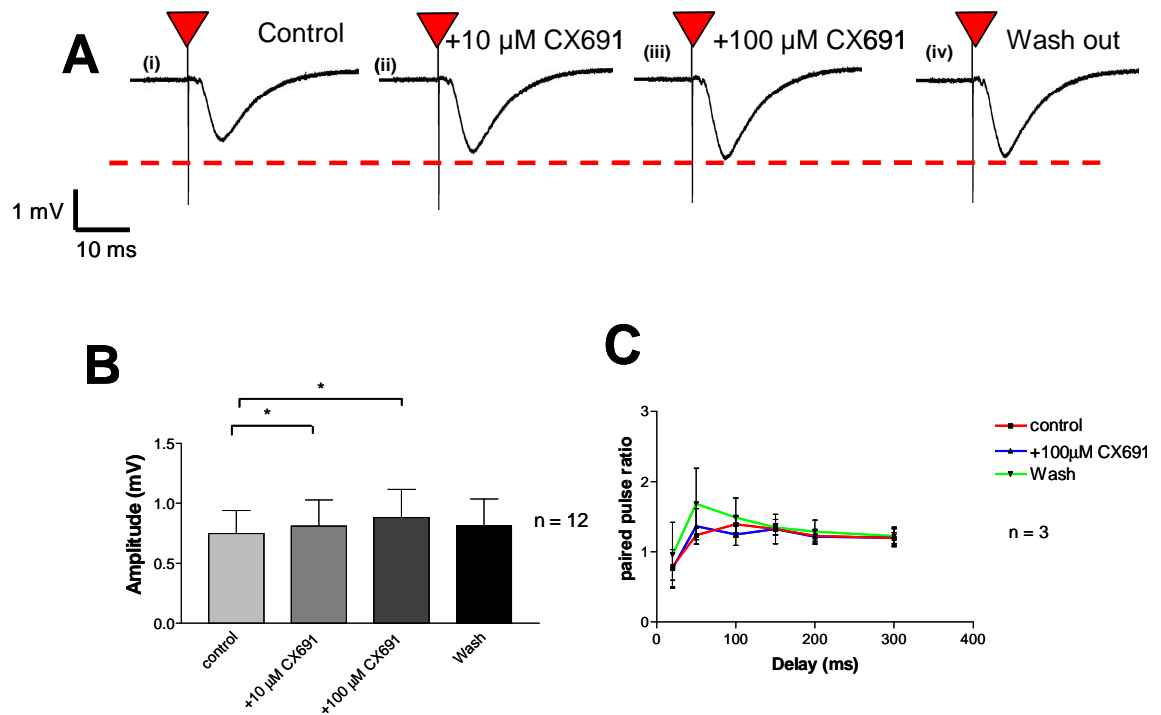
As ampakines positively modulate synaptic transmission, it is important to evaluate the pro-epileptogenic potential of these compounds at the level of the network. In order to characterise the effects of ampakines on network activity, the ampakines CX546 and CX691 were applied to coronal hippocampal slices displaying either no network activity (fig 5.3), or four mechanistically distinct models of epileptiform activity (fig 5.3.1-8).

Initially the ability of ampakines to induce oscillatory network activity was investigated. The ampakines CX546 and CX691 were applied to naïve hippocampal coronal slices and emergent network activity was monitored.

The effect of application of CX546 on naïve slices

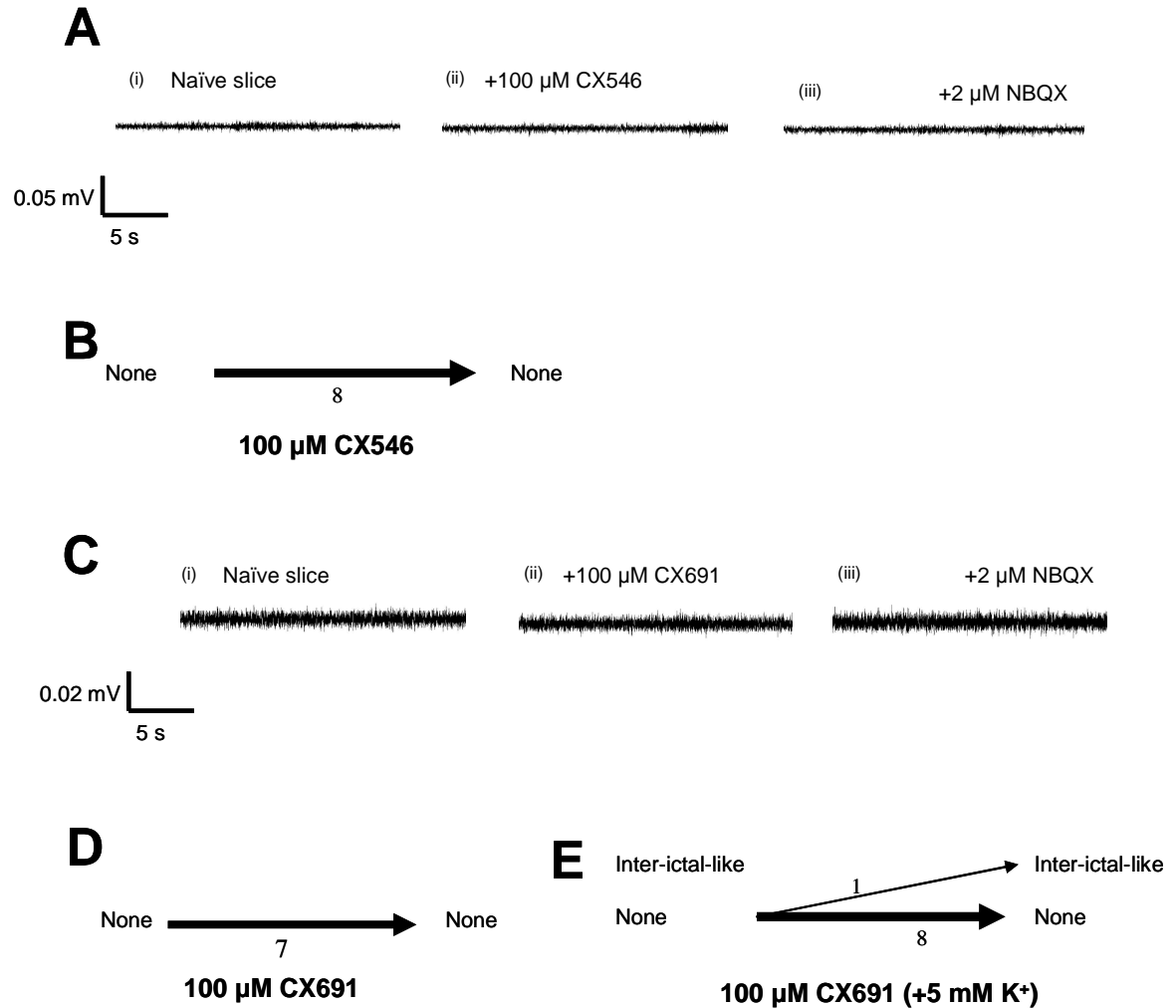
Application of $100 \mu\text{M}$ CX546 to naïve hippocampal slices did not produce any detectable field events or oscillatory activity in all slices tested (8/8, see fig 5.3.B). In fig 5.3.A the expanded trace shows there was no change from the background signal following addition of $100 \mu\text{M}$ CX546.

Fig 5.2.2 Investigation into the effect of application of the ampakine CX691 on the amplitude of field excitatory post-synaptic potentials



A. Representative trace examples showing (i) a control field excitatory post-synaptic potential (fEPSP) (ii) the fEPSP in the presence of 10 μM CX691 (iii) the fEPSP in the presence of 100 μM CX691 and (iv) wash out of the ampakine CX691. **B.** Summary histograms showing the concentration dependent increase in amplitude of fEPSP following application of 10-100 μM CX691. **C.** Time-ratio plot showing that there is no difference in the paired pulse ratio in the presence and absence of 100 μM CX691.

Fig 5.3 Investigation into the effect of the application of ampakines on naïve hippocampal slices



A. Representative trace examples showing (i) the naïve hippocampal slice (ii) application of the ampakine 100 μ M CX546 and (iii) subsequent application of the AMPA/kainate receptor antagonist NBQX. Note no overt network activity is observed following application of CX546. **B.** Trend chart showing application of 100 μ M CX546 does not induce or lead to a change in network activity. **C.** Representative trace examples showing extracellular field recordings from (i) a naïve hippocampal slice, (ii) the effect of application of 100 μ M CX691 on the hippocampal slice and (iii) subsequent application of 2 μ M NBQX. **D** and **E.** Trend charts showing no change in oscillatory activity following application of 100 μ M CX691 to naïve hippocampal slices in **(D)** normal ACSF and only 1/9 slices change in **(E)** elevated extracellular [K⁺] ACSF.

The effect of application of CX691 on naïve slices

Application of 100 μM CX691 to naïve hippocampal slices also did not induce oscillatory activity (fig 5.3.C). The trend diagram (fig 5.3.D) shows that no activity was observed in all (7/7) slices tested following application of 100 μM CX691. Even in the presence of a raised extracellular $[\text{K}^+]_o$ of 5 mM, to increase neuronal excitability by depolarising neurones (Traub and Dingledine, 1990), only 11% (1/9) of slices displayed oscillatory activity in response to application of 100 μM CX691. This activity was in the form of inter-ictal-like events.

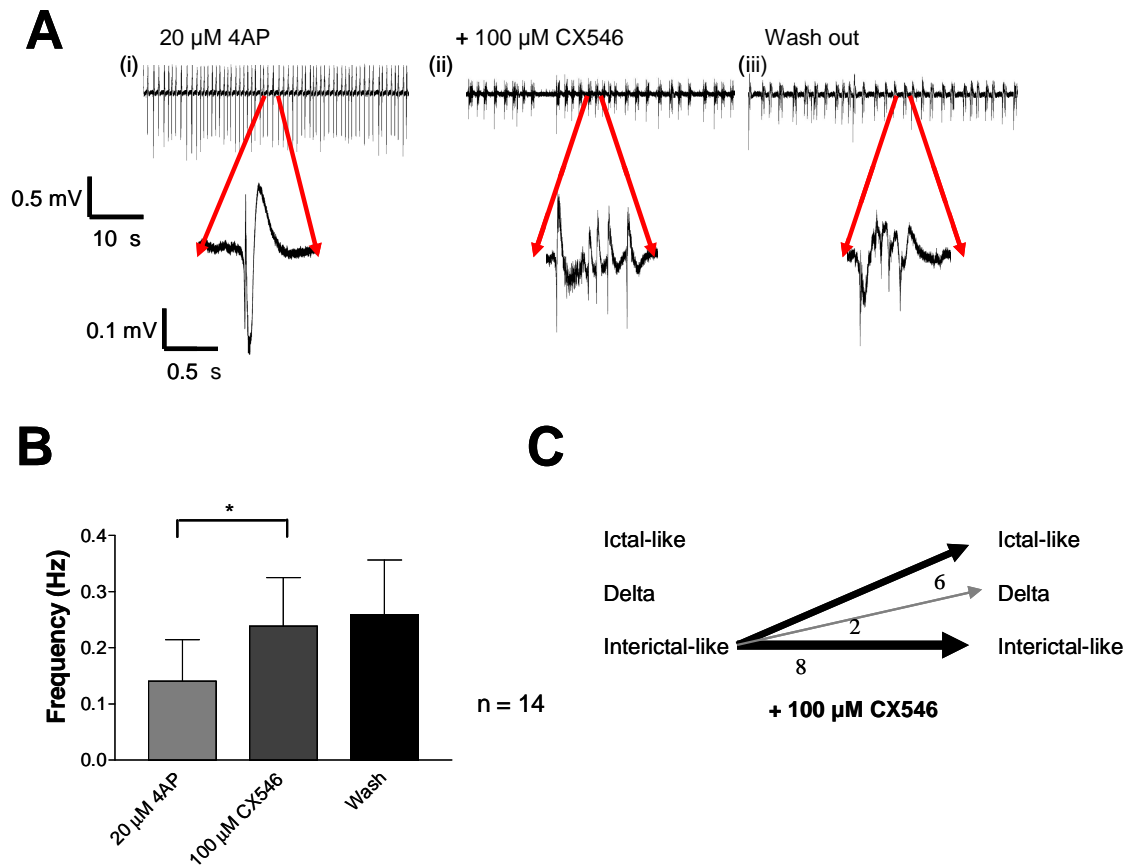
5.3.1 The effect of application of CX546 on 4-AP-induced inter-ictal-like activity

As observed above ampakines are not overtly oscillogenic in naïve slices. However, in naïve slices basal glutamate and GABA release are likely to be low, which may not best represent the *in vivo* situation. To truly assess the potential pro-epileptogenic nature of ampakines in hippocampal slices ongoing AMPA receptor activation is required.

Ampakines affect glutamatergic synaptic transmission through positive modulation of AMPA receptors (Ito et al., 1990) and it has therefore been postulated that ampakines may be pro-epileptogenic (Qi et al., 2006). Thus, the ampakines CX546 and CX691 were applied to 4-AP, bicuculline, low extracellular Mg^{2+} and a 4-AP/NBQX slow inter-ictal-like event models to investigate their effect on established epileptiform activity.

Blockade of the potassium currents I_D and I_A by 4-AP induces inter-ictal-like events (see fig 4.2.1). 4-AP activates pyramidal cells to increase glutamate release in the hippocampus (Buzsaki and Draguhn, 2004). Application of 100 μM CX546 to slices exhibiting ongoing 4-AP-induced inter-ictal-like activity increased the frequency of inter-ictal-like activity and often led to a change in the mode of activity (fig 5.3.1). The inter-ictal-like events induced by application of 20 μM 4-AP were converted into ictal-like events (37.5%, 6/16 slices) following application 100 μM CX546, as shown in fig 5.3.1.C. Also on occasion delta frequency oscillatory network activity was observed in a small subset (12.5%, 2/16) of slices.

Fig 5.3.1 Investigation into the effect of CX546 on hippocampal slices displaying inter-ictal-like activity induced by application of 4-AP



A. Representative trace examples showing (i) interictal-like activity induced by application of 20 μM 4-AP, (ii) the effect of application of the positive AMPA-receptor allosteric modulator CX546 (100 μM , *inset*- expanded trace) and (iii) wash out of CX546 (*inset*- expanded trace). Upon application of CX546 the inter-ictal-like activity tends change into ictal-like events (as shown by the insets), which is partially reversible on wash out. **B.** Summary histogram showing the significant increase in the rate of 4-AP-induced interictal-like activity induced by the application of 100 μM CX546. **C.** Trend chart showing that the 50% of the slices displaying interictal-like activity continue to display interictal-like activity (8/16 slices) and 37.5 % began to display ictal-like events (6/16 slices).

Application of 100 μM CX546 significantly ($P = 0.0006$) the frequency of 20 μM 4-AP-induced inter-ictal-like events increased (from 0.14 ± 0.07 to 0.24 ± 0.09 Hz, $n = 14$) (fig 5.3.1.B). This effect was not reversible upon wash out of CX546 (0.26 ± 0.10 Hz, $n = 13$).

5.3.2 The effect of application of CX691 on 4-AP-induced inter-ictal-like activity

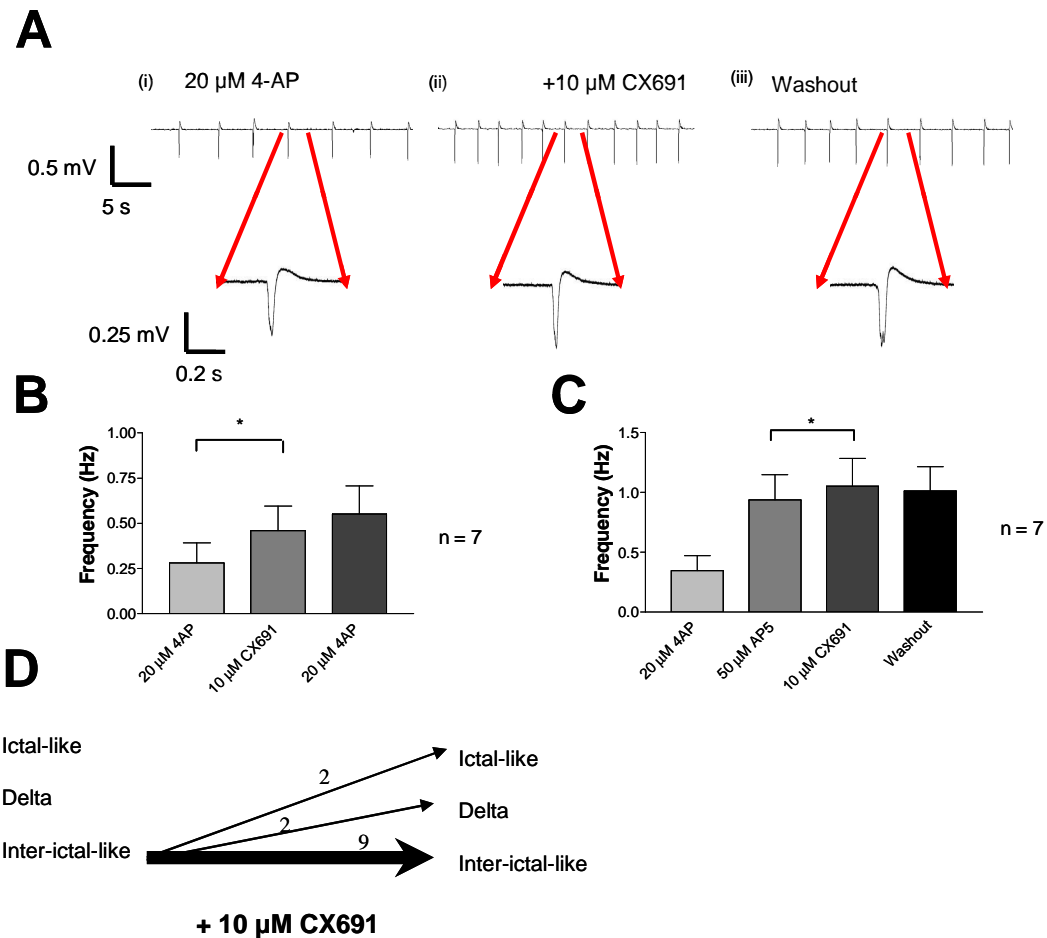
Application of CX691 to 4-AP-induced inter-ictal-like activity led to an increase in inter-ictal-like event frequency, but did not lead to a change in the mode of oscillatory activity (fig 5.3.2.). Application of 10 μM CX691 to 20 μM 4-AP induced inter-ictal-like activity led to a significant ($P = 0.016$) increase (from 0.28 ± 0.11 to 0.46 ± 0.13 Hz, $n = 7$) in the mean frequency of 4-AP-induced inter-ictal-like events (fig 5.3.2.B). This increase was not reversible upon wash out (0.55 ± 0.16 Hz, $n = 7$). In order to investigate the mechanism of the irreversible nature of the CX691-induced increase in inter-ictal-like frequency, the NMDA receptor antagonist 2-AP5 (50 μM) was applied before CX691 to prevent NMDA mediated network plasticity. Application of 2-AP5 itself significantly ($P = 0.009$) increased (from 0.34 ± 0.12 Hz to 0.94 ± 0.21 Hz, $n = 7$) the frequency of 4-AP induced inter-ictal-like events. In the presence of the NMDA receptor antagonist 50 μM 2-AP5, 10 μM CX691 caused a significant increase in inter-ictal-like event frequency (from 0.94 ± 0.21 to 1.05 ± 0.23 Hz, $n = 7$, $P = 0.016$), which was partially reversible (to 1.01 ± 0.20 Hz) (fig 5.3.2.C).

Following application of 10 μM CX691 to 20 μM 4-AP-induced inter-ictal-like activity the majority (69%, 9/13) of slices continued to display inter-ictal-like activity (fig 5.3.2.D) and only 15% displayed ictal-like activity. Again in a small subset (15%, 2/13) of slices delta frequency oscillatory network activity was observed.

5.3.3 The effect of application of CX546 on bicuculline-induced inter-ictal-like activity

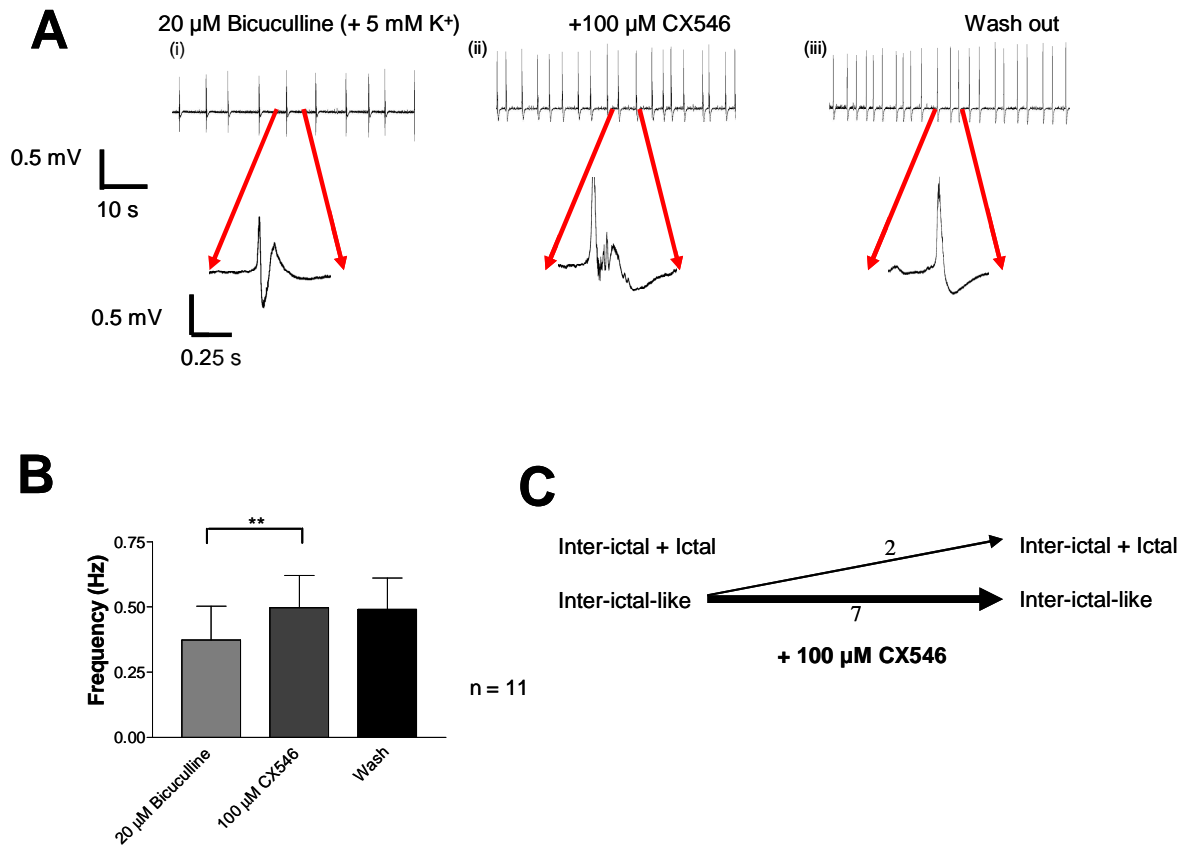
Bicuculline induces oscillatory network activity through the blockade of GABA_A receptors, allowing summation of EPSPs throughout the network, and the development of paroxysmal depolarising shifts within pyramidal cells (see chapter 4).

Fig 5.3.2 Investigation into the effect of CX691 on the frequency of inter-ictal-like events induced by 4-AP



A. Representative trace examples showing (i) inter-ictal-like activity induced by the application of 20 μ M 4-AP, (ii) subsequent application of the ampakine CX691 (10 μ M, *inset*- expanded trace) and (iii) wash out of CX691. Note the increase in inter-ictal-like event frequency. **B-C.** Summary histograms showing the application of 10 μ M CX691 to 4-AP induced activity which increases the rate of inter-ictal-like activity. Note that the increase in activity is not reversible upon washout. **C** The application of the NMDA receptor antagonist AP5 (50 μ M) prior to application of CX691 (10 μ M) does not prevent the CX691-mediated increase in inter-ictal-like event frequency, which is reversible on wash out of CX691. **D** Trend charts showing that of slices initially displaying inter-ictal-like activity the majority of slices continue to display inter-ictal-like activity. (9/13 slices).

Fig 5.3.3 Investigation into the effect of CX546 on the frequency of inter-ictal-like events induced by bicuculline (+5 mM K⁺)



A. Representative trace examples showing (i) 20 μM bicuculline (+5 mM [K⁺])-induced inter-ictal-like activity, (ii) the effect of the application of 100 μM CX546 upon this bicuculline-induced activity (*inset*- expanded inter-ictal-like event) and (iii) wash out of the ampakine CX546. **B.** Summary histogram showing a significant increase in inter-ictal-like event frequency following application of the ampakine CX546. **C.** Trend chart showing that in the majority of slices in which inter-ictal-like activity is established subsequent application of 100 μM CX546 does not lead to a change in the mode of activity (7/9 slices).

Application of 100 μM CX546 to 20 μM bicuculline (+5 mM $[\text{K}^+]$)-induced inter-ictal-like activity led to a significant ($P = 0.002$) increase (from 0.39 ± 0.13 to 0.50 ± 0.13 Hz, $n = 11$) in the frequency of inter-ictal-like activity (fig 5.3.3.B). The increase was not reversible upon wash out of CX546 (0.49 ± 0.12 Hz). Of the slices displaying inter-ictal-like activity in response to application of 20 μM bicuculline (+5 mM $[\text{K}^+]$), 78% (7/9) of slices continued to display inter-ictal-like activity in the presence of 100 μM CX546, whilst ictal-like activity emerged in 22% of slices.

5.3.4 The effect of application of CX691 on bicuculline-induced inter-ictal-like activity

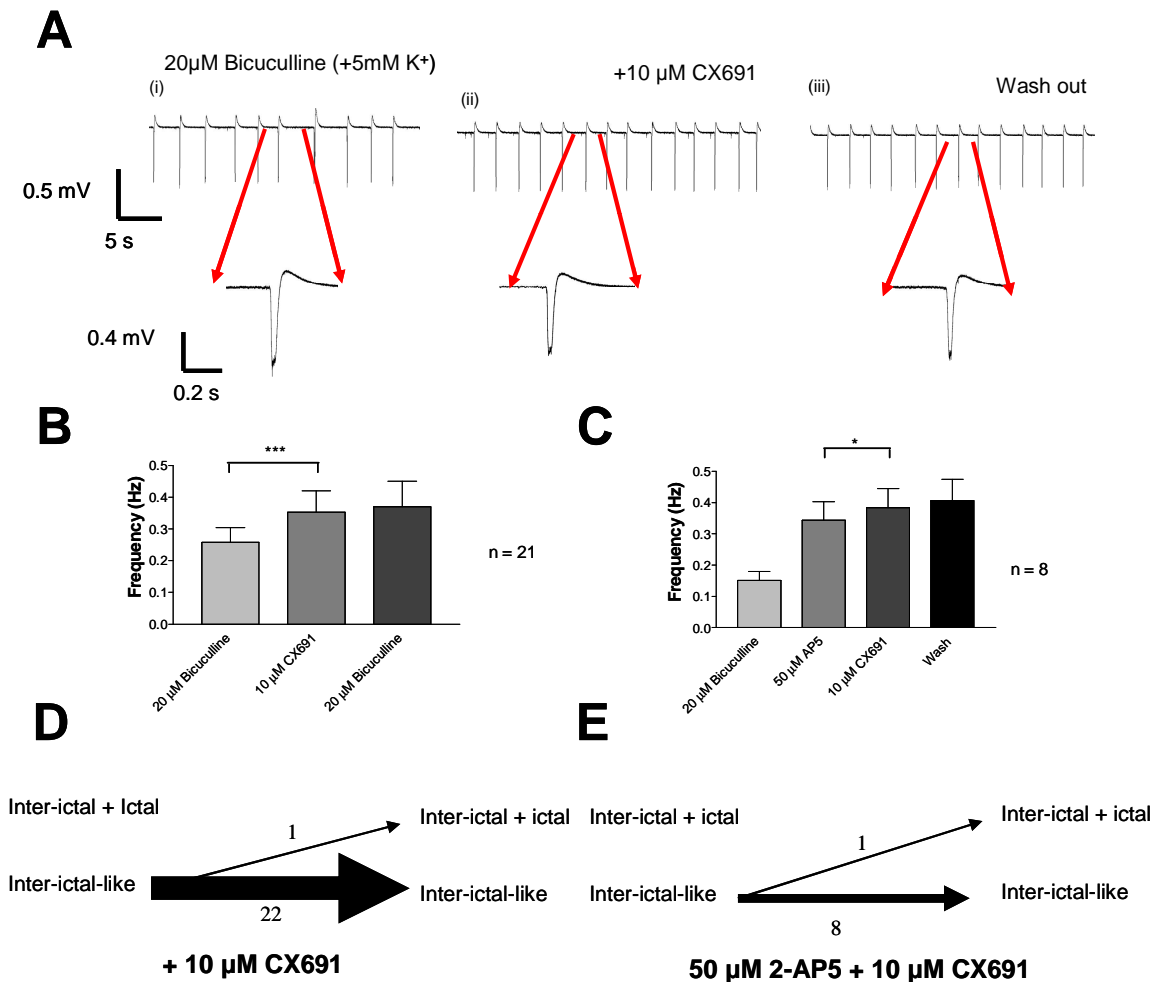
The frequency of 20 μM bicuculline (+5 mM $[\text{K}^+]$)-induced inter-ictal-like activity was similarly increased in response to the application of 10 μM CX691. However CX691 did not induce ictal-like activity (fig 5.3.4). Application of 10 μM CX691 led to a significant ($P = 0.0006$) increase (from 0.26 ± 0.05 to 0.35 ± 0.07 Hz, $n = 21$) in the mean inter-ictal-like event frequency (fig 5.3.4.B), which was again not reversible upon wash out of 10 μM CX691 (frequency = 0.37 ± 0.08). Prior application of 50 μM 2-AP5 increased the frequency of inter-ictal-like events (0.15 ± 0.03 to 0.34 ± 0.06 Hz, $n = 8$) and did not prevent the 10 μM CX691-induced significant ($P = 0.047$) increase (0.34 ± 0.06 to 0.38 ± 0.06 Hz, $n = 8$) in mean inter-ictal-like activity (fig 5.3.4.C). Wash out of 10 μM CX691 in the same experiment did not result in a decrease in event frequency (0.41 ± 0.07 Hz, $n = 8$).

Application of 10 μM CX691 to bicuculline -induced inter-ictal-like events did not change the mode of activity in 96% (22/23) of slices tested (fig 5.3.4.D), and 88% (7/8) slices continued to display inter-ictal-like activity following application of 100 μM CX691. In the presence of 50 μM 2-AP5 88% (8/9) of slices did not change the mode of activity in response to the application of 10 μM CX691 (fig 5.3.4.E).

5.3.5 The effect of the application of CX546 on low extracellular magnesium-induced inter-ictal-like activity

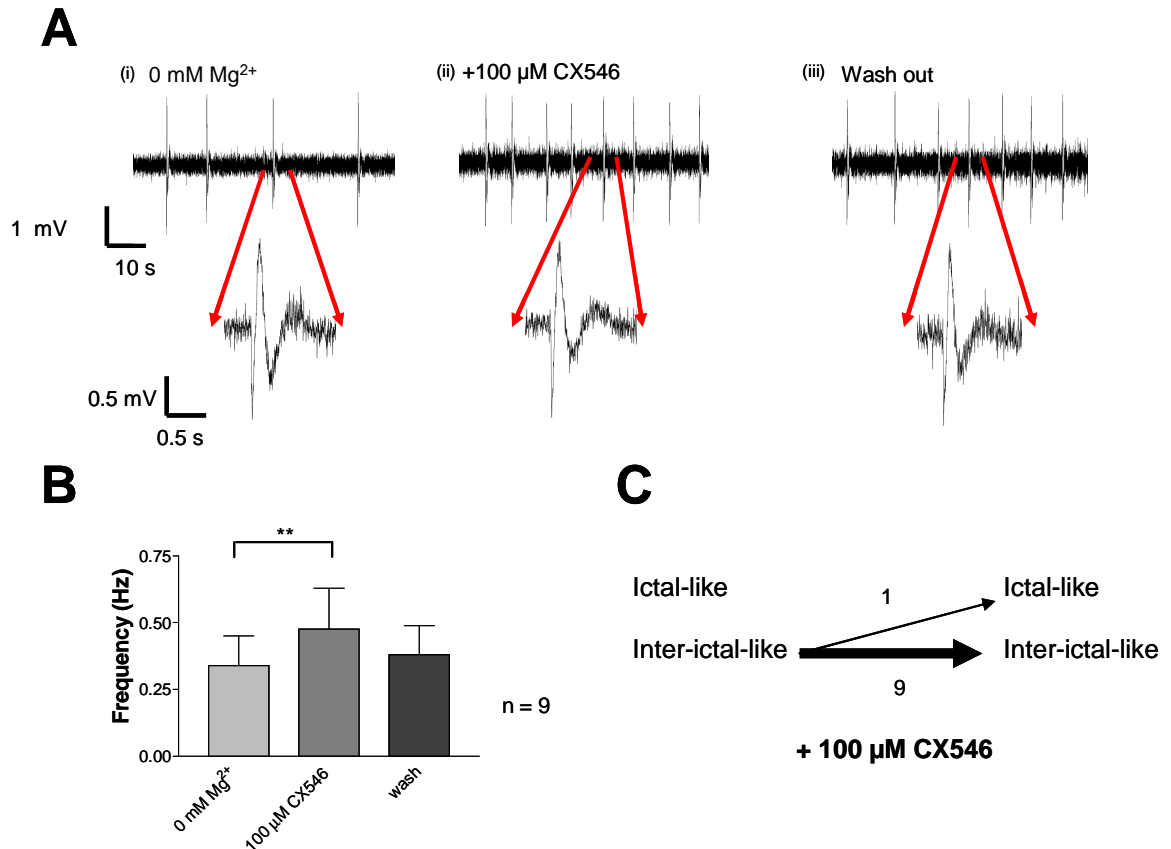
Removal of extracellular magnesium leads to emergent inter-ictal-like network activity through the removal of the voltage dependent magnesium block of the NMDA receptor (Traub et al., 1994).

Fig 5.3.4 Investigation into the effect of CX691 on the frequency of bicuculline-induced inter-ictal-like events



A. Representative trace examples showing (i) the GABA_A receptor antagonist 20 μM bicuculline (+5 mM extracellular [K⁺])-induced inter-ictal-like activity, (ii) subsequent application of 10 μM CX691 (*inset*- expanded inter-ictal-like event) and (iii) wash out of the ampakine CX691. **B & C.** Summary histograms showing (B) the application of 10 μM CX691 on bicuculline induced inter-ictal-like activity leads to a increase in the frequency of inter-ictal-like events, which is not reversible upon wash out of the ampakine. 10 μM CX691 causes a significant increase in inter-ictal-like event frequency in the presence of 50 μM AP5, but again wash out of CX691 does not reverse the increase in frequency (C). **D & E.** Trend charts showing (D) the effect of application of 10 μM CX691 on bicuculline-induced inter-ictal-like activity. No change in the oscillatory activity is observed in 21/22 slices. Application of 50 μM 2-AP5 prior to the application of 10 μM CX691 (E) does not promote other oscillatory activities (8/9 slices tested).

Fig 5.3.5 Investigation into the effect of CX546 on low Mg^{2+} induced inter-ictal-like activity



A. Representative trace examples showing (i) inter-ictal-like activity occurs following removal of Mg^{2+} ions from the extracellular bathing medium, (ii) an increase in the frequency of inter-ictal-like events following addition of 100 μM CX546, which is reversible upon wash out (iii). **B.** Summary histogram showing a significant increase in inter-ictal event frequency due to addition of 100 μM CX546 to inter-ictal-like activity induced by the removal of Mg^{2+} ions from the extracellular bathing medium. This is reversible on wash out of CX546. **C.** Trend chart showing only 1 out of 10 slices changes the mode of activity from inter-ictal-like activity to ictal-like activity following the application of 100 μM CX546.

The gradual emergence of these inter-ictal-like events is described in the previous chapter (fig 4.2.7).

Application of 100 μ M CX546 increased the frequency of low magnesium induced inter-ictal-like activity but did not change the mode of activity in the majority of slices.

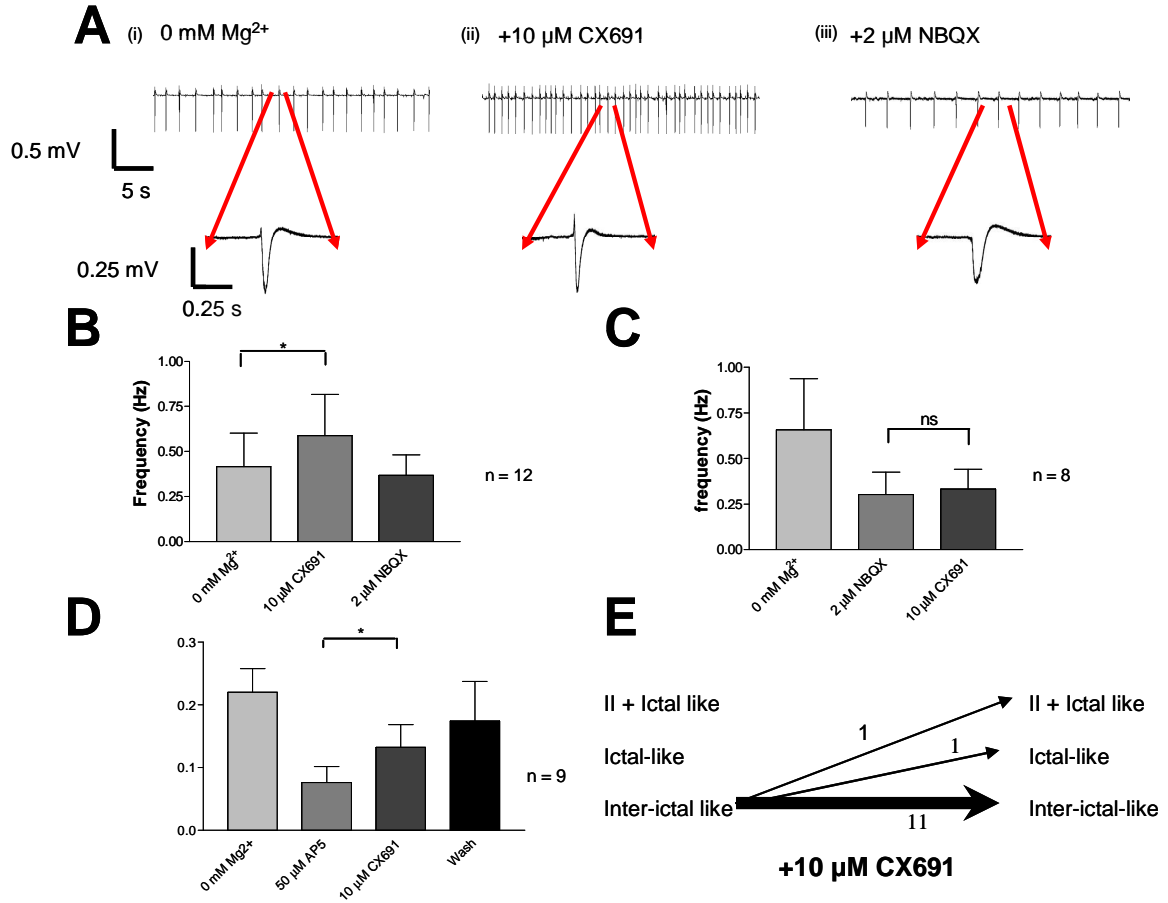
Application of 100 μ M CX546 caused a significant ($P = 0.0020$) increase (from 0.34 ± 0.11 to 0.48 ± 0.15 Hz, $n = 10$) in the low-magnesium-induced inter-ictal-like activity frequency (fig 5.3.5.B) that was reversible on wash out of 100 μ M CX546 (frequency = 0.38 ± 0.11 Hz, $n = 10$). Application of 100 μ M CX546 did not change the mode of activity in 90% (9/10) of slices tested, with the exception of one slice in which ictal-like events were observed following its application.

5.3.6 The effect of the application of CX691 on low extracellular magnesium-induced inter-ictal-like activity

Application of 10 μ M CX691 led to a significant ($P = 0.014$) increase in the frequency (0.49 ± 0.22 to 0.67 ± 0.27 Hz, $n = 12$) of low extracellular magnesium-induced inter-ictal-like events (fig 5.3.6.B) that was reversed by the subsequent application of the AMPA/kainate antagonist NBQX (0.37 ± 0.11 Hz). Application of 100 μ M CX691 also led to a significant ($P = 0.020$) increase (from 0.48 ± 0.13 to 0.73 ± 0.19 Hz, $n = 7$, not shown) in the frequency of the low extracellular magnesium-induced inter-ictal-like activity that was reversible upon subsequent application of 2 μ M NBQX (0.53 ± 0.08 Hz, $n = 7$). Application of 2 μ M NBQX prior to the addition of 10 μ M CX691 prevented (0.30 ± 0.12 to 0.33 ± 0.11 Hz, $n = 8$) the increase ($P = 0.15$) in low extracellular magnesium-induced inter-ictal-like event frequency induced by CX691 (fig 5.3.6.C).

Application of 50 μ M 2-AP5 caused a significant ($P = 0.005$) decrease in the inter-ictal-like event frequency (from 0.22 ± 0.03 Hz to 0.08 ± 0.03 Hz, $n = 9$). In the presence of 50 μ M 2-AP5, 10 μ M CX691 caused a significant ($P = 0.03$) increase (to 0.13 ± 0.04 Hz, $n = 9$) in low extracellular magnesium-induced inter-ictal-like event frequency. This increase was not reversible upon wash out of the CX691 in the presence of 50 μ M 2-AP5 (0.17 ± 0.06 Hz, $n = 9$).

Fig 5.3.6 Investigation into the effect of CX691 on low Mg^{2+} -induced inter-ictal-like events



A. Representative trace examples showing (i) inter-ictal-like activity induced by removal of Mg^{2+} ions from the bathing solution (ii) the effect of subsequent application of 10 μM CX691 (*inset*- expanded inter-ictal-like event) and (iii) the effect of the addition of the AMPA/kainate receptor antagonist NBQX (2 μM). **B-D.** Summary histograms showing the effect of application of the ampakine CX691 on low Mg^{2+} -induced inter-ictal-like activity. A significant increase in the inter-ictal-like event frequency is observed following application of (B) 10 μM CX691, which is reversible upon addition of 2 μM NBQX or wash out of the ampakine (data not shown). **C.** This increase is abolished by the addition of 2 μM NBQX prior to the application of 10 μM CX691. **D.** The significant increase in inter-ictal-like event frequency is not abolished by the addition of the NMDA receptor antagonist 50 μM AP5 before application of the ampakine CX691 (10 μM). **E.** Trend charts showing the effect of application of the ampakine CX691 on low Mg^{2+} -induced inter-ictal-like activity. The majority of slices (11/13) do not change the mode of activity in response to the application of 10 μM CX691.

The majority (85%, 11/13) of slices did not change in the mode of activity from low extracellular magnesium-induced inter-ictal-like activity following application of 10 μM CX691 (fig 5.3.6.E). All slices (9/9) continued to display low extracellular magnesium-induced inter-ictal-like activity following application of 100 μM CX691. In the presence of 2 μM NBQX or 50 μM 2-AP5, subsequent application of 10 μM CX691 did not change the mode of activity from low extracellular magnesium-induced inter-ictal-like activity in all slices tested (8/8 and 9/9 slices respectively).

5.3.7 The effect of CX546 on 4-AP/NBQX-induced slow inter-ictal-like events

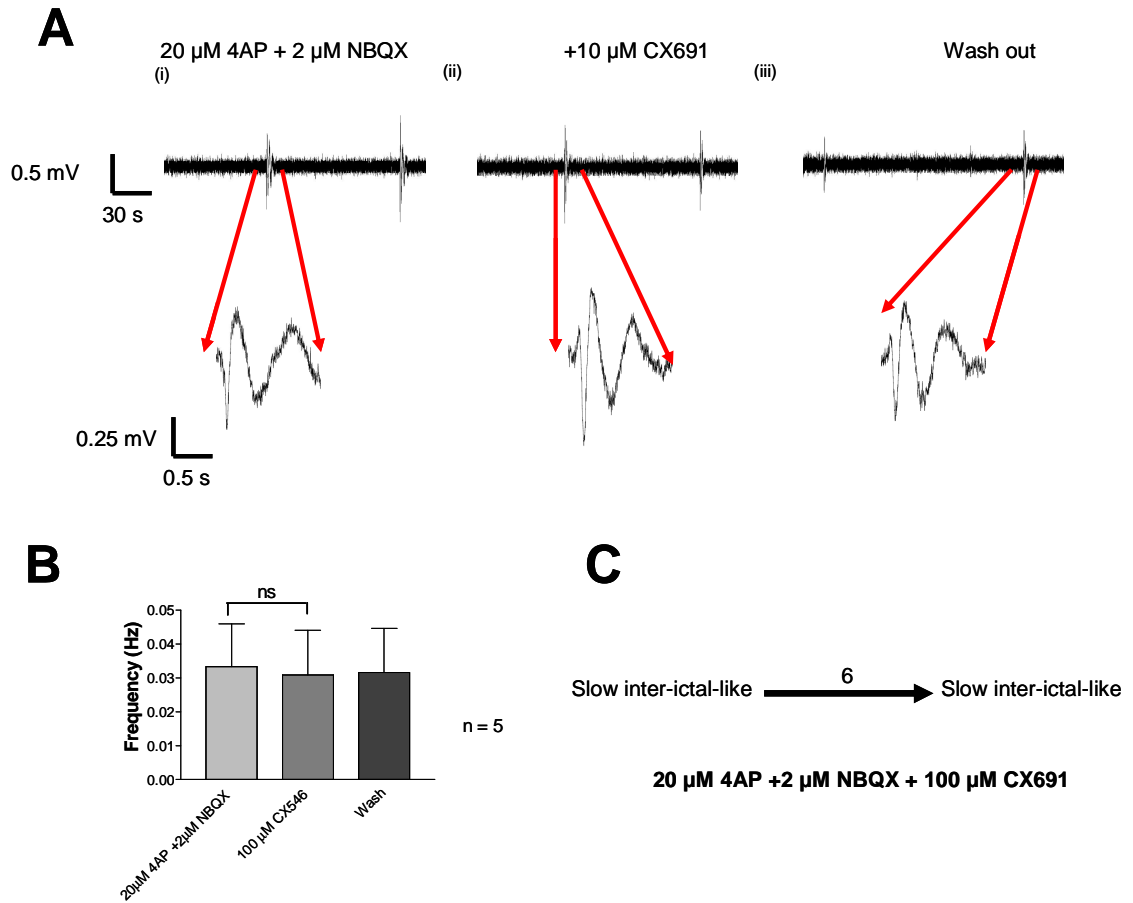
In order to ensure that the ampakines investigated acted through the modulation of AMPA receptors, ampakines were applied the 4-AP/NBQX induced slow inter-ictal-like event model. Application of ampakines to this model should not alter the mode or frequency of emergent network activity, as the antagonist NBQX blocks all AMPA/kainate receptors. If the ampakines are acting through other receptor systems to increase the frequency of 4-AP-induced oscillations in the absence of NBQX (figs 5.3.1 and 5.3.2), then an increase in frequency would be expected to occur in the presence of NBQX.

The frequency of 20 μM 4-AP/2 μM NBQX induced slow inter-ictal-like events was not altered by application of 100 μM CX546 (fig 5.3.7). There was no significant change ($P = 0.50$, from 0.033 ± 0.013 to 0.031 ± 0.013 Hz, $n = 5$) in the mean slow inter-ictal-like event frequency (fig 5.3.7.B), which again did not alter upon wash out (0.032 ± 0.013 Hz, $n = 5$). In all slices (6/6) displaying 4-AP/NBQX induced slow inter-ictal-like events the slices continued to show this mode of activity following addition of 100 μM CX546 (fig 5.3.7.C).

5.3.8 The effect of application of CX691 on 4-AP/NBQX-induced slow inter-ictal like events

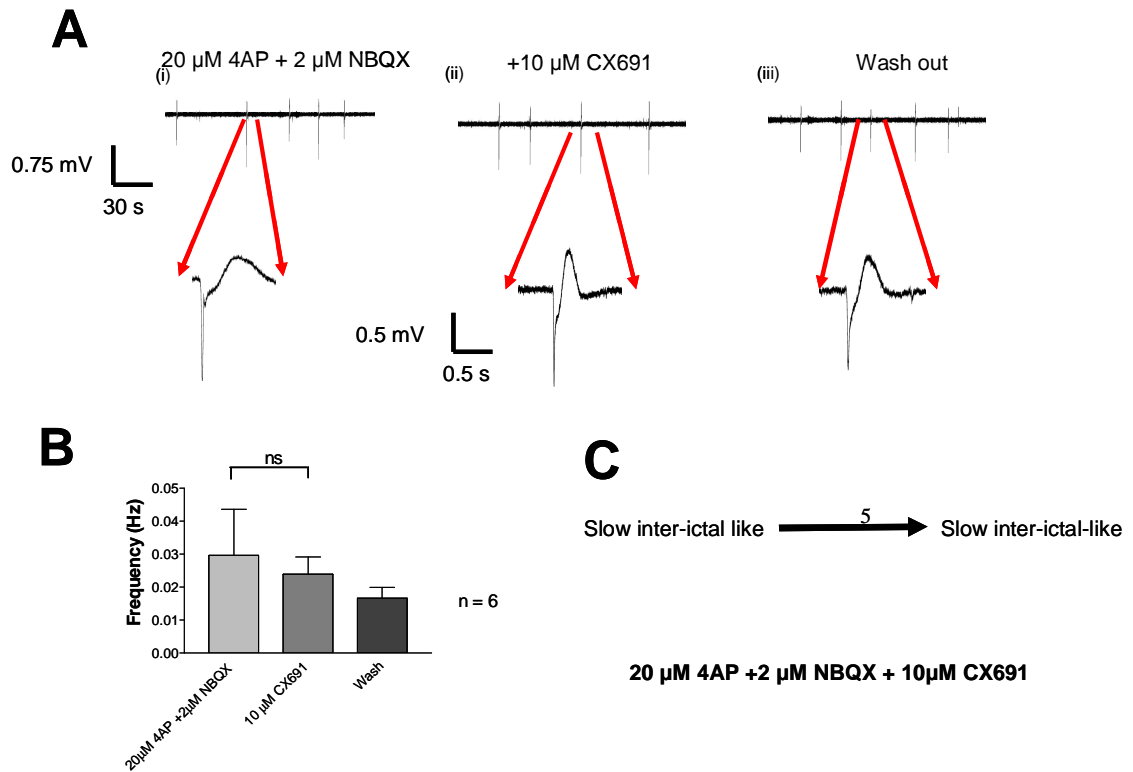
The frequency of 20 μM 4-AP/2 μM NBQX induced slow inter-ictal-like events was not altered by 10 μM CX691 (fig 5.3.8).

Fig 5.3.7 CX546 does not alter the frequency of 4-AP/NBQX induced slow inter-ictal-like events



A. Representative trace examples showing (i) 4-AP/NBQX-induced slow inter-ictal-like events (*inset*- expanded event), (ii) the effect of subsequent application of 100 μ M CX546 and (iii) wash out of CX546. **B.** Summary histogram showing there is no significant change in the frequency of slow inter-ictal-like events following application of 100 μ M CX546. **C.** Trend chart showing there is no change in the mode of activity following application of 100 μ M CX546 (n = 6).

Fig 5.3.8 CX691 does not alter the frequency of 4-AP/NBQX induced slow inter-ictal-like events



A. Representative trace examples showing (i) 20 μ M 4AP and 2 μ M NBQX-induced inter-ictal-like events, (ii) the effect of the subsequent application of 10 μ M CX691 (*inset*- slow inter-ictal-like event) and (iii) wash out of the ampakine CX691. **B.** Summary histogram showing there is no significant change in the frequency of slow inter-ictal like events following application of 10 μ M CX691. **C.** Trend chart showing there is no change in the mode of the oscillatory activity following application of 10 μ M CX691 on slow inter-ictal like events in 5 out of 5 slices tested.

There was a slight non-significant ($P = 0.69$) decrease (from 0.030 ± 0.014 to 0.024 ± 0.005 Hz, $n = 6$) in the mean slow inter-ictal-like event frequency following application of $10 \mu\text{M}$ CX691 (fig 5.3.8.B), which decreased further upon wash out (0.017 ± 0.003 Hz, $n = 6$). In all slices (5/5) displaying 4-AP/NBQX induced slow inter-ictal-like events the slices continued to show this mode of activity following addition of $10 \mu\text{M}$ CX691 (fig 5.3.8.C).

5.4 Discussion

In this chapter the effect of two ampakines on hippocampal networks was investigated. CX546 is an ampakine that causes a significant increase in the open time of AMPA receptors, increasing the width of the EPSC. CX691 is a 20-50 times more potent analogue of the ampakine CX516, which significantly increases the current flow through the AMPA receptor by increasing the amplitude of the EPSC (Arai et al., 2004). The main findings of this chapter are as follows;

1. Ampakines promote synaptic transmission at the Schaffer collateral-CA1 synapse.
2. Ampakines do not induce emergent oscillatory activity when applied to naïve hippocampal slices.
3. Ampakines increase the frequency of inter-ictal-like events in three mechanistically distinct models of epileptiform activity.
4. The ampakine CX546 also promotes ictal-like activity in hippocampal slices displaying 4-AP-induced inter-ictal-like activity.
5. Ampakines have no effect on the mode or frequency of the slow inter-ictal-like events induced by co-application of 4-AP and NBQX.

Ampakines are of interest as the facilitation of fast glutamatergic transmission is known to improve cognitive function in many disparate tasks and species (Ingvar et al., 1997; Hampson et al., 1999; Jones et al., 2005), but the potential of these drugs to be used as nootropic agents is hindered by the fact they may possibly induce seizures.

The older generation ampakine, CX546, and the newer ampakine, CX691, facilitate glutamatergic transmission at the Schaffer collateral-CA1 synapse as shown in section 5.2. The facilitation of glutamatergic transmission is thought to underlie the pro-cognitive action of ampakines (Black, 2005).

Although the effect of CX546 is to increase the deactivation time of the AMPA receptor (Arai et al., 2004), this is manifest as an increase in the amplitude of the fEPSP. The fEPSP is predominantly made up of current flow into pyramidal cell dendrites, and is proportional to the excitability of pyramidal cells (Balestrino et al., 1986). It is possible that an increase in the temporal summation of EPSPs from Schaffer collaterals can occur in the presence of

CX546. Temporal summation occurs when membrane depolarisations occur within dendrites within a short amount of time (Rall, 1964; Sjostrom et al., 2008). This increases the excitability of pyramidal cells and probability of action potential firing, increasing the amplitude of the fEPSP. CX691 does not change the temporal component of the EPSC, but rather increases the amplitude of the EPSC (Arai et al., 2004). The increased amplitude of the EPSC leads to a greater depolarisation of the CA3 pyramidal cells in the network for each EPSP, increasing the probability of suprathreshold potentials in pyramidal cells in the presence of CX691.

CX546 and CX691 appear to exert the majority of their effect on normal synaptic transmission at the post-synaptic locus as they do not change the paired pulse ratio. The paired pulse ratio is a measure of the change in the amplitude of the EPSP that occurs in response to a second stimulus due to a raised residual $[Ca^{2+}]$ in the pre-synaptic bouton following the initial stimulus (Schulz et al., 1994). Thus if the paired pulse ratio changes following an experimental intervention, then the locus of that effect is pre-synaptic.

AMPA receptor activation is crucial in the electrophysiological phenomenon that is thought to represent memory formation, long term potentiation (LTP) (Malinow and Malenka, 2002; Sprengel, 2006) which is a long-term increase in the glutamatergic synaptic strength. Ampakines have been shown to increase the amplitude of LTP at the Schaffer collateral-CA1 synapse (Arai et al., 2004). Both pre- and post-synaptic loci have been implicated in the molecular changes that occur in LTP, but the changes that occur in the presence of the ampakines above would be likely to be at a postsynaptic locus.

Application of either of the ampakines, CX546 and CX691, did not induce any detectable oscillatory network activity in naïve hippocampal slices. As ampakines are positive allosteric modulators of AMPA receptors (Ito et al., 1990), they do not directly activate AMPA receptors. Ampakines require AMPA receptor activation by endogenous or exogenous AMPA receptor agonists, like glutamate, to have an effect. Neuronal activity underlies both glutamate release (Hamberger et al., 1979) and oscillatory network activity (Traub et al., 2004). Therefore ongoing neuronal activity is required for ampakines to exert their effect, and in slices in which no detectable oscillatory activity is observed it is likely that the majority of neurones are quiescent (Connors et al., 1982). The absence of network oscillatory activity following application of ampakines to quiescent slices was therefore expected. Even following the increase of $[K^+]_o$ up to 5 mM, which increases the probability of neuronal activity by depolarising neurones closer to action potential firing threshold (Kaila et al. 1997), the ampakines largely did not promote network oscillatory activity.

In the slices that were not quiescent in either normal ACSF or raised extracellular $[K^+]_o$, the ampakines CX546 and CX691 were able to potentiate oscillatory activity. The activities induced were highly variable and relatively rare, so no quantifiable measure of the facilitation of these activities by the ampakines was possible. However, the facilitation of both the physiological and pathophysiological oscillatory network activities in these slices was expected as the ongoing activity indicates glutamate was being released and AMPA receptors activated (Whittington et al., 1997).

The effect of these ampakines on four different models of epileptiform activity was then investigated. Both of the ampakines caused a significant increase in the frequency of inter-ictal-like activity in three of the epileptiform models tested. The 4-AP model induces epileptiform activity in hippocampal networks through the generation of paroxysmal depolarising shifts within principal cells (Perreault and Avoli, 1991). Paroxysmal depolarising shifts are initiated by the summation of glutamate mediated EPSPs within the network. As CX546 increases the width of the AMPA-mediated EPSC (Arai et al., 2004), an increase in the temporal summation of EPSPs increases the probability, and thus the frequency, of action potential firing. As action potential firing increases the frequency of paroxysmal depolarising shifts (see chapter 4), the inter-ictal-like event frequency increases in the presence of CX546. As mentioned above, an increase in the amplitude of the EPSC leads to greater action potential firing in the presence of CX691. This property also increases the frequency of paroxysmal depolarisation shifts, and as such inter-ictal-like events within the network.

This increase in the decay time of EPSCs following application of CX546 displayed a tendency to induce a change from inter-ictal-like events to ictal-like events in the 4-AP model of epileptiform activity. For ictal-like events to be manifest, a transient decrease in GABAergic inhibition from interneurons is required, either through depolarisation block of interneurons, or a reversal in the chloride gradient making GABA_A potentials excitatory (Isomura et al., 2003; Fujiwara-Tsukamoto et al., 2004; Ziburkus et al., 2006). AMPA receptors are located on interneurons and display shorter rise and decay times than AMPA receptors in pyramidal cells (Geiger et al., 1997; Povysheva et al., 2006). CX546 would lengthen the temporal component of AMPA receptor mediated EPSCs on interneurons, and the temporal summation of EPSPs within interneurons may lead to depolarisation block of OLM interneurons, to a sufficient degree that ictal-like events could occur as in the Ziburkus model detailed in the previous chapters. It is also possible that increased neuronal activity reverses the chloride gradient so that GABA_A receptor mediated potentials are excitatory, as in the Fujiwara-Tsukamoto model. Ictal-like activity

would not be induced by CX546 in the bicuculline model as depolarising GABA potentials are blocked in this model.

The increase in inter-ictal-like event frequency following the application of CX691 was not reversible upon wash out of the ampakine. It was postulated that this irreversibility may have been due to some plasticity associated with enhanced network activity, perhaps due to the recruitment of NMDA receptor mediated potentiation. To investigate this further the NMDA receptor antagonist 2-AP5 was used to block the NMDA receptor prior to the ampakine application. Application of 2-AP5 did allow a partial reversal of the inter-ictal-like event frequency following wash out of CX691, suggesting that the irreversible nature of the increase in event frequency on washout of CX691 is at least partially mediated by the NMDA receptor. NMDA receptor mediated plasticity is involved in LTP in which strong depolarisations in the postsynaptic membrane lead to increases in synaptic strength (Bliss and Collingridge 1993). As CX691 allows greater post-synaptic potentials by increasing the amplitude of the EPSC than in normal conditions, some plasticity of this fashion would be expected.

Interestingly there was a significant increase in inter-ictal-like event frequency following application of 2-AP5. As this is a glutamate receptor antagonist, application of 2-AP5 may be expected, if anything, to decrease the frequency of inter-ictal-like events. Indeed other studies have shown that NMDA antagonists are anticonvulsant (Aram et al., 1989), but some have shown NMDA antagonists to be pro-convulsant (Stafstrom et al., 1997). It is likely the NMDA receptors are activated following 4-AP application (Perreault and Avoli 1992). Thus it appears that the activation of NMDA receptor negatively regulates inter-ictal-like event frequency. Two possible mechanistic explanations of this effect include:

1. Ca^{2+} activated K^+ channels are activated in the network by NMDA receptor activity as open NMDA receptors are permeable to Ca^{2+} (Faber et al., 2005; Faber and Sah 2007). This allows K^+ ions to flow out of pyramidal cells through SK channels, which mediates the medium after-hyperpolarisation potential (mAHP) (Sah and Faber 2002). Blockade of the NMDA receptor mediated Ca^{2+} entry by 2-AP5 may stop the activation of this channel and allow depolarisation of pyramidal cells.
2. NMDA receptors, which are expressed in interneurons (Standaert et al., 1996), may be involved in feed forward inhibition of pyramidal cells. Block of these NMDA receptors decreases interneurone excitation by pyramidal cells and subsequent GABA mediated inhibition of pyramidal cells.

In order to gain further mechanistic insight into the physiological networks that underlie the increase in inter-ictal-like event frequency induced by ampakines and the NMDA antagonist 2-AP5, these compounds were applied to a range of mechanistically distinct models of epileptiform activity.

Inter-ictal-like events are also induced by application of the GABA_A receptor antagonist bicuculline. Bicuculline abolishes fast GABA_A mediated synaptic inhibition leading to the gradual emergence of inter-ictal-like events *in vivo* (Campbell and Holmes 1984) and *in vitro* (Hwa et al., 1991). These inter-ictal-like events are mediated through fast glutamatergic transmission (Hwa and Avoli 1991), and so ampakines are well positioned to modulate the events induced by application of bicuculline. Application of both CX546 and CX691 lead to significant increases in the frequency of the inter-ictal-events induced by bicuculline. As for the 4-AP model of epileptiform activity, application of ampakines increases the frequency of the inter-ictal events by increasing the magnitude of EPSPs, following the increase in open time (for CX546) or current flux (for CX691) of the AMPA receptor in the presence of the ampakines (Arai et al., 2004).

In contrast to the 4-AP model, application of CX546 does not show a tendency to induce ictal-like activity in the bicuculline induced inter-ictal-like event model. Application of CX691 also does not induce ictal-like activity in the majority of slices tested. A straightforward explanation for this could be the absence of depolarising GABA_A mediated potentials within this model (Isomura et al., 2003). It is also possible that the lower inter-ictal-like event frequency in the bicuculline model means that the effect of the increased open time of the AMPA receptor in the presence of CX546 is negated. With a lower frequency the potential for temporal summation, and subsequent depolarisation block, is decreased.

As in the 4-AP induced inter-ictal-like event model, the increase in inter-ictal-like event frequency was not reversed upon wash out of the ampakine, indicating some longer term changes in synaptic strength may have occurred. Unlike the 4-AP-induced inter-ictal-like event model, the frequency of the bicuculline-induced events did not reverse upon washout of the ampakine in the presence of the NMDA receptor antagonist 2-AP5. Therefore these changes were not totally mediated by the NMDA receptor, so NMDA receptor independent plasticity changes must have occurred. Ca²⁺ entry into pyramidal cells via voltage-gated Ca²⁺ channels (Johnston et al., 1992) or Ca²⁺ permeable AMPA receptors (receptors that lack the GluR2 subunit) have been reported to lead to NMDA receptor independent plasticity (Jia et al., 1996). Application of ampakines would enhance the current flow

through GluR2 containing AMPA receptors, possibly increasing the degree of NMDA receptor independent plasticity by increasing Ca^{2+} entry via the AMPA receptor route. Also, as ampakines act to depolarise pyramidal cells by increasing AMPA receptor mediated EPSCs, application of the ampakines would increase the levels of activation of voltage gated Ca^{2+} channels. As this NMDA independent plasticity occurred only in the bicuculline model, it is possible that the NMDA-dependent plasticity observed in other models occurs through the interneurons, and the NMDA-independent plasticity occurs through direct effects on pyramidal cells or through modulation of GABA_B receptor function.

As in the 4-AP model, application of 2-AP5 caused a significant increase in the frequency of the inter-ictal-like events in the bicuculline model. The direct effects on pyramidal cells would remain in place in this model. It is possible that although GABA_A mediated signalling from interneurons is removed; post-synaptic GABA_B -mediated inhibition may still regulate inter-ictal-like event frequency. The removal of GABA_B mediated inhibition, by reducing the excitability of interneurons through NMDA receptor block, may allow the increase in inter-ictal-event frequency observed in the bicuculline model following application of 2-AP5. The role of GABA_B could be further elucidated using specific antagonists such as CGP55845 (Davies et al., 1993).

As shown in the previous chapter, removal of Mg^{2+} ions from the extracellular medium leads to the gradual emergence of inter-ictal-like events within hippocampal slices (Tancredi et al., 1990). Subsequent application of both CX546 and CX691 lead to a further increase in the inter-ictal-like event frequency. The low- Mg^{2+} induced events occur following the removal of the Mg^{2+} block of the NMDA receptor channel. This is confirmed by the significant reduction in inter-ictal-like event frequency following application of the NMDA receptor antagonist 2-AP5. Paroxysmal depolarising shifts in pyramidal cells within the CA3 subfield of the hippocampus leads to the formation of inter-ictal-like events. Although these events are initiated by the opening of the NMDA receptor, the recurrent synaptic connections and EPSPs that make up paroxysmal depolarisation shifts are largely mediated through AMPA/kainate receptors, as indicated by the significant reduction in event frequency following application of NBQX.

CX546 increases the open time of the AMPA receptor, allowing increased temporal summation of EPSPs and action potential firing within pyramidal cells. CX691 increases the amplitude of the AMPA mediated EPSC, which causes an increased magnitude of each EPSP. This increased action potential firing increases the frequency of inter-ictal-like

events as noted above. There is not a dependency on NMDA receptor activation to increase the frequency of the low Mg^{2+} -induced inter-ictal-like events following application of the ampakines, as NMDA receptor activation is ongoing in this model (Tancredi et al., 1988). Indeed, CX691 increased the frequency of inter-ictal-like events in the presence of 2-AP5.

In the low Mg^{2+} model, application of 2-AP5 caused a significant decrease in the frequency of inter-ictal-like events. This is expected as the major effect on pyramidal cells by removing Mg^{2+} is the activation of the NMDA receptor (Tancredi et al., 1990).

However, IPSPs that are present in this model are also blocked by 2-AP5, indicating the role of NMDA activation in the recruitment of interneurons. This adds evidence to the putative NMDA mediated interneurone recruitment as a possible mechanism for the increase in inter-ictal-like events following 2-AP5 application in the other epileptiform models described above.

The combination of 4-AP and NBQX induces slow inter-ictal-like events in the hippocampus. This model was predominantly used to check the functional specificity of the ampakines for AMPA receptors at the level of the network, using a competitive antagonist of AMPA receptors. These events rely on $GABA_A$ mediated transmission and are depolarising at the intracellular level (Perreault and Avoli, 1992). Subsequent application of CX546 and CX691 did not lead to a significant change in the frequency or mode of the slow inter-ictal-like events, indicating that the ampakines are functionally selective for AMPA/kainate receptors in hippocampal network oscillatory models.

5.5 Conclusion

The main conclusion from the experiments in this chapter is that ampakines increase the frequency of inter-ictal-like activity in a range of models of epileptiform activity. The ampakines investigated increase the amplitude of the fEPSP through their actions on postsynaptic glutamate receptors. They do not induce emergent network activity in quiescent hippocampal slices. CX691 is likely to be more useful than CX546 as a putative nootropic drug as CX691 does not robustly induce ictal-like activity in any of the models investigated, and is therefore likely to be less pro-convulsant than CX546.

Ampakines are potentially useful clinical drugs as they have been shown to significantly improve cognitive function. In the *in vitro* slice preparation, application of the ampakine CX546 often changed the mode of activity from inter-ictal- to ictal-like activity, and in the rest of the models some of the slices displayed ictal-like events following application of the

both ampakines. In individuals who do not display seizures but who are pre-disposed to epilepsy, ampakine treatment may tip the balance of excitation too far and these individuals may then develop epilepsy. If these individuals are representative of the range of susceptibilities of a population to epilepsy, a large proportion of the more vulnerable may suffer seizures following ampakine treatment.

6 Changes in protein expression following environmental enrichment

6.1 Introduction

As discussed in the previous chapters, treatment with nootropic drugs is an approach to enhance cognitive performance. However, other approaches have been shown to improve performance in cognitive tasks, including exposure to an enriched environment for a period of time (Hebb, 1949). In this protocol, animals are either kept in an environment containing ladders, running wheels and tubing, which is moved on a regular basis, or alternatively in a sparse environment containing only minimal shelter and stimulation (see methods chapter). Changes in spine density, dendritic length and behaviour can be observed between the two groups (Varty et al., 2000) and subsequent biochemical analysis shows changes in gene expression (Huang et al., 2006).

Changes in protein expression also occur following exposure to an enriched environment. In McNair *et al* (2007), differential in-gel electrophoresis (DiGE) along with matrix assisted laser desorption-ionisation time of flight (MALDI-ToF) and Q-STAR mass spectrometry allowed the identification of hippocampal proteins that significantly change in expression in response to exposure to an enriched environment. Subsequent database searching and gene ontology analysis revealed the majority (>70%) of proteins regulated were involved in energy metabolism, cytoplasmic organisation/biogenesis, and signal transduction.

The focus of this chapter is the initial confirmation of some of the protein changes that occur in response to the enrichment protocol using a 2-dimensional western blot technique. This allows antibodies raised against the protein of interest to identify changes in the charge or size of the protein. The expression of a further protein, MeCP2, a histone modification protein, will be compared between the animals exposed to the enriched environment and the poor environment using a conventional 1D western blot. This protein is involved in the epigenetic regulation of gene expression and deficits in this protein are known to induce developmental deficits (Amir et al., 1999).

The aims of this chapter were to

1. Confirm the observations from the DiGE experiment identifying several proteins that significantly changed in expression in response to an enriched environment
2. Quantify the expression of MeCP2 in response to an enriched environment

The possible implications of the changes that occur at the proteomic level, with respect to the cognitive enhancement that occurs following exposure to this model, will be discussed.

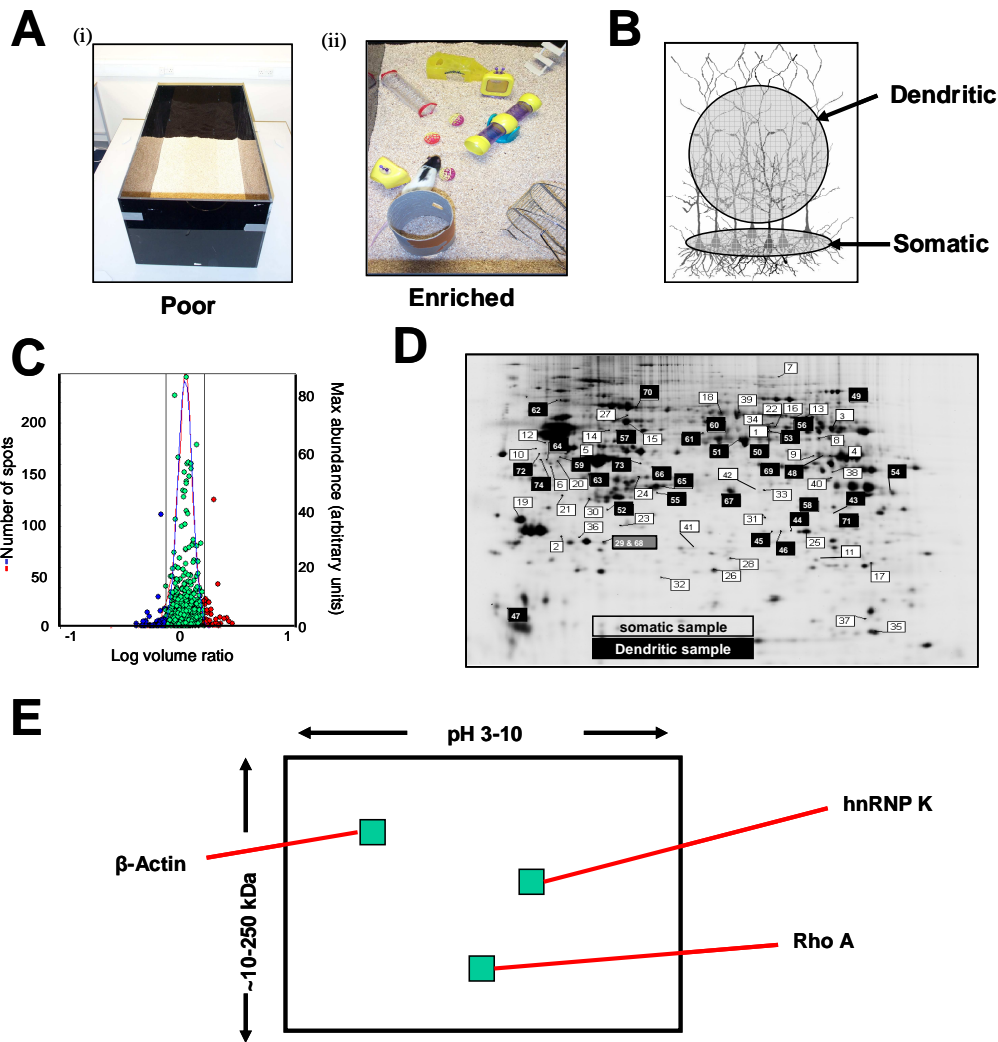
6.2 Effect of a model of environmental enrichment on global hippocampal protein expression

Figure 6.2 is reproduced here from McNair *et al* (2007) with permission. Upon initiation of the enrichment protocol, animals were housed in an open field (fig 6.2.A.i) or an enriched environment (fig 6.2.A.ii), containing many objects that were moved on a regular basis. This enhances spatial re-mapping ability and improves cognitive performance (Duffy *et al.*, 2001; Escorihuela *et al.*, 1994; Escorihuela *et al.*, 1995), and promotes synaptic plasticity (Duffy *et al.* 2001). Following a six week enrichment regime, the hippocampi were rapidly removed and chilled (see methods). The somatic and dendritic layers of the hippocampus were separated to isolate the predominantly principal cell soma from the dendritic field neuropil.

The entire proteome was then labelled for DiGE to allow quantification of individual protein spot abundance levels in control and enriched animals. The scatter plot (fig 6.2.C) shows the change in the log abundance of proteins from the somatic layer following the environmental enrichment protocol, in which only 137 of 2469 protein spots displayed a change in abundance greater than 1.5 fold. Using biological variance analysis it was revealed that only 71 of the proteins significantly ($P < 0.05$) changed in abundance following the environmental enrichment protocol (see fig 6.2.D), with slightly fewer somatic proteins changing expression (32) than dendritic proteins (42). Only 2 proteins significantly changed in abundance in both the somatic and dendritic regions. Following MALDI-ToF/Q-STAR mass spectrometry several of these proteins were identified and displayed in tables 1 and 2 in the appendix.

The schematic representation of the DiGE gel shows the approximate locations of where a significant ($P < 0.05$) change in the expression of β -Actin, Rho A, and hnRNP K occurs, as identified by the MALDI-ToF/Q-STAR mass spectrometry (see appendix). These locations correspond to the locations on the 2D western blots where protein changes were observed.

Fig 6.2 The effect of an environmental enrichment protocol on the global protein expression of the hippocampus



A. These pictures show the environmental conditions for the animals exposed to an open field (i) or an enriched (ii) environment for a total period of 6 weeks. **B.** Hippocampal tissue was then isolated from either predominantly dendritic or somatic regions (shaded areas). **C.** Total protein extracts from area CA1 stratum pyramidale of the enriched animals show a number of proteins change in abundance relative to the control animals. The scatter plot shows the log abundance ratio of individual sample spot pairs against the maximum protein spot abundance. Individual protein spots show decreased (●), unaltered (●) and increased (●) log abundance ratios. The vertical lines indicate 1.5 fold change in abundance. The red curve shows the frequency distribution of the log abundance ratios, and the blue curve shows the normalised modal frequency fitted to a modal peak of zero. Note that the majority of protein spots remain unaltered by the enrichment protocol. **D.** The gel image indicates that the environmental enrichment protocol induced significant ($P < 0.05$) changes in protein abundance in 71 proteins revealed by biological variance analysis. Of these proteins 42 displayed differential abundance only in the somatic layer (open squares), whilst 32 showed significantly altered abundance in the somatic layer (black squares), and only 2 proteins significantly changed abundance in both the somatic and dendritic layers (grey squares). **E.** Schematic of a DiGE gel showing the approximate locations of the proteins β -Actin, Rho A, and hnRNP K, as identified by MALDI-ToF mass spectrometry. The indicated location of β -Actin, which can be observed in several locations throughout the gel, is the one identified as significantly changing in the DiGE analysis.

6.3 The change in expression of the proteins β -Actin, Rho A, and hnRNP K following exposure to a model of environmental enrichment

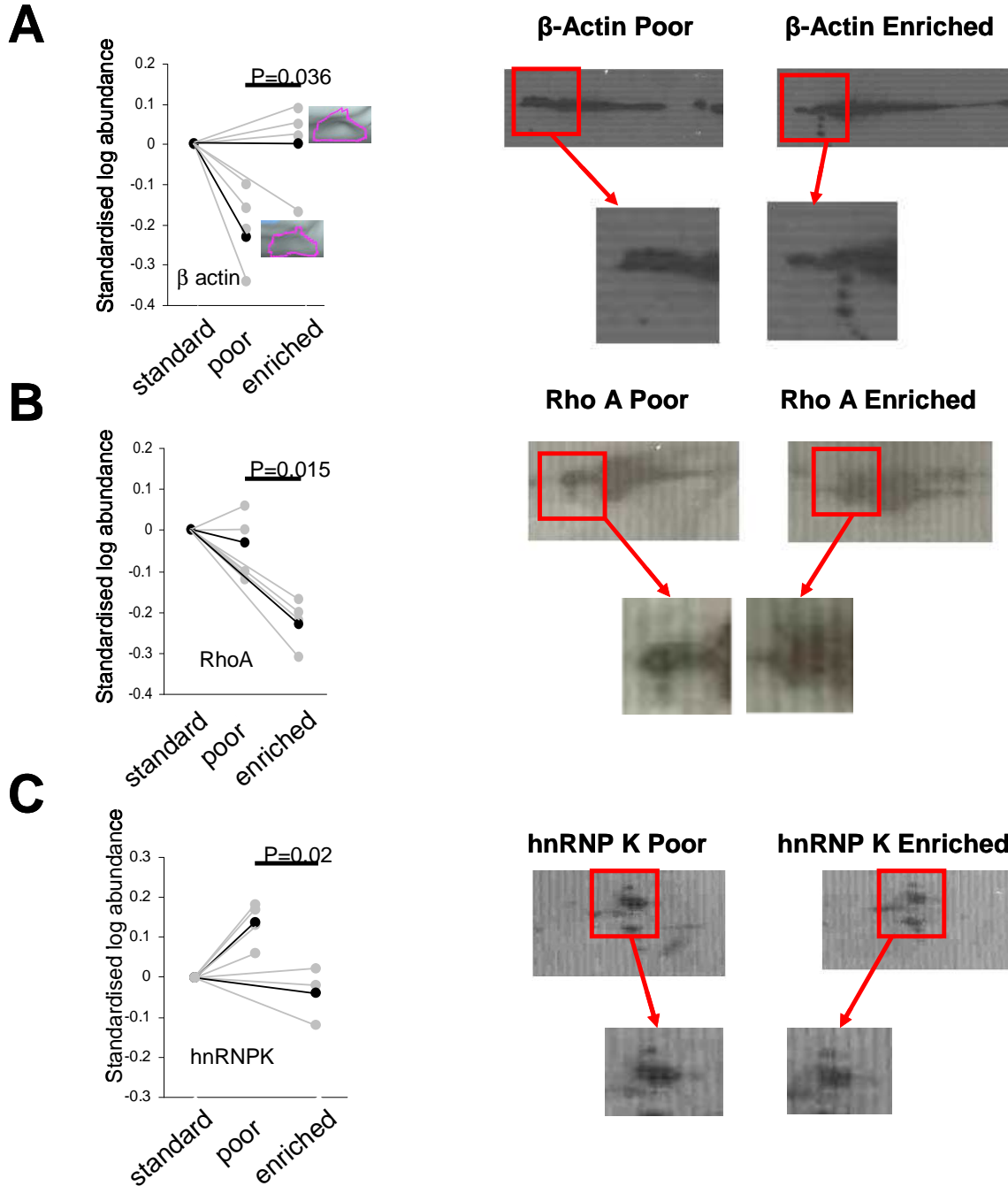
The DiGE analysis revealed the altered expression of a number of hippocampal proteins following environmental enrichment. To confirm and validate the findings of the DiGE experiment using a different experimental approach, representative proteins were selected from the DiGE study. Commercial antibodies selective for these proteins were then used to identify these proteins.

In order to confirm the changes in expression of these proteins, 2 dimensional western blots were performed for β -Actin, Rho A, and hnRNP K. β -Actin, the cell structural protein, increases in expression at the locus identified following the enrichment protocol (fig 6.2.1.B). Three extra protein spots can be observed following the enrichment protocol as opposed to the control showing the change in the pattern of expression of β -Actin. The enrichment protocol causes a decrease in the expression of the cell signalling protein Rho A. Rho A displays a weaker but more disparate protein spot in the tissue taken from the hippocampus of the animals exposed to an enriched environment than the poor environment. Similarly, hnRNP K decreased in expression in response to exposure to the enriched environment, as shown by the expanded gel image, which validates the findings of the DiGE experiment.

6.4 The change in expression of MeCP2 in response to a model of environmental enrichment

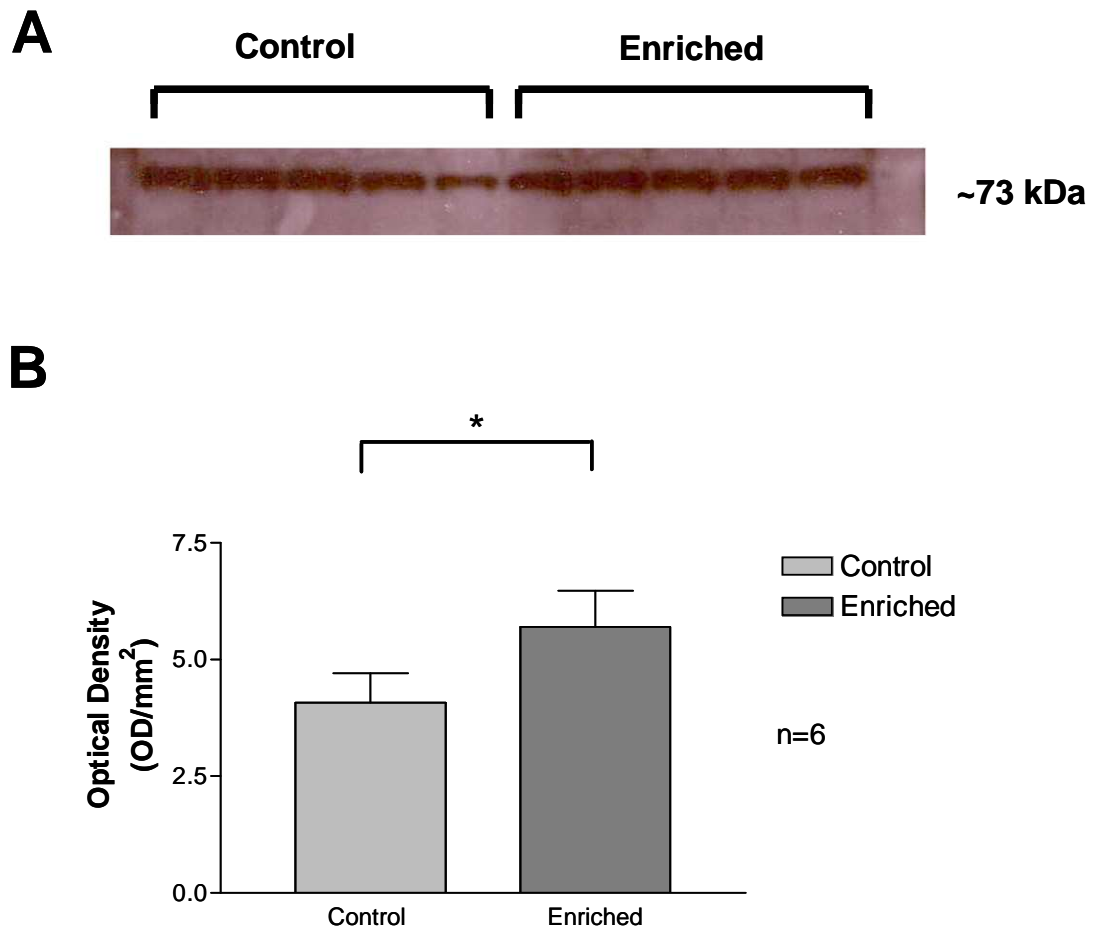
To assess the effect of environmental enrichment on the DNA methyl binding protein MeCP2, 1D western blot experiments were performed using a commercially available anti-MeCP2 antibody. The representative bands from the 1 dimensional western blot (fig 6.4) show that the enrichment protocol increases the expression of MeCP2. The theoretical size from the amino acid sequence of MeCP2 is 52 kDa but the band migrates to around 73 kDa (Myaki and Nagai 2006). The summary histogram (fig 6.4.B) shows that there is a significant ($P = 0.04$) increase in the mean ($n = 6$) expression of MeCP2 in the hippocampus of animals exposed to an enriched environment as opposed to a poor environment. This is reflected in the increase in the optical density in the bands corresponding to MeCP2.

Fig 6.3 The effect of an enriched environment upon the expression of β -Actin, Rho-A, and hnRNP K



A-C Representative scatter plots showing examples of identified protein spots displaying increased (i, β -Actin) and decreased (ii, Rho A & iii, hnRNP.K) protein abundance in hippocampal tissues isolated following environmental enrichment. Grey points represent individual DiGE gel replicates whilst black points indicate mean abundance in tissues from rats exposed to 'poor' (open field) and enriched conditions. Also, 2D western blots showing the difference in expression pattern of identified proteins between poor and enriched animals. **A.** The enrichment protocol increases the expression of β -Actin at this locus, shown by a change in size and intensity of the β -Actin bands. Note there are a number of spots of β -Actin observed in the enriched animals that are not present in the control animals. **B.** The enrichment protocol causes a decrease in the expression of Rho A at this locus. **C.** An decrease in the expression of hnRNP K can be observed following exposure to an enriched environment.

Fig 6.4 Quantification of expression change of MeCP2 in response to enriched environment



A. Representative 1 dimensional western blot showing the effect of an enrichment protocol on the expression of the histone modification protein MeCP2, taken from a combined sample of 3 animals. **B.** Summary histogram showing environmental enrichment causes a significant ($P = 0.04$) increase in the mean ($n = 6$) expression of MeCP2. Each individual experiment is taken from a combined protein sample of 3 animals, with 5 replicates per gel, across 6 gels. The pairing of the data approaches significance ($P = 0.07$).

6.5 Discussion

As well as the electrophysiological approaches in the previous chapter, it is important to analyse the changes that occur at the proteomic level following cognitive enhancing strategies, allowing the isolation of cognition-related biomarkers and the identification of novel molecular entities involved in cognitive processes. The pharmaceutical industry is especially interested in the reversal of cognitive deficits that are associated with neurological conditions like Alzheimer's Disease and schizophrenia (Buchanan et al., 2007; Chamberlain et al., 2006).

The cognitive enhancing strategy investigated in this chapter was environmental enrichment, which is reported to result in improvements in a range of cognitive tasks (Duffy et al., 2001). Regular changes in the features of the environment in which the rodents were housed ensured the rodents underwent spatial re-mapping (Jankowsky et al., 2005), thought to be crucial in the enhancement of cognition that occurs in this environment.

Previous studies showed that the expression of genes performing a range of different functions varied following an environmental enrichment regime (Rampon et al., 2000). Fig 6.2 shows that the expression of proteins also changes following exposure to the six-week environmental enrichment protocol. The majority of the proteins that change are involved in signalling, metabolism, biogenesis and cytoplasmic organisation (see appendix). It is likely that as structural and metabolic proteins are more highly abundant than other classes of proteins, one may expect a higher proportion of proteins from these classes to be identified. In the dendritic sample, a substantially greater proportion of signalling proteins change in expression as compared to the somatic fraction (fig 3, appendix), perhaps due to the enhancement of synaptic transmission, and therefore synaptic remodelling, which occurs in the dendrites following the enrichment protocol (Duffy et al., 2001; Huang et al., 2006).

Three proteins that significantly changed in expression were selected for further analysis – the structural protein β -Actin, the signalling protein Rho A, and the heterogeneous nuclear ribonuclear protein complex K (hnRNP K). These proteins were chosen as representative examples of the proteins investigated as they perform different functions within neurones, and they are expressed in different compartments of the neurone. Also an important consideration for the 2D western analysis is the availability of an antibody for the

particular protein of interest. One of the proteins initially chosen, CRMP2, an important protein in axonal growth that promotes microtubule assembly (Fukata et al., 2002), was eventually rejected due to the unavailability of a specific CRMP2 antibody. These proteins were chosen to perform 2D western blot experiments as the location of the gel spot on the DiGE experiment could be related to the position of the spot identified by the specific antibody to the protein. Performing 2D (as opposed to 1D) western blots also allowed the change in charge of the protein to be identified. The activation state of proteins, which can be changed by processes such as phosphorylation, can be differentiated even if the total expression level does not change. These proteins all changed spot density in the direction predicted by the DiGE experiment, confirming the validity of the conclusion that the proteins changed in expression following exposure to an enriched environment.

The DiGE experiment highlighted the wide range of proteins that change in expression following an environmental enrichment protocol. These experiments showed that β -actin, a widely expressed protein and one often used as a protein loading control in western blots (Dennis-Sykes et al., 1985; Towbin et al., 1979), is dynamically regulated and can change in expression in response to environmental conditions. β -Actin is a cytoskeletal protein that regulates the leading edge of cell growth (Wallar and Alberts, 2003). A change in the total expression of β -Actin demonstrates that changes in the synaptic morphology may occur during the enrichment protocol. Indeed, spine formation and synapse re-modelling is important in the expression of long term potentiation (Popov et al., 2004), and actin polymerisation is implicated in LTP formation (Huntley et al., 2002; Krucker et al., 2000).

Rho A is part of a family of Rho GTPases which are small proteins involved in the transduction of extracellular signals to the nucleus (Jaffe and Hall, 2005). Rho GTPases are known to play a role in hippocampal neuronal plasticity (O'Kane et al., 2003; O'Kane et al., 2004). In particular, RhoA is known to be important in the maintenance of neuronal structures (Threadgill et al., 1997). RhoA was found to increase in expression following exposure to an enriched environment. Activated RhoGTPases, including RhoA, are involved in the enhancement of learning and memory in mice (Diana et al., 2007), suggesting that an increased level of RhoA would be beneficial to the processes that occur during spatial re-mapping. The conditional knockout or pharmacological inhibition of RhoA during the environmental enrichment protocol would lead to a greater understanding of the role RhoA plays in the enhancement of cognition.

The protein kinase hnRNP K is involved in the control of transcription of a number of cell cycle regulators (Michelotti et al., 1996), and activation of hnRNP K involves an increase

in RNA synthesis of its target genes (Lee et al., 1996). Expression of hnRNP K is increased in the model of environmental enrichment, and thus the expression of the genes controlled by hnRNP K may be involved in the enhancement of cognition observed following the enrichment protocol. An increase in RNA synthesis is involved in the process of long term potentiation, and as such, activated hnRNP K may act to transcribe target genes in this process.

However, activated hnRNP K can antagonise the effects of the neuronal nicotinic acetylcholine receptor promoter (Du et al., 1998), amongst other protein targets. Activation of the neuronal nicotinic acetylcholine receptor is widely reported to be pro-cognitive (Ferguson et al., 2007; Hodgkiss and Kelly, 2001; Timmermann et al., 2007). This suggests that if an increase in the expression of hnRNP K is mediating the enhancement of cognitive function, it must be pro-cognitive despite its detrimental effect upon nicotinic acetylcholine receptor expression.

There are clearly several advantages and disadvantages to this method of investigating changes in protein expression. This approach allows an unbiased evaluation of the whole proteome, and all the proteins that do significantly change in expression can be identified following the DiGE experiment. This allows the identification of proteins previously not associated with the changes that occur following cognitive enhancing strategies. The confirmation of the change in protein expression by the 2D western blotting analysis provides an extra assurance of the veracity of the conclusions made following the DiGE experiments. However, conclusions obtained using a DiGE approach must include several caveats. With such a large data set generated, this consequently increases the chance of false positives and negatives being generated. Many proteins, especially membrane bound proteins, do not run onto the gels and therefore cannot be identified by the DiGE approach. Proteins with a low abundance are less likely to be identified by mass spectrometry than proteins with an abundant expression. As only one time point was chosen (6 weeks in this case) other proteins important in the development of cognitive enhancement may be missed. As such, further experiments investigating proteins that are identified by this approach should be carried out to evaluate the precise temporal and spatial expression and function of the proteins. This would allow further understanding of the roles of these proteins in cognitive enhancement.

The second approach used to investigate changes in protein expression that occur following exposure to an enrichment environment was the use of a conventional 1D western blot. The protein chosen was methyl-CpG binding protein 2 (MeCP2), a protein

that is aberrantly expressed in the neurodevelopmental disorder known as Rett syndrome (Lewis et al., 1992; Meehan et al., 1992a; Meehan et al., 1992b). MeCP2 is an X-linked protein and binds to methylated CpG islands of DNA and suppresses gene transcription at these locations (Nan et al., 1998). The condition is X-linked (Amir et al., 1999) and female patients develop severe autistic-like and other symptoms after 6-18 months of apparently normal development (Chahrour and Zoghbi, 2007). Other autistic spectrum disorders are linked to mutations in the *MECP2* gene in males (Jan et al., 1999; Moretti and Zoghbi, 2006). MeCP2 is thought to play a role in neuronal maturation and plasticity through transcriptional repression (Nan et al., 1997) and modification of RNA splicing (Young et al., 2005).

The main finding of this section was the demonstration that the expression of MeCP2 does significantly increase following exposure to an enriched environment. The enrichment protocol, through the regularly changing environment, causes spatial re-mapping in the hippocampus and therefore changes in the plasticity of the neurones must occur (Duffy et al., 2001). The upregulation of MeCP2 may therefore be required to allow these plasticity changes to occur. As MeCP2 is involved in neuronal maturation then an upregulation of MeCP2 may occur as neurogenesis increases in the hippocampus following environmental enrichment (Nilsson et al., 1999).

The upregulation of MeCP2, a transcriptional repressor, fits with the fact that the majority of proteins identified as significantly changing expression decreased in expression following exposure to the model of environmental enrichment. It is possible that expression of MeCP2 is important in the subsequent down-regulation of many genes (Rampon et al., 2000) and proteins (see appendix) following the enrichment protocol. In contrast to the findings above, immunohistochemical studies (Zhou et al., 2006) have shown that total levels of MeCP2 expression do not change in response to environmental stimuli, but the level of phosphorylation of the protein is activity dependent. As the antibody used above was raised such that it was not selective between the phosphorylated and dephosphorylated states of MeCP2, the activation state of the protein could not be assessed following the enrichment regime. Interestingly, changes in either the gene or protein expression of MeCP2 were not identified by the microarray (Rampon et al., 2000) or DiGE (see appendix) studies.

It is also tempting to speculate that the environmentally poor model is essentially a model of Rett syndrome, as there is a lower expression of this protein than in the enrichment model. MeCP2 deficient mice display altered social interactions (Moretti et al., 2005).

When compared to the enrichment model, there was a decreased expression of this protein, and a measurable cognitive impairment as in Rett syndrome. However, as introducing mutations into MeCP2 can produce further cognitive deficits, the environmentally poor environment is a model of a mild form of Rett syndrome at best. Cognitive impairment may occur through other mechanisms, and this model would have to be characterised further to evaluate its potential use as a model of mild Rett syndrome.

An important proviso in interpreting the results from the environmental enrichment model is that the animals exposed to the enriched environment were likely to get more exercise than the animals exposed to the poor environment. Exercise can change protein expression (Ding et al., 2006; Ueda et al., 2003) and improve cognitive function (Hicks and Birren, 1970; Radak et al., 2001). It is difficult to control for and separate these changes from the changes induced by the spatial re-mapping and exploratory behaviour.

Both approaches, despite the fact that the somatic and dendritic regions were separated for the DiGE experiment, can not provide any information at the cellular or regional levels of protein expression. There are many distinct cell types within the hippocampus, including the pyramidal cells, the interneurons, the glial cells, the blood vessels etc. Important changes that occur in one region that do not occur in another may not be identified by the proteomic approaches used above. One way to overcome this problem is to identify the cell type using immunohistochemistry single cell RT-PCR. Another approach is to genetically label a sub-population of cells with fluorescent markers linked to markers of that cell type, and use fluorescence activated cell sorting (FACS) to separate this particular population of cells (Herzenberg et al., 2002). This would allow proteomics to be subsequently performed upon a particular cell type.

The environmental enrichment model confirms that improvements in cognition do not necessarily cause epileptogenesis, as some of the approaches to enhancing cognition investigated in the previous chapters do. Environmental enrichment can actually decrease seizure susceptibility in rodents (Young et al., 1999), indicating an increase in cellular excitability to the point of increased seizure susceptibility is not required to improve cognitive function.

6.6 Conclusion

In this chapter a further strategy shown previously by several groups to enhance cognition, an environmental enrichment model, was investigated. A vast number of proteins in many

different classes, that perform many different functions, changed in expression following the enrichment protocol. An indication of the extremely large range of proteins that are modulated in expression following a cognitive enhancing strategy was gained from the DiGE experiment and the subsequent western blots. As MeCP2 was not identified as significantly changing in expression following exposure to the enriched environment in the proteomic analysis, but was in the 1D western blot approach, this indicates the proteomic approach cannot identify all of the relevant proteins at the same time. A combination of approaches using genetics, molecular biology, pharmacology, electrophysiology, and proteomics and is required to gain further insight into the processes that underlie cognitive enhancement.

7 Summary and conclusions

7.1 Introduction

The major focus of this thesis was the investigation of hippocampal physiology, pharmacology and protein expression with respect to cognitive enhancing strategies. Two approaches to cognitive enhancement, one using nootropic drugs to induce oscillations and another using an environmental enrichment, were investigated. Initially, potentially nootropic compounds were investigated to establish the propensity of these compounds to induce network oscillatory activity in hippocampal slices. Network oscillations are correlated with specific brain functions, and an enhancement of oscillatory activity has been proposed to rectify cognitive impairment in a number of different conditions (Cobb and Davies, 2005). Many compounds that can enhance cognitive function also show a tendency to be epileptogenic, and so the effects of these compounds were investigated in models of epileptiform activity. The hippocampus is an ideal brain region in which to study these processes, as the hippocampus is a region involved in mnemonic processes, but is also an area that is highly susceptible to the generation of seizures (Schwartzkroin, 1993). The protein changes that occur following exposure to an enriched environment, an experimental paradigm which is known to improve cognitive function, were identified using a global proteomic approach, following which the changes in expression of selected proteins were confirmed by western blots. The findings of these experiments, and the potential implications for the development of cognitive enhancing strategies, are discussed below.

7.2 The effect of mAChRs on hippocampal neurophysiology

Application of mAChR agonists to hippocampal slices leads to the emergence of a range of oscillatory activities. Both physiological and pathophysiological oscillations induced by the application of mAChR agonists have long been identified within the hippocampus (Rutecki and Yang, 1998; Williams and Kauer, 1997). The selective M₁ mAChR agonist 77-LH-281 behaves very differently from non-M₁ selective mAChR agonists in that it may possess desirable pro-oscillatory/cognitive properties whilst not producing unwanted pathophysiological oscillatory responses.

In naïve hippocampal slices, application of a range of mAChR agonists, including carbachol, oxotremorine, and pilocarpine, have been shown to induce epileptiform-like activity. These agonists also induce seizures within laboratory animals (Turski et al., 1989). As the mAChR agonists are also putatively pro-cognitive and promote synaptic

plasticity (Huerta and Lisman, 1993; Messer et al., 1990), an agonist that can promote mAChR-mediated transmission, but does not promote epileptiform activity, is a potentially useful therapeutic strategy to promote cognitive function. 77-LH-281, an allosteric M₁ mAChR agonist, promotes gamma frequency oscillations in hippocampal slices, which are associated with cognition (Tallon-Baudry and Bertrand, 1999). Promoting gamma activity is a potential therapeutic strategy in reversing the cognitive decline that is observed in schizophrenics, as a reduced power of gamma frequency oscillatory activity is observed in schizophrenic patients (Haig et al., 2000). In the majority of both naïve slices, and slices in which a range of mechanistically distinct epileptiform-like activities were induced, 77-LH-281 did not promote pathophysiological epileptiform-like activity. This is in contrast to the non-subtype-selective mAChR agonist oxotremorine-M.

Gamma frequency oscillations are also initiated by the application of kainate. However, application of kainate to laboratory animals leads to the eventual emergence of seizure-like activity (Ben-Ari et al., 1981). Thus further *in vivo* studies are required to evaluate the potential epileptogenic potential of 77-LH-281.

Profound differences in the emergent network activities were observed depending on the orientation in which the slices are made. The main difference observed between the slices was a greater tendency for slices prepared in the coronal orientation to display gamma frequency oscillatory activity in response to kainate and 77-LH-281, whereas gamma frequency oscillations were absent in slices prepared in the parasagittal orientation. This is likely to be due to basket cells interneurone arborizations being predominant in the coronal sections, with stratum oriens-lacunosum moleculare being the predominant interneurone class within parasagittal slices (Gloveli et al., 2005).

Previously, cholinergically induced gamma frequency oscillations have been shown to be sensitive to antagonists of both fast glutamatergic synaptic transmission and fast GABAergic synaptic transmission (Fisahn et al., 1998; Mann et al., 2005). Similarly, the gamma frequency oscillation induced by 77-LH-281 is also sensitive to antagonists of ionotropic glutamate and GABA_A receptors.

A range of mechanistically distinct models of epileptiform activity allowed both the potential pro-epileptogenic nature of mAChR agonists to be investigated, and insight into the network that underlies these oscillations. In the main, oxotremorine-M increased the frequency of inter-ictal-like events and induced ictal-like activity in three of the four epileptiform models studied. In contrast, 77-LH-281 did not induce ictal-like activity in

any of the models studied and only increased the frequency of inter-ictal-like events in the bicuculline model. This indicates that 77-LH-281 displays a lower potential to be epileptogenic than oxotremorine-M.

Inter-ictal-like events are characterised by paroxysmal depolarising shifts within the pyramidal cells. The frequency of paroxysmal depolarisation shifts is increased with a greater excitability of the network; this in turn increases the frequency of inter-ictal-like events. Excitability is manifest as an increased pyramidal cell action potential firing within the hippocampus (Rutecki et al., 1985). mAChR agonists depolarise and cause action potentials within pyramidal cells partially through M_1 mAChRs (Fisahn et al., 2002), so the absence of an increase in inter-ictal-like event frequency in both the 4-AP and low Mg^{2+} modes following M_1 mAChR activation is somewhat surprising. It is possible that an increased activation of interneurons occurs in these models leading to an increase in $GABA_A$ mediated IPSPs in pyramidal cells. In the bicuculline model this form of inhibition is removed allowing an increase in inter-ictal-like event frequency. As inter-ictal-like event frequency has been correlated with $[K^+]_o$ it would be interesting to record the $[K^+]_o$ with ionic sensitive electrodes.

The application of oxotremorine-M to hippocampal slices leads to pathophysiological ictal-like activity in both quiescent hippocampal slices and slices in which inter-ictal-like events are ongoing. This ictal-like activity is dependent upon AMPA/kainate mediated glutamate signalling, and is not replicated by M_1 mAChRs. Ictal-like events are characterised by a transient decrease in inhibition from interneurons, with $GABA_B$ prominent in the bicuculline model. Greater insight into the mechanism of ictal generation in hippocampal networks in a variety of these epileptiform models would be provided by intracellular recordings from pyramidal cells and morphologically distinct classes of interneurons in the hippocampus. In hindsight a more thorough investigation of the role of the $GABA_B$ receptor in these models would have been of interest.

As a strategy to enhance cognition, the development of a specific M_1 mAChR agonist appears to show a greater tendency to induce gamma oscillations, and less of a propensity to induce pathophysiological epileptiform-like activity, than non-subtype-selective mAChR agonists. 77-LH-281 therefore has a more favourable electrophysiological profile for use as a potential cognitive enhancer than non-subtype selective mAChR agonists.

7.3 The effect of ampakines in hippocampal slices

Another class of compounds that are potentially useful cognitive enhancing drugs are the ampakines. These are positive allosteric modulators of AMPA type glutamate receptors, and potentiate fast glutamatergic synaptic transmission. Compounds with this property have long been associated with cognitive enhancement (Ingvar et al., 1997; Ito et al., 1990), but, like mAChR agonists, they have the potential to be pro-epileptogenic (Qi et al., 2006). Here the effects of two ampakines were investigated, one that increases the amplitude of current flow through the AMPA receptor, and the other that increases the time the ion pore is open. The potential pro-epileptogenic effect of the ampakines was tested in the same models of epileptiform activity used in the investigations of 77-LH-281.

In quiescent slices both ampakines did not induce any oscillatory activity. In the epileptiform models, both CX546 and CX691 significantly increased the frequency of inter-ictal-like events. This increase in the frequency of inter-ictal-like events corresponds to an increase in excitability in the network. CX546 showed a tendency to promote ictal-like activity only the 4-AP model, possibly due to an increase in the window of temporal summation for EPSPs acting on interneurons to lead to an eventual depolarisation block of the interneurons. This may only happen in the 4-AP model as the frequency of inter-ictal-like events, and paroxysmal depolarising shifts, is higher than in the other models investigated. It is also possible that an increased level of excitation reverses the chloride gradient to make GABA_A mediated potentials excitatory.

These experiments show that these ampakines are potentially pro-epileptogenic, as they increase the frequency of inter-ictal-like events in hippocampal slices. The ampakines only display a tendency to promote epileptiform activity in slices in which epileptiform activity was induced prior to the application of the ampakine: in less excitable physiological networks ampakines did not promote epileptiform-like activity. It is possible that in non-epileptics ampakines may have a wide enough therapeutic index to promote cognitive function without promoting pathological oscillations. The ampakines that enhance the single channel conductance of the AMPA receptor, like CX691, are more likely to be safer than ampakines that increase the open time of the ion channel, like CX546. Conversely, as oscillatory activity is associated with mnemonic function (Traub et al., 1998), it may be that ampakines in the same class as CX546, which promote oscillatory activity, are better cognitive enhancers. Further *in vivo* studies investigating the cognitive and pro-epileptic potential of these ampakines could be performed to determine the potential use of these compounds as cognitive enhancers in the clinic.

7.4 The environmental enrichment protocol

The environmental enrichment protocol is a well-characterised method of improving the cognitive ability of rodents (Varty et al., 2000). Changes in protein expression that occurred following exposure to an enriched environment were investigated. Several of these proteins were identified using a non-biased proteomic approach, and one protein was selected due to the phenotype of severe cognitive impairment that occurs following disruption of this protein. These complementary approaches also allowed a comparison of the methods used to select these proteins.

There were many proteins, of several functional classes, that changed in expression following exposure to the environmental enrichment protocol. Some or all of these may play a role in the cognitive enhancement that occurs following exposure to the enriched environment. The ones selected for confirmation of the change in expression by 2D western blot analysis were known to perform different roles within the neurones.

These proteins significantly changed in expression and were identified using MALDI-ToF mass spectrometry. Database searches were then performed to identify these proteins, and antibodies for these proteins were then selected. All of these tasks have limitations. If the protein does not resolve on the gel the protein cannot be identified. This is a particular problem with hydrophobic proteins like neurotransmitter receptors. If the proteins are not picked up by the mass spectrometer or do not appear within the database they cannot be identified. 2D proteomics provides a greater weighting to the more abundantly expressed proteins, and as such the proteins that are present in small amounts within the cells are less likely to be identified as significantly changing. No emphasis is given to proteins that play a more prominent role in the changes that are observed between the two groups. A 'single gene' approach often provides more detailed insight into the key proteins that underlie changes that occur in following interventions like environmental enrichment, though an appreciation of the network that protein exists in is crucial to understanding these complex changes.

MeCP2 is an important protein in the regulation of the expression of many genes (Nan et al., 1998). In the model of environmental enrichment many different genes are regulated (Rampon et al., 2000) and it is likely that epigenetic factors play a role in changes of expression of these genes. Recently environmental enrichment has been shown to help ameliorate the cognitive decline that occurs in Rett syndrome mice (Kondo et al., 2008; Nag et al., 2009). It was therefore decided to investigate the expression of MeCP2 in

environmentally enriched animals. MeCP2 is a protein that is known to be important in cognitive function, as disruption of MeCP2 leads to Rett syndrome (Amir et al., 1999). MeCP2 is significantly increased in expression in the enriched model, despite the fact that the DiGE approach did not identify MeCP2 as significantly changing in expression. A change in the expression of MeCP2 would have many downstream effects on the expression of many genes that are regulated by MeCP2, and these changes may partially underlie the changes in the global proteome that occur following exposure to an enriched environment. This emphasises some of the limitations of the 2D DiGE approach. Prior selection of protein targets that may be involved in cognitive enhancement would lead to important proteins in this process being missed. As such, combined proteomic approaches are required to investigate fully the changes in protein expression that underlie cognitive enhancement.

7.5 Combination of approaches investigating cognitive enhancement

In this thesis two experimental approaches to enhance cognition, the application of nootropic drugs, and exposure to an environment that improves cognitive function, were investigated. It would be interesting to combine both of these, and other, approaches to investigate further cognitive enhancement. Following the chronic or acute treatment of animals with putatively nootropic drugs, such as 77-LH-281 or ampakines, the behavioural, electrophysiological and proteomic changes that occur following drug application could be compared to the changes that occur in enriched animals. Also, it would be interesting to see if the deficits in cognitive function that occur in the poor environment can be reversed by treatment with cognitive enhancers. Protein changes that occur may provide a reliable biomarker for cognitive impairment, a useful way of identifying the effectiveness of future nootropic drugs, and even provide possible new targets for cognitive enhancement strategies.

7.6 Conclusions

This thesis has provided insight into both electrophysiological properties and protein expression within the hippocampus, and the relation of these to the field of cognitive enhancement. Mechanistic insight into the role of specific mAChR subtypes in oscillations, and the effect of nootropic compounds on emergent network activity has been gained. Importantly, the novel specific M₁ mAChR 77-LH-281 has been shown to induce an oscillatory rhythm that is associated with cognition, and to not promote ictal-like

epileptiform activity. Ampakines show a tendency to promote some forms of pathophysiological activity. This thesis also showed the wide range of proteins that change in expression following exposure to an enriched environment, indicating the complex sub-cellular response to this cognitive enhancing strategy. The studies performed in this thesis can hopefully underpin further research into cognitive enhancing strategies, and to help ameliorate cognitive decline in diseases such as Alzheimer's disease and schizophrenia.

List of References

- Alban, A., S.O. David, L. Bjorkesten, C. Andersson, E. Sloge, S. Lewis, and I. Currie, 2003, A novel experimental design for comparative two-dimensional gel analysis: two-dimensional difference gel electrophoresis incorporating a pooled internal standard, *Proteomics* 2003 3(1):36.
- Amir, R.E., I.B. Van den Veyver, M. Wan, C.Q. Tran, U. Francke and H.Y. Zoghbi, 1999, Rett syndrome is caused by mutations in X-linked MECP2, encoding methyl-CpG-binding protein 2, *Nat Genet* 23, 185.
- Andrade, R., R.C. Malenka and R.A. Nicoll, 1986, A G protein couples serotonin and GABA_B receptors to the same channels in hippocampus, *Science* 234, 1261.
- Arai, A.C. and M. Kessler, 2007, Pharmacology of ampakine modulators: from AMPA receptors to synapses and behavior, *Curr Drug Targets* 8, 583.
- Arai, A.C., Y.F. Xia and E. Suzuki, 2004, Modulation of AMPA receptor kinetics differentially influences synaptic plasticity in the hippocampus, *Neurosci* 123, 1011.
- Arai, J. and K. Natsume, 2006, The properties of carbachol-induced beta oscillation in rat hippocampal slices, *Neurosci Res* 54, 95.
- Aram, J.A., D. Martin, M. Tomczyk, S. Zeman, J. Millar, G. Pohler and D. Lodge, 1989, Neocortical epileptogenesis in vitro: studies with N-methyl-D-aspartate, phencyclidine, sigma and dextromethorphan receptor ligands, *J Pharmacol Exp Ther* 248, 320.
- Avoli, M., M. Barbarosie, A. Lucke, T. Nagao, V. Lopantsev and R. Kohling, 1996, Synchronous GABA-mediated potentials and epileptiform discharges in the rat limbic system in vitro, *J Neurosci* 16, 3912.
- Balestrino, M., P.G. Aitken, G.G. Somgen, 1986, The effects of moderate changes of extracellular K⁺ and Ca²⁺ on synaptic and neural function in the CA1 region of the hippocampal slice, *Brain Res* 377(2), 229.
- Bartos, M., I. Vida, M. Frotscher, A. Meyer, H. Monyer, J.R. Geiger and P. Jonas, 2002, Fast synaptic inhibition promotes synchronized gamma oscillations in hippocampal interneuron networks, *Proc Natl Acad Sci U S A* 99, 13222.
- Bartos, M., I. Vida and P. Jonas, 2007, Synaptic mechanisms of synchronized gamma oscillations in inhibitory interneuron networks, *Nat Rev Neurosci* 8, 45.
- Bartus, R.T., R.L. Dean, 3rd, B. Beer and A.S. Lippa, 1982, The cholinergic hypothesis of geriatric memory dysfunction, *Science* 217, 408.
- Behrends, J.C. and G. ten Bruggencate, 1993, Cholinergic modulation of synaptic inhibition in the guinea pig hippocampus in vitro: excitation of GABAergic interneurons and inhibition of GABA-release, *J Neurophysiol* 69, 626.
- Ben-Ari, Y., Seizures beget seizures: the quest for GABA as a key player, 2006, *Crit Rev Neurobiol*, 18(1-2), 135.
- Ben-Ari, Y., E. Cherubini, R. Corradetti, J.L. Gaiarsa, 1989, Giant synaptic potentials in immature rat CA3 hippocampal neurones, *J Physiol* 416, 303-25.
- Ben-Ari, Y., E. Tremblay, D. Riche, G. Ghilini and R. Naquet, 1981, Electrographic, clinical and pathological alterations following systemic administration of kainic acid, bicuculline or pentetrazole: Metabolic mapping using the deoxyglucose method with special reference to the pathology of epilepsy, *Neurosci* 6, 1361.
- Bernard, C., 2005, Dogma and dreams: experimental lessons for epilepsy mechanism chasers, *Cell Mol Life Sci* 62, 1177.
- Birdsall, N.J., A.S. Burgen and E.C. Hulme, 1978, The binding of agonists to brain muscarinic receptors, *Mol Pharmacol* 14, 723.
- Black, M.D., 2005, Therapeutic potential of positive AMPA modulators and their relationship to AMPA receptor subunits. A review of preclinical data, *Psychopharmacol (Berl)* 179, 154.

- Bland, B.H., S.D. Oddie, L.V. Colom and R.P. Vertes, 1994, Extrinsic modulation of medial septal cell discharges by the ascending brainstem hippocampal synchronizing pathway, *Hippocampus* 4, 649.
- Bliss, T.V. and G.L. Collingridge, 1993, A synaptic model of memory: long-term potentiation in the hippocampus, *Nature* 361, 31.
- Blozovski D., A. Cudennec, D. Garrigou D, 1977, Deficits in passive-avoidance learning following atropine in the developing rat, *Psychopharmacol (Berl)* 54(2),139.
- Boddeke, H.W., R. Best and P.H. Boeijinga, 1997, Synchronous 20 Hz rhythmic activity in hippocampal networks induced by activation of metabotropic glutamate receptors in vitro, *Neurosci* 76, 653.
- Bormann, J., O.P. Hamill and B. Sakmann, 1987, Mechanism of anion permeation through channels gated by glycine and gamma-aminobutyric acid in mouse cultured spinal neurones, *J Physiol* 385, 243.
- Brazhnik, E.S. and S.E. Fox, 1999, Action potentials and relations to the theta rhythm of medial septal neurons in vivo, *Exp Brain Res* 127, 244.
- Brothwell, S.L., J.L. Barber, D.T. Monaghan, D.E. Jane, A.J. Gibb and S. Jones, 2008, NR2B- and NR2D-containing synaptic NMDA receptors in developing rat substantia nigra pars compacta dopaminergic neurones, *J Physiol* 586, 739.
- Brown, J.T., C.H. Gill, C.E. Farmer, C. Lanneau, A.D. Randall, M.N. Pangalos, G.L. Collingridge and C.H. Davies, 2003, Mechanisms contributing to the exacerbated epileptiform activity in hippocampal slices of GABA_B1 receptor subunit knockout mice, *Epilepsy Res* 57, 121.
- Brown, J.T. and A.D. Randall, 2009, Activity-dependent depression of the spike after-depolarization generates long-lasting intrinsic plasticity in hippocampal CA3 pyramidal neurons, *J Physiol* 587(Pt 6),1265.
- Buchanan, R.W., R. Freedman, D.C. Javitt, A. Abi-Dargham and J.A. Lieberman, 2007, Recent advances in the development of novel pharmacological agents for the treatment of cognitive impairments in schizophrenia, *Schizophr Bull* 33, 1120.
- Buckley, N.J., T.I. Bonner and M.R. Brann, 1988, Localization of a family of muscarinic receptor mRNAs in rat brain, *J Neurosci* 8, 4646.
- Buhl, E.H., G. Tamas and A. Fisahn, 1998, Cholinergic activation and tonic excitation induce persistent gamma oscillations in mouse somatosensory cortex in vitro, *J Physiol* 513 (Pt 1), 117.
- Buzsaki, G., 2002, Theta oscillations in the hippocampus, *Neuron* 33, 325.
- Buzsaki, G. and A. Draguhn, 2004, Neuronal oscillations in cortical networks, *Science* 304, 1926.
- Campbell, A.M. and O. Holmes, 1984, Bicuculline epileptogenesis in the rat, *Brain Res* 323, 239.
- Carey, G.J., W. Billard, I. Binch, Herbert, M. Cohen-Williams, G. Crosby, M. Grzelak, H. Guzik, J.A. Kozlowski and D.B. Lowe, 2001, SCH 57790, a selective muscarinic M2 receptor antagonist, releases acetylcholine and produces cognitive enhancement in laboratory animals, *Eur J Pharmacol* 431, 189.
- Castillo, P.E., R.C. Malenka and R.A. Nicoll, 1997, Kainate receptors mediate a slow postsynaptic current in hippocampal CA3 neurons, *Nature* 388, 182.
- Caulfield, M.P. and N.J. Birdsall, 1998, International Union of Pharmacology. XVII. Classification of muscarinic acetylcholine receptors, *Pharmacol Rev* 50, 279.
- Cavalheiro, E.A., J.P. Leite, Z.A. Bortolotto, W.A. Turski, C. Ikonomidou and L. Turski, 1991, Long-term effects of pilocarpine in rats: structural damage of the brain triggers kindling and spontaneous recurrent seizures, *Epilepsia* 32, 778.
- Chahrouh, M. and H.Y. Zoghbi, 2007, The story of rett syndrome: from clinic to neurobiology, *Neuron* 56, 422.
- Chamberlain, S.R., U. Muller, T.W. Robbins and B.J. Sahakian, 2006, Neuropharmacological modulation of cognition, *Curr Opin Neurol* 19, 607.

- Chamberlin, N.L., R.D. Traub and R. Dingledine, 1990, Role of EPSPs in initiation of spontaneous synchronized burst firing in rat hippocampal neurons bathed in high potassium, *J Neurophysiol* 64, 1000.
- Changeux, J.P. and S.J. Edelman, 1998, Allosteric receptors after 30 years, *Neuron* 21, 959.
- Chapman, C.A. and J.C. Lacaille, 1999, Cholinergic induction of theta-frequency oscillations in hippocampal inhibitory interneurons and pacing of pyramidal cell firing, *J Neurosci* 19, 8637.
- Cobb, S.R., E.H. Buhl, K. Halasy, O. Paulsen and P. Somogyi, 1995, Synchronization of neuronal activity in hippocampus by individual GABAergic interneurons, *Nature* 378, 75.
- Cobb, S.R., D.O. Bulters and C.H. Davies, 2000, Coincident activation of mGluRs and mAChRs imposes theta frequency patterning on synchronised network activity in the hippocampal CA3 region, *Neuropharmacol* 39, 1933.
- Cobb, S.R., D.O. Bulters, S. Suchak, G. Riedel, R.G. Morris and C.H. Davies, 1999, Activation of nicotinic acetylcholine receptors patterns network activity in the rodent hippocampus, *J Physiol* 518 (Pt 1), 131.
- Cobb, S.R. and C.H. Davies, 2005, Cholinergic modulation of hippocampal cells and circuits, *J Physiol* 562, 81.
- Cobb, S.R., K. Halasy, I. Vida, G. Nyiri, G. Tamas, E.H. Buhl and P. Somogyi, 1997, Synaptic effects of identified interneurons innervating both interneurons and pyramidal cells in the rat hippocampus, *Neurosci* 79, 629.
- Cole, A.E. and R.A. Nicoll, 1983, Acetylcholine mediates a slow synaptic potential in hippocampal pyramidal cells, *Science* 221, 1299.
- Cole, A.E. and R.A. Nicoll, 1984a, Characterization of a slow cholinergic post-synaptic potential recorded in vitro from rat hippocampal pyramidal cells, *J Physiol* 352, 173.
- Cole, A.E. and R.A. Nicoll, 1984b, The pharmacology of cholinergic excitatory responses in hippocampal pyramidal cells, *Brain Res* 305, 283.
- Colino, A. and J.V. Halliwell, 1993, Carbachol potentiates Q current and activates a calcium-dependent non-specific conductance in rat hippocampus in vitro, *Eur J Neurosci* 5, 1198.
- Colom, L.V., S. Nassif-Caudarella, C.T. Dickson, J.W. Smythe and B.H. Bland, 1991, In vivo intrahippocampal microinfusion of carbachol and bicuculline induces theta-like oscillations in the septally deafferented hippocampus, *Hippocampus* 1, 381.
- Connors, B.W., M.J. Gutnick and D.A. Prince, 1982, Electrophysiological properties of neocortical neurons in vitro, *J Neurophysiol* 48, 1302.
- Cunningham, M.O., C.H. Davies, E.H. Buhl, N. Kopell and M.A. Whittington, 2003, Gamma oscillations induced by kainate receptor activation in the entorhinal cortex in vitro, *J Neurosci* 23, 9761.
- Davies, C.H., M.F. Pozza and G.L. Collingridge, 1993, CGP 55845A: a potent antagonist of GABA_B receptors in the CA1 region of rat hippocampus, *Neuropharmacol* 32, 1071.
- de Sevilla, D.F., C. Cabezas, A.N.O. de Prada, A. Sanchez-Jimenez and W. Buno, 2002, Selective muscarinic regulation of functional glutamatergic Schaffer collateral synapses in rat CA1 pyramidal neurons *J Physiol* 545, 51.
- Deng, L. and G. Chen, 2003, Cyclothiazide potently inhibits gamma-aminobutyric acid type A receptors in addition to enhancing glutamate responses, *Proc Natl Acad Sci U S A* 100, 13025.
- Dennis-Sykes, C.A., W.J. Miller and W.J. McAleer, 1985, A quantitative Western Blot method for protein measurement, *J Biol Stand* 13, 309.
- Diana, G., G. Valentini, S. Travaglione, L. Falzano, M. Pieri, C. Zona, S. Meschini, A. Fabbri and C. Fiorentini, 2007, Enhancement of learning and memory after activation of cerebral Rho GTPases, *Proc Natl Acad Sci U S A* 104, 636.

- Ding, Q., S. Vaynman, P. Souda, J.P. Whitelegge and F. Gomez-Pinilla, 2006, Exercise affects energy metabolism and neural plasticity-related proteins in the hippocampus as revealed by proteomic analysis, *Eur J Neurosci* 24, 1265.
- Dingledine, R., K. Borges, D. Bowie and S.F. Traynelis, 1999, The glutamate receptor ion channels, *Pharmacol Rev* 51, 7.
- Du, Q., I.N. Melnikova and P.D. Gardner, 1998, Differential Effects of Heterogeneous Nuclear Ribonucleoprotein K on Sp1- and Sp3-mediated Transcriptional Activation of a Neuronal Nicotinic Acetylcholine Receptor Promoter 10.1074/jbc.273.31.19877, *J Biol Chem* 273, 19877.
- Duffy, S.N., K.J. Craddock, T. Abel and P.V. Nguyen, 2001, Environmental enrichment modifies the PKA-dependence of hippocampal LTP and improves hippocampus-dependent memory, *Learn Mem* 8, 26.
- Dutar, P. and R.A. Nicoll, 1988, Pre- and postsynaptic GABA_B receptors in the hippocampus have different pharmacological properties, *Neuron* 1, 585.
- Egorov, A.V., P.R. Angelova, U. Heinemann and W. Muller, 2003, Ca²⁺-independent muscarinic excitation of rat medial entorhinal cortex layer V neurons, *Eur J Neurosci* 18, 3343.
- Engel, A., P. Konig, A. Kreiter and W. Singer, 1991, Interhemispheric synchronization of oscillatory neuronal responses in cat visual cortex, *Science* 252, 1177.
- Escorihuela, R.M., A. Tobena and A. Fernandez-Teruel, 1994, Environmental enrichment reverses the detrimental action of early inconsistent stimulation and increases the beneficial effects of postnatal handling on shuttlebox learning in adult rats, *Behav Brain Res* 61, 169.
- Escorihuela, R.M., A. Tobena and A. Fernandez-Teruel, 1995, Environmental enrichment and postnatal handling prevent spatial learning deficits in aged hypoemotional (Roman high-avoidance) and hyperemotional (Roman low-avoidance) rats. *Learn Mem* 2, 40.
- Faber, E.S., A.J. Delaney and P. Sah, 2005, SK channels regulate excitatory synaptic transmission and plasticity in the lateral amygdala, *Nat Neurosci* 8, 635.
- Faber, E.S. and P. Sah, 2007, Functions of SK channels in central neurons, *Clin Exp Pharmacol Physiol* 34, 1077.
- Fabian-Fine, R., P. Skehel, M.L. Errington, H.A. Davies, E. Sher, M.G. Stewart and A. Fine, 2001, Ultrastructural distribution of the alpha7 nicotinic acetylcholine receptor subunit in rat hippocampus, *J Neurosci* 21, 7993.
- Fellous, J.M. and T.J. Sejnowski, 2000, Cholinergic induction of oscillations in the hippocampal slice in the slow (0.5-2 Hz), theta (5-12 Hz), and gamma (35-70 Hz) bands, *Hippocampus* 10, 187.
- Ferguson, S.M., G. Brasnjo, M. Hayashi, M. Wolfel, C. Collesi, S. Giovedi, A. Raimondi, L.W. Gong, P. Ariel, S. Paradise, E. O'Toole, R. Flavell, O. Cremona, G. Miesenbock, T.A. Ryan and P. De Camilli, 2007, A selective activity-dependent requirement for dynamin 1 in synaptic vesicle endocytosis, *Science* 316, 570.
- Fibiger, H.C., 1991, Cholinergic mechanisms in learning, memory and dementia: a review of recent evidence, *Trends Neurosci* 14, 220.
- Finnerty, G.T. and J.G. Jefferys, 1993, Functional connectivity from CA3 to the ipsilateral and contralateral CA1 in the rat dorsal hippocampus, *Neurosci* 56, 101.
- Fisahn, A., 2005, Kainate receptors and rhythmic activity in neuronal networks: hippocampal gamma oscillations as a tool, *J Physiol* 562, 65.
- Fisahn, A., A. Contractor, R.D. Traub, E.H. Buhl, S.F. Heinemann and C.J. McBain, 2004, Distinct roles for the kainate receptor subunits GluR5 and GluR6 in kainate-induced hippocampal gamma oscillations, *J Neurosci* 24, 9658.
- Fisahn, A., F.G. Pike, E.H. Buhl and O. Paulsen, 1998, Cholinergic induction of network oscillations at 40 Hz in the hippocampus in vitro, *Nature* 394, 186.

- Fisahn, A., M. Yamada, A. Duttaroy, J.W. Gan, C.X. Deng, C.J. McBain and J. Wess, 2002, Muscarinic induction of hippocampal gamma oscillations requires coupling of the M1 receptor to two mixed cation currents, *Neuron* 33, 615.
- Fischer, A., F. Sananbenesi, X. Wang, M. Dobbin and L.H. Tsai, 2007, Recovery of learning and memory is associated with chromatin remodelling, *Nature* 447, 178.
- Fischer, Y., 2004, The hippocampal intrinsic network oscillator, *J Physiol* 554, 156.
- Fischer, Y., B.H. Gahwiler and S.M. Thompson, 1999, Activation of intrinsic hippocampal theta oscillations by acetylcholine in rat septo-hippocampal cocultures, *J Physiol* 519 Pt 2, 405.
- Fisher, A., E. Heldman, D. Gurwitz, R. Haring, Y. Karton, H. Meshulam, Z. Pittel, D. Marciano, R. Brandeis, E. Sadot, Y. Barg, R. Pinkas-Kramarski, Z. Vogel, I. Ginzburg, T.A. Treves, R. Verchovsky, S. Klimowsky and A.D. Korczyn, 1996, M1 agonists for the treatment of Alzheimer's disease. Novel properties and clinical update, *Ann N Y Acad Sci* 777, 189.
- Fonnum, F., 1984, Glutamate: a neurotransmitter in mammalian brain, *J Neurochem* 42, 1.
- Frerking, M., R.C. Malenka and R.A. Nicoll, 1998, Synaptic activation of kainate receptors on hippocampal interneurons, *Nat Neurosci* 1, 479.
- Freund, T.F. and G. Buzsaki, 1996, Interneurons of the hippocampus, *Hippocampus* 6, 347.
- Friedman, J.I., 2004, Cholinergic targets for cognitive enhancement in schizophrenia: focus on cholinesterase inhibitors and muscarinic agonists, *Psychopharmacol (Berl)* 174, 45.
- Fujiwara-Tsukamoto, Y., Y. Isomura, K. Kaneda and M. Takada, 2004, Synaptic interactions between pyramidal cells and interneurone subtypes during seizure-like activity in the rat hippocampus, *J Physiol* 557, 961.
- Fujiwara-Tsukamoto, Y., Y. Isomura, A. Nambu and M. Takada, 2003, Excitatory GABA input directly drives seizure-like rhythmic synchronization in mature hippocampal CA1 pyramidal cells, *Neurosci* 119, 265.
- Fukata, Y., T.J. Itoh, T. Kimura, C. Menager, T. Nishimura, T. Shiromizu, H. Watanabe, N. Inagaki, A. Iwamatsu, H. Hotani and K. Kaibuchi, 2002, CRMP-2 binds to tubulin heterodimers to promote microtubule assembly, *Nat Cell Biol* 4, 583.
- Garner, H.L., M.A. Whittington and Z. Henderson, 2005, Induction by kainate of theta frequency rhythmic activity in the rat medial septum-diagonal band complex in vitro, *J Physiol* 564, 83.
- Geiger, J.R., J. Lubke, A. Roth, M. Frotscher, P. Jonas, 1997, Submillisecond AMPA receptor-mediated signaling at a principal neuron-interneuron synapse, *Neuron* 18 (6), 1009.
- Gloveli, T., T. Dugladze, H.G. Rotstein, R.D. Traub, H. Monyer, U. Heinemann, M.A. Whittington and N.J. Kopell, 2005, Orthogonal arrangement of rhythm-generating microcircuits in the hippocampus. *Proc Natl Acad Sci U S A* 102, 13295.
- Goddard, G.V., D.C. McIntyre and C.K. Leech, 1969, A permanent change in brain function resulting from daily electrical stimulation, *Experimental Neurol* 25, 295.
- Grauer, E. and J. Kapon, 1996, Differential effects of anticholinergic drugs on paired discrimination performance, *Pharmacol Biochem and Behav* 53, 463.
- Gray, C.M. and W. Singer, 1989, Stimulus-specific neuronal oscillations in orientation columns of cat visual cortex, *Proc Natl Acad Sci U S A* 86, 1698.
- Gruslin, E., S. Descombes and C. Psarropoulou, 1999, Epileptiform activity generated by endogenous acetylcholine during blockade of GABAergic inhibition in immature and adult rat hippocampus, *Brain Res* 835, 290.
- Guilarte, T.R., C.D. Toscano, J.L. McGlothlan and S.A. Weaver, 2003, Environmental enrichment reverses cognitive and molecular deficits induced by developmental lead exposure, *Ann Neurol* 53, 50.

- Gulyas-Kovacs, A., J. Doczi, I. Tarnawa, L. Detari, I. Banczerowski-Pelyhe and I. Vilagi, 2002, Comparison of spontaneous and evoked epileptiform activity in three in vitro epilepsy models, *Brain Res* 945, 174.
- Gutnick, M.J., B.W. Connors and D.A. Prince, 1982, Mechanisms of neocortical epileptogenesis in vitro, *J Neurophysiol* 48, 1321.
- Guy, J., J. Gan, J. Selfridge, S. Cobb and A. Bird, 2007, Reversal of neurological defects in a mouse model of Rett syndrome, *Science* 315, 1143.
- Haig, A.R., E. Gordon, V. De Pascalis, R.A. Meares, H. Bahramali and A. Harris, 2000, Gamma activity in schizophrenia: evidence of impaired network binding?, *Clin Neurophysiol* 111, 1461.
- Hajos, N., J. Palhalmi, E.O. Mann, B. Nemeth, O. Paulsen and T.F. Freund, 2004, Spike timing of distinct types of GABAergic interneuron during hippocampal gamma oscillations in vitro, *J Neurosci* 24, 9127.
- Hajos, N., E.C. Papp, L. Acsady, A.I. Levey and T.F. Freund, 1998, Distinct interneuron types express m2 muscarinic receptor immunoreactivity on their dendrites or axon terminals in the hippocampus, *Neurosci* 82, 355.
- Halliwel, J.V. and P.R. Adams, 1982, Voltage-clamp analysis of muscarinic excitation in hippocampal neurons, *Brain Res* 250, 71.
- Hamberger, A.C., G.H. Chiang, E.S. Nylén, S.W. Scheff and C.W. Cotman, 1979, Glutamate as a CNS transmitter. I. Evaluation of glucose and glutamine as precursors for the synthesis of preferentially released glutamate, *Brain Res* 168, 513.
- Hampson, R.E., G. Rogers, G. Lynch and S.A. Deadwyler, 1998, Facilitative effects of the ampakine CX516 on short-term memory in rats: enhancement of delayed-nonmatch-to-sample performance, *J Neurosci* 18, 2740.
- Hampson, R.E., J.D. Simeral and S.A. Deadwyler, 1999, Distribution of spatial and nonspatial information in dorsal hippocampus, *Nature* 402, 610.
- Harries, M.H., N.A. Samson, J. Cilia and A.J. Hunter, 1998, The profile of sabcomeline (SB-202026), a functionally selective M1 receptor partial agonist, in the marmoset, *Br J Pharmacol* 124, 409.
- Hasselmo, M.E. and E. Schnell, 1994, Laminar selectivity of the cholinergic suppression of synaptic transmission in rat hippocampal region CA1: computational modeling and brain slice physiology, *J Neurosci* 14, 3898.
- Hentschke, H., M.G. Perkins, R.A. Pearce and M.I. Banks, 2007, Muscarinic blockade weakens interaction of gamma with theta rhythms in mouse hippocampus, *Eur J Neurosci* 26, 1642.
- Herzenberg, L.A., D. Parks, B. Sahaf, O. Perez, M. Roederer and L.A. Herzenberg, 2002, The History and Future of the Fluorescence Activated Cell Sorter and Flow Cytometry: A View from Stanford, *Clin Chem* 48, 1819.
- Hicks, L.H. and J.E. Birren, 1970, Aging, brain damage, and psychomotor slowing, *Psychol Bull* 74, 377.
- Hille, B., A.M. Woodhull and B.I. Shapiro, 1975, Negative surface charge near sodium channels of nerve: divalent ions, monovalent ions, and pH, *Philos Trans R Soc Lond B Biol Sci* 270, 301.
- Hodgkiss, J.P. and J.S. Kelly, 2001, Effect of FK960, a putative cognitive enhancer, on synaptic transmission in CA1 neurons of rat hippocampus, *J Pharmacol Exp Ther* 297, 620.
- Hollmann, M., M. Hartley and S. Heinemann, 1991, Ca²⁺ permeability of KA-AMPA-gated glutamate receptor channels depends on subunit composition, *Science* 252, 851.
- Hollmann, M. and S. Heinemann, 1994, Cloned Glutamate Receptors. *Annu Rev Neurosci* 17, 31.

- Honore, T., S.N. Davies, J. Drejer, E.J. Fletcher, P. Jacobsen, D. Lodge and F.E. Nielsen, 1988, Quinoxalinediones: potent competitive non-NMDA glutamate receptor antagonists, *Science* 241, 701.
- Huang, F.L., K.P. Huang, J. Wu and C. Boucheron, 2006, Environmental enrichment enhances neurogranin expression and hippocampal learning and memory but fails to rescue the impairments of neurogranin null mutant mice, *J Neurosci* 26, 6230.
- Huerta, P.T. and J.E. Lisman, 1993, Heightened synaptic plasticity of hippocampal CA1 neurons during a Cholinergically induced rhythmic state, *Nature* 364, 723.
- Huguenard, J.R., D.A. Coulter, and D.A. Prince, 1991, A fast transient potassium current in thalamic relay neurons: kinetics of activation and inactivation, *J Neurophysiol* 66(4), 1304
- Hunter, A.J. and F.F. Roberts, 1988, The effect of pirenzepine on spatial learning in the Morris Water Maze, *Pharmacol Biochem Behav* 30, 519.
- Huntley, G.W., D.L. Benson and D.R. Colman, 2002, Structural Remodeling of the Synapse in Response to Physiological Activity, *Cell* 108, 1.
- Hwa, G.G. and M. Avoli, 1991, The involvement of excitatory amino acids in neocortical epileptogenesis: NMDA and non-NMDA receptors, *Exp Brain Res* 86, 248.
- Hwa, G.G., M. Avoli, A. Oliver and J.G. Villemure, 1991, Bicuculline-induced epileptogenesis in the human neocortex maintained in vitro, *Exp Brain Res* 83, 329.
- Ingvar, M., J. Ambros-Ingerson, M. Davis, R. Granger, M. Kessler, G.A. Rogers, R.S. Schehr and G. Lynch, 1997, Enhancement by an ampakine of memory encoding in humans, *Exp Neurol* 146, 553.
- Isomura, Y., M. Sugimoto, Y. Fujiwara-Tsukamoto, S. Yamamoto-Muraki, J. Yamada and A. Fukuda, 2003, Synaptically activated Cl⁻ accumulation responsible for depolarizing GABAergic responses in mature hippocampal neurons, *J Neurophysiol* 90, 2752.
- Ito, I., S. Tanabe, A. Kohda and H. Sugiyama, 1990, Allosteric potentiation of quisqualate receptors by a nootropic drug aniracetam., *J Physiol* 424, 533.
- Jaffe, A.B. and A. Hall, 2005, Rho GTPases: biochemistry and biology, *Annu Rev Cell Dev Biol* 21, 247.
- Jahr, C.E. and C.F. Stevens, 1990, Voltage dependence of NMDA-activated macroscopic conductances predicted by single-channel kinetics, *J Neurosci* 10, 3178.
- Jan, M.M., J.M. Dooley and K.E. Gordon, 1999, Male Rett syndrome variant: application of diagnostic criteria, *Pediatr Neurol* 20, 238.
- Jankowsky, J.L., T. Melnikova, D.J. Fadale, G.M. Xu, H.H. Slunt, V. Gonzales, L.H. Younkin, S.G. Younkin, D.R. Borchelt and A.V. Savonenko, 2005, Environmental enrichment mitigates cognitive deficits in a mouse model of Alzheimer's disease, *J Neurosci* 25, 5217.
- Jia, Z., N. Agopyan, P. Miu, Z. Xiong, J. Henderson, R. Gerlai, F.A. Taverna, A. Velumian, J. MacDonald, P. Carlen, W. Abramow-Newerly and J. Roder, 1996, Enhanced LTP in Mice Deficient in the AMPA Receptor GluR2, *Neuron* 17, 945.
- Johnson, S.A., N. T. Luu, T. A. Herbst, R. Knapp, D. Lutz, A. Arai, G. A. Rogers and G. Lynch, 1999, Synergistic interactions between ampakines and antipsychotic drugs, *J Pharmacol Exp Ther* 289 (1), 392.
- Johnston, D., S. Williams, D. Jaffe and R. Gray, 1992, NMDA-receptor-independent long-term potentiation, *Annu Rev Physiol* 54, 489.
- Jones, N., M.J. O'Neill, M. Tricklebank, V. Libri and S.C. Williams, 2005, Examining the neural targets of the AMPA receptor potentiator LY404187 in the rat brain using pharmacological magnetic resonance imaging, *Psychopharmacol (Berl)* 180, 743.
- Kaila, K., K. Lamsa, S. Smirnov, T. Taira and J. Voipio, 1997, Long-Lasting GABA-Mediated Depolarization Evoked by High-Frequency Stimulation in Pyramidal Neurons of Rat Hippocampal Slice Is Attributable to a Network-Driven, Bicarbonate-Dependent K⁺ Transient, *J Neurosci* 17, 7662.
- Kandel, E.R., 1997, Genes, synapses, and long-term memory, *J Cell Physiol* 173, 124.

- Kaneko, S., H. Iwasa and M. Okada, 2002, Genetic identifiers of epilepsy, *Epilepsia* 43 Suppl 9, 16.
- Kang, H., A.A. Welcher, D. Shelton and E.M. Schuman, 1997, Neurotrophins and time: different roles for TrkB signaling in hippocampal long-term potentiation, *Neuron* 19, 653.
- Khawaled, R., A. Bruening-Wright, J.P. Adelman and J. Maylie, 1999, Bicuculline block of small-conductance calcium-activated potassium channels, *Pflugers Arch* 438, 314.
- Kitaichi, K., T. Hori, L.K. Srivastava and R. Quirion, 1999, Antisense oligodeoxynucleotides against the muscarinic m2, but not m4, receptor supports its role as autoreceptors in the rat hippocampus, *Brain Res Mol Brain Res* 67, 98.
- Klausberger, T., L.F. Marton, J. O'Neill, J.H. Huck, Y. Dalezios, P. Fuentealba, W.Y. Suen, E. Papp, T. Kaneko, M. Watanabe, J. Csicsvari and P. Somogyi, 2005, Complementary roles of cholecystokinin- and parvalbumin-expressing GABAergic neurons in hippocampal network oscillations, *J Neurosci* 25, 9782.
- Klausberger, T. and P. Somogyi, 2008, Neuronal diversity and temporal dynamics: the unity of hippocampal circuit operations, *Science* 321, 53.
- Kondo, M., L.J. Gray, G.J. Pelka, J. Christodoulou, P.P. Tam, A.J. Hannan, 2008, Environmental enrichment ameliorates a motor coordination deficit in a mouse model of Rett syndrome- *Mecp2* gene dosage effects and BDNF expression, *Eur J Neurosci* 27 (12), 3342.
- Krucker, T., G.R. Siggins and S. Halpain, 2000, Dynamic actin filaments are required for stable long-term potentiation (LTP) in area CA1 of the hippocampus. *Proc Natl Acad Sci U S A* 97, 6856.
- Krystal, J.H., L.P. Karper, J.P. Seibyl, G.K. Freeman, R. Delaney, J.D. Bremner, G.R. Heninger, M.B. Bowers, Jr. and D.S. Charney, 1994, Subanesthetic effects of the noncompetitive NMDA antagonist, ketamine, in humans. Psychotomimetic, perceptual, cognitive, and neuroendocrine responses, *Arch Gen Psychiatry* 51, 199.
- Kuhnt, U. and L.L. Voronin, 1994, Interaction between paired-pulse facilitation and long-term potentiation in area CA1 of guinea-pig hippocampal slices: application of quantal analysis, *Neurosci* 62, 391.
- Kukkonen, J., J. Nasman, P. Ojala, C. Oker-Blom and K. Akerman, 1996, Functional properties of muscarinic receptor subtypes Hm1, Hm3 and Hm5 expressed in Sf9 cells using the baculovirus expression system, *J Pharmacol Exp Ther* 279, 593.
- Langmead, C. J., N. E. Austin, C. L. Branch, J. T. Brown, K. A. Buchanan, C. H. Davies, I. T. Forbes, V. A. H. Fry, J. J. Hagan, H. J. Herdon, G. A. Jones, R. Jeggo, J. N. C. Kew, A. Mazzali, R. Melarange, N. Patel, J. Pardoe, A. D. Randall, C. Roberts, A. Roopun, K. R. Starr, A. Teriakidis, M. D. Wood, M. Whittington, Z. Wu and J. Watson, 2008, Characterization of a CNS penetrant, selective M1 muscarinic receptor agonist, 77-LH-28-1, *Br J Pharmacol* 154 (5), 1104.
- Langmead, C.J., V.A. Fry, I.T. Forbes, C.L. Branch, A. Christopoulos, M.D. Wood and H.J. Herdon, 2006, Probing the molecular mechanism of interaction between 4-n-butyl-1-[4-(2-methylphenyl)-4-oxo-1-butyl]-piperidine (AC-42) and the muscarinic M(1) receptor: direct pharmacological evidence that AC-42 is an allosteric agonist, *Mol Pharmacol* 69, 236.
- Lasztocki, B. and J. Kardos, 2006, Cyclothiazide prolongs low $[Mg^{2+}]$ -induced seizure-like events, *J Neurophysiol* 96, 3538.
- Laube, B., J. Kuhse and H. Betz, 1998, Evidence for a tetrameric structure of recombinant NMDA receptors, *J Neurosci* 18, 2954.
- Lee, M.-H., S. Mori and P. Raychaudhuri, 1996, trans-Activation by the hnRNP K Protein Involves an Increase in RNA Synthesis from the Reporter Genes. *J Biol Chem* 271, 3420.
- Leung, L.S., K.J. Canning and B. Shen, 2005, Hippocampal afterdischarges after GABA_B-receptor blockade in the freely moving rat, *Epilepsia* 46, 203.

- Levey, A., S. Edmunds, V. Koliatsos, R. Wiley and C. Heilman, 1995, Expression of m1-m4 muscarinic acetylcholine receptor proteins in rat hippocampus and regulation by cholinergic innervation, *J Neurosci* 15, 4077.
- Levy, R., P. Ashby, W.D. Hutchison, A.E. Lang, A.M. Lozano and J.O. Dostrovsky, 2002, Dependence of subthalamic nucleus oscillations on movement and dopamine in Parkinson's disease, *Brain* 125, 1196.
- Lewis, J.D., R.R. Meehan, W.J. Henzel, I. Maurer-Fogy, P. Jeppesen, F. Klein and A. Bird, 1992, Purification, sequence, and cellular localization of a novel chromosomal protein that binds to Methylated DNA, *Cell* 69, 905.
- Lockhart, B.P., M. Rodriguez, S. Mourlevat, P. Peron, S. Catesson, N. Villain, J.P. Galizzi, J.A. Boutin and P. Lestage, 2007, S18986: a positive modulator of AMPA-receptors enhances (S)-AMPA-mediated BDNF mRNA and protein expression in rat primary cortical neuronal cultures, *Eur J Pharmacol* 561, 23.
- Lorente de No, R., 1934, Studies on the structure of the cerebral cortex II. Continuation of the study of the Ammonic system. *J Psychol Neurol* 46: 113.
- Luciano, D., 1993, Partial seizures of frontal and temporal origin, *Neurol Clin* 11, 805.
- Lundh, H. and S. Thesleff, 1977, The mode of action of 4-aminopyridine and guanidine on transmitter release from motor nerve terminals, *Eur J Pharmacol* 42, 411.
- Lynch, G., 2004, AMPA receptor modulators as cognitive enhancers, *Curr Opin Pharmacol* 4, 4.
- Lynch, G. and C.M. Gall, 2006, Ampakines and the threefold path to cognitive enhancement, *Trends Neurosci* 29, 554.
- Maccaferri, G., M. Mangoni, A. Lazzari and D. DiFrancesco, 1993, Properties of the hyperpolarization-activated current in rat hippocampal CA1 pyramidal cells, *J Neurophysiol* 69, 2129.
- MacDermott, A.B., M.L. Mayer, G.L. Westbrook, S.J. Smith and J.L. Barker, 1986, NMDA-receptor activation increases cytoplasmic calcium concentration in cultured spinal cord neurones, *Nature* 321, 519.
- MacVicar, B.A., N. Ropert and K. Krnjevic, 1982, Dye-coupling between pyramidal cells of rat hippocampus in vivo, *Brain Res* 238, 239.
- MacVicar, B.A. and F.W. Tse, 1989, Local neuronal circuitry underlying cholinergic rhythmical slow activity in CA3 area of rat hippocampal slices, *J Physiol* 417, 197.
- Malinow, R. and R.C. Malenka, 2002, AMPA receptor trafficking and synaptic plasticity. *Annu Rev Neurosci* 25, 103.
- Mann, E.O. and O. Paulsen, 2005, Mechanisms underlying gamma ('40 Hz') network oscillations in the hippocampus--a mini-review, *Prog Biophys Mol Biol* 87, 67.
- Mann, E.O., J.M. Suckling, N. Hajos, S.A. Greenfield and O. Paulsen, 2005, Perisomatic feedback inhibition underlies cholinergically induced fast network oscillations in the rat hippocampus in vitro, *Neuron* 45, 105.
- Marinissen, M.J. and J.S. Gutkind, 2001, G-protein-coupled receptors and signaling networks: emerging paradigms, *Trends in Pharmacol Sci* 22, 368.
- Marino, M.J., S.T. Rouse, A.I. Levey, L.T. Potter and P.J. Conn, 1998, Activation of the genetically defined m1 muscarinic receptor potentiates N-methyl-D-aspartate (NMDA) receptor currents in hippocampal pyramidal cells, *Proc Natl Acad Sci U S A* 95, 11465.
- Markram, H. and M. Segal, 1990, Long-lasting facilitation of excitatory postsynaptic potentials in the rat hippocampus by acetylcholine, *J Physiol* 427, 381.
- Marshall, F.H., J. White, M. Main, A. Green and A. Wise, 1999, GABA_B receptors function as heterodimers, *Biochem Soc Trans* 27, 530.
- Martin, L.F., W.R. Kem and R. Freedman, 2004, Alpha-7 nicotinic receptor agonists: potential new candidates for the treatment of schizophrenia, *Psychopharmacol (Berl)* 174, 54.

- Matsuda, S., Y. Kamiya and M. Yuzaki, 2005, Roles of the N-terminal Domain on the Function and Quaternary Structure of the Ionotropic Glutamate Receptor, *J Biol Chem* 280, 20021.
- Matsumoto, H. and C.A. Marsan, 1964, Cortical Cellular Phenomena in Experimental Epilepsy: Ictal Manifestations, *Exp Neurol* 9, 305.
- McMahon, L.L., J.H. Williams and J.A. Kauer, 1998, Functionally distinct groups of interneurons identified during rhythmic carbachol oscillations in hippocampus in vitro, *J Neurosci* 18, 5640.
- Meehan, R., J. Lewis, S. Cross, X. Nan, P. Jeppesen and A. Bird, 1992a, Transcriptional repression by methylation of CpG, *J Cell Sci Suppl* 16, 9.
- Meehan, R.R., J.D. Lewis and A.P. Bird, 1992b, Characterization of MeCP2, a vertebrate DNA binding protein with affinity for methylated DNA, *Nucleic Acids Res* 20, 5085.
- Meshi, D., M.R. Drew, M. Saxe, M.S. Ansorge, D. David, L. Santarelli, C. Malapani, H. Moore and R. Hen, 2006, Hippocampal neurogenesis is not required for behavioral effects of environmental enrichment, *Nat Neurosci* 9, 729.
- Messer, W.S., M. Bohnett and J. Stibbe, 1990, Evidence for a preferential involvement of M1 muscarinic receptors in representational memory, *Neurosci Letters* 116, 184.
- Michelotti, E., G. Michelotti, A. Aronsohn and D. Levens, 1996, Heterogeneous nuclear ribonucleoprotein K is a transcription factor, *Mol Cell Biol* 16, 2350.
- Miles, R. and R.K. Wong, 1987, Inhibitory control of local excitatory circuits in the guinea-pig hippocampus, *J Physiol* 388, 611.
- Misgeld, U., M. Bijak and W. Jarolimek, 1995, A physiological role for GABA_B receptors and the effects of baclofen in the mammalian central nervous system, *Prog Neurobiol* 46, 423.
- Moretti, P., J.A. Bouwknecht, R. Teague, R. Paylor and H.Y. Zoghbi, 2005, Abnormalities of social interactions and home-cage behavior in a mouse model of Rett syndrome, *Hum Mol Genet* 14, 205.
- Moretti, P. and H.Y. Zoghbi, 2006, MeCP2 dysfunction in Rett syndrome and related disorders, *Curr Opin Genet Dev* 16, 276.
- Morton, R.A., N.A. Manuel, D.O. Bulters, S.R. Cobb and C.H. Davies, 2001, Regulation of muscarinic acetylcholine receptor-mediated synaptic responses by GABA_B receptors in the rat hippocampus, *J Physiol* 535, 757.
- Motalli, R., M. D'Antuono, J. Louvel, I. Kurcewicz, G. D'Arcangelo, V. Tancredi, M. Manfredi, R. Pumain and M. Avoli, 2002, Epileptiform synchronization and GABA_B receptor antagonism in the juvenile rat hippocampus, *J Pharmacol Exp Ther* 303, 1102.
- Motalli, R., J. Louvel, V. Tancredi, I. Kurcewicz, D. Wan-Chow-Wah, R. Pumain and M. Avoli, 1999, GABA_B receptor activation promotes seizure activity in the juvenile rat hippocampus, *J Neurophysiol* 82, 638.
- Nag, N., J.M. Moriuchi, C.G. Peitzman, B.C. Ward, N.H. Kolodny, and J.E. Berger-Sweeney, 2009, Environmental enrichment alters locomotor behaviour and ventricular volume in Mecp2 floxed mice, *Behav Brain Res* 196 (1), 44.
- Nagao, T., A. Alonso and M. Avoli, 1996, Epileptiform activity induced by pilocarpine in the rat hippocampal-entorhinal slice preparation, *Neurosci* 72, 399.
- Nagarajan, N., C. Quast, A.R. Boxall, M. Shahid and C. Rosenmund, 2001, Mechanism and impact of allosteric AMPA receptor modulation by the ampakine CX546, *Neuropharmacol* 41, 650.
- Najm, I., Z. Ying and D. Janigro, 2001, Mechanisms of epileptogenesis, *Neurol Clin* 19, 237.
- Nakanishi, S., 1992, Molecular diversity of glutamate receptors and implications for brain function, *Science* 258, 597.
- Nan, X., F.J. Campoy and A. Bird, 1997, MeCP2 is a transcriptional repressor with abundant binding sites in genomic chromatin, *Cell* 88, 471.

- Nan, X., S. Cross and A. Bird, 1998, Gene silencing by methyl-CpG-binding proteins, *Novartis Found Symp* 214, 6.
- Nayeem, N., T.P. Green, I.L. Martin and E.A. Barnard, 1994, Quaternary structure of the native GABAA receptor determined by electron microscopic image analysis, *J Neurochem* 62, 815.
- Newhouse, P.A., A. Potter and E.D. Levin, 1997, Nicotinic system involvement in Alzheimer's and Parkinson's diseases. Implications for therapeutics, *Drugs Aging* 11, 206.
- Nilsson, M., E. Perfilieva, U. Johansson, O. Orwar and P.S. Eriksson, 1999, Enriched environment increases neurogenesis in the adult rat dentate gyrus and improves spatial memory, *J Neurobiol* 39, 569.
- Nilsson, O.G., G. Leanza, C. Rosenblad, D.A. Lappi, R.G. Wiley and A. Bjorklund, 1992, Spatial learning impairments in rats with selective immunolesion of the forebrain cholinergic system, *Neuroreport* 3, 1005.
- Nowak, L., P. Bregestovski, P. Ascher, A. Herbet and A. Prochiantz, 1984, Magnesium gates glutamate-activated channels in mouse central neurones, *Nature* 307, 462.
- O'Kane, E.M., T.W. Stone and B.J. Morris, 2003, Activation of Rho GTPases by synaptic transmission in the hippocampus, *J Neurochem* 87, 1309.
- O'Kane, E.M., T.W. Stone and B.J. Morris, 2004, Increased long-term potentiation in the CA1 region of rat hippocampus via modulation of GTPase signalling or inhibition of Rho kinase, *Neuropharmacol* 46, 879.
- O'Keefe, J. and J. Dostrovsky, 1971, The hippocampus as a spatial map. Preliminary evidence from unit activity in the freely-moving rat, *Brain Res* 34, 171.
- O'Keefe, J. and M.L. Recce, 1993, Phase relationship between hippocampal place units and the EEG theta rhythm, *Hippocampus* 3, 317.
- Pena, F. and N. Alavez-Perez, 2006, Epileptiform activity induced by pharmacologic reduction of M-current in the developing hippocampus in vitro, *Epilepsia* 47, 47.
- Pena, F. and R. Tapia, 2000, Seizures and neurodegeneration induced by 4-aminopyridine in rat hippocampus in vivo: role of glutamate- and GABA-mediated neurotransmission and of ion channels, *Neurosci* 101, 547.
- Penttonen, M., A. Kamondi, L. Acsady and G. Buzsaki, 1998, Gamma frequency oscillation in the hippocampus of the rat: intracellular analysis in vivo, *Eur J Neurosci* 10, 718.
- Perkins D.N., D.J. Pappin, D.M. Creasy, and J.S. Cottrell, 1999, Probability-based protein identification by searching sequence databases using mass spectrometry data, *Electrophoresis* 20 (18), 3551.
- Perreault, P. and M. Avoli, 1991, Physiology and pharmacology of epileptiform activity induced by 4-aminopyridine in rat hippocampal slices, *J Neurophysiol* 65, 771.
- Perreault, P. and M. Avoli, 1992, 4-aminopyridine-induced epileptiform activity and a GABA-mediated long-lasting depolarization in the rat hippocampus, *J Neurosci* 12, 104.
- Perry, E.K., M. Curtis, D.J. Dick, J.M. Candy, J.R. Atack, C.A. Bloxham, G. Blessed, A. Fairbairn, B.E. Tomlinson and R.H. Perry, 1985, Cholinergic correlates of cognitive impairment in Parkinson's disease: comparisons with Alzheimer's disease, *J Neurol Neurosurg Psychiatry* 48, 413.
- Pham, T.M. and J.C. Lacaille, 1996, Multiple postsynaptic actions of GABA via GABA_B receptors on CA1 pyramidal cells of rat hippocampal slices, *J Neurophysiol* 76, 69.
- Pietersen, A.N., N. Patel, J.G. Jefferys, and M. Vreugdenhil, 2009, Comparison between spontaneous and kainate-induced gamma oscillations in the mouse hippocampus in vitro, *Eur J Neurosci* 21 (11), 2145
- Pike, F.G., R.S. Goddard, J.M. Suckling, P. Ganter, N. Kasthuri and O. Paulsen, 2000, Distinct frequency preferences of different types of rat hippocampal neurones in response to oscillatory input currents, *J Physiol* 529 (Pt 1), 205.

- Pin, J.-P. and R. Duvoisin, 1995, The metabotropic glutamate receptors: Structure and functions, *Neuropharmacol* 34, 1.
- Pitler, T.A. and B.E. Alger, 1990, Activation of the pharmacologically defined M3 muscarinic receptor depolarizes hippocampal pyramidal cells, *Brain Res* 534, 257.
- Poolos, N.P., M.D. Mauk and J.D. Kocsis, 1987, Activity-evoked increases in extracellular potassium modulate presynaptic excitability in the CA1 region of the hippocampus, *J Neurophysiol* 58, 404.
- Popov, V.I., H.A. Davies, V.V. Rogachevsky, I.V. Patrushev, M.L. Errington, P.L.A. Gabbott, T.V.P. Bliss and M.G. Stewart, 2004, Remodelling of synaptic morphology but unchanged synaptic density during late phase long-term potentiation (LTP): A serial section electron micrograph study in the dentate gyrus in the anaesthetised rat, *Neurosci* 128, 251.
- Porter, A.C., F.P. Bymaster, N.W. DeLapp, M. Yamada, J. Wess, S.E. Hamilton, N.M. Nathanson and C.C. Felder, 2002, M1 muscarinic receptor signaling in mouse hippocampus and cortex, *Brain Res* 944, 82.
- Pouille, F. and M. Scanziani, 2001, Enforcement of temporal fidelity in pyramidal cells by somatic feed-forward inhibition, *Science* 293, 1159.
- Povysheva, N.V., G. Gonzalez-Burgos, A.V. Zaitsev, S. Kroner, G. Barrionuevo, D.A. Lewis and L.S. Krimer, 2006, Properties of excitatory synaptic responses in fast-spiking interneurons and pyramidal cells from monkey and rat prefrontal cortex, *Cereb Cortex* 16, 541.
- Power, J.M. and P. Sah, 2002, Nuclear calcium signaling evoked by cholinergic stimulation in hippocampal CA1 pyramidal neurons, *J Neurosci* 22, 3454.
- Psarropoulou, C. and S. Descombes, 1999, Differential bicuculline-induced epileptogenesis in rat neonatal, juvenile and adult CA3 pyramidal neurons in vitro, *Develop Brain Res* 117, 117.
- Qi, J., Y. Wang, M. Jiang, P. Warren and G. Chen, 2006, Cyclothiazide induces robust epileptiform activity in rat hippocampal neurons both in vitro and in vivo, *J Physiol* 571, 605.
- Rabilloud T., C. Valette, J.J. Lawrence, 1994, Sample application by in-gel rehydration improves the resolution of two-dimensional electrophoresis with immobilized pH gradients in the first dimension, *Electrophoresis* 15 (12), 1552.
- Radak, Z., T. Kaneko, S. Tahara, H. Nakamoto, J. Pucsek, M. Sasvari, C. Nyakas and S. Goto, 2001, Regular exercise improves cognitive function and decreases oxidative damage in rat brain, *Neurochem International* 38, 17.
- Rampon, C., C.H. Jiang, H. Dong, Y.P. Tang, D.J. Lockhart, P.G. Schultz, J.Z. Tsien and Y. Hu, 2000, Effects of environmental enrichment on gene expression in the brain, *Proc Natl Acad Sci U S A* 97, 12880.
- Reutens, D.C. and S.F. Berkovic, 1995, Idiopathic generalized epilepsy of adolescence: are the syndromes clinically distinct?, *Neurol* 45, 1469.
- Rodriguez-Moreno, A., O. Herreras and J. Lerma, 1997, Kainate receptors presynaptically downregulate GABAergic inhibition in the rat hippocampus, *Neuron* 19, 893.
- Roshan-Milani, S., L. Ferrigan, M.J. Khoshnood, C.H. Davies and S.R. Cobb, 2003, Regulation of epileptiform activity in hippocampus by nicotinic acetylcholine receptor activation, *Epilepsy Res* 56, 51.
- Rouse, S.T., M.J. Marino, L.T. Potter, P.J. Conn and A.I. Levey, 1999, Muscarinic receptor subtypes involved in hippocampal circuits, *Life Sci* 64, 501.
- Rutecki, P.A., F.J. Lebeda and D. Johnston, 1985, Epileptiform activity induced by changes in extracellular potassium in hippocampus, *J Neurophysiol* 54, 1363.
- Rutecki, P.A., F.J. Lebeda and D. Johnston, 1987, 4-Aminopyridine produces epileptiform activity in hippocampus and enhances synaptic excitation and inhibition, *J Neurophysiol* 57, 1911.
- Rutecki, P.A. and Y. Yang, 1998, Ictal Epileptiform Activity in the CA3 Region of Hippocampal Slices Produced by Pilocarpine, *J Neurophysiol* 79, 3019.

- Sah, P. and E.S. Faber, 2002, Channels underlying neuronal calcium-activated potassium currents, *Prog Neurobiol* 66, 345.
- Sakai, R., G.T. Swanson, K. Shimamoto, T. Green, A. Contractor, A. Ghetti, Y. Tamura-Horikawa, C. Oiwa and H. Kamiya, 2001, Pharmacological Properties of the Potent Epileptogenic Amino Acid Dysiherbaine, a Novel Glutamate Receptor Agonist Isolated from the Marine Sponge *Dysidea herbacea*, *J Pharmacol Exp Ther* 296, 650.
- Schuler, V., C. Luscher, C. Blanchet, N. Klix, G. Sansig, K. Klebs, M. Schmutz, J. Heid, C. Gentry, L. Urban, A. Fox, W. Spooren, A.L. Jatton, J. Vigouret, M. Pozza, P.H. Kelly, J. Mosbacher, W. Froestl, E. Kaslin, R. Korn, S. Bischoff, K. Kaupmann, H. van der Putten and B. Bettler, 2001, Epilepsy, hyperalgesia, impaired memory, and loss of pre- and postsynaptic GABA_B responses in mice lacking GABA_B(1), *Neuron* 31, 47.
- Schulz, P., E. Cook and D. Johnston, 1994, Changes in paired-pulse facilitation suggest presynaptic involvement in long-term potentiation, *J Neurosci* 14, 5325.
- Scoville, W.B. and B. Milner, 1957, Loss of recent memory after bilateral hippocampal lesions, *J Neurol Neurosurg Psychiatry* 20, 11.
- Seguela, P., J. Wadiche, K. Dineley-Miller, J.A. Dani and J.W. Patrick, 1993, Molecular cloning, functional properties, and distribution of rat brain alpha 7: a nicotinic cation channel highly permeable to calcium, *J Neurosci* 13, 596.
- Sharma, A.C. and S.K. Kulkarni, 1991, Effects of MK-801 and ketamine on short-term memory deficits in passive avoidance step-down task paradigm in mice, *Methods Find Exp Clin Pharmacol* 13, 155.
- Sheardown, M.J., E.O. Nielsen, A.J. Hansen, P. Jacobsen and T. Honore, 1990, 2,3-Dihydroxy-6-nitro-7-sulfamoyl-benzo(F)quinoxaline: a neuroprotectant for cerebral ischemia, *Science* 247, 571.
- Shimono, K., F. Brucher, R. Granger, G. Lynch and M. Taketani, 2000, Origins and distribution of cholinergically induced beta rhythms in hippocampal slices, *J Neurosci* 20, 8462.
- Shinoe, T., M. Matsui, M.M. Taketo and T. Manabe, 2005, Modulation of synaptic plasticity by physiological activation of M1 muscarinic acetylcholine receptors in the mouse hippocampus, *J Neurosci* 25, 11194.
- Sieghart, W., K. Fuchs, V. Tretter, V. Ebert, M. Jechlinger, H. Hoger and D. Adamiker, 1999, Structure and subunit composition of GABA_A receptors, *Neurochem Int* 34, 379.
- Sjostrom, P.J., E.A. Rancz, A. Roth and M. Hausser, 2008, Dendritic excitability and synaptic plasticity, *Physiol Rev* 88(2), 769.
- Slobounov, S.M., K. Fukada, R. Simon, M. Rearick and W. Ray, 2000, Neurophysiological and behavioral indices of time pressure effects on visuomotor task performance, *Brain Res Cogn Brain Res* 9, 287.
- Spalding, T.A., J.N. Ma, T.R. Ott, M. Friberg, A. Bajpai, S.R. Bradley, R.E. Davis, M.R. Brann and E.S. Burstein, 2006, Structural requirements of transmembrane domain 3 for activation by the M1 muscarinic receptor agonists AC-42, AC-260584, clozapine, and N-desmethylclozapine: evidence for three distinct modes of receptor activation, *Mol Pharmacol* 70, 1974.
- Spalding, T.A., C. Trotter, N. Skjaerbaek, T.L. Messier, E.A. Currier, E.S. Burstein, D. Li, U. Hacksell and M.R. Brann, 2002, Discovery of an ectopic activation site on the M(1) muscarinic receptor, *Mol Pharmacol* 61, 1297.
- Spencer, S.S., D.D. Spencer, P.D. Williamson and R.H. Mattson, 1981, Ictal effects of anticonvulsant medication withdrawal in epileptic patients, *Epilepsia* 22, 297.
- Sprengel, R., 2006, Role of AMPA receptors in synaptic plasticity, *Cell Tissue Res* 326, 447.

- Stafstrom, C.E., P. Tandon, A. Hori, Z. Liu, M.A. Mikati and G.L. Holmes, 1997, Acute effects of MK801 on kainic acid-induced seizures in neonatal rats, *Epilepsy Res* 26, 335.
- Standaert, D.G., G. Bernhard Landwehrmeyer, J.A. Kerner, J.B. Penney and A.B. Young, 1996, Expression of NMDAR2D glutamate receptor subunit mRNA in neurochemically identified interneurons in the rat neostriatum, neocortex and hippocampus, *Mol Brain Res* 42, 89.
- Staubli, U., Y. Perez, F.B. Xu, G. Rogers, M. Ingvar, S. Stone-Elander and G. Lynch, 1994, Centrally active modulators of glutamate receptors facilitate the induction of long-term potentiation in vivo, *Proc Natl Acad Sci U S A* 91, 11158.
- Storm, J.F., 1988, Temporal integration by a slowly inactivating K⁺ current in hippocampal neurons, *Nature* 336, 379.
- Sur, C., P.J. Mallorga, M. Wittmann, M.A. Jacobson, D. Pascarella, J.B. Williams, P.E. Brandish, D.J. Pettibone, E.M. Scolnick and P.J. Conn, 2003, N-desmethylozapine, an allosteric agonist at muscarinic 1 receptor, potentiates N-methyl-D-aspartate receptor activity, *Proc Natl Acad Sci U S A* 100, 13674.
- Swash, M., 2005, John Hughlings Jackson (1835-1911), *J Neurol* 252(6):745.
- Szente, M. and A. Baranyi, 1987, Mechanism of aminopyridine-induced ictal seizure activity in the cat neocortex, *Brain Res* 413, 368.
- Szerb, J.C., 1984, Storage and release of endogenous and labelled GABA formed from [3H]glutamine and [14C]glucose in hippocampal slices: effect of depolarization, *Brain Res* 293, 293.
- Tallon-Baudry, C. and O. Bertrand, 1999, Oscillatory gamma activity in humans and its role in object representation, *Trends Cogn Sci* 3, 151.
- Tallon, C., O. Bertrand, P. Bouchet and J. Pernier, 1995, Gamma-range activity evoked by coherent visual stimuli in humans, *Eur J Neurosci* 7, 1285.
- Tancredi, V., M. Avoli and G.G. Hwa, 1988, Low-magnesium epilepsy in rat hippocampal slices: inhibitory postsynaptic potentials in the CA1 subfield, *Neurosci Lett* 89, 293.
- Tancredi, V., G.G. Hwa, C. Zona, A. Brancati and M. Avoli, 1990, Low magnesium epileptogenesis in the rat hippocampal slice: electrophysiological and pharmacological features, *Brain Res* 511, 280.
- Tapia, R., 1996, Release and uptake of glutamate as related to excitotoxicity, *Rev Bras Biol* 56 Su 1 Pt 1, 165.
- Threadgill, R., K. Bobb and A. Ghosh, 1997, Regulation of dendritic growth and remodeling by Rho, Rac, and Cdc42, *Neuron* 19, 625.
- Timmermann, D.B., J.H. Gronlien, K.L. Kohlhaas, E.O. Nielsen, E. Dam, T.D. Jorgensen, P.K. Ahring, D. Peters, D. Holst, J.K. Christensen, J. Malysz, C.A. Briggs, M. Gopalakrishnan and G.M. Olsen, 2007, An allosteric modulator of the alpha7 nicotinic acetylcholine receptor possessing cognition-enhancing properties in vivo, *J Pharmacol Exp Ther* 323, 294.
- Toscano, C.D., J.L. McGlothan and T.R. Guilarte, 2003, Lead exposure alters cyclic-AMP response element binding protein phosphorylation and binding activity in the developing rat brain, *Brain Res Dev Brain Res* 145, 219.
- Toscano, C.D., J.L. McGlothan and T.R. Guilarte, 2006, Experience-dependent regulation of zif268 gene expression and spatial learning, *Exp Neurol* 200, 209.
- Towbin, H., T. Staehelin and J. Gordon, 1979, Electrophoretic transfer of proteins from polyacrylamide gels to nitrocellulose sheets: procedure and some applications, *Proc Natl Acad Sci U S A* 76, 4350.
- Traub, R.D., A. Bibbig, F.E. LeBeau, E.H. Buhl and M.A. Whittington, 2004, Cellular mechanisms of neuronal population oscillations in the hippocampus in vitro, *Annu Rev Neurosci* 27, 247.

- Traub, R.D. and R. Dingledine, 1990, Model of synchronized epileptiform bursts induced by high potassium in CA3 region of rat hippocampal slice. Role of spontaneous EPSPs in initiation, *J Neurophysiol* 64, 1009.
- Traub, R.D., J.G. Jefferys and M.A. Whittington, 1994, Enhanced NMDA conductance can account for epileptiform activity induced by low Mg^{2+} in the rat hippocampal slice, *J Physiol* 478 Pt 3, 379.
- Traub, R.D., R. Miles and G. Buzsaki, 1992, Computer simulation of carbachol-driven rhythmic population oscillations in the CA3 region of the in vitro rat hippocampus, *J Physiol* 451, 653.
- Traub, R.D., N. Spruston, I. Soltesz, A. Konnerth, M.A. Whittington and G.R. Jefferys, 1998, Gamma-frequency oscillations: a neuronal population phenomenon, regulated by synaptic and intrinsic cellular processes, and inducing synaptic plasticity, *Prog Neurobiol* 55, 563.
- Traub, R.D., M.A. Whittington, E.H. Buhl, J.G. Jefferys and H.J. Faulkner, 1999, On the mechanism of the gamma --> beta frequency shift in neuronal oscillations induced in rat hippocampal slices by tetanic stimulation, *J Neurosci* 19, 1088.
- Traub, R.D., M.A. Whittington, S.B. Colling, G. Buzsaki and J.G. Jefferys, 1996, Analysis of gamma rhythms in the rat hippocampus in vitro and in vivo, *J Physiol* 493 (Pt 2), 471.
- Turski, L., C. Ikonomidou, W.A. Turski, Z.A. Bortolotto and E.A. Cavalheiro, 1989, Review: cholinergic mechanisms and epileptogenesis. The seizures induced by pilocarpine: a novel experimental model of intractable epilepsy, *Synapse* 3, 154.
- Ueda, H., Y. Urano, T. Sakurai, T. Kizaki, Y. Hitomi, H. Ohno and T. Izawa, 2003, Enhanced expression of neuronal nitric oxide synthase in islets of exercise-trained rats, *Biochem and Biophys Res Com* 312, 794.
- Vanderwolf, C.H., 1969, Hippocampal electrical activity and voluntary movement in the rat, *Electroencephalogr Clin Neurophysiol* 26, 407.
- Varty, G.B., M.P. Paulus, D.L. Braff and M.A. Geyer, 2000, Environmental enrichment and isolation rearing in the rat: effects on locomotor behavior and startle response plasticity, *Biol Psychiatry* 47, 864.
- Vida, I., M. Bartos and P. Jonas, 2006, Shunting inhibition improves robustness of gamma oscillations in hippocampal interneuron networks by homogenizing firing rates, *Neuron* 49, 107.
- von Linstow Roloff, E., D. Harbaran, J. Micheau, B. Platt and G. Riedel, 2007, Dissociation of cholinergic function in spatial and procedural learning in rats, *Neurosci* 146, 875.
- Wallar, B.J. and A.S. Alberts, 2003, The formins: active scaffolds that remodel the cytoskeleton, *Trends in Cell Biol* 13, 435.
- Whittington, M.A., I.M. Stanford, S.B. Colling, J.G. Jefferys and R.D. Traub, 1997, Spatiotemporal patterns of gamma frequency oscillations tetanically induced in the rat hippocampal slice, *J Physiol* 502 (Pt 3), 591.
- Widmer, H., L. Ferrigan, C.H. Davies and S.R. Cobb, 2006, Evoked slow muscarinic acetylcholinergic synaptic potentials in rat hippocampal interneurons, *Hippocampus* 16, 617.
- Williams, J.H. and J.A. Kauer, 1997, Properties of carbachol-induced oscillatory activity in rat hippocampus, *J Neurophysiol* 78, 2631.
- Wong, R.K., S.C. Chuang and R. Bianchi, 2002, Metabotropic Glutamate Receptors and Epileptogenesis, *Epilepsy Curr* 2, 81.
- Wu, L.G., and Saggau P., 1995, GABA_B mediated presynaptic inhibition in guinea-pig hippocampus is caused by a reduction of presynaptic Ca^{2+} influx, *J Physiol* 15;485 (Pt 3):649.
- Xia, Y.F. and A.C. Arai, 2005, AMPA receptor modulators have different impact on hippocampal pyramidal cells and interneurons, *Neurosci* 135, 555.

- Young, D., P.A. Lawlor, P. Leone, M. Dragunow and M.J. During, 1999, Environmental enrichment inhibits spontaneous apoptosis, prevents seizures and is neuroprotective, *Nat Med* 5, 448.
- Young, J.I., E.P. Hong, J.C. Castle, J. Crespo-Barreto, A.B. Bowman, M.F. Rose, D. Kang, R. Richman, J.M. Johnson, S. Berget and H.Y. Zoghbi, 2005, Regulation of RNA splicing by the methylation-dependent transcriptional repressor methyl-CpG binding protein 2, *Proc Natl Acad Sci U S A* 102, 17551.
- Zhang, W., A.S. Basile, J. Gomeza, L.A. Volpicelli, A.I. Levey and J. Wess, 2002, Characterization of Central Inhibitory Muscarinic Autoreceptors by the Use of Muscarinic Acetylcholine Receptor Knock-Out Mice, *J Neurosci* 22, 1709.
- Zhou, Z., E.J. Hong, S. Cohen, W.N. Zhao, H.Y. Ho, L. Schmidt, W.G. Chen, Y. Lin, E. Savner, E.C. Griffith, L. Hu, J.A. Steen, C.J. Weitz and M.E. Greenberg, 2006, Brain-specific phosphorylation of MeCP2 regulates activity-dependent Bdnf transcription, dendritic growth, and spine maturation, *Neuron* 52, 255.
- Ziburkus, J., J.R. Cressman, E. Barreto and S.J. Schiff, 2006, Interneuron and pyramidal cell interplay during in vitro seizure-like events, *J Neurophysiol* 95, 3948.

Bibliography

- Engel J. (1989) *Seizures and epilepsy*, F A Davis, Philadelphia
- Glaze DG (1990) Drug effects. In: *Current practice of clinical electroencephalography*, ed 2 (Daly DD, Pedley TA, eds), pp 489-512. New York: Raven.
- Hebb DO (1949) *The Organization of Behavior: A Neuropsychological Theory* New York, Wiley
- Jeffeys J.G. (1993) "The pathophysiology of Epilepsies" In *A text book of epilepsy*. Laidlaw, J. Richens, A Chadwick, D.W. (ed.) Churchill Livingstone, Edinburgh
- Rall WA. (1964) Theoretical significance of dendritic trees for neuronal input-output relations. In: *Neural Theory and Modeling*, edited by Reiss RF. Stanford, CA: Stanford Univ. Press, p. 73-97
- Schwartzkroin PA (1993) *Epilepsy: models, mechanisms, and concepts*, p 544

GLOBAL CHANGES IN THE HIPPOCAMPAL PROTEOME FOLLOWING EXPOSURE TO AN ENRICHED ENVIRONMENT

K. McNAIR,^a J. BROAD,^a G. RIEDEL,^b C. H. DAVIES^c
AND S. R. COBB^{a*}

^aDivision of Neuroscience and Biomedical Systems, IBLS, University of Glasgow, Glasgow, G12 8QQ, UK

^bSchool of Medical Sciences, University of Aberdeen, Forresterhill, Aberdeen, AB25 2ZD, UK

^cPsychiatry Centre for Excellence in Drug Discovery, GlaxoSmithKline Pharmaceuticals, Third Avenue, Harlow CM19 5AW, UK

Abstract—Exposure to an enriched environment promotes neurochemical, structural and neurophysiological changes in the brain and is associated with enhanced synaptic plasticity and improved hippocampal-dependent learning. Using a global proteomics-based approach we have now been able to reveal the altered expression of a diverse range of hippocampal proteins following exposure to an enriched environment. Male Hooded Lister rats (8 weeks) were subjected to a 6-week regimen in which they were housed in either non-enriched (open field) or enriched conditions (toys, wheels etc.). Whole protein extracts from stratum pyramidale and stratum radiatum of area CA1 were then isolated and subjected to differential gel electrophoresis [McNair K, Davies CH, Cobb SR (2006) Plasticity-related regulation of the hippocampal proteome. *Eur J Neurosci* 23(2):575–580]. Of the 2469 resolvable protein spots detected in this study, 42 spots (1.7% of the detectable proteome) derived from predominantly somatic fractions and 32 proteins spots from dendritic fractions (1.3% of detectable proteome) were significantly altered in abundance following exposure to an enriched environment (somatic: 14 increased/28 decreased abundance, range –1.5 to +1.4-fold change; dendritic: 16 increased, 16 decreased abundance, range –1.6 to +3.0-fold change). Following in-gel tryptic digestion and MALDI-ToF/Q-star mass spectrometry, database searching revealed the identity of 50 protein spots displaying environmental enrichment-related modulation of expression. Identified proteins belonged to a variety of functional classes with gene ontology analysis revealing the majority (>70%) of regulated proteins to be part of the energy metabolism, cytoplasmic organization/biogenesis and signal transduction processes. © 2006 IBRO. Published by Elsevier Ltd. All rights reserved.

Key words: hippocampus, environmental enrichment, proteomics, glutamate, plasticity, proteome.

An enriched environment where animals are introduced to novel, complex and stimulating surroundings has long been known to promote structural changes in the brain and

*Corresponding author. Tel: +44-0141-330-2914; fax: +44-0141-330-2923.

E-mail address: s.cobb@bio.gla.ac.uk (S. Cobb).

Abbreviations: ACSF, artificial cerebrospinal fluid; BVA, biological variance analysis; DiGE, difference gel electrophoresis; LTP, long-term potentiation; PMF, peptide mass fingerprint.

0306-4522/07/\$30.00+0.00 © 2006 IBRO. Published by Elsevier Ltd. All rights reserved.
doi:10.1016/j.neuroscience.2006.12.033

to enhance learning and memory performance in rodents (Hebb, 1947). Indeed, more recent studies have confirmed exposure to an enriched environment to result in altered expression of various neurochemical markers (Huang et al., 2006; Naka et al., 2005) as well as neurophysiological changes such as enhanced synaptic plasticity (Irvine and Abraham, 2005). For instance, environmental enrichment is reported to modify the PKA-dependence of long-term potentiation (LTP) as well as improving hippocampal-dependent memory (Duffy et al., 2001).

However, the exact cellular and molecular basis for enrichment-induced structural or neurophysiological modifications remains unknown. Altered intracellular signaling and modified synaptic strength may support enrichment-induced cognitive changes. Microarray studies following short- and long-term environmental enrichment exposure have identified genes involved in DNA/RNA synthesis, neuronal signaling, neuronal growth/structure, cell death and protein processing (Rampon et al., 2000) as possible targets for neuronal adaptations in response to environmental enrichment. However, a global assessment of alterations in expression at the protein level remains to be undertaken. Therefore, to better understand the degree and patterns of altered protein expression underlying environmental enrichment, we have used difference gel electrophoresis (DiGE) to analyze differential global protein expression in the rat hippocampus following several weeks of exposure to a complex and stimulating environment. DiGE permits pairwise comparison between protein samples on a single gel by labeling each protein sample with a distinct fluor with the beneficial incorporation of an internal standard (Unlu et al., 1997; Lilley and Friedman, 2004).

The unique anatomical structure of the hippocampus in which the overwhelming majority of principal cells are co-aligned enables the separation of dendritic fields from soma. In the current study we have taken advantage of this feature to enable a simple form of tissue pre-fractionation in which the somatic tissues are separated from the synaptic transmission domain of the cell to allow independent analysis of these two areas.

We report altered expression of a diverse range of proteins isolated from somatic and dendritic hippocampal regions in response to environmental enrichment. The results indicate that proteins involved in neuronal signaling, structural alterations and protein metabolism, among others, are altered following exposure of rats to a complex and stimulating environment.

EXPERIMENTAL PROCEDURES

Animals

Hooded Lister rats (male, aged 8 weeks) were obtained from Harlan (Bicester, UK) and initially housed in groups of five in standard cages from 3 months prior to the beginning of the study. They were given *ad libitum* access to food and water and were kept on a 12-h light/dark cycle. Upon commencement of the enrichment study the enriched group was placed in a black Perspex box 100×50 cm in size which contained a food corner, suspended drinking bottle and sawdust base in addition to several novel objects including tubes, running wheels, platforms, beams, ladders etc. These enrichment objects were re-arranged and some were removed and replaced by novel items on a weekly basis. This ensured a degree of spatial novelty and learning about objects and their relationships. Control groups were placed in the same size and type of box, with a food corner, suspended drinking bottle and sawdust base with no additional enrichment objects. Both enriched and control groups were placed in their corresponding environments overnight for 15 h, 5 days per week for a total experimental period of 6 weeks.

Tissue harvest

At the end of the 6-week regimen, control and enriched rats were killed with an overdose of intraperitoneally injected tribromoethanol followed by cervical dislocation in accordance with local ethical guidelines and UK legislation [Animals (Scientific Procedure) Act, 1986]. All efforts were made to minimize the suffering and number of animals used in each experiment. Brains were rapidly transferred into ice cold (0–3 °C), oxygenated (95% O₂, 5% CO₂) artificial cerebrospinal fluid (ACSF) of the following composition (mM): NaCl 124, KCl 3, NaHCO₃ 26, NaH₂PO₄ 1.25, MgSO₄ 1, D-glucose 10 and CaCl₂ 2. The hippocampi were dissected free and transverse 500 μm thick slices cut using a McIlwain tissue chopper (Camden Instruments, Loughborough, UK). In oxygenated ice cold ACSF and under a dissection microscope, hippocampal area CA1 was dissected free from surrounding regions following which the stratum radiatum and stratum pyramidale were collected separately and snap frozen in liquid nitrogen and stored at –70 °C prior to proteomic analysis.

DIGE sample extraction and preparation

For each individual protein sample the CA1 region from three to four hippocampal slices were pooled and lysed in 150 μl of buffer containing 10 mM Tris pH 8, 5 mM magnesium acetate, 8 M urea and 2% ASB14. Lysed tissue was then subjected to five freeze–thaw cycles and left at room temperature for 1 h to aid solubilization of proteins. Samples were subsequently sonicated (4×4 min with 2 min intervals to prevent the overheating of urea in lysis buffer) and centrifuged at 13,000 r.p.m. for 15 min. Following sample cleanup using an ammonium acetate precipitation, protein pellets were re-suspended in approximately 70 μl of lysis buffer and protein concentration determined using Pierce's BCA Protein Assay Kit (Perbio Science UK Ltd., Cheshire, UK).

Sample CyDye labeling

Fifty micrograms of each protein sample was labeled with 400 pmol of either Cy2, 3 or 5 according to the manufacturer's instructions (GE Healthcare, Amersham, Little Chalfont, UK). Treatment samples were assigned randomly across six to eight gels (supplementary methods Table 1). Prior to the 1st dimension Cy2, 3 and 5 samples were pooled and added to the same volume of 2× sample buffer containing 8 M urea, 2% ASB14, 20 mg/ml DTT and 2% IPG buffer and then corrected to a final volume of 450 μl using rehydration buffer (8 M urea, 2% ASB14, 2 mg/ml DTT and 1% IPG buffer).

2D gel electrophoresis

The 1st dimension of the 2D gel electrophoresis process was performed using the rehydration method (Rabilloud et al., 1994). Isoelectric focusing was carried out on pH 3–10 non-linear (NL) 24 cm IPG strips. The second dimension was run on 12.5%, homogenous polyacrylamide gels poured between low fluorescence glass plates (GE Health Care). Gels were scanned immediately after the running of the second dimension on a Typhoon™ 9400 variable mode imager.

DiGE gel analysis

For initial studies (Fig. 1D), gel images were analyzed in differential in-gel analysis (DIA) mode in DeCyder software with spots displaying greater than 1.5-fold change in spot density being tentatively defined as being differentially expressed. All subsequent experiments incorporated a Cy2 internal standard. Following gel-to-gel matching of spots, statistical analysis (Student's *t*-test) of normalized protein abundance changes between samples was performed using BVA software module as described (Alban et al., 2003).

Spot picking and mass spectrometry analysis

Protein spots shown to be significantly different ($P < 0.05$) from control following treatment were picked, digested (porcine trypsin 0.2 μg, Promega, UK) and spotted onto a Voyager DE-Pro MALDI-ToF target plate for subsequent mass spectrometry analysis (Perceptive Biosystems, CA, USA) using the Ettan Spot Handling Workstation (GE Health Care). MALDI-ToF mass spectrometry was performed in positive reflector mode using a laser setting around 2350. The low mass gate setting was set at 750 Da, and the spectra were acquired over a range of 750–3500 Da. The accelerating voltage was 20 kV, the grid voltage set to 76% and the guide wire voltage set to 0.006%, with an extraction delay time of 160 ns. One hundred shots per spectrum were collected, with a combination of three spectra per spot.

Spectra were then exported to Data Explorer™ (version 4, Applied Biosystems, Cheshire, UK) where they were internally calibrated using the 842.5099 and 2211.1046 trypsin peaks, processed to reduce background noise, and a monoisotopic peak list was generated and entered into the Mascot peptide mass fingerprint (PMF) database. Data were searched using the NCBI nr database.

Those peptide mixtures that were unidentified by MALDI-ToF analysis were sent for tandem MS analysis. Tryptic peptides were solubilized in 0.5% formic acid and fractionated by nanoflow HPLC on a C18 reverse phase column, eluting with a continuous linear gradient to 40% acetonitrile over 20 min. The eluate was analyzed by online electrospray tandem mass spectrometry using a Qstar Pulsar (Applied Biosystems). Mass spectrometric analysis was performed in IDA mode (AnalystQS software, Applied Biosystems), selecting the four most intense ions for MSMS analysis. A survey scan of 400–1500 Da was collected for 3 s followed by 5 s MSMS scans of 50–2000 Da using the standard rolling collision energy settings. Masses were then added to the exclusion list for 3 min. Peaks were extracted using the Mascot script (BioAnalyst, Applied Biosystems) and automatically exported to the Mascot (Matrix Science, London, UK) search engine.

For both the PMF and MS/MS searches, proteins were matched with the identified peptides and each protein was assigned a Mascot score, which was a probability-based Mowse score (Perkins et al., 1999). In the case of PMF the significance threshold was 62, and in the case of MS/MS this threshold was 36.

Table 1. Hippocampal proteins (somatic fraction) showing differential expression following long term exposure to an enriched environment

Spot no. ^a	Master no. ^b	Protein ID ^c	Av. Ratio ^d	Control vs. enriched (<i>t</i> -test) ^e	Mass ^f	NCBI Acc no. ^g	Mowse Score ^h	Class ⁱ
1	1297		1.4	0.034				
2	2081		1.28	0.0017				
3	1312	ATP synthase α (M)	1.28	0.021	58904	gi 114523	95	NM
4	1584	Citrate synthase	1.26	0.0063	52176	gi 18543177	174	E/M
		Phosphoglycerate kinase 1			44909	gi 40254752	111	CM
5	1672	Actin, β	1.2	0.036	42066	gi 71620	261	CO&B
6	1642		1.19	0.0055				
7	491	Dynamin 1	1.18	0.00048	96209	gi 18093102	215	CO&B
8	1395	4-Aminobutyrate transaminase	1.16	0.0055	57178	gi 2143559	66	NT
9	1566		1.16	0.045				
10	1465		1.13	0.043				
11	2232	Proteasome subunit, β type 2	1.12	0.033	23069	gi 8394079	272	PM&T
		Auh protein			33605	gi 34873875	132	E/M
		ATP synthase α (M)			58904	gi 114523	82	NM
		RAB7			23075	gi 92022	39	ST
12	1400		1.1	0.011				
13	1098		1.1	0.046				
14	1253		1.07	0.02				
15	1141	Protein phosphatase 3 (α)	-1.1	0.046	59291	gi 8394030	105	ST
16	1101	Isoform of PSD-95/SAP90	-1.11	0.028	92685	gi 1517938	49	NT
17	2270	Dynactin 3	-1.11	0.029	24867	gi 34867161	144	CP
		ATP synthase, subunit D (M)			18827	gi 220904	104	NM
18	1034	CRMP-2 (<i>Mus musculus</i>)	-1.12	0.023	62638	gi 40254595	125	NG
19	1998	14-3-3	-1.13	0.0095	29274	gi 13928824	63	PM&T
		Tropomyosin isoform 6			29245	gi 29336093	71	MC
		GFAP δ			48809	gi 5030428	50	CO&B
20	1608		-1.13	0.02				
21	1898	Tubulin, β chain 15	-1.13	0.027	50361	gi 92930	148	CO&B
22	1210		-1.14	0.032				
23	2034		-1.14	0.035				
24	1723	Enol protein	-1.14	0.045	51736	gi 38649320	355	E/M
		Tubulin β chain 15			50361	gi 92930	319	CO&B
		Tubulin, β 2-like			50225	gi 40018568	291	CO&B
		Tubulin, β 5			50095	gi 27465535	287	CO&B
		Tubulin, α 2			50804	gi 34740335	256	CO&B
		Tubulin, α 1			50788	gi 11560133	237	CO&B
		GTP-binding regulatory protein			40568	gi 71911	135	ST
		Go						
		Isocitrate dehydrogenase 3 (NAD ⁺)			40044	gi 16758446	102	E/M
		Tubulin, β 3			50711	gi 21245098	90	CO&B
		Enolase (neuronal)			47495	gi 1363309	87	E/M
		Actin β			42066	gi 71620	75	CO&B
25	2086	Phosphoglycerate mutase (B)	-1.16	0.012	28942	gi 8248819	121	CM
26	2253		-1.16	0.032				
27	1054	hnRNPk protein	-1.17	0.02	51230	gi38197650	63	T/T
28	2209	RhoA	-1.18	0.015	22110	gi 31542143	142	ST
29	2133	Ubiquitin thiolesterase	-1.18	0.021	25096	gi 92934	168	PM&T
30	1919	Tubulin, β	-1.18	0.04	50377	gi 34875329	72	CO&B
31	1995	Glutathione transferase ω a 1	-1.18	0.049	27936	gi 12585231	56	E/M
32	2287		-1.19	0.017				
33	1865	Dynamin 1	-1.21	0.037	96209	gi 18093102	235	CO&B
		Malate dehydrogenase 1			36631	gi 15100179	226	E/M
		NAD						
34	1150	Synapsin lib	-1.22	0.0057	52822	gi 112350	329	ST
		Tyrosyl-tRNA synthetase			63385	gi 34871588	241	PM&T
		Mammalian fusca gene			53964	gi 871528	214	NG
35	2431	Peptidylprolyl isomerase A	-1.28	0.028	18091	gi 8394009	74	PM&T
36	2105		-1.29	0.022				
37	2405	Destrin	-1.31	0.013	18661	gi 7441446	205	CO&B
38	1724		-1.39	0.0029				

Table 1. continued

Spot no. ^a	Master no. ^b	Protein ID ^c	Av. Ratio ^d	Control vs. enriched (<i>t</i> -test) ^e	Mass ^f	NCBI Acc no. ^g	Mowse Score ^h	Class ⁱ
39	1032	CRMP-2 (<i>Mus musculus</i>)	−1.4	0.006	62638	gi 40254595	157	NG
40	1768		−1.41	0.011				
41	2156		−1.5	0.0023				
42	1824	Malate dehydrogenase 1	−1.5	0.0066	36631	gi 15100179	214	E/M
		NAD Glycerol 3-phosphate dehydrog			38001	gi 2317252	57	E/M

Abbreviations: CO&B, cytoplasmic organization and biogenesis; E/M, energy and metabolism; PM&T, protein modification and transport; ST, signal transduction; NM, nucleotide metabolism; NG, neurogenesis; CM, carbohydrate metabolism; NT, neurotransmitter release and production; CP, cell proliferation; MC, muscle contraction; T/T, transcription and translation.

List details proteins found to be significantly ($P < 0.05$) differentially expressed compared to tissues isolated from non-enriched rats.

^a Spot number corresponds to the annotation found in figure 1C.

^b Master number is the number assigned by DeCyder BVA software to each individual protein spot.

^c Protein i.d. assigned to each individual protein spot following mascot database searching using the Rattus taxonomy.

^d Average abundance ratio of individual protein spots (+ = increase, − = decrease in expression). Fold changes ranged from 40% decrease in expression (−1.4) to a 50% increase in expression (1.5).

^e Student's *t*-test value assigned by DeCyder BVA software, $P < 0.05$ determines significance.

^{f,g,h} Mass, NCBI accession number and Mowse score obtained following Mascot PMF or MS/MS ion searching following either MALDI-ToF (bold) or Qstar mass spectrometry.

ⁱ Protein biological processes were determined using the Fatigo gene ontology database. Proteins belong to a wide variety of functional classes.

RESULTS

To investigate global changes in hippocampal protein expression associated with environmental enrichment, adult male hooded Lister rats (8 weeks old) were exposed to an overnight-enriched environment regimen for six consecutive weeks (see Experimental Procedures). The enriched chamber comprised a 100 cm by 50 cm open box containing an assortment of plastic toys, balls, cardboard tubes, ladders and running wheels (Fig. 1B) while control group animals were placed in an identical open arena which contained only wood shavings and a single cardboard tube shelter (Fig. 1A). Animals exposed to the enriched conditions noticeably displayed overt exploratory activity and appeared inquisitive when the cage top was removed for routine husbandry. In contrast, animals in the control arena were typically less active and displayed little exploratory behavior. When quiescent, both groups of animals tended to nest together in a corner of the arenas. At the end of the 6-week enrichment program brain tissue was harvested and hippocampi were dissected free from the surrounding tissues and transverse slices cut with the aid of a McIlwain tissue chopper. Isolated tissue samples of predominantly somatic or dendritic origin were subsequently obtained by carefully dissecting area CA1 stratum pyramidale and stratum radiatum respectively (Fig. 1C). The entire hippocampal proteome was labeled for DIGE to separate component proteins and enable the quantification of individual protein spot abundance levels in tissues from enriched and non-enriched subjects. Initial differential in-gel analysis revealed the majority of protein spots to remain unchanged in both stratum pyramidale- (Fig. 1D) and stratum radiatum- (not shown) derived tissues. However, a small discrete population of 137 protein spots did exhibit modest (>1.5-fold) changes in spot density between enriched and non-

enriched samples. For a more detailed analysis, multiple gel replicates were analyzed in biological variance analysis (BVA) mode (Fig. 1E). Of the 2469 protein spots resolved across both somatic and dendritic fractions, 32 (1.3% of the detectable proteome) showed significantly altered abundance levels following environmental enrichment within the dendritic fraction compared with non-enriched controls (16 increased/16 decreased abundance (−1.58- to 2.98-fold change), all $P < 0.05$). In tissues isolated from stratum radiatum, BVA analysis revealed 42 (1.7% of the detectable proteome) protein spots displaying altered abundance following environmental enrichment (14 increased/28 decreased abundance (−1.5- to 1.4-fold change), all $P < 0.05$).

Following in-gel tryptic digestion and MALDI-ToF/Q-star mass spectrometry, database searching revealed the identity of 50 protein spots with more than half of such spots representing a single protein entity (Tables 1 and 2 for somatic and dendritic samples respectively). Fig. 2 shows representative plots of individual spots together with examples of 3D protein intensity plots (A–B) or 2D Western blot validation of altered expression (C–D).

Identified proteins belonged to a diverse variety of functional classes including postsynaptic density proteins (e.g. SAP90), presynaptic proteins (e.g. dynamin 1) and proteins associated with signaling such as small GTPase signaling pathways (e.g. RhoA). Identified proteins were more formally grouped by biological function using Fatigo (Al-Shahrour et al., 2004) gene ontology analysis (Fig. 3) which confirmed that protein spots exhibiting enrichment-related altered expression spanned a wide range of functional classes. However, in both stratum radiatum- and stratum pyramidale-derived fractions, cytoplasmic organization and biogenesis (structural) and energy metabolism were the predominant classes of protein displaying enrichment-related differential protein spot expression.

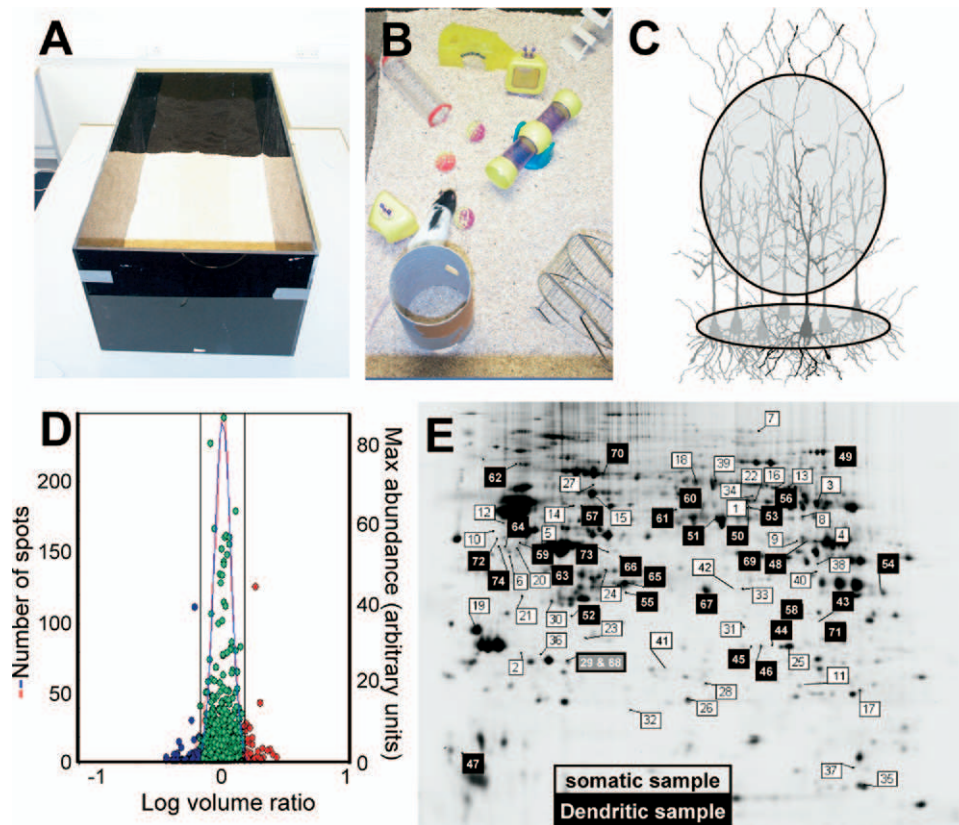


Fig. 1. Exposure to an enriched environment results in the altered expression of hippocampal proteins. Rats were exposed to either (A) an open field arena or (B) an identical-sized enriched environment for a total experimental period of 6 weeks (see Experimental Procedures). (C) Hippocampal tissues were subsequently isolated from either predominantly dendritic or somatic lamina (shaded areas) of hippocampal area CA1. (D) Total protein extracts from area CA1 stratum pyramidale following exposure to environmental enrichment revealed a distribution of protein spots corresponding to both increased and decreased abundance when compared with control treated tissues. Scatter plot shows log abundance ratios of individual vehicle/glutamate sample spot pairs (○) against maximum protein spot abundance. Individual protein spots show decreased (left, blue ●), unaltered (center, green ●) and increased (right, red ●) log abundance ratios. Vertical lines are included as a guide to indicate a level of 1.5-fold change in abundance (see Experimental Procedures). The red curve shows the frequency distribution of the log abundance ratios, whereas the blue curve is the normalized modal frequency fitted to a modal peak of zero. Note that a minority of protein spots display enrichment-related increase or decrease in expression but that the expression levels of majority of protein spots remain unaltered. (E) Statistical comparison of environmental enrichment-associated alterations in protein abundance (four gel replicates per group comprising six pooled subjects) using BVA revealed 74 protein spots with significant changes in abundance ($P < 0.05$) as indicated on gel image. Of the observed changes in abundance, 42 were confined to tissues isolated from predominantly somatic regions (open squares) while 32 protein spots displayed differential abundance only in the dendritic layer fraction (black squares). Only two spots (gray squares) showed significantly altered abundance levels in both somatic and dendritic later fractions. For interpretation of the references to color in this figure legend, the reader is referred to the Web version of this article.

DISCUSSION

The main finding of the current study is that chronic exposure of an enriched environment leads to the altered expression of a diverse range of hippocampal proteins.

Overall, the number of protein species showing altered expression was in the range of 1–2% of the proteome within the detectable range of the DiGE technique, the altered expression of somatic and dendritic fractions being broadly similar (1.7 and 1.3% altered respectively). Moreover, subsequent gene ontology analysis of the protein classes showing enrichment-related alterations in expression revealed a very similar pattern of alteration when the proteins were grouped by biological function. That the cytoplasmic organization and biosynthesis (structural) and energy metabolism were the dominant classes in terms of percentage of the altered proteome is consistent with

structural and metabolic alterations occurring in association with enhanced hippocampal activity (McNair et al., 2006). However, structural and metabolic proteins are typically highly abundant proteins in hippocampus (Yang et al., 2004) and will thus be more readily detectable using protein dyes with a finite sensitivity. That said, the results clearly indicate that these abundant proteins including ‘housekeeping’ proteins do indeed show altered expression in relation to environmental enrichment. Furthermore, less abundant proteins such as those associated with signal transduction were also identified as displaying altered expression. In this respect it is interesting to note that while structural and metabolic proteins showed altered expression throughout both somatic and dendritic fractions, alterations in the expression signaling proteins were much more pronounced in dendritic sam-

Table 2. Hippocampal proteins (dendritic fraction) showing differential expression following long term exposure to an enriched environment

Spot no. ^a	Master no. ^b	Protein ID ^c	Av. Ratio ^d	Control vs. enriched (dendritic) (<i>t</i> -test) ^e	Mass ^f	NCBI Acc no. ^g	Mowse Score ^h	Class ⁱ
43	2030	ATP synthase α (M)	2.98	0.0058	58904	gi 114523	293	NM
		VAMP-associated protein B						ST
		VAMP-associated protein A			27476	gi 61889097	59	ST
		Glyceraldehyde 3-phosphate-dehydrogenase			36098	gi 56188	320	E/M
44	2080	Phosphoglycerate mutase B	1.48	0.00083	28942	gi 8248819	98	E/M
		Hsc 70-psl			71112	gi 56385	402	CO&B
		Rho-associated coiled-coil forming kinase 2			160475	gi 6981478	31	ST
45	2075	Pgam1 protein	1.43	0.025	28928	gi 12805529	97	CM
		Chain F, Enoyl-Coa hydratase complexed with octanoyl-Coa			28555	gi 3212683	145	E/M
46	2078	Pgam1 protein	1.41	0.0096	28928	gi 12805529	225	CM
		Proteasome 26S non-ATPase subunit 9			24985	gi 18426862	121	PM&T
47	2365	ATP synthase, subunit D (M)	1.4	0.043	18809	gi 9506411	424	NM
		Enolase (neuronal)			47495	gi 1363309	58	E/M
		Transgelin 3			24981	gi 13928938	48	CO&B
		Ubiquitin-conjugating enzyme			42505	gi 34933268	36	PM&T
48	1579	Pyruvate dehydrogenase E1 α	1.27	0.014	43853	gi 57657	781	E/M
		Phosphoglycerate kinase 1			44909	gi 40254752	281	E/M
		SEC14-like protein 2			46593	gi 21542226	158	T/T
		Citrate synthase			52176	gi 18543177	104	E/M
		RNA binding protein p42 AUF1			36164	gi 9588098	72	T/T
49	757	Aconitase 2, mitochondrial	1.26	0.035	86121	gi 40538860	682	CM
		GFAP δ			48809	gi 5030428	63	CO&B
50	1288	Heat shock protein 60 precursor	1.25	0.024	58061	gi 1334284	87	CO&B
51	1365	Enolase 1	1.23	0.036	47428	gi 56107	98	E/M
52	1289	Aldehyde dehydrogenase 7, A1	1.21	0.0097	25313	gi 25090044	49	E/M
53	1967	Actin, β	1.21	0.019	42066	gi 71620	260	CO&B
		Tubulin, β			50095	gi 27465535	39	CO&B
54	1844	Malate dehydrogenase (M)	1.18	0.027	36117	gi 42476181	112	E/M
55	1858	GFAP δ	1.15	0.043	48809	gi 5030428	122	CO&B
56	1301		1.15	0.047				
57	1266		1.1	0.041				
58	1931	Fumarylacetoacetate hydrolase	1.08	0.038	40884	gi 34858672	66	E/M
		Creatine kinase (M)			47398	gi 57539	44	E/M
		Glyceraldehyde 3-phosphate-dehydrogenase			36090	gi 37590767	43	E/M
59	1574	GFAP δ	-1.08	0.047	48809	gi 5030428	86	CO&B
60	1144	GRP58	-1.09	0.021	57044	gi 38382858	174	PM&T
61	1296		-1.13	0.019				
62	859	Heat shock 70 kD protein 5	-1.15	0.016	72473	gi 38303969	78	CO&B
63	1719	GNBP α inhibiting 2	-1.17	0.019	41043	gi 13591955	511	ST
		GTP-binding regulatory protein Go α chain, splice form α -2			40568	gi 71911	222	ST
		A326s Mutant of an inhibitory α subunit			36325	gi 3891516	166	ST
		Tubulin, α			50804	gi 34740335	162	CO&B
		Actin, β			42066	gi 71620	88	CO&B
		GNBP3			40781	gi 27465609	81	ST
		GNBP α 13			44326	gi 61557003	63	ST
64	1588	Actin, β	-1.2	0.03	42066	gi 71620	276	CO&B
		Tubulin, β 5			50095	gi 27465535	153	CO&B
		Tubulin β chain 15			50361	gi 95930	146	CO&B
		GFAP δ			48809	gi 5030428	127	CO&B
		Hsc70-psl			71112	gi 56385	68	CO&B
65	1663		-1.21	0.044				
66	1793	Lactate dehydrogenase B	-1.21	0.047	36874	gi 6981146	79	E/M
67	1908	Septin 5	-1.23	0.035	44349	gi 16758814	66	ST
		Crystallin, 1			35717	gi 28461157	78	E/M
68	2133	Ubiquitin thiolesterase	-1.24	0.032	25096	gi 92934	168	PM&T
69	1637		-1.25	0.023				
70	934	ATPase, H ⁺ transporting, V1 subunit A, isoform 1	-1.28	0.036	68584	gi 34869154	56	NM
71	2005	Cyclin-dependent kinase 5	-1.29	0.0073	33689	gi 18266682	232	NG

Table 2. continued

Spot no. ^a	Master no. ^b	Protein ID ^c	Av. Ratio ^d	Control vs. enriched (dendritic) (<i>t</i> -test) ^e	Mass ^f	NCBI Acc no. ^g	Mowse Score ^h	Class ⁱ
		VDAC 3			31178	gi 3786204	69	ST
		Inducible carbonyl reductase			30920	gi 1906812	80	E/M
		B-36 VDAC			32327	gi 299036	68	ST
		Lymphocyte protein tyrosine kinase			58366	gi 34871627	55	ST
		ATP synthase γ			29972	gi 310190	55	NM
		Protein tyrosine kinase			57290	gi 57582	52	ST
72	1526		-1.3	0.028				
73	1617		-1.31	0.017				
74	1586	Diacylglycerol kinase ζ	-1.58	0.006	105426	gi 13592131	56	E/M

Abbreviations: CO&B, cytoplasmic organization and biogenesis; E/M; energy and metabolism; PM&T, protein modification and transport; ST, signal transduction; NM, nucleotide metabolism; NG, neurogenesis; CM, carbohydrate metabolism; NT, neurotransmitter release and production; CP, cell proliferation; T/T, transcription and translation.

List details proteins found to be significantly ($P < 0.05$) differentially expressed compared to tissues isolated from non-enriched rats.

^a Spot number corresponds to the annotation found in figure 1C.

^b Master number is the number assigned by DeCyder BVA software to each individual protein spot.

^c Protein i.d. assigned to each individual protein spot following mascot database searching using the Rattus taxonomy.

^d Average abundance ratio of individual protein spots (+ = increase, - = decrease in expression). Fold changes range from a 198% decrease (-2.98) in expression to a 58% increase in expression (1.58).

^e Student's *t*-test value assigned by DeCyder BVA software.

^{f,g,h} Mass, NCBI accession number and Mowse score obtained following Mascot PMF or MS/MS ion searching following either Maldi-Tof (bold) or Qstar mass spectrometry.

ⁱ Protein biological processes were determined using the Fatigo gene ontology database. Proteins belong to a wide variety of functional classes.

ples. Indeed, changes in synaptosomal protein contents may result in behavioral alterations (Kirchner et al., 2004) and environmental enrichment has, possibly as a result of such differential protein expression, consistently enhanced behavioral learning (Duffy et al., 2001; Huang et al., 2006).

Proteins involved in small GTPase signaling pathways (RhoA, Rho-associated coil-forming kinase 2), guanine nucleotide binding proteins (GNBP) and protein tyrosine kinase pathways in particular were shown to display altered expression. This may be consistent with the role of GTPase and tyrosine kinase signaling pathways in hippocampal neuronal plasticity (O'Kane et al., 2004; O'Dell et al., 1991; Ho et al., 2004). RhoA in particular is known to be important in the maintenance of dendritic structures in rat hippocampal neurones (Nakayama et al., 2000).

A feature unique to the current study is that only a single protein entity was found to display altered abundance in both dendritic and somatic fractions. Spot number 2133 subsequently identified as ubiquitin thiolesterase was found to decrease in both fractions. This finding suggests that while overall numerous proteins throughout the somato-dendritic axis display altered expression, these changes in abundance are nevertheless specific for the domain in terms of whether they occur in the perisomatic or axon termination zones, and these changes are not necessarily accessible when the hippocampus as a whole is considered (Yang et al., 2004).

Environmental-related alterations in motor activity and other exercise related processes may potentially contribute to the alterations in expression observed. Indeed, environmental enrichment has been reported to result in increased dendritic spine density in motor cortex and striatum (Turner et al., 2003). However, the same study did

not find any change in granule cell spine density in the same animals. That said, the possible contribution of exercise or other physiological processes on environmental enrichment-related alterations in the hippocampal proteome cannot be excluded.

The current study focused upon a single time point at 6 weeks following the introduction of the enriched environment. This time-point was chosen as it has been shown in many previous studies that, by around this point, rodents exhibit alterations in synaptic plasticity mechanisms (Artola et al., 2006; Duffy et al., 2001) as well as hippocampal dependent learning (Rampon et al., 2000; Williams et al., 2001). Also around this time structural changes, including changes in spine density and size as well as increases in neuronal number are apparent (Turner et al., 2003). Such structural modifications are also found in this study as indicated by the relatively large number of altered proteins belonging to the cytoplasmic organization and biogenesis class of biological function. Given that environmental enrichment-associated neurogenesis is widely reported to be predominantly restricted to the dentate gyrus (Bruehl-Jungerman et al., 2005), it is likely that the altered expression of structurally related proteins in CA1 is mainly due to the structural reorganization of existing neurones. This would be consistent with morphological studies showing experience-dependent plasticity to be associated with the creation of new and bulking up of existing synapses (Faherty et al., 2003; Turner et al., 2003). Indeed, a recent report by Meshi et al. (2006) demonstrated behavioral effects of environmental enrichment such as improved hippocampal-dependent spatial learning and habituation to an unfamiliar environment to be independent of neurogenesis and instead may be due to changes in morphology

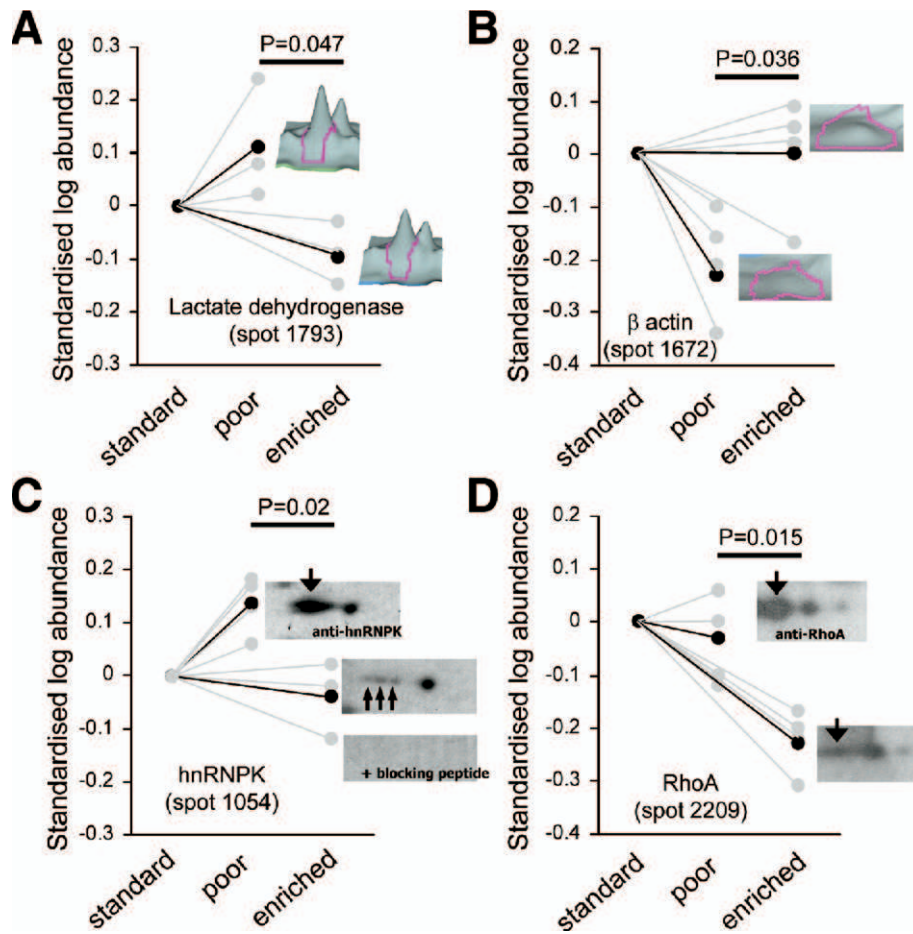


Fig. 2. Effects of environmental enrichment on identified hippocampal proteins. Representative scatter plots showing examples of identified protein spots displaying decreased (A, C–D) and increased (B) spot protein abundance in hippocampal tissues isolated following environmental enrichment. Gray points represent individual DiGE gel replicates while black points indicate mean abundance in tissues from rats exposed to ‘poor’ (open field) and enriched conditions. Insets in A and B show representative spot profile (protein intensity peak) of identified proteins on DiGE gels in poor and enriched group samples. Insets in C and D show 2D Western blot validation for enrichment-related altered hnRNPk and RhoA spot intensity respectively. Note that the prominent anti-hnRNPk spot in the ‘poor’ sample (downward arrow) is reduced in intensity in enriched sample to reveal a chain of small spots (upward arrows) likely representing a charge chain. Control gel below shows hnRNPk blocking peptide to abolish immunoreactivity.

such as increased synaptogenesis (van Praag et al., 2000).

As discussed, the current study demonstrates a degree of overlap with complementary microarray-based gene expression studies (Rampon et al., 2000). Rampon et al. (2000) investigated gene expression following both short and long term exposure of mice to an enriched environment. Both our study and the Rampon et al. (2000) report provide a consensus finding in which a variety of mRNAs and corresponding proteins display altered expression following environmental enrichment. Overall, for example, the small GTPase RhoA, the structural protein actin and other molecules including GRP-78 and PSD-95 were shown to display altered abundance at both mRNA and protein levels. The alteration in RhoA and in hnRNPk expression identified using the DiGE approach was additionally confirmed by Western blot. Furthermore, we here extend previous studies by identifying several novel environmental enrichment-related proteins including hnRNPk

which is thought to be involved in the translation of mRNAs (Evans et al., 2003) and which we have previously identified as differentially expressed shortly after the induction of hippocampal plasticity (McNair et al., 2006). Overall, it is interesting to note that 18% of proteins identified in this study have been shown to be regulated during LTP using an identical DiGE approach *in vitro* (McNair et al., 2006). This may suggest that synaptic plasticity-related changes are indeed a major component of the altered expression seen with environmental enrichment. Indeed, several other proteins identified in this study have also previously been linked to synaptic plasticity-related processes such as LTP, LTD, learning and memory. These include PSD-95 (Migaud et al., 1998; Stein et al., 2003), synapsin (Sato et al., 2000), Rock (O’Kane et al., 2004) and CDK-5 (Wang et al., 2004) and provide compelling evidence for the notion that environmental enrichment recruits mechanisms similar to those activated during neuronal plasticity.

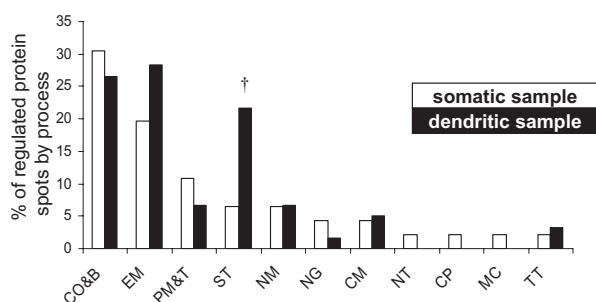


Fig. 3. Gene ontology analysis of hippocampal proteins showing altered abundance in response to exposure to an enriched environment. Bar chart illustrating a functional cluster analysis of identified proteins classed by biological function contained within spots showing environmental enrichment-associated altered abundance in whole protein extracts from cell body layer ('somatic samples,' open boxes) and dendritic layer ('dendritic sample,' black-filled boxes) tissues. Note that the majority of identified proteins belong to the cytoplasmic organization and biogenesis (cytoskeletal and associated proteins) and energy metabolism groups but that dendritic sample additionally exhibits a substantial proportion of synaptic transmission-related proteins displaying differential expression (†). Abbreviations: CO&B, cytoplasmic organization and biogenesis; E/M, energy and metabolism; PM&T, protein modification and transport; ST, signal transduction; NM, nucleotide metabolism; NG, neurogenesis; CM, carbohydrate metabolism; NT, neurotransmitter release and production; CP, cell proliferation; MC, muscle contraction; T/T, transcription and translation.

One of the main limitations of the current study is the inability to resolve very low abundance proteins as well as highly membrane bound proteins, which tend not to enter the second dimension of the 2D gels. This is an important consideration given that there are likely to be many environmental enrichment-related changes occurring with the population of membrane bound proteins. For instance, [Naka et al. \(2005\)](#) reported alterations in AMPA receptor subunits following environmental enrichment while [Rampon et al. \(2000\)](#) reported alterations in the expression of genes involved in NMDA receptor expression. However, the current report complements these studies by demonstrating that proteins with non-membranous and in many cases non-synaptic loci also show altered abundance in relation to environmental enrichment. Moreover, while the [Rampon et al. \(2000\)](#) report demonstrated altered expression at the mRNA level, it is likely that many of the changes reported here are not only due to alterations in de novo synthesis but also due to altered protein degradation and posttranslational modifications. That a limited subset of proteins identified in this study corresponds to differentially expressed mRNAs identified in the [Rampon et al. \(2000\)](#) study likely reflects the fact that the current analysis is restricted to more soluble and abundant proteins. However, this limitation is tempered by the ability to identify actual changes in functional protein levels per se, including alterations due to differential mRNA-independent post-translational modification, trafficking and degradation.

CONCLUSION

In conclusion, the current study demonstrates a significant alteration in a diverse range of hippocampal proteins fol-

lowing exposure to an enriched environment and extends previous findings describing enrichment-related alterations in gene expression. The findings highlight the occurrence of structural, metabolic and signaling changes associated with environmental enrichment and suggest that the associated cognitive benefits may result from selective adaptations, which differ for synaptosomal and somatic compartment of the neurons.

Acknowledgments—This work was supported by the MRC and GlaxoSmithKline. The authors thank Drs. Richard Burchmore and Andy Pitt at the Sir Henry Wellcome Functional Genomics Facility for advice in all aspects of proteomic analysis and Drs. Patricia Dorward and Lianne Robinson (University of Aberdeen) for help with the enrichment protocol.

REFERENCES

- Alban A, David SO, Bjorkesten L, Andersson C, Sloge E, Lewis S, Currie I (2003) A novel experimental design for comparative two-dimensional gel analysis: two-dimensional difference gel electrophoresis incorporating a pooled internal standard. *Proteomics* 3(1):36–44.
- Al-Shahrour F, Diaz-Uriate R, Dopazo J (2004) FatiGO: a web tool for finding significant associations of gene ontology terms. *Bioinformatics* 20(4):578–580.
- Artola A, von Frijtag JC, Fermont PC, Gispen WH, Schrama LH, Kamal A, Spruijt BM (2006) Long-lasting modulation of the induction of LTD and LTP in rat hippocampal CA1 by behavioural stress and environmental enrichment. *Eur J Neurosci* 23(1):261–272.
- Bruel-Jungerman E, Laroche S, Rampon C (2005) New neurons in the dentate gyrus are involved in the expression of enhanced long-term memory following environmental enrichment. *Eur J Neurosci* 21(2):513–521.
- Duffy SN, Craddock KJ, Abel T, Nguyen PV (2001) Environmental enrichment modifies the PKA-dependence of hippocampal LTP and improves hippocampus-dependent memory. *Learn Mem* 8(1):26–34.
- Evans JR, Mitchell SA, Spriggs KA, Ostrowski J, Bomsztyk K, Ostarek D, Willis AE (2003) Members of the poly (rC) binding protein family stimulate the activity of the c-myc internal ribosome entry segment in vitro and in vivo. *Oncogene* 22(39):8012–8020.
- Faherty CJ, Kerley D, Smeyne RJ (2003) A Golgi-Cox morphological analysis of neuronal changes induced by environmental enrichment. *Brain Res Dev Brain Res* 141(1–2):55–61.
- Hebb DO (1947) The effects of early experience on problem-solving at maturity. *Am Psychol* 2:306–307.
- Ho OH, Delgado JY, O'Dell TJ (2004) Phosphorylation of proteins involved in activity-dependent forms of synaptic plasticity is altered in hippocampal slices maintained in vitro. *J Neurochem* 91(6):1344–1357.
- Huang FL, Huang KP, Wu J, Boucheron C (2006) Environmental enrichment enhances neurogranin expression and hippocampal learning and memory but fails to rescue the impairments of neurogranin null mutant mice. *J Neurosci* 26(23):6230–6237.
- Irvine GI, Abraham WC (2005) Enriched environment exposure alters the input-output dynamics of synaptic transmission in area CA1 of freely moving rats. *Neurosci Lett* 391(1–2):32–37.
- Kirchner L, Weitzdoerfer R, Hoeger H, Urc A, Schmidt P, Engelmann M, Villara SR, Fountoulakis M, Lubec G, Lubec B (2004) Impaired cognitive performance in neuronal nitric oxide synthase knockout mice is associated with hippocampal protein derangements. *Nitric oxide* 11:316–330.
- Lilley KS, Friedman DB (2004) All about DIGE: quantification technology for differential-display 2D-gel proteomics. *Expert Rev Proteomics* 1(4):401–409.

- McNair K, Davies CH, Cobb SR (2006) Plasticity-related regulation of the hippocampal proteome. *Eur J Neurosci* 23(2):575–580.
- Meshi D, Drew MR, Saxe M, Ansorge MS, David D, Santarelli L, Malapani C, Moore H, Hen R (2006) Hippocampal neurogenesis is not required for behavioural effects of environmental enrichment. *Nat Neurosci* 9(6):729–731.
- Migaud M, Charlesworth P, Dempster M, Webster LC, Watabe AM, Makhinson M, He Y, Ramsay MF, Morris RG, Morrison JH, O'Dell TJ, Grant SG (1998) Enhanced long-term potentiation and impaired learning in mice with mutant postsynaptic density-95 protein. *Nature* 396(6710):433–439.
- Naka F, Narita N, Okada N, Narita M (2005) Modification of AMPA receptor properties following environmental enrichment. *Brain Dev* 27(4):275–278.
- Nakayama AY, Harms MB, Luo L (2000) Small GTPases Rac and Rho in the maintenance of dendritic spines and branches in hippocampal pyramidal neurons. *J Neurosci* 20(14):5329–5338.
- O'Dell TJ, Kandel ER, Grant SG (1991) Long-term potentiation in the hippocampus is blocked by tyrosine kinase inhibitors. *Nature* 353(6344):558–560.
- O'Kane EM, Stone TW, Morris BJ (2004) Increased long-term potentiation in the CA1 region of rat hippocampus via modulation of GTPase signalling or inhibition of Rho kinase. *Neuropharmacology* 46(6):879–887.
- Perkins DN, Pappin DJ, Creasy DM, Cottrell JS (1999) Probability-based protein identification by searching sequence databases using mass spectrometry data. *Electrophoresis* 20(18):3551–3567.
- Rabilloud T, Valette C, Lawrence JJ (1994) Sample application by in-gel rehydration improves the resolution of two-dimensional electrophoresis with immobilized pH gradients in the first dimension. *Electrophoresis* 15(12):1552–1558.
- Rampon C, Jiang CH, Dong H, Tang YP, Lockhart DJ, Schultz PG, Tsien JZ, Hu Y (2000) Effects of environmental enrichment on gene expression in the brain. *Proc Natl Acad Sci U S A* 97(23):12880–12884.
- Sato K, Morimoto K, Suemaru S, Sato T, Yamada N (2000) Increased synapsin I immunoreactivity during long-term potentiation in rat hippocampus. *Brain Res* 872(1–2):219–222.
- Stein V, House DR, Bredt DS, Nicoll RA (2003) Postsynaptic density-95 mimics and occludes hippocampal long-term potentiation and enhances long-term depression. *J Neurosci* 23(13):5503–5506.
- Turner CA, Lewis MH, King MA (2003) Environmental enrichment: effects on stereotyped behavior and dendritic morphology. *Dev Psychobiol* 43(1):20–27.
- Unlu M, Morgan ME, Minden JS (1997) Difference gel electrophoresis: a single gel method for detecting changes in protein extracts. *Electrophoresis* 18(11):2071–2077.
- van Praag H, Kempermann G, Gage F (2000) Neural consequences of environmental enrichment. *Nat Rev Neurosci* 1(3):191–198.
- Wang Q, Walsh DM, Rowan MJ, Selkoe DJ, Anwyl R (2004) Block of long-term potentiation by naturally secreted and synthetic amyloid beta-peptide in hippocampal slices is mediated via activation of the kinases c-Jun N-terminal kinase, cyclin-dependent kinase 5, and p38 mitogen-activated protein kinase as well as metabotropic glutamate receptor type 5. *J Neurosci* 24(13):3370–3378.
- Williams BM, Luo Y, Ward C, Redd K, Gibson R, Kuczaj SA, McCoy JG (2001) Environmental enrichment: effects on spatial memory and hippocampal CREB immunoreactivity. *Physiol Behav* 73(4):649–658.
- Yang J-W, Czech T, Lubec G (2004) Proteomic profiling of human hippocampus. *Electrophoresis* 25:1169–1174.

(Accepted 11 December 2006)
(Available online 29 January 2007)